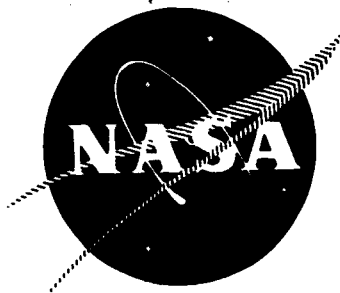


25

NASA CR-72379



R-7427

INTERIM REPORT
INDUCER DYNAMICS, PARTIAL FLOW
HYDRAULIC TURBINE DRIVE

GPO PRICE \$ _____

CFSTI PRICE(S) \$ _____

Hard copy (HC) 3.00

Microfiche (MF) _____

By

J. A. King

Prepared For

ff 653 July 65

National Aeronautics and Space Administration

Contract NAS3-10280

FACILITY FORM 602

N68-22094

(ACCESSION NUMBER)

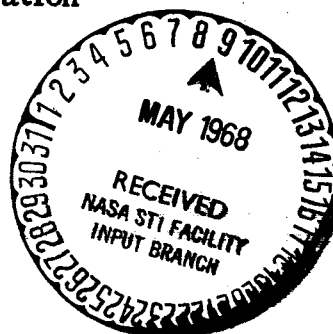
184
(PAGES)

NASA CR 72379
(NASA CR OR TMX OR AD NUMBER)

(THRU)

(CODE)

(CATEGORY)



Rocketdyne
A Division of North American Rockwell Corporation
Canoga Park, California

INTERIM REPORT

INDUCER DYNAMICS, PARTIAL FLOW
HYDRAULIC TURBINE DRIVE

by

J. A. King

Prepared for

NATIONAL AERONAUTICS AND SPACE ADMINISTRATION

February 1968

CONTRACT NAS 3-10280

Technical Management
NASA Lewis Research Center
Cleveland, Ohio
Large Engine Technology Branch
W. A. Rostafinski

ROCKETDYNE
A Division of North American Rockwell Corporation
6633 Canoga Avenue
Canoga Park, California

PRECEDING PAGE BLANK NOT FILMED.

FOREWORD

Rocketdyne, a Division of North American Rockwell Corporation, has prepared this report under National Aeronautics and Space Administration, Lewis Research Center, Contract NAS3-10280, G.O. 08983. This report covers the period from July 1967 through January 1968.

ABSTRACT

Two computer programs, an analog and a digital, have been developed that will predict the transient performance of a low-speed inducer driven by a hydraulic turbine. An inducer-turbine unit has been designed and fabrication is in progress. Steady-state maps of the pertinent components of this unit have been constructed from existing test data and by synthetic mapping procedures. These maps have been used in the computer programs to predict the performance of this unit in the system in which it will eventually be tested. Parametric studies have been made to determine the effect of selected changes in this system. The computer program has also been used to investigate several inducer-turbine combinations in simulated rocket engine installations.

PRECEDING PAGE BLANK NOT FILMED.

CONTENTS

Foreword	iii
Abstract	iii
Introduction	1
Objective	3
Design of a Partial-Flow, Hydraulic Turbine-Driven Inducer . .	5
Hydrodynamic Design	5
Mechanical Design	22
Dynamic Performance Models	33
Equation Development	33
Feed Line Description	49
Preinducer Description	50
Pump Description	51
Hydraulic Turbine Description	51
System Data	51
Computer Programs	55
Digital Model	55
Analog Model	56
Program Comparison	56
Parametric Studies	63
Introduction	63
Parameter Survey	64
Test System Performance	82
Engine System Operation	118
Summary and Conclusions	125
<u>Appendix A</u>	129
Equation Nomenclature	130
Basic Equations	131
Model Nomenclature	139
Digital Model Program Listings	143
Preinducer Analog Model Diagram	165

ILLUSTRATIONS

1. Optimum Efficiency of a Full-Admission Turbine	9
2. Preinducer Hydraulic Turbine (H_2O) Velocity Diagram	11
3. Preinducer Turbine Nozzle	12
4. Preinducer Turbine Nozzle	13
5. Preinducer Turbine Rotor	14
6. Preinducer Turbine Rotor	15
7. J-2 Oxidizer Pump Performance	17
8. J-2 Oxidizer Pump Performance	18
9. J-2 Oxidizer Pump Suction Performance	19
10. J-2 Oxidizer Preinducer Predicted Performance	20
11. J-2 Oxidizer Preinducer Predicted Suction Performance	21
12. Torque of Preinducer Hydraulic Turbine in Water	23
13. Pressure-Flow Curve of Preinducer Hydraulic Turbine in Water	24
14. Preinducer Cross Section	25
15. Test System Schematic	34
16. Model Logic for Inducer-Pump Test System	37
17. Preinducer Heat Capacity Characteristic	38
18. Preinducer Torque Capacity Characteristic	39
19. Preinducer Cavitation Correction	40
20. Preinducer (H_2O) Cavitation Correction Parameter	41
21. Hydraulic Turbine Torque Map	42
22. Hydraulic Turbine Flow Characteristic	43
23. Main Pump Head Capacity Characteristic	44
24. Main Pump Torque Capacity Characteristic	45
25. Main Pump, Cavitation Correction	46
26. Main Pump Cavitation Correction Parameter	47
27. Main Pump Inlet Compliance	48
28. Inducer and Main Pump Speed, Closed-Coupled Configuration	57
29. Inducer Pump Pressures, Close-Coupled Configuration	58
30. Inducer Pump Flowrate, Close-Coupled Configuration	59

31.	Inducer and Main Pump Speed, Remote-Coupled Configuration	60
32.	Pump Inlet Pressures, Remote-Coupled Configuration	61
33.	Inducer Pump Flowrate, Remote-Coupled Configuration	62
34.	Close-Coupled Reference Start	65
35.	Remote-Coupled Reference Start	66
36.	Close-Coupled, Two-Stage Turbine	68
37.	Remote-Coupled Two-Stage Turbine	69
38.	Close-Coupled Low Moment of Inertia	71
39.	Remote-Coupled Low Moment of Inertia	72
40.	Close-Coupled High Moment of Inertia	73
41.	Remote-Coupled High Moment of Inertia	74
42.	Remote-Coupled Low Coupling Line Fluid Inertia	75
43.	Close-Coupled Low Turbine Feed Line Resistance	76
44.	Remote-Coupled Low Turbine Feed Line Resistance	77
45.	Close-Coupled High Turbine Feed Line Resistance	78
46.	Remote-Coupled High Turbine Feed Line Resistance	79
47.	Close-Coupled Low Turbine Feed Line Fluid Inertia	80
48.	Remote-Coupled Low Turbine Feed Line Fluid Inertia	81
49.	Close-Coupled Low-Head Inducer	83
50.	Close-Coupled Test Start to 100-Percent Q/N, 1.5-Second Speed Ramp	85
51.	Remote-Coupled Test Start to 100-Percent Q/N, 1.5-Second Speed Ramp	86
52.	Close-Coupled Test Start to 100-Percent Q/N, 2.0-Second Speed Ramp	87
53.	Remote-Coupled Test Start to 100-Percent Q/N, 2.0-Second Speed Ramp	88
54.	Close-Coupled Test Start to 100-Percent Q/N, 2.5-Second Speed Ramp	89
55.	Remote-Coupled Test Start to 100-Percent Q/N, 2.5-Second Speed Ramp	90
56.	Close-Coupled Test Start to 100-Percent Q/N, 3.0-Second Speed Ramp	91
57.	Remote-Coupled Test Start to 100-Percent Q/N, 3.0-Second Speed Ramp	92

58.	Close-Coupled Test Start to 100-Percent Q/N, 4.0-Second Speed Ramp	93
59.	Remote-Coupled Test Start to 100-Percent Q/N, 4.0-Second Speed Ramp	94
60.	Close-Coupled Test Start to 120-Percent Q/N, 2.0-Second Speed Ramp	95
61.	Remote-Coupled Test Start to 120-Percent Q/N, 2.0-Second Speed Ramp	96
62.	Close-Coupled Test Start to 120-Percent Q/N, 3.0-Second Speed Ramp	97
63.	Remote-Coupled Test Start to 120-Percent Q/N, 3.0-Second Speed Ramp	98
64.	Close-Coupled Test Start to 120-Percent Q/N, 4.0-Second Speed Ramp	99
65.	Remote-Coupled Test Start to 120-Percent Q/N, 4.0-Second Speed Ramp	100
66.	Remote-Coupled Test Throttling, 1.0-Second Deceleration, 0.5-Second Acceleration	101
67.	Close-Coupled Test Throttling, 2.0-Second Deceleration, 1.0-Second Acceleration	102
68.	Close-Coupled Test Throttling, 2.0-Second Deceleration, 1.0-Second Acceleration	103
69.	Remote-Coupled Test Throttling, 2.0-Second Deceleration, 1.0-Second Acceleration	104
70.	Close-Coupled Test Throttling, 2.0-Second Deceleration, 1.0-Second Acceleration	105
71.	Close-Coupled Test Throttling, 3.0-Second Deceleration, 1.5-Second Acceleration	106
72.	Close-Coupled Test Throttling, 3.0-Second Deceleration, 1.5-Second Acceleration	107
73.	Remote-Coupled Test Throttling, 3.0-Second Deceleration, 1.5-Second Acceleration	108
74.	Remote-Coupled Test Throttling, 3.0-Second Deceleration, 1.5-Second Acceleration	109

75.	Close-Coupled Test Throttling, 4.0-Second Deceleration, 2.0-Second Acceleration	110
76.	Close-Coupled Test Throttling, 4.0-Second Deceleration, 2.0-Second Acceleration	111
77.	Remote-Coupled Test Throttling, 4.0-Second Deceleration, 2.0-Second Acceleration	112
78.	Remote-Coupled Test Throttling, 4.0-Second Deceleration, 2.0-Second Acceleration	115
79.	Close-Coupled Test Throttling, 5.0-Second Deceleration, 4.0-Second Acceleration	114
80.	Close-Coupled Test Throttling, 5.0-Second Deceleration, 4.0-Second Acceleration	115
81.	Remote-Coupled Test Throttling, 5.0-Second Deceleration, 4.0-Second Acceleration	116
82.	Remote-Coupled Test Throttling, 5.0-Second Deceleration, 4.0-Second Acceleration	117
83.	LH ₂ Preinducer Performance	119
84.	LH ₂ Hydraulic Turbine Performance	120
85.	LH ₂ Mark 29-F Pump Performance	121
86.	Typical J-2S Valve Sequencing and Pump Speed Buildup	122
87.	Simulated Oxidizer Engine Feed System, 25-Feet NPSH	123
88.	Simulated Oxidizer Feed System, 16-Feet NPSH	124
89.	Simulated Fuel Feed System	126

TABLES

1. System Data	52
2. Test System Operating Point	54
3. Transient Test Conditions	84

INTRODUCTION

A major objective in turbopump design is to minimize turbopump weight. This can be done best by using high rotative speeds. A second major objective is to operate reliably at low suction pressures; this is very difficult to accomplish with high-speed turbomachinery. However, the objective can be met by using a low-speed inducer upstream of the high-speed pump to generate sufficient head rise to permit the main pump to operate at all times without cavitating. The low-speed inducer can be driven in a variety of ways, one of which is by using part of the high-pressure discharge flow from the main pump to power a hydraulic turbine that drives the inducer. This research program is concerned with the theory, design, construction, and testing of such a partial-flow, hydraulic turbine-driven, low-speed inducer. Of particular interest is the ability of this inducer to perform as required during conditions of rapid pump acceleration, throttling, and shutdown. Can the transient performance of the inducer be predicted accurately? And if so, what are the variables that most affect this transient performance?

OBJECTIVE

The object of this contract is to develop a computer program that will accurately predict the transient performance of a low-speed inducer driven by a partial-flow, hydraulic turbine. The program then will be used to investigate the transient behavior of a variety of inducer-turbine combinations in a particular system and to determine the effect of selected parameter changes in the system on this transient behavior. The validity of the computer program will be verified by designing, constructing, and testing a turbine-driven inducer to determine its steady-state and transient characteristics. The test results then will be compared with the predicted results. If necessary, the mathematical model will be refined to include measured rather than assumed constants.

DESIGN OF A PARTIAL-FLOW, HYDRAULIC TURBINE-DRIVEN INDUCER

HYDRODYNAMIC DESIGN

Nomenclature

D	= diameter, inches
D _m	= mean diameter, inches
Δ H	= head rise, feet
HP	= horsepower
N	= rotational speed, rpm
N _{ss}	= suction specific speed, $N_{ss} = N \sqrt{Q}/(\text{NPSH})^{3/4}$
NPSH	= net positive suction head, feet
Δ P	= pressure rise, lb/sq in.
Q	= volume flow, gal/min
W	= weight flow, lb/sec

Design Points for LO₂ and Water

The contract specified that, at the design point, the inducer NPSH should be 8 feet, in water, and that its characteristics were to be compatible with those of the J-2 oxidizer pump, which was to serve as the high-pressure pump. A J-2 fuel pump inducer design modified to a larger scale was to be used for the preinducer design. These basic "ground rules" did not fix the size or the speed of the unit. Calculations were made on a variety of sizes, with both NPSH and facility limitations being considered. The calculations indicated that the inlet diameter of the inducer should be about 10 inches. Accordingly, a standard-size pipe was selected; the pipe was schedule 40 stainless with an OD of 10.750 inches and an ID of 10.020 inches.

The optimum flow coefficient of the J-2 fuel pump inducer is 0.07, and the inlet diameter of the pipe is 8.015 inches. It was desired to have the same value of Q/ND^3 for the modified inducer. For the J-2:

$$\phi = 0.2292 \ Q/N$$

$$\frac{Q}{ND^3} = \frac{\phi}{0.2292D^3} = \frac{0.07}{(0.2292)(8.015)^3} = \frac{1}{1685.88192}$$

For the preinducer in water:

$$D = 10.020 \text{ inches; NPSH} = 8 \text{ feet; } N_{ss} = 40,000 \text{ (44,250 from test data)}$$

$$(NPSH)^{3/4} = (8)^{3/4} = 4.75682847$$

$$N\sqrt{Q} = (40,000)(4.75682847) = 190,273.1388$$

$$\frac{Q}{ND^3} = \frac{Q\sqrt{Q}}{N\sqrt{Q} D^3} = \frac{Q\sqrt{Q}}{(190,273.1388)(10.020)^3} = \frac{1}{1685.88192}$$

$$Q\sqrt{Q} = 113,541.2036; Q = 2344.79; N = 3929.40$$

The inducer head was obtained from a curve of the test data, so the complete values for the preinducer design point in water are:

$$Q = 2345 \text{ gpm} \qquad \Delta H = 171 \text{ feet}$$

$$N = 3930 \text{ rpm} \qquad \Delta P = 74.2 \text{ psi}$$

$$\phi = 0.07 \qquad HP = 135$$

$$N_{ss} = 40,000 \qquad W = 326 \text{ lb/sec}$$

$$NPSH = 8 \text{ feet}$$

The ratio of the pipe size is $R = 10.020/8.015 = 1.25$. So every dimension of the scaled-up inducer is 1.25 times that of the J-2 fuel pump inducer.

Although the design point of the preinducer provided some indication of the flow through the high-pressure pump (inducer flow plus recirculation flow), it did not fix the head and speed of the pump. These variables were open to arbitrary selection. It was decided that if the final unit successfully passed all its tests, it might, with a few modifications, be made available for an actual rocket engine test. Rocketdyne has made many studies on uprated J-2 engines, and the version on which the pre-inducer would be of most use is the 265K engine. On this engine, the LO_2 pump speed would increase by an approximate ratio of 265:200. The NPSH, therefore, would increase by the square of this ratio, or 1.756. A preinducer would be desirable if such an engine were ever tested. Calculations showed that a 265K engine would require a throughflow of 3314 gpm and a head of 3258 feet. The preinducer running on such an engine would operate at the following values:

Q	= 3314 gpm	ΔH	= 342 feet
N	= 5554 rpm	ΔH	= 168.2 psi
W	= 523 lb/sec	HP	= 434
NPSH	= 16 feet		

Under these conditions, the high-pressure pump would produce a head of 2916 feet and a flow of 4090 gpm at a speed of 10,560 rpm. At the design point in water, the corresponding head of the high-pressure pump is 1459 feet at a flow of 2893 gpm and a speed of 7471 rpm.

Inducer Guide Vanes

The inducer imparts a large amount of whirl to the fluid so that the guide vanes must turn the fluid through an angle of 59.6 degrees to remove all the rotation. It was decided that the best way to accomplish this was to use a scaled-up model of the stator following the J-2 fuel pump inducer (Fig. 14, page 25). This row of 19 airfoils removes 35.6 degrees of rotation and converts most of the velocity head into static pressure. The remaining 24 degrees of rotation is removed by a second

cascade containing 19 double-circular-arc blades, each with a chord of 4 inches and a maximum thickness of 0.4 inch. Each vane has 5 holes of 1/4-inch diameter for the passage of the return flow to the turbine. The total area of these holes is 4.6633 sq in. and the flow through them is 549 gpm with a resultant velocity of 37.7 ft/sec and a velocity head of 22 feet.

The 19 blade stator following the J-2 fuel pump inducer was carefully designed to avoid cavitation; test results have shown that the inducer cavitates first.

Hydraulic Turbine Design

Preliminary calculations were made on several types of turbines. These included a partial admission turbine driving a shrouded inducer through the shroud and a full-admission turbine driving the inducer through a shaft. A three-stage, full-admission turbine was the most promising. In 1966, under Contract Nonr 4507(00) for the Office of Naval Research, Dr. O. E. Balje' issued a Rocketdyne report (R-6805) that presented the results of a study program for the prediction of turbine performance. In the Performance Diagrams section of this report is a figure giving the optimum performance of full-admission axial-flow turbines. This diagram is shown reproduced in Fig. 1. To put the values into the same units as used by Dr. Balje' we have for the LOX conditions

$$D = 5.816/12 = 0.48467 \text{ feet}; Q = 122.30/70.79 = 1.727645 \text{ cfs}$$

$$\sqrt{Q} = 1.31440; N = 5554.31 \text{ rpm}$$

$$Had^{1/4} = (805.17)^{1/4} = (28.37552)^{1/2} = 5.326868$$

$$Had^{3/4} = 151.15265$$

$$D_s = \frac{(0.48467)(5.326868)}{1.3144} = 1.9642$$

$$N_s = \frac{(5554.31)(1.3144)}{151.15265} = 48.30$$

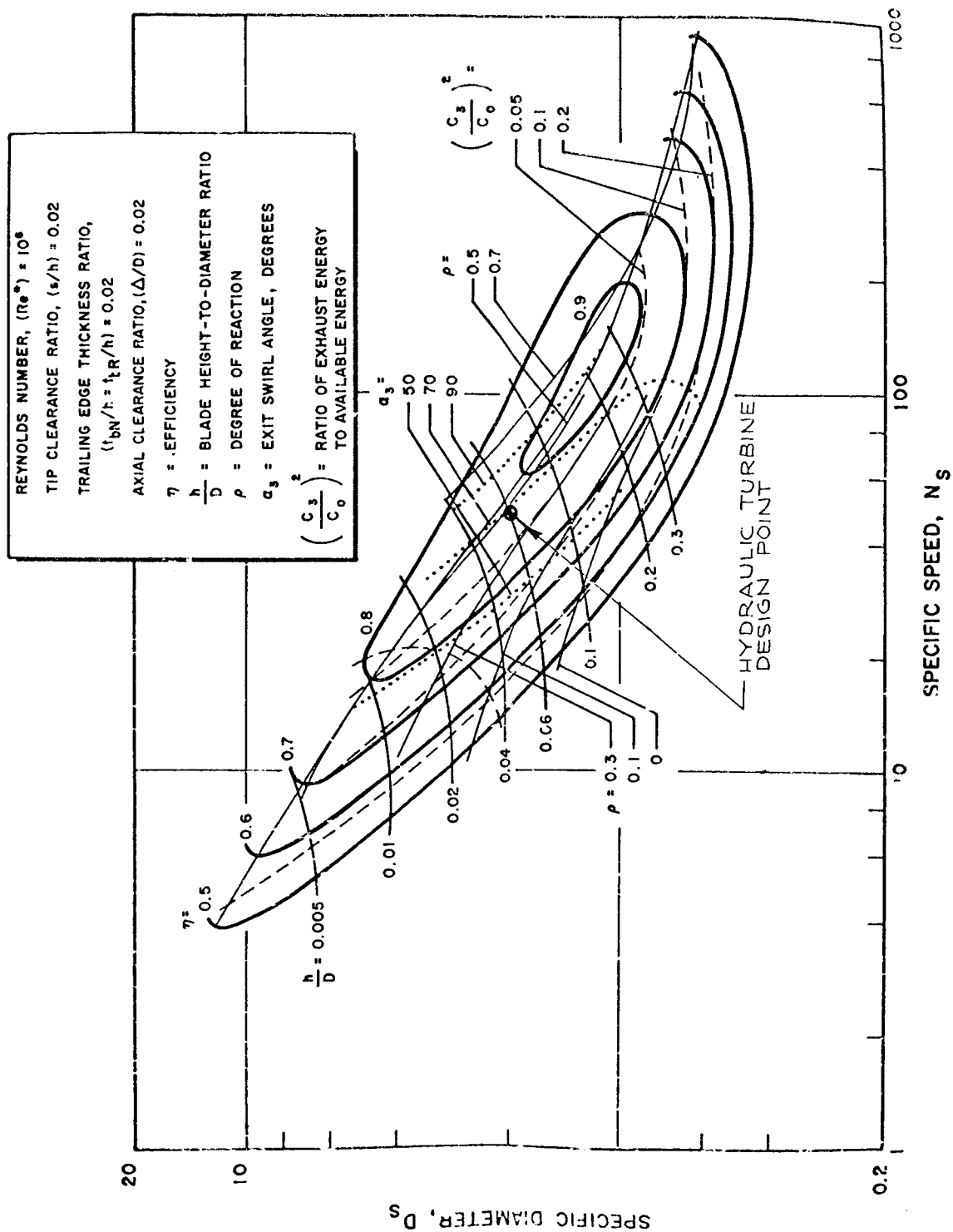


Figure 1. Optimum Efficiency of a Full-Admission Turbine

On this map is shown the operating point of the three-stage hydraulic turbine with a predicted efficiency of over 85 percent. A partial-admission turbine would have an efficiency of approximately half this value and would, thus, require twice the recirculated flow. Additional advantages of the full-admission turbine are:

1. A more easily maintained tip clearance
2. A better dynamically balanced unit
3. A smaller rotating diameter with little or no increase in unit length
4. An unshrouded inducer that is easier to manufacture. Shrouding would change the performance of the J-2 inducer.
5. Seal diameters and speeds that are lower

In view of these advantages, it was decided to use the full-admission turbine.

A generous allowance was made for the head drop in the return line between the high-pressure pump and the turbine. This permitted the insertion of a flowmeter for measuring the return flow and a valve for controlling the speed of the turbine. The remaining head was assumed to drop uniformly across the three stages. This gave a head drop across each stage of 403 feet in water with an Euler head of 325 feet. The resultant Euler efficiency was approximately 80 percent. The resultant turbine flow to provide the inducer design horsepower was 549 gpm. Figure 2 shows the velocity diagram for the three-stage turbine. Figures 3 through 6 show the shapes of the nozzles and rotors as defined by the turbine designer.

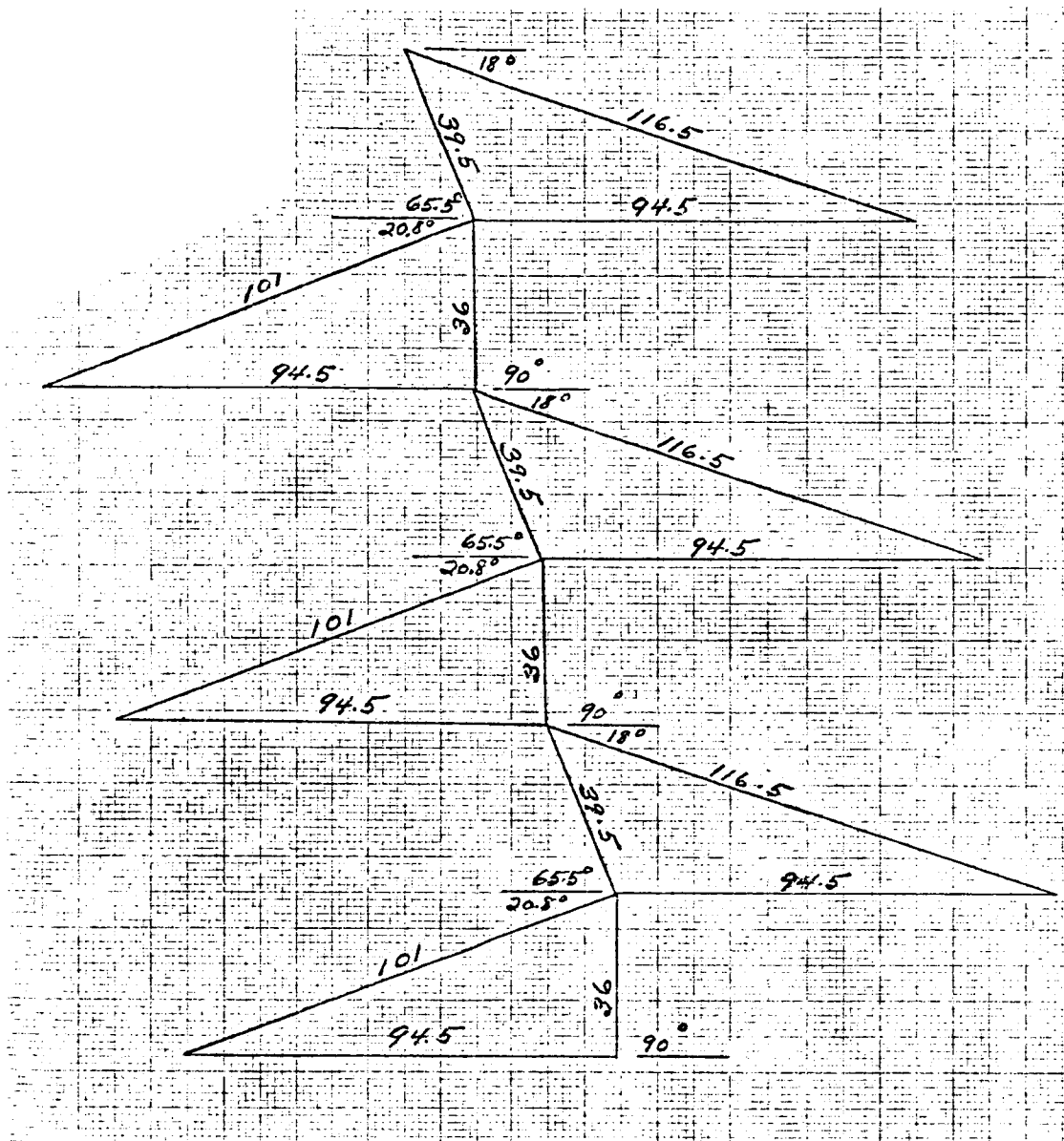


Figure 2. Preinducer Hydraulic Turbine (H_2O) Velocity Diagram

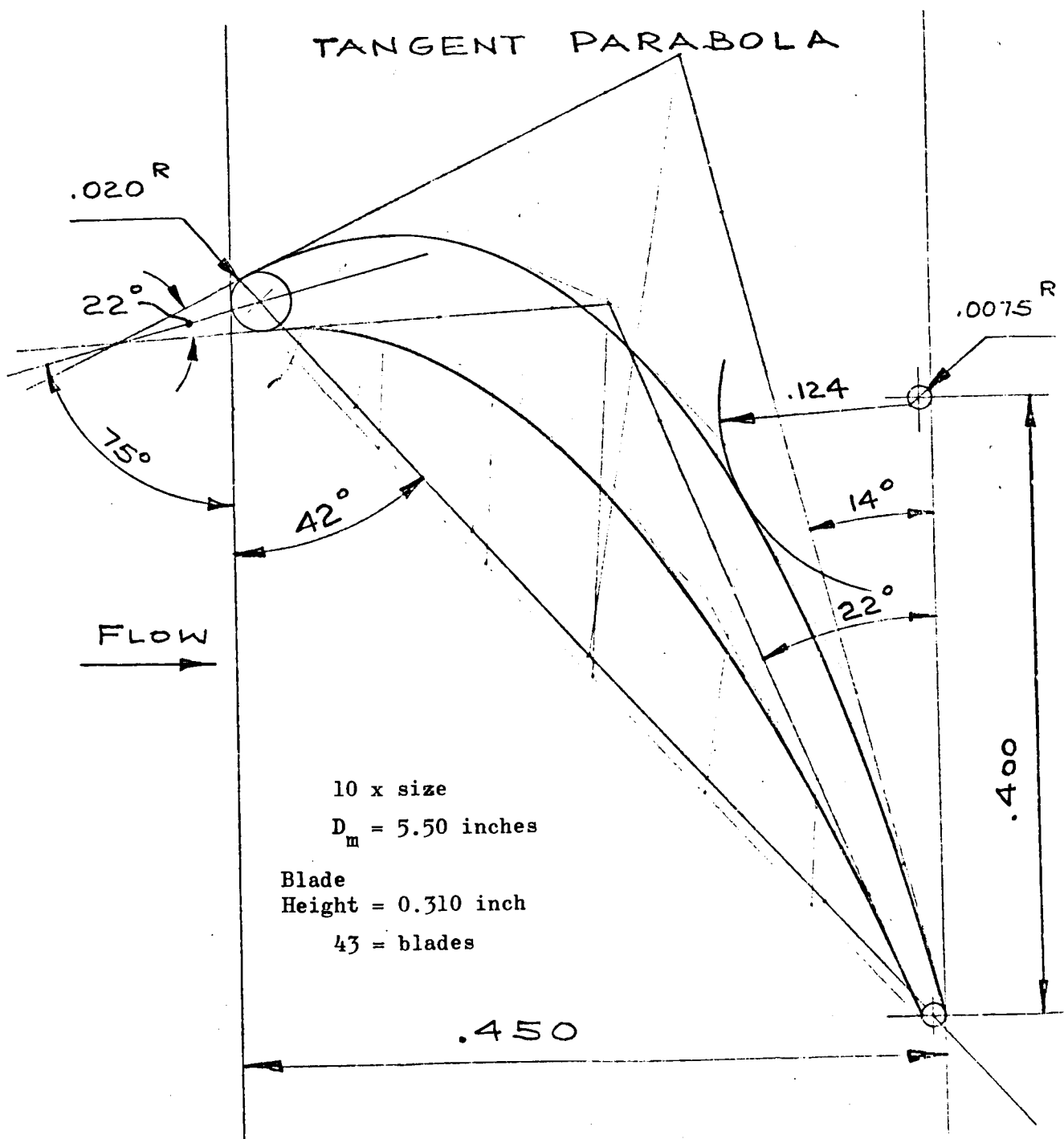


Figure 3. Preinducer Turbine Nozzle

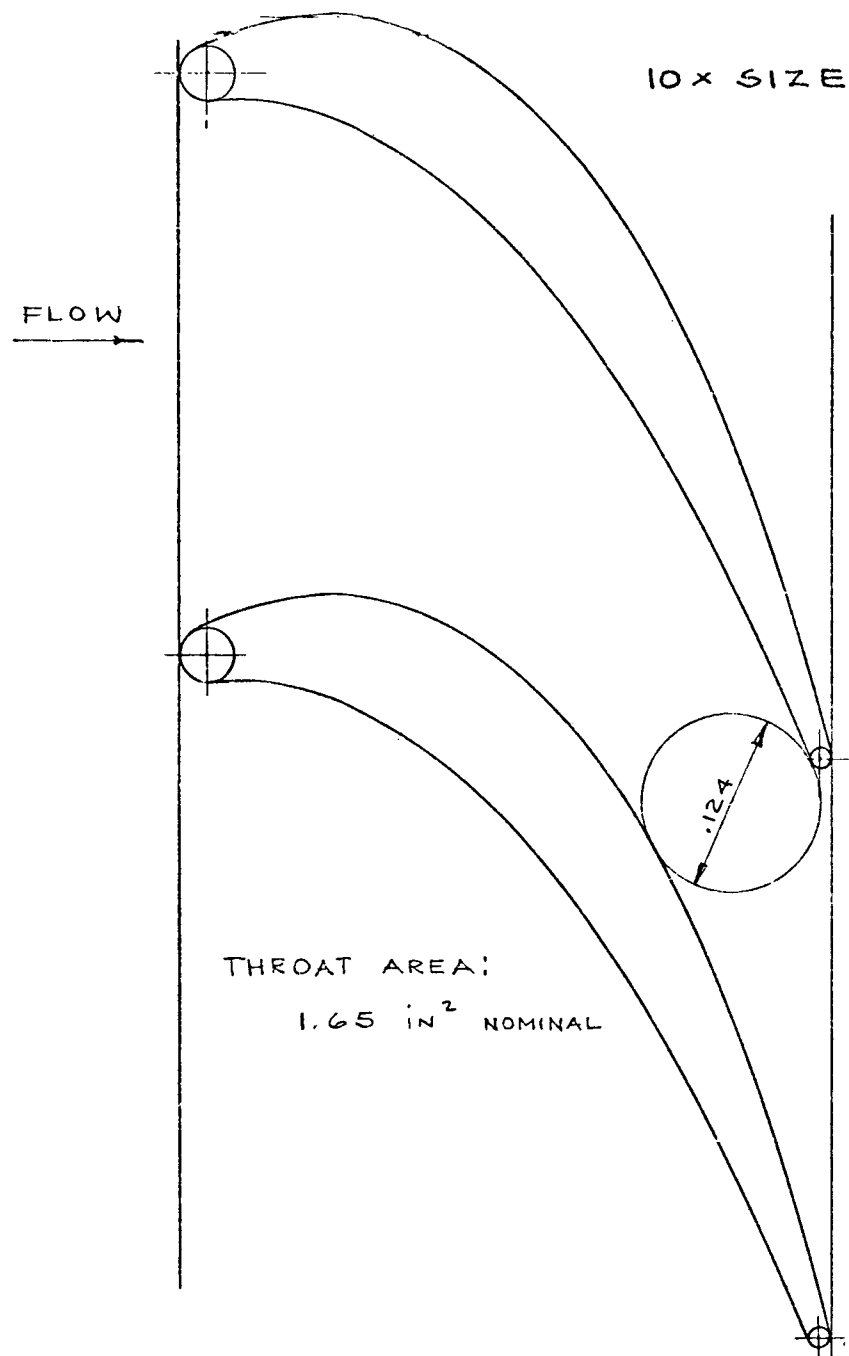
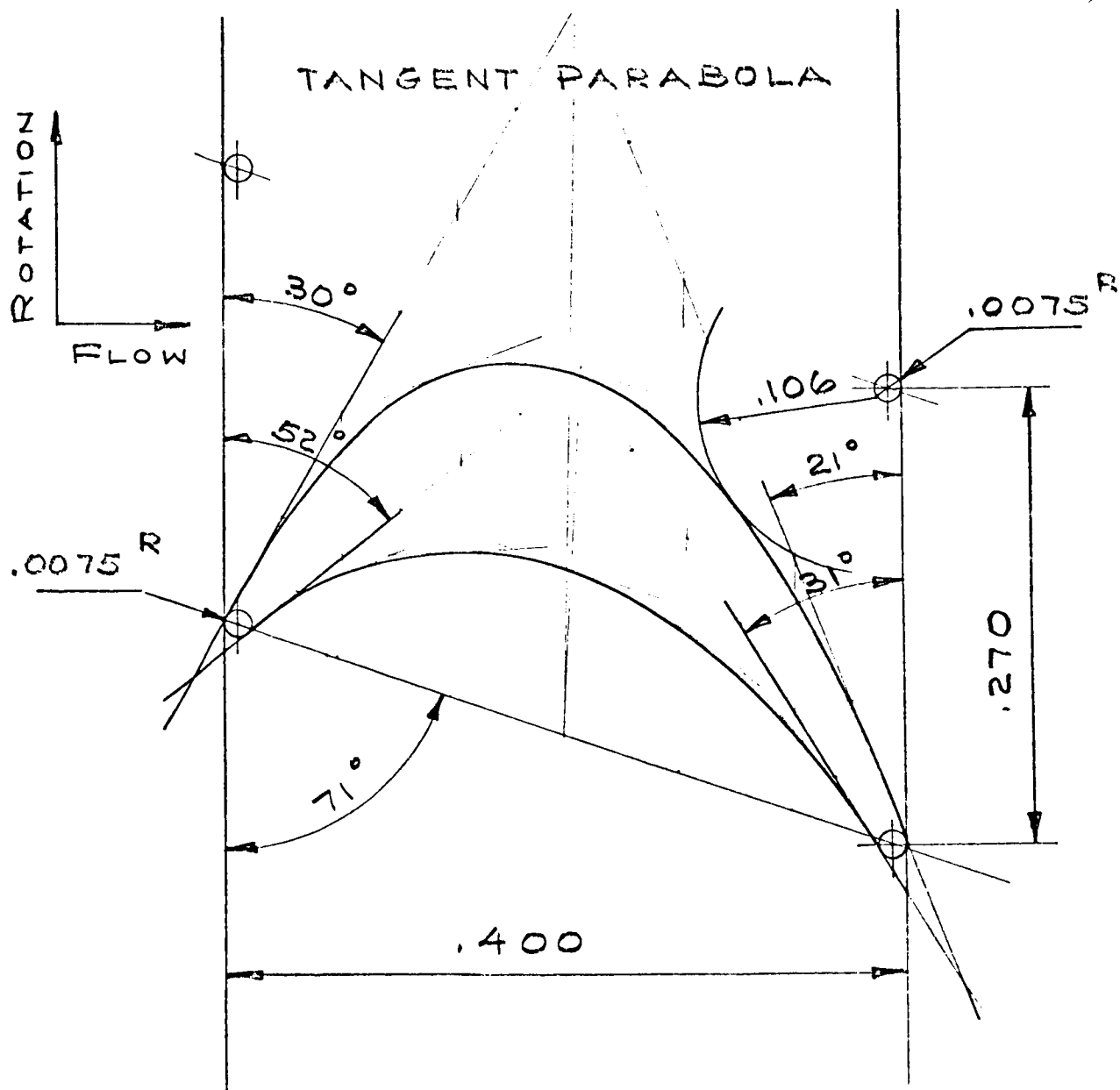


Figure 4. Preinducer Turbine Nozzle



10 x Size
 $D_m = 5.50$ inches
 Blade
 Height = 0.310 inch
 64 = blades

Figure 5. Preinducer Turbine Rotor

10 x SIZE

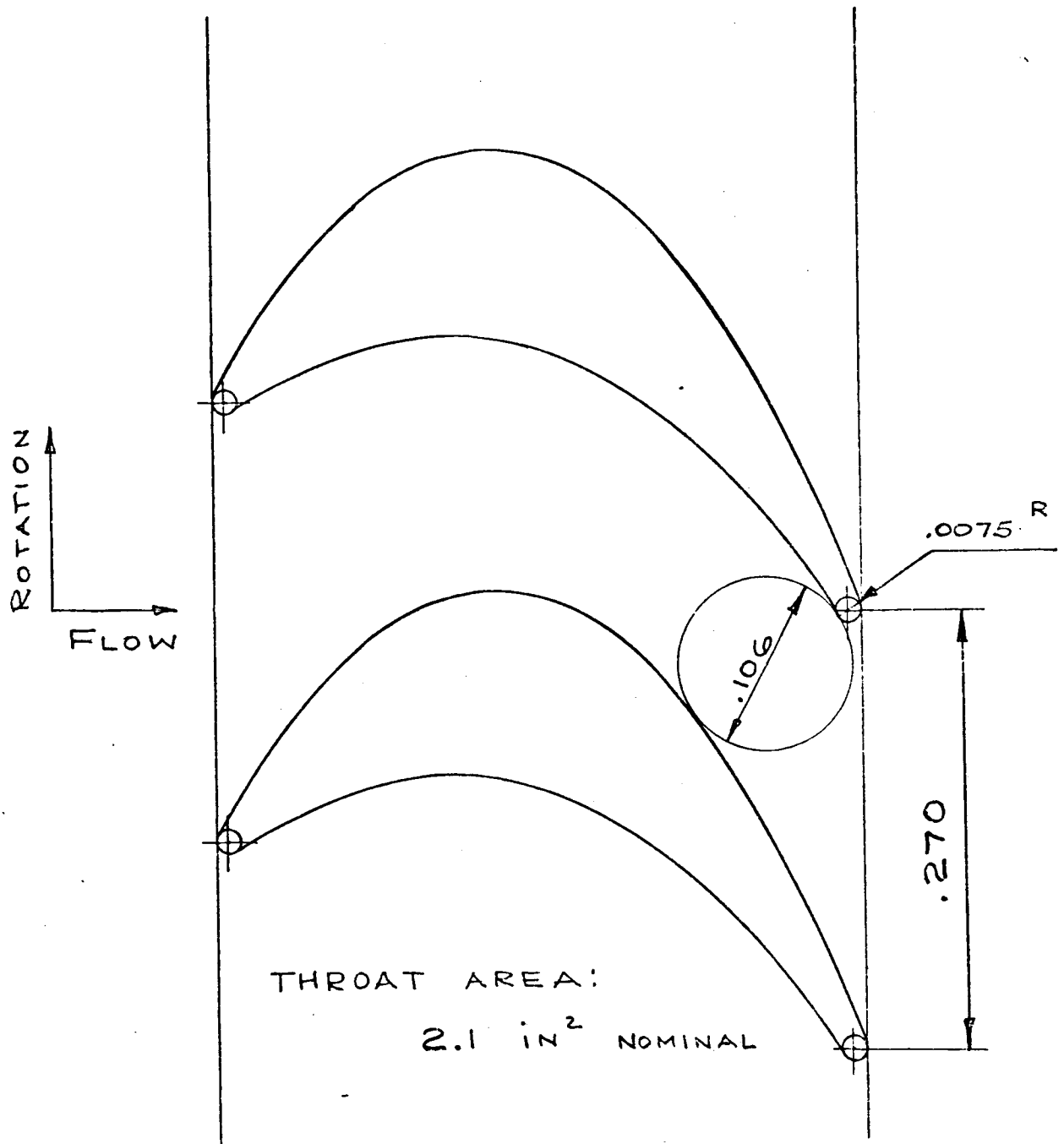


Figure 6. Preinducer Turbine Rotor

Steady-State Maps

The computer programs required steady-state performance maps of the various components as inputs. These include the head, flow, efficiency, and NPSH as a function of speed for both the inducer and the high-pressure pump and the torque, pressure drop and flow as a function of speed for the hydraulic turbine. The high-pressure pump (J-2 oxidizer pump) and the J-2 fuel pump inducer have both been tested at Rocketdyne. Figure 7 shows the nondimensional H-Q performance of the high-pressure pump while Fig. 8 and 9 give the efficiency and NPSH. The nondimensional H-Q and efficiency of the preinducer are shown in Fig. 10, and the cavitation performance is shown in Fig. 11. The H-Q map was taken from calibration tests made on J-2 fuel pumps at full speed in liquid hydrogen. The inlet head was the total head at the inlet of the pump; the discharge head was measured with a static wall tap at the discharge of the stator row that follows the inducer. To this static head was added the head corresponding to the axial component of velocity. It was assumed that the static pressure remained constant through the second row of vanes of the preinducer (the losses were equal to the velocity head recovery associated with the removal of the fluid rotation). The map, thus, includes the effect of incidence on the first row of stators and is accurate at off-design conditions. The maps for the preinducer have been modified by the affinity laws to account for the fact that the inducer is 1.25 times as large as the J-2 fuel pump inducer.

It was necessary to calculate the turbine map because no data were available. The calculated map was based on the following assumptions:

1. The turbine is of the full-admission, repeating-stage type.
2. The flow is two-dimensional and the design is fixed by a velocity diagram at only one radius.
3. The flow is incompressible.

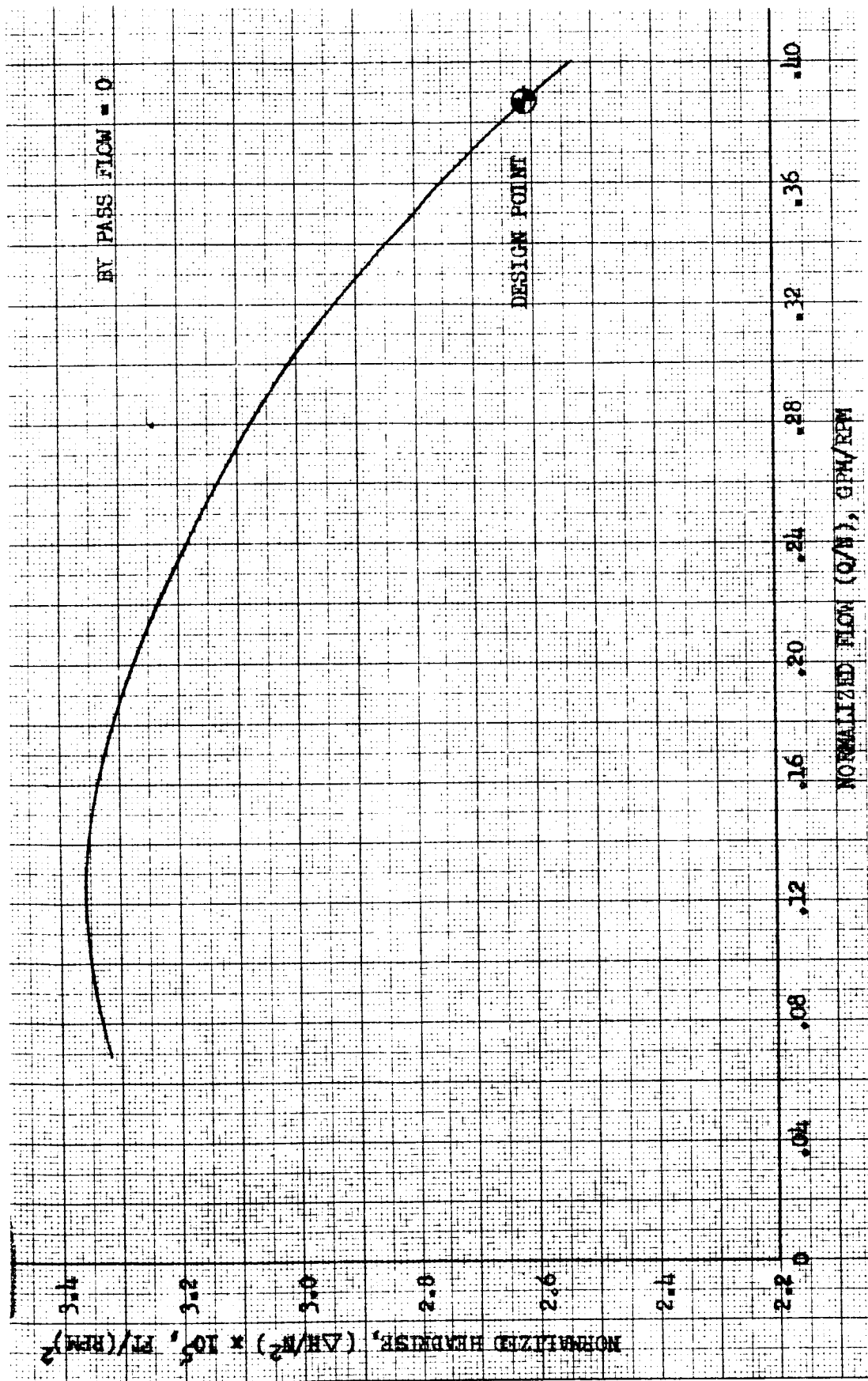


Figure 7. J-2 Oxidizer Pump Performance

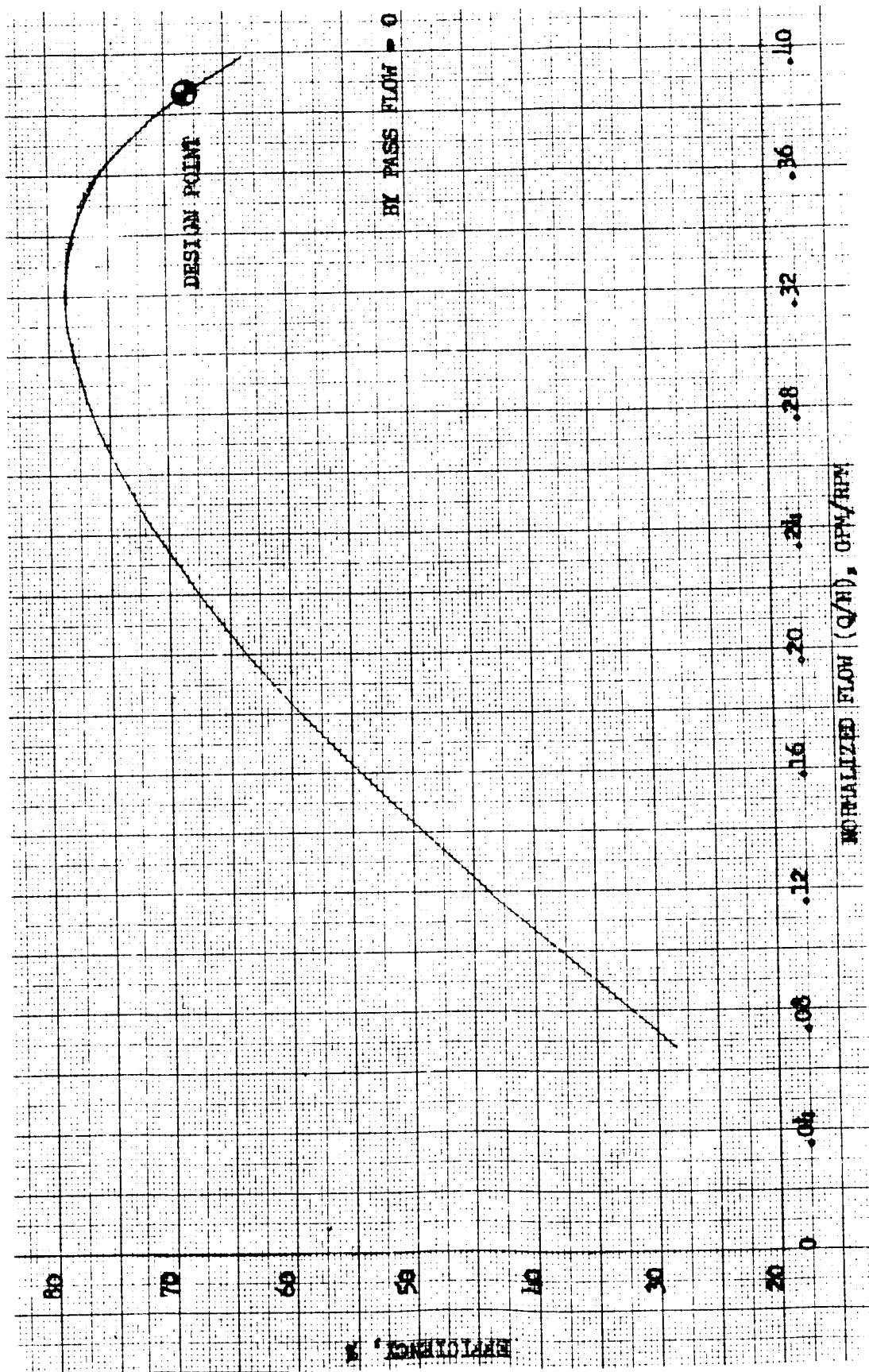


Figure 8. J-2 Oxidizer Pump Performance

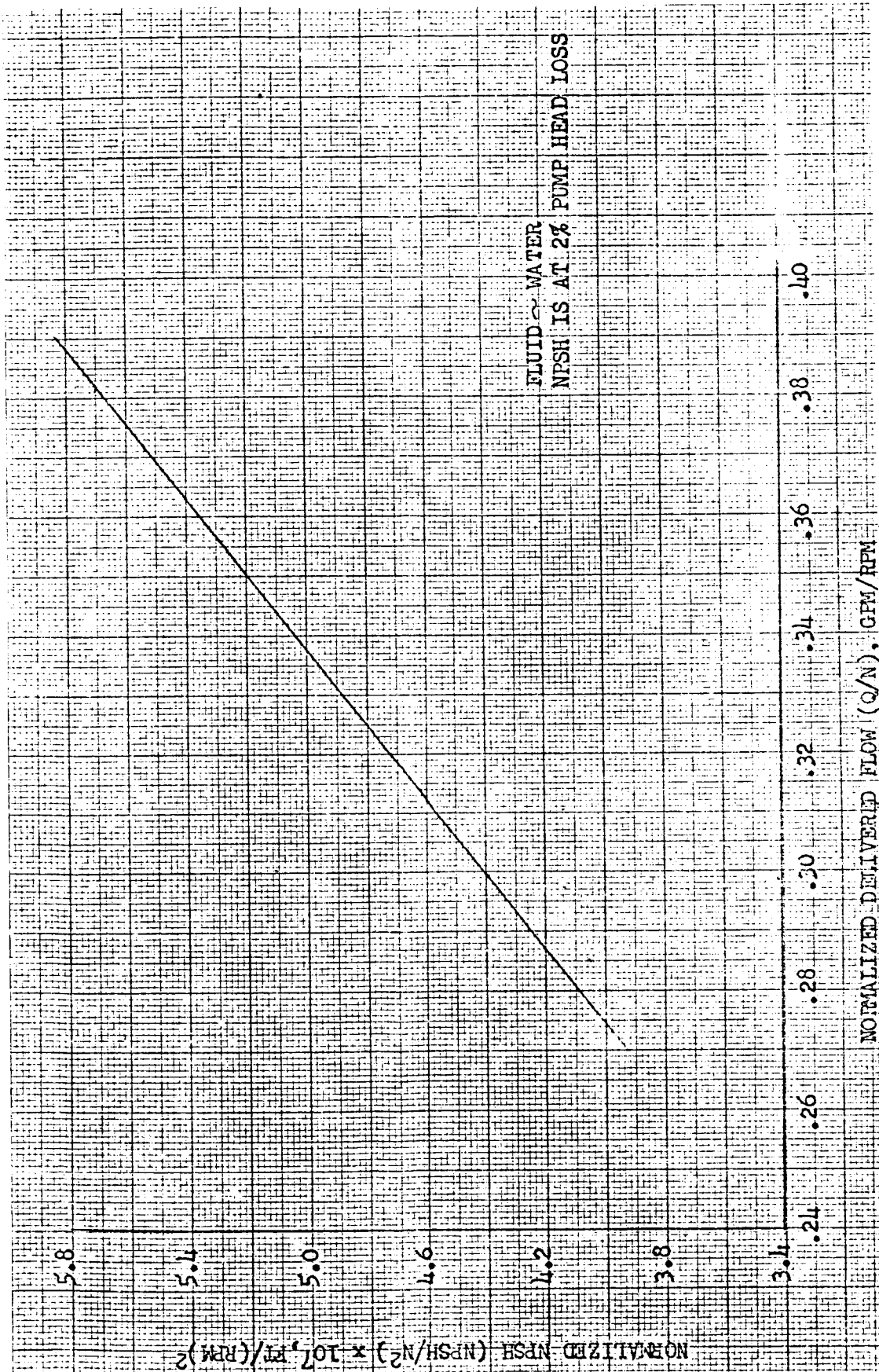


Figure 9. J-2 Oxidizer Pump Suction Performance

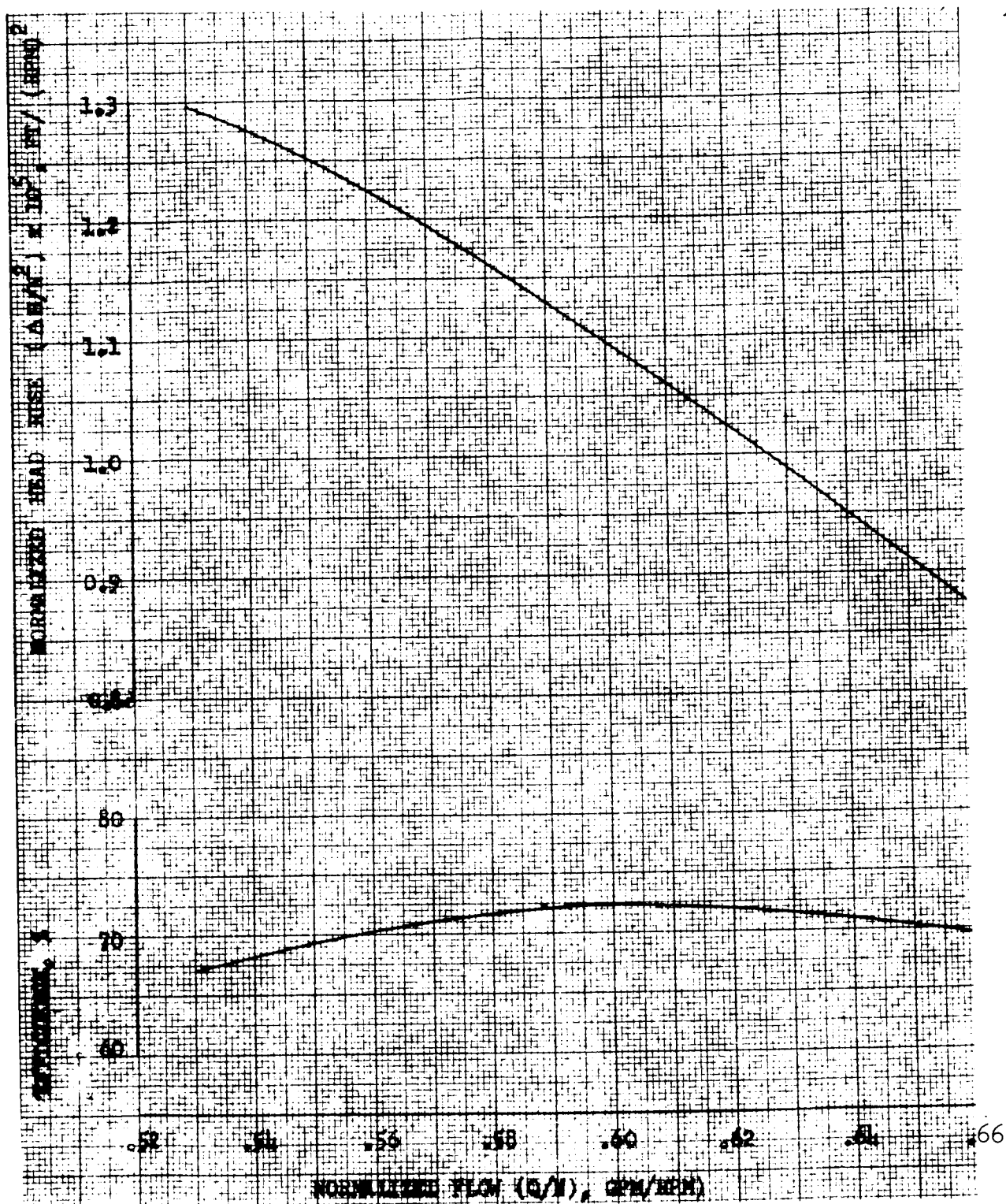


Figure 10. J-2 Oxidizer Preinducer Predicted Performance

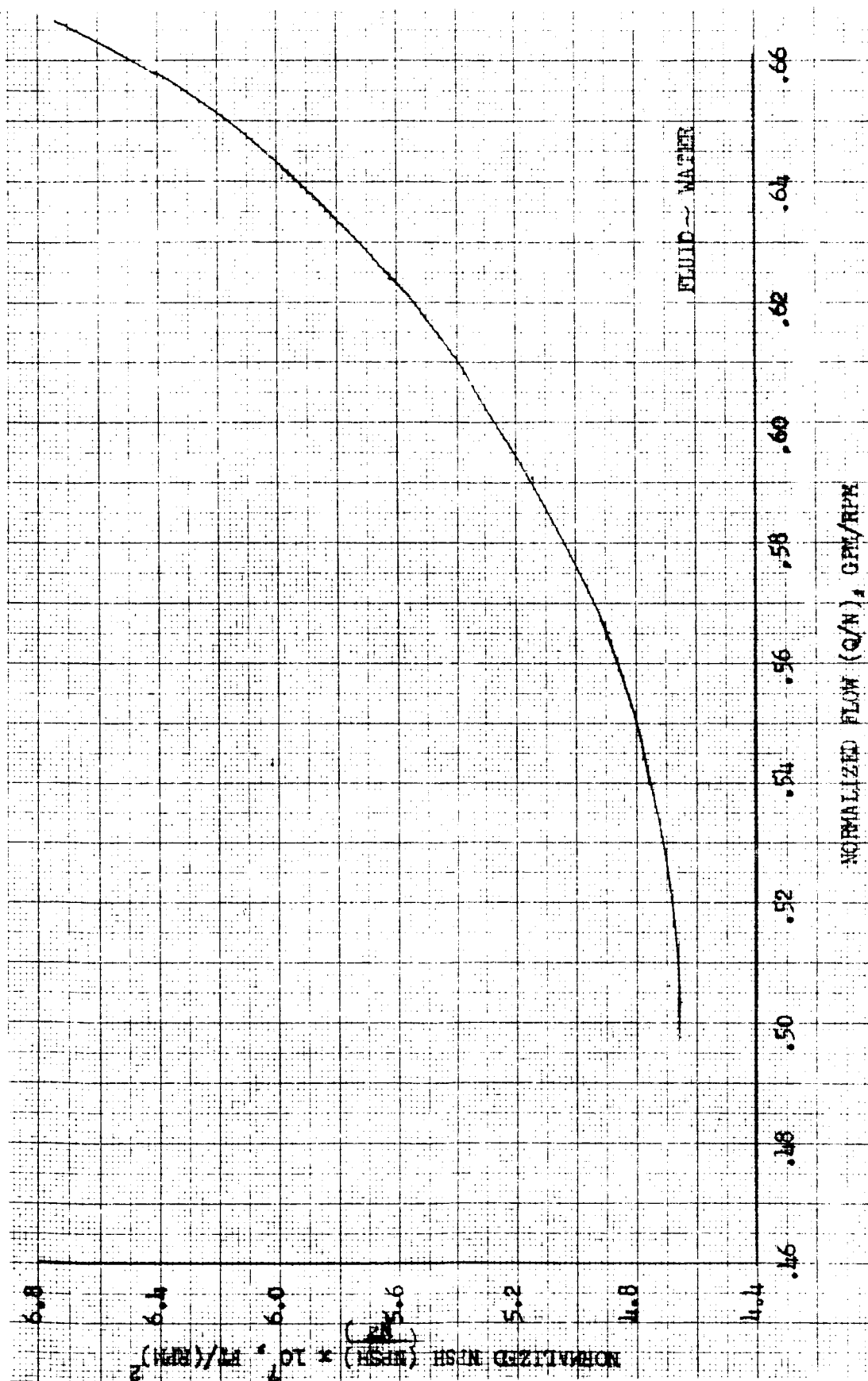


Figure 11. J-2 Oxidizer Preinducer Predicted Suction Performance

4. The nozzle and rotor discharge angles as determined by the basic velocity diagram at the design point are attained by a properly designed set of blades; at off-design points these angles remain unchanged (the deviation angle is not affected by incidence angle).
5. The efficiency at the design point is known (by calculation or estimation). This efficiency is expressed as a loss coefficient applied to the nozzle and rotor spouting velocities; this loss coefficient is held constant at all off-design points. It also is assumed that additional losses are caused by positive or negative incidence angles on both rotor and stator at off-design points. These losses are equal to the velocity head of the component normal to the design inlet velocity vector.

With these assumptions, it was a simple matter to set up the equations and write an IBM program to calculate turbine maps. Figures 12 and 13 show the maps generated by the program. The curve for the three-stage turbine is for the turbine that is being fabricated. The curves for the two- and four-stage turbines were made for parametric studies of the effect of the degree of turbine reaction on the transient performance of the unit. The two-stage turbine was close to being a pure impulse turbine (11.72 percent reaction); the three-stage turbine had 41.14 percent reaction, and the four-stage turbine had 55.86 percent. At first, it was assumed that all turbines had the same axial velocity at the design point. However, this assumption for the two-stage turbine produced too flat an angle leaving the nozzle. This angle (with the tangent) was increased to 14 degrees by increasing the axial velocity.

MECHANICAL DESIGN

A cross section of the preinducer is shown in Fig. 14, with the major hardware components identified. Flow enters the inducer from the left

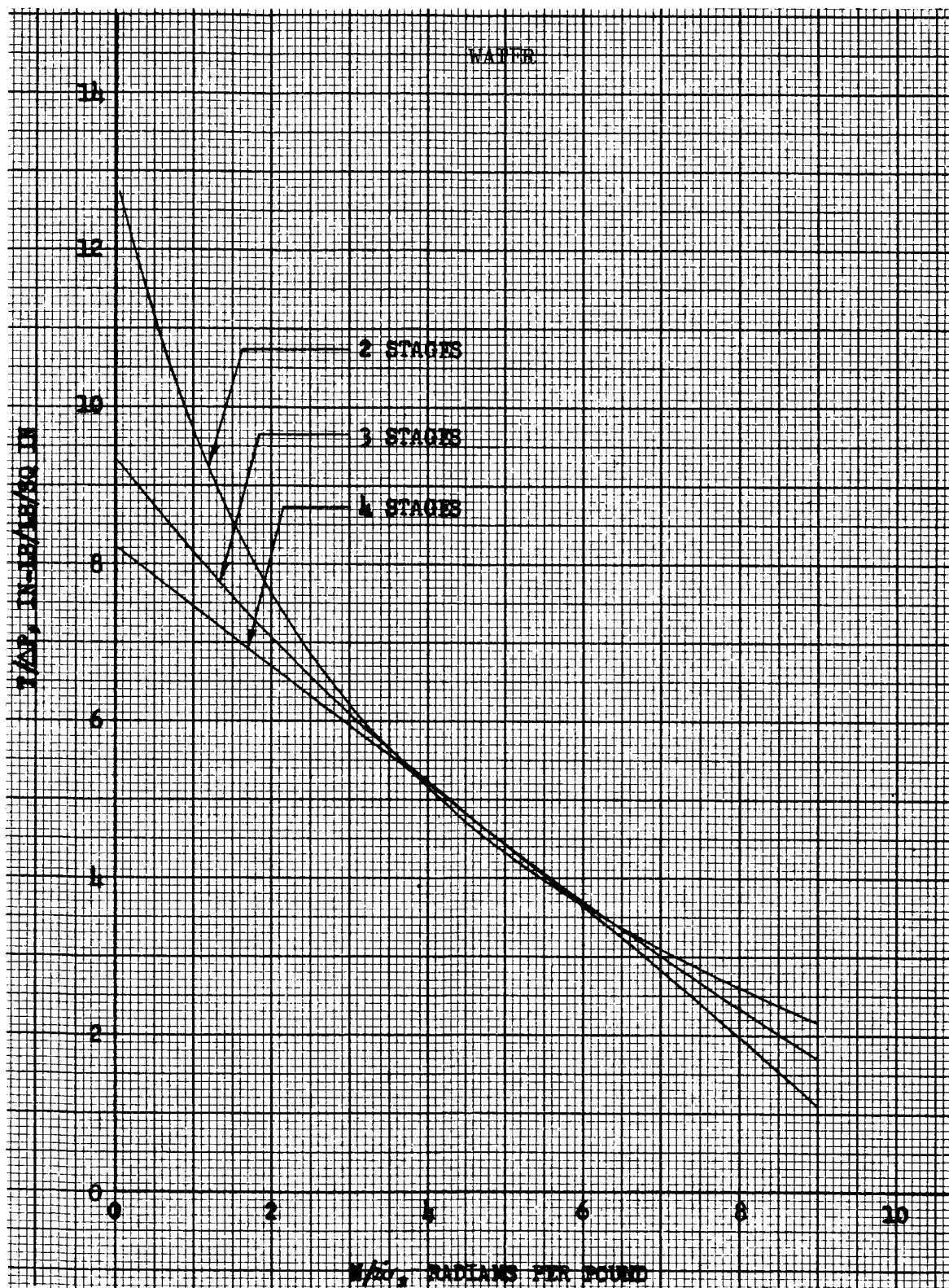


Figure 12. Torque of Preinducer Hydraulic Turbine in Water

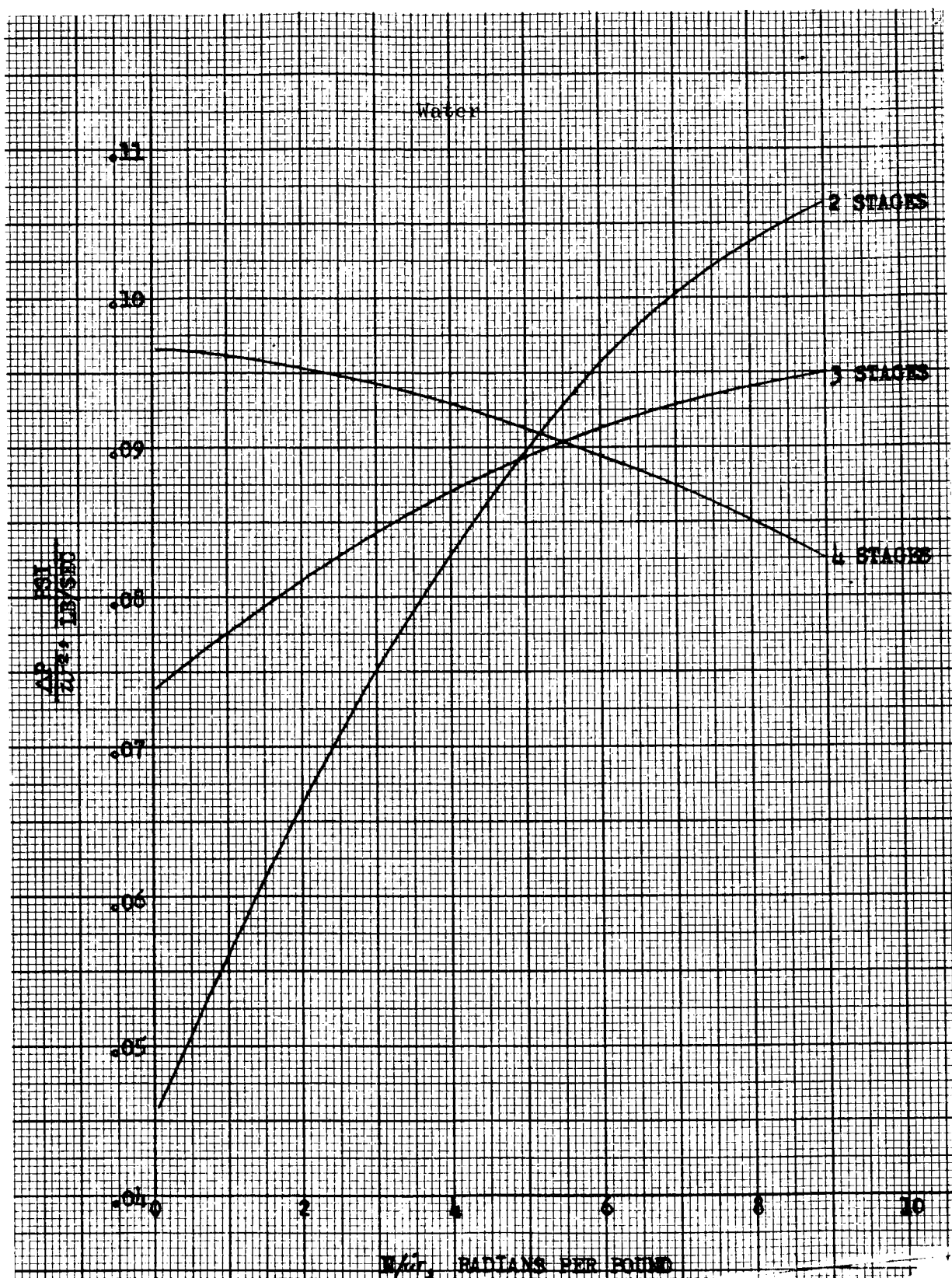


Figure 13. Pressure-Flow Curve of Preinducer Hydraulic Turbine in Water

THRUST BALANCE
SEAL

INLET HOUSING

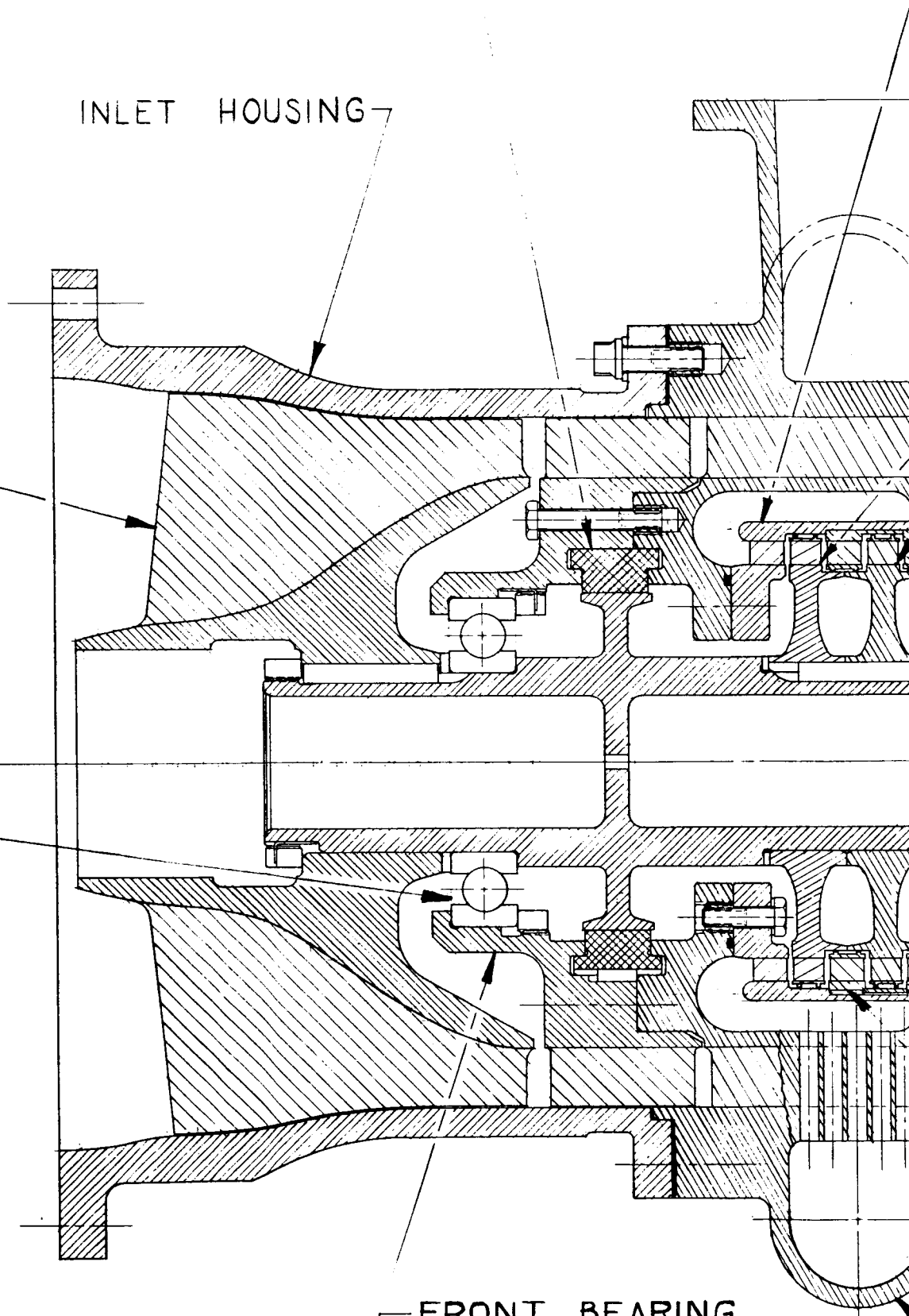
INDUCER

FRONT
BEARING

— FRONT BEARING
SUPPORT

R-7427

FOLDOUT FRAME /



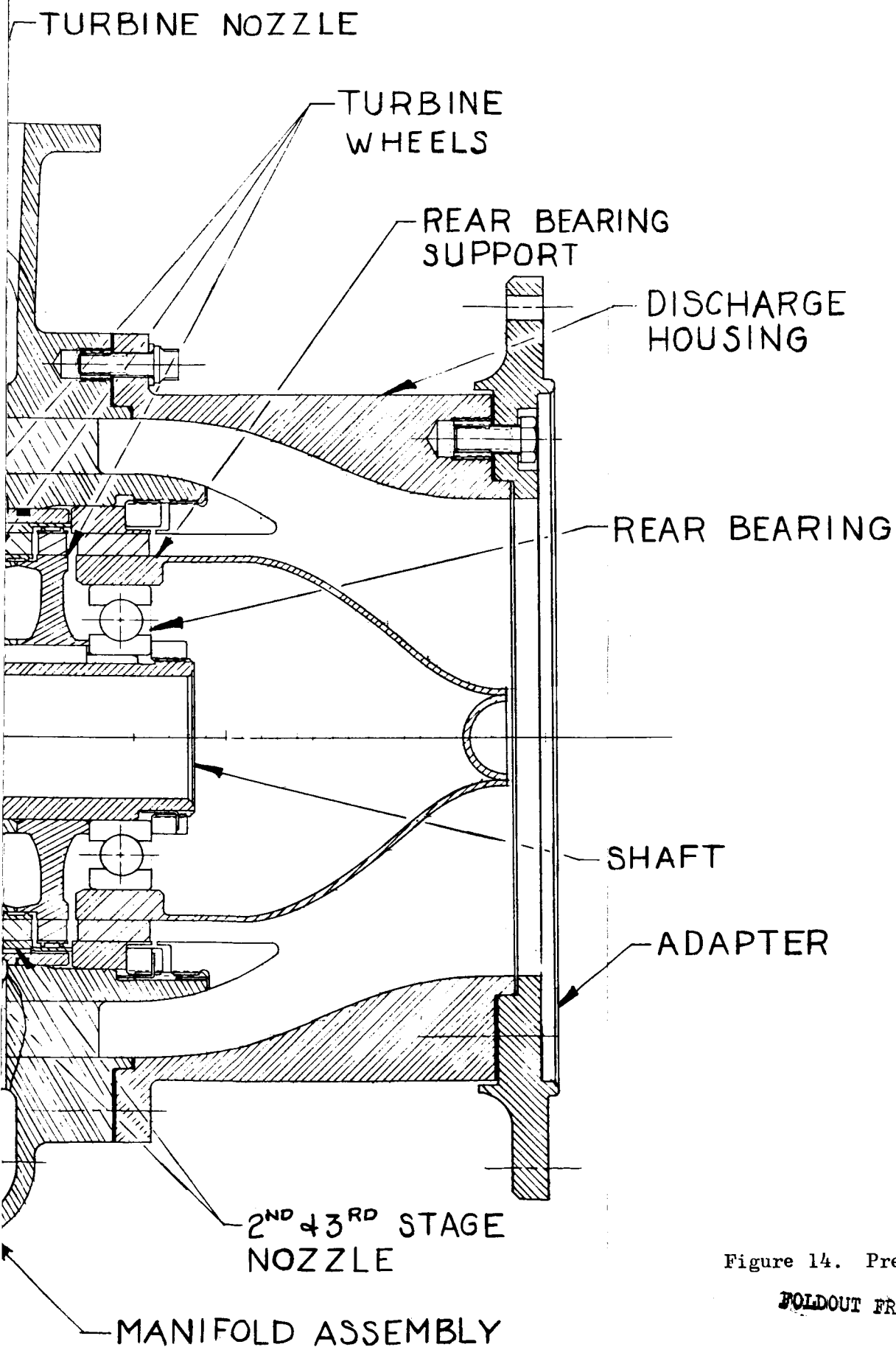


Figure 14. Preinducer Cross Section

FOLDOUT FRAME ↘

and is discharged into a two-row cascade. Most of the whirl is removed by the first row of nineteen airfoils; the remaining whirl is removed by the second row. The second-row vanes are used also as structural vanes to support the bearings and the walls of the turbine. The turbine is driven by high-pressure fluid from the discharge of the high-pressure pump. This fluid enters a circumferential manifold through a single inlet and is distributed around the outer periphery from which it passes to the inner circumferential manifold through five radial holes drilled in each of the nineteen vanes. After the fluid has expelled its energy in the turbine, it blends with the inducer discharge flow and enters the high-pressure pump.

The rotor assembly is a flightweight design so that realistic rotor dynamics will be displayed. A critical speed analysis indicates that no critical speed problems will exist throughout the operating range. If a conservative bearing spring rate of 10^5 lb/in. is assumed, the critical speed will be greater than 14,000 rpm. Other numbers pertinent to the rotating assembly are:

Weight	15.67 pounds
Center of Gravity	5.58 inches from inducer end at the hub
Moment of Inertia in Roll	92.83 lb-in. ²
Diametral Moment of Inertia	214.95 lb-in. ²

The axial thrust of the turbine is in the aft direction; it exceeds the forward thrust of the inducer. The thrust difference is compensated by a thrust balance disk which senses the inducer discharge pressure on the forward side and the turbine nozzle discharge pressure on the aft side. The diameter of the disk is such that a balance is obtained at the design point.

In contrast to the rotor assembly, the housings are heavy to simplify machining and to provide a sturdy support for the rotor.

Inlet Housing

The inlet housing converges the flow from the facility ducting to the inducer inlet OD. It is also the inducer housing and contains the speed pickup. The speed pickup is a Bently transducer located at the inducer blade leading edge OD. The inlet housing wall was left thick to minimize machining costs. As a result of this, the stress level in the housing from both operating and mounting loads is low. The inlet housing is machined from 6061-T651 aluminum alloy hand forging.

Inducer

The inducer is a scaled-up version of the J-2 fuel pump inducer. It is machined from a 7075-T73 aluminum alloy hand forging. A pilot diameter and inducer nut are used for retention to the shaft with a single key to transmit torque. The centrifugal blade loading stresses are quite low; the hydrodynamic blade loading is the largest, being approximately half of the blade design capability. The maximum possible weight has been removed from the inducer hub to keep the rotor assembly flightweight.

Front Bearing Support

The front bearing support incorporates the diffuser vanes as an integral part. It has a retention flange for the thrust balance labyrinth seal. The bearing support is bolted to the manifold assembly, and the bearing is installed in the conventional manner with a bearing shoulder, nut, and lock tab washer. It is machined from a 6061-T651 aluminum alloy hand forging.

Manifold Assembly

The manifold assembly consists of the outer manifold, the second row of diffuser vanes, and the outer shell of the turbine. The vanes, along with the two walls, are machined from solid 6061 aluminum stock, and the

five radial fluid passage holes then are drilled in each vane. The manifold inlet and the manifold ring are separately machined from 6061, then the entire assembly is welded together. This is followed by heat treat and final machining. The maximum stress in this assembly occurs at the elliptical section of the inlet. At the maximum operating pressure, this stress is half the capability of the material. The assembly will be proof pressure tested to 925 psi. The maximum stress at this pressure in the elliptical section will be approximately two-thirds the capability of the material.

Shaft

An aluminum shaft was selected over the conventional steel shaft because the stress levels in the shaft are low. The shaft is hollow and, with the aluminum material, this produces a lightweight low-inertia shaft for fast acceleration response and good rotor dynamics. The shaft is machined from a 6061 aluminum alloy bar. The thrust balance disk is machined as an integral part of the shaft. The finished shaft is heat treated to a T6 condition as per MIL-H-6088. It is hard anodized at the bearing journals and thrust balance seal surface to a thickness of 0.0010 inch. The remaining surface of the shaft is hard anodized to a thickness of 0.0002 to 0.0003 inch. The shaft threads are dry film lubricated to prevent galling.

Turbine Nozzle

The turbine nozzle is machined from 6061-T651 aluminum alloy. There are 43 vanes in the nozzle ring. A cylinder that retains the second- and third-stage nozzle ring is welded to the outer shroud of the turbine nozzle. The turbine nozzle is bolted to the manifold assembly by a flange which is machined on the inner shroud. The split lines between turbine nozzle and the manifold assembly are sealed with O-rings. The highest stress occurs as hoop compression in the welded-on cylinder. This stress is approximately one-half of the material capability.

Second and Third Stage Nozzles

The second- and third-stage nozzles are identical and interchangeable. Their flow passage is the same as that of the turbine nozzle. They are machined from 6061-T651 aluminum alloy; two lips are machined on the inner periphery of the inner shroud to form a seal and reduce fluid leakage between the stationary nozzle and the rotating wheel rim. The nozzle torque is restrained by keying each nozzle stage at the outer shroud to the cylinder of the turbine nozzle. The maximum stress in each nozzle state is in bending at the vane tips where the torque resistance is transferred from each vane into the outer shroud. The stress level in this area is less than one-half of the design capability.

Turbine Wheels

The three turbine wheels are identical except for the spacing rim. The center wheel has the spacing rim on each side, while the first- and third-stage wheels have the rim removed from the front and back side, respectively. The turbine blades are machined without an outer shroud and as an integral part of the disk. The outer shrouds are installed with a dip braze over the blade tips. Two lips are machined on the outer periphery of each shroud to form a seal and reduce fluid leakage over the wheel OD. The turbine wheels are keyed to the shaft. The nozzle-to-wheel axial clearance is set with a spacer between the first-stage wheel hub and the shaft shoulder. The wheels are held on the shaft by the rear bearing nut. The three turbine wheels are machined from 6061-T651 aluminum alloy and heat treated to a T6 condition after the dip brazing process. The highest stress occurs at the blade roots, and this stress is well within the design capability.

Rear Bearing Support

The rear bearing support is machined from 6061 aluminum alloy. The discharge cone is formed from 6061 aluminum sheet and welded to the bearing support. Fifteen vanes are used in the fluid passageway to transmit the bearing loads into the manifold assembly. These vanes are straight and radial and remove any rotation remaining in the fluid. The bearing support is held in place by a single, large-diameter retaining nut.

Discharge Housing

The discharge housing covers the flow passage from the inducer discharge diameter to the J-2 oxidizer inlet diameter. It is machined from a 6061-T651 aluminum alloy hand forging. The stress level here, as in the inlet housing, is low because the walls were left thick to minimize machining costs.

Bearings

Two ball bearings are used to support the rotor assembly, one aft of the inducer and one aft of the turbine. The two bearings used are the same bearings used in the J-2 oxidizer turbopump. 440-C steel is used for the race and ball material. The bearing cage is made of Armalon with riveted aluminum side bands. Axial retention is maintained on both the inner and outer races of the front bearing. The rear bearing is retained at the inner race only while the outer race is allowed to move axially. The front bearing is lubricated by fluid leakage through the balance disk seal. The rear bearing is lubricated with turbine discharge fluid. This fluid flows to the low pressure inlet through a controlling orifice in the center of the shaft.

Thrust Balance Seal

The thrust balance seal is incorporated into the design to counteract the axial thrust produced by the turbine. The rotating thrust balance disk portion of the seal is machined as an integral part of the shaft. The seal proper is a smooth cylindrical seal machined from Kel-F. The pressure drop across the seal produces a force on the disk opposite that of the turbine thrust.

Adapter

The preinducer discharge housing bolt circle is smaller in diameter than the J-2 oxidizer turbopump inlet flange bolt circle. The preinducer will be installed next to the turbopump, and also in a remote position upstream of the turbopump. Because of these installation locations, the adapter is incorporated to eliminate large bolt circle diameter flanges on the facility ducting and preinducer discharge. The adapter is machined from 6061-T6 aluminum alloy plate. The stresses in this part are low.

DYNAMIC PERFORMANCE MODELS

A mathematical model of the CTL-1 water test facility (including the main pump and drive mechanism, the hydraulic turbine/low-speed preinducer unit, and required feed lines) was formulated for the purpose of (1) studying the transient and low-frequency dynamic behavior of the test system, (2) determining the effect of variations in the preinducer design parameters and test system line configurations, and (3) predicting rocket engine feed system performance incorporating hydraulic turbine-driven preinducers with liquid hydrogen and liquid oxygen propellants.

The system equations and component descriptions were programmed for solution on both an analog and digital computer. The digital model provides the capability for using detailed component performance descriptions (due to larger programming capacity), a means to evaluate any model simplifications required for the analog program, and a concise program deck which can be used at other computing installations. This model was used as a cross check for the analog model and to predict preinducer operation in a simulated rocket engine.

The analog model provides the capability for determining the effect of various system variables in a short period of time. This model was used to conduct system parametric studies, and will be used for model correlation with test data.

EQUATION DEVELOPMENT

The system that was mathematically simulated was the pump test configuration as installed in the CTL-1 water test facility. This system, shown schematically in Fig. 15, consists of a water supply tank with a tube bundle resistance at the outlet, a preinducer inlet feed line, a hydraulically driven preinducer either close or remote coupled to a high-head

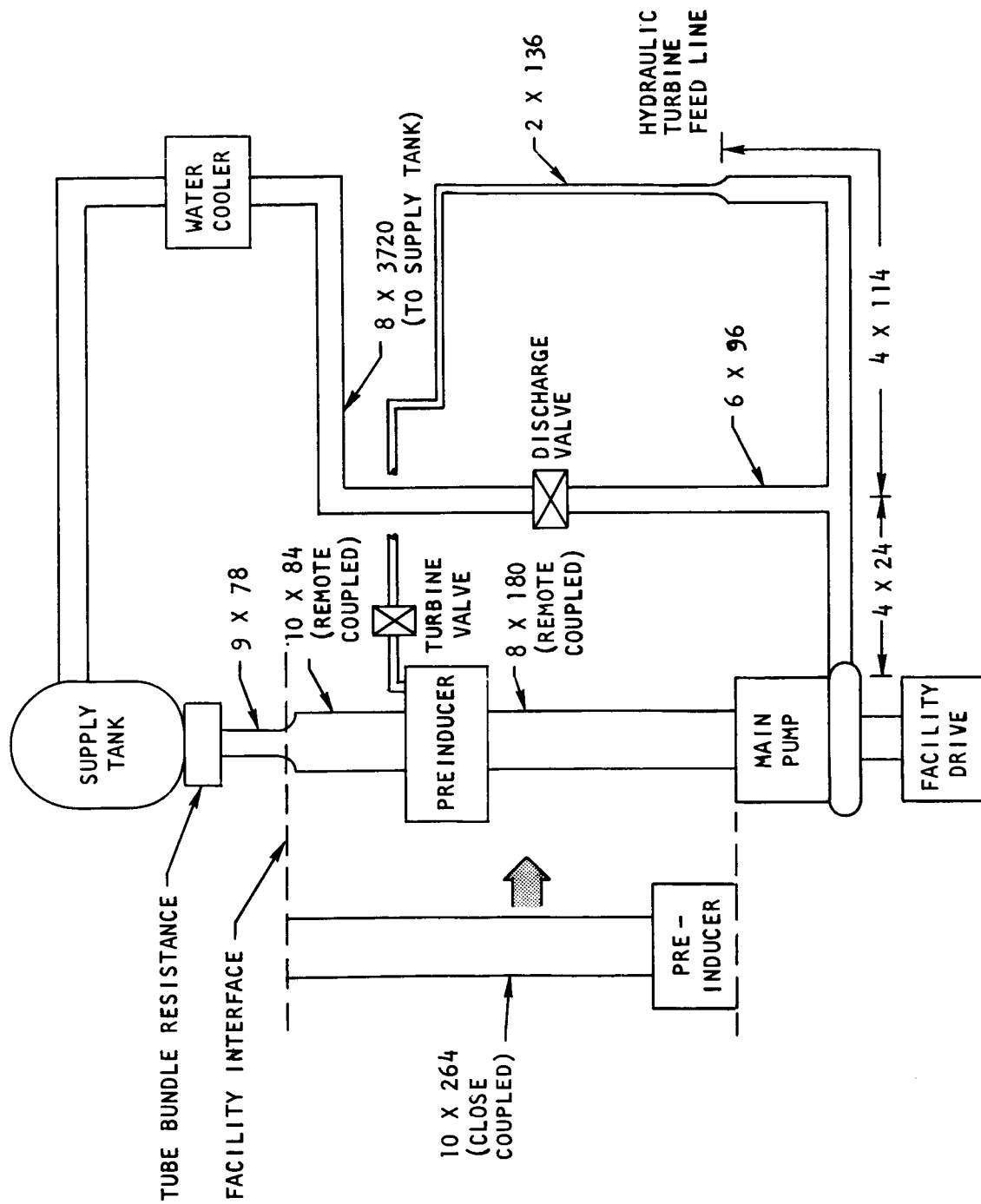


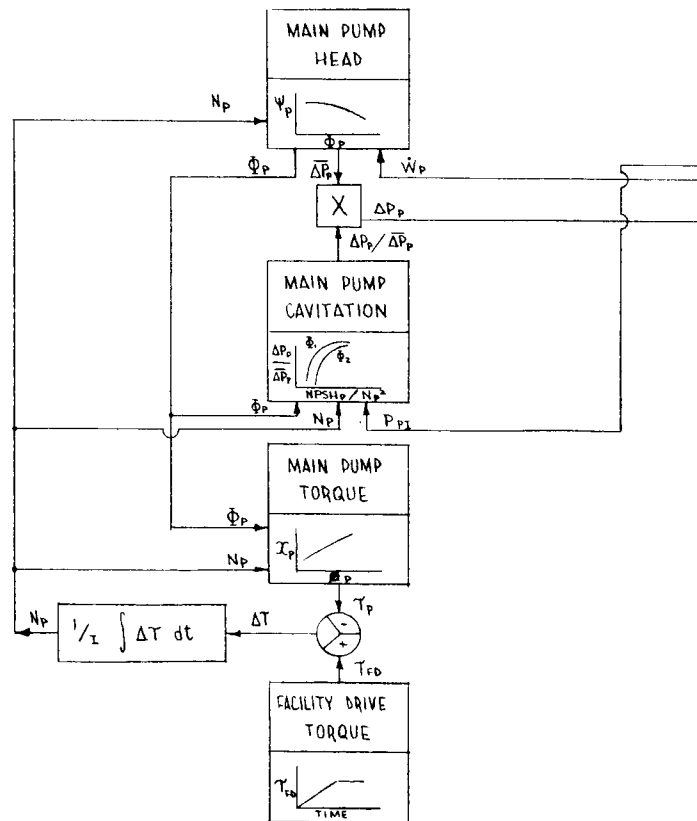
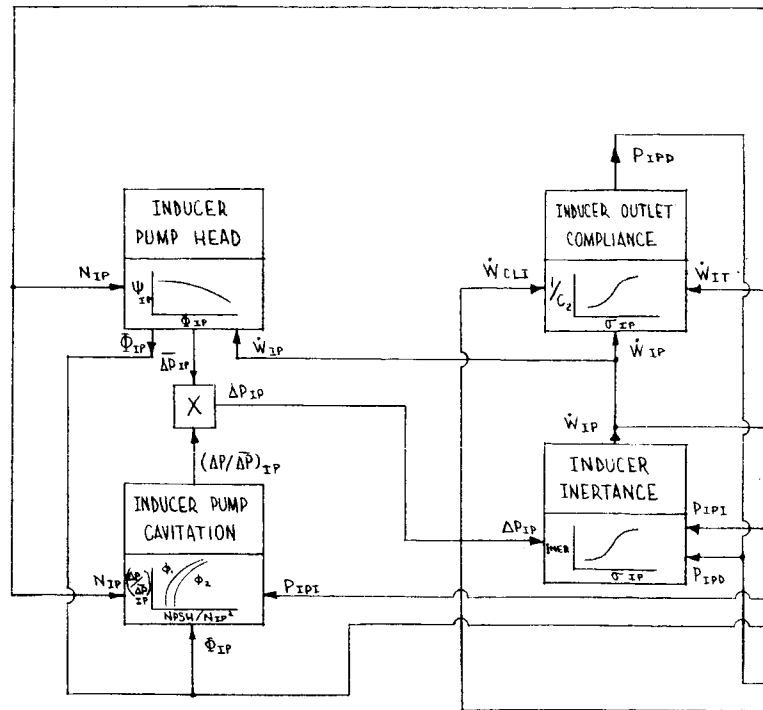
Figure 15. Test System Schematic

(main) pump, a feed line from the main pump discharge to the hydraulic turbine inlet, a return line from the main pump discharge to the supply tank, and an electric-motor drive for the main pump. With the exception of the main pump drive and tube bundle, the equations required for simulation of the test facility are applicable to an engine feed system with changes in appropriate constants. The electric drive and tube bundle are applicable only to the test facility, the electric drive being used in place of a turbine, and the tube bundle being used to reduce the inducer inlet pressure for low NPSH operation.

The logic flow chart used for developing the models is presented in Fig. 16, which shows the various components, performance curves, and information flow between elements that were considered in building the simulation. The dynamic operation of the pump, turbine, and inducer were represented by performance curves in addition to algebraic and differential equations describing their dynamic behavior. Feed system dynamics were described by distributed or lumped parameter equations, as applicable. The equations used to construct the model are presented in the appendix. Component performance curves are presented in Fig. 17 through 27.

The modeling was based on the following basic criteria and assumptions:

1. The model must be capable of responding to frequencies up to 50 cps.
2. The test fluid (water) density is constant.
3. Pressure drops are proportional to the flowrate squared.
4. Heat transfer can be neglected.
5. Preinducer cavitation dynamics can be represented by a combination of an inlet and outlet compliance separated by an inertance.



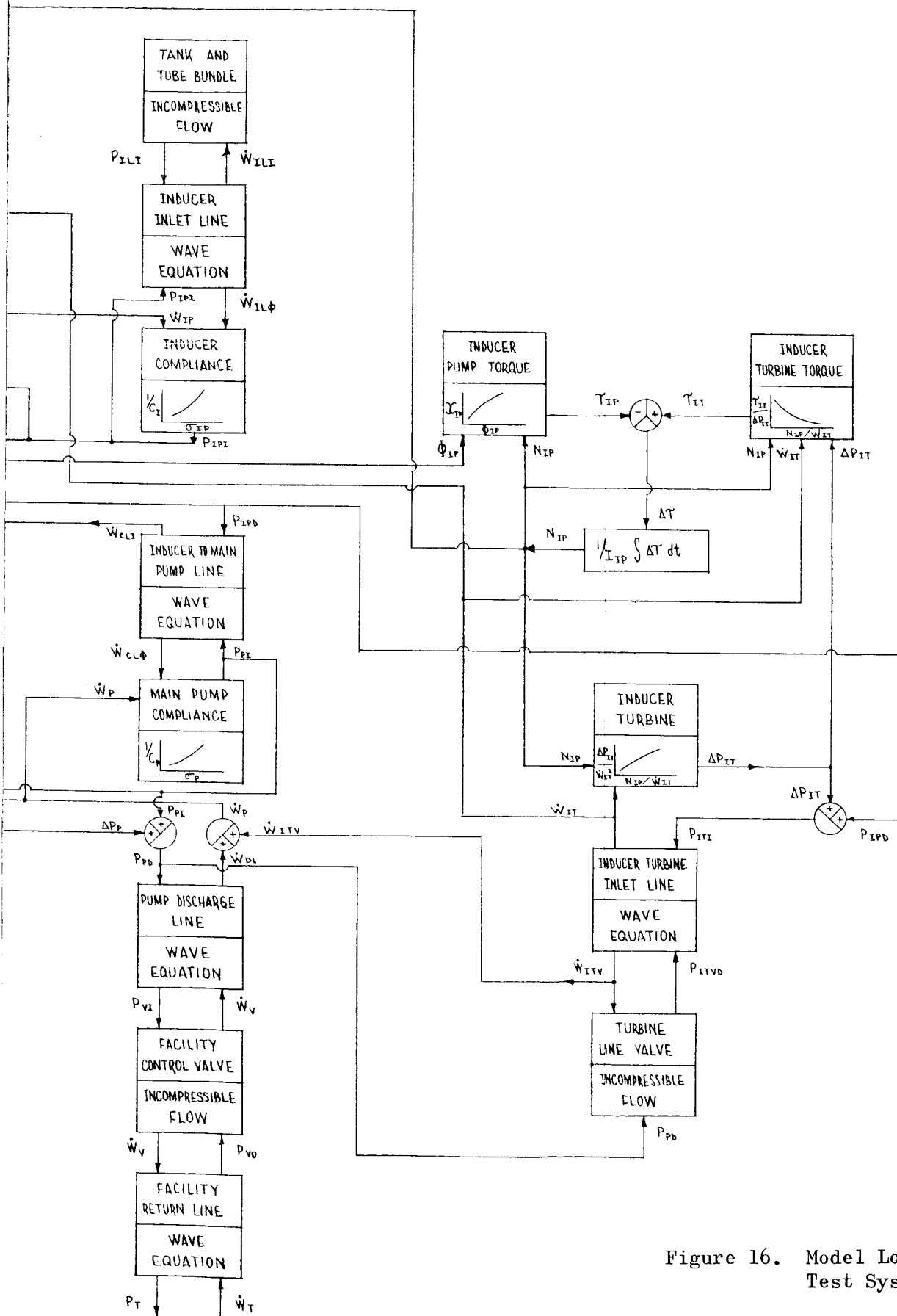


Figure 16. Model Logic for Inducer-Pump Test System

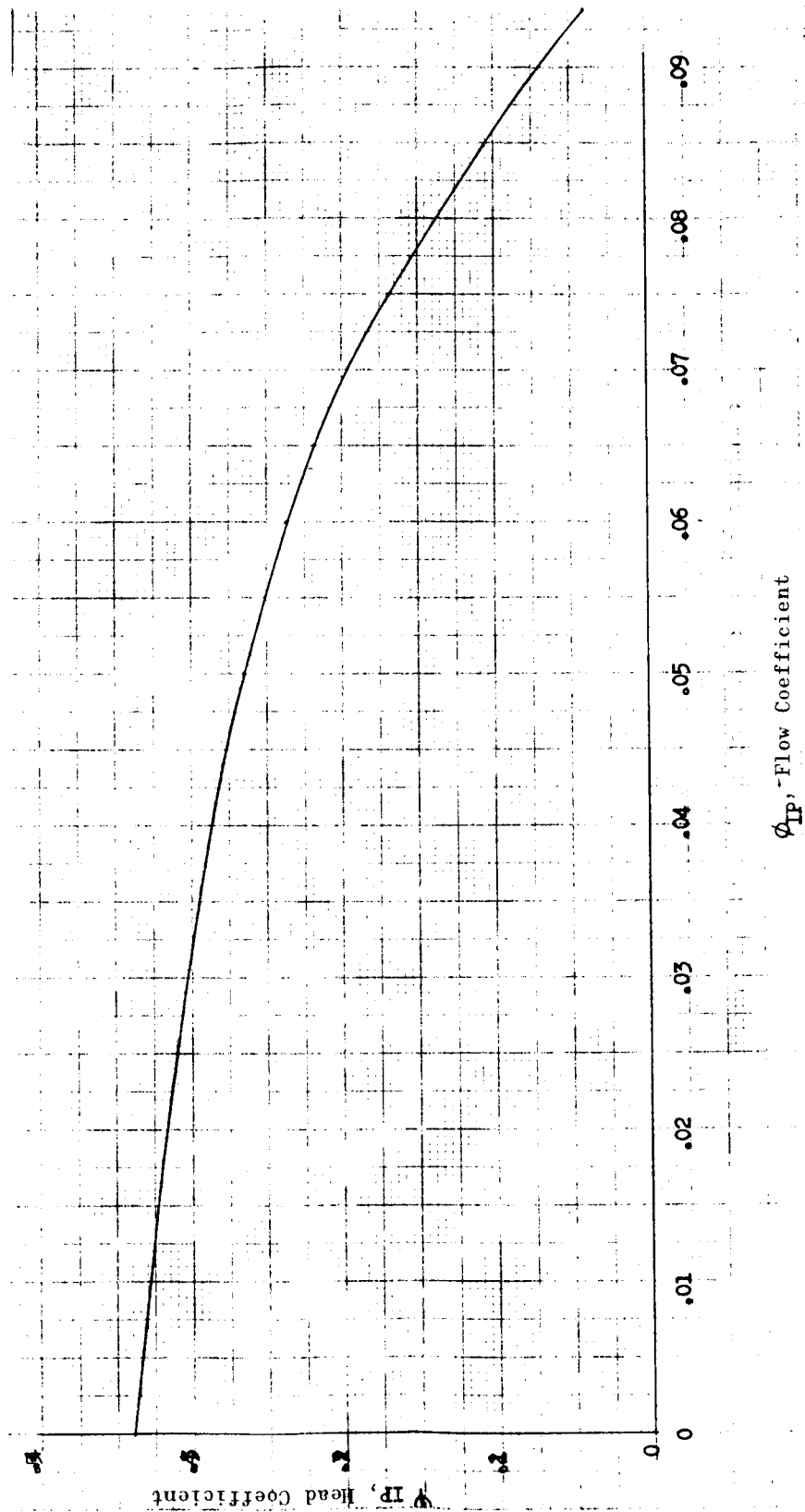


Figure 17. Preinducer Head Capacity Characteristic

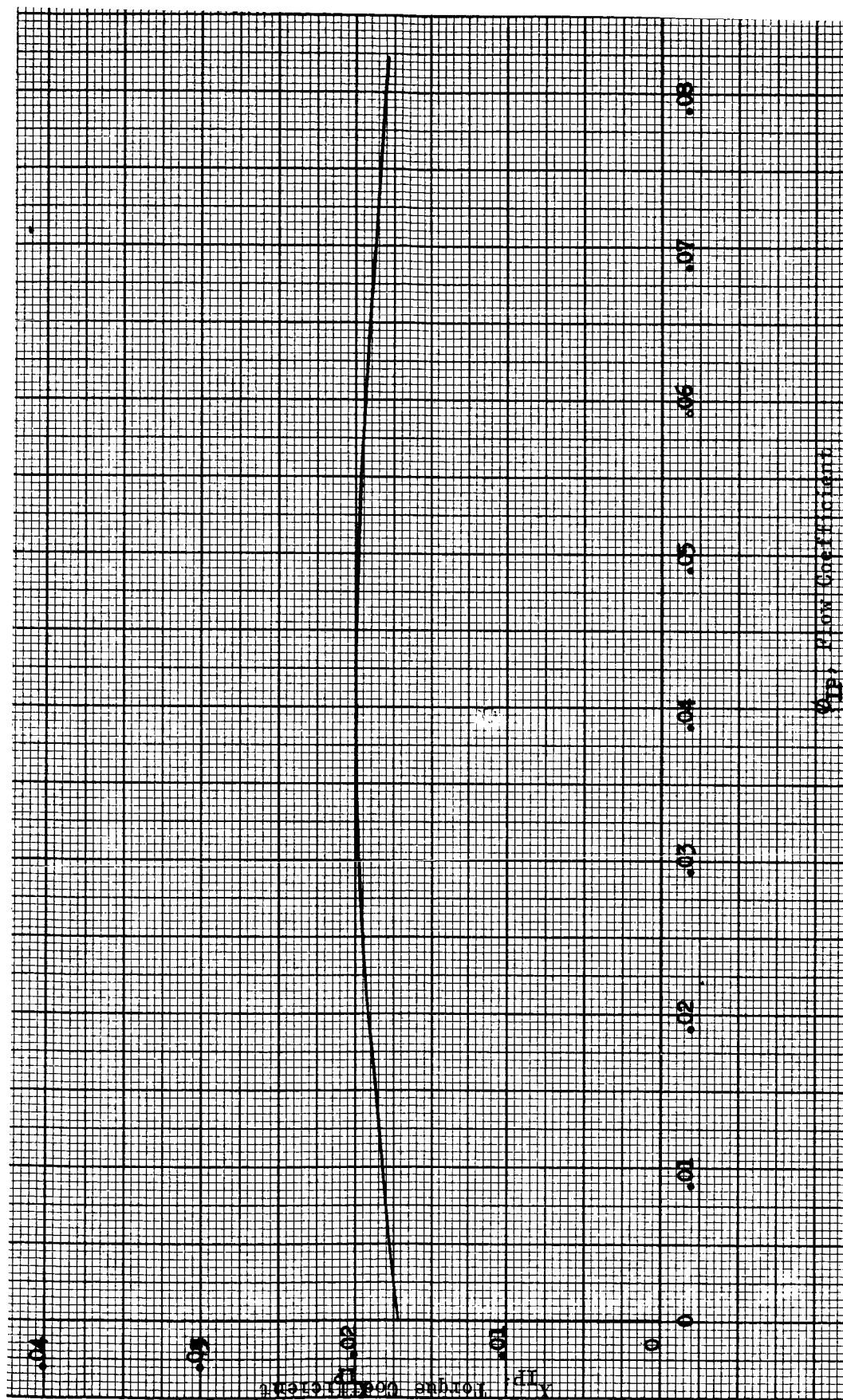


Figure 18. Preinducer Torque Capacity Characteristic

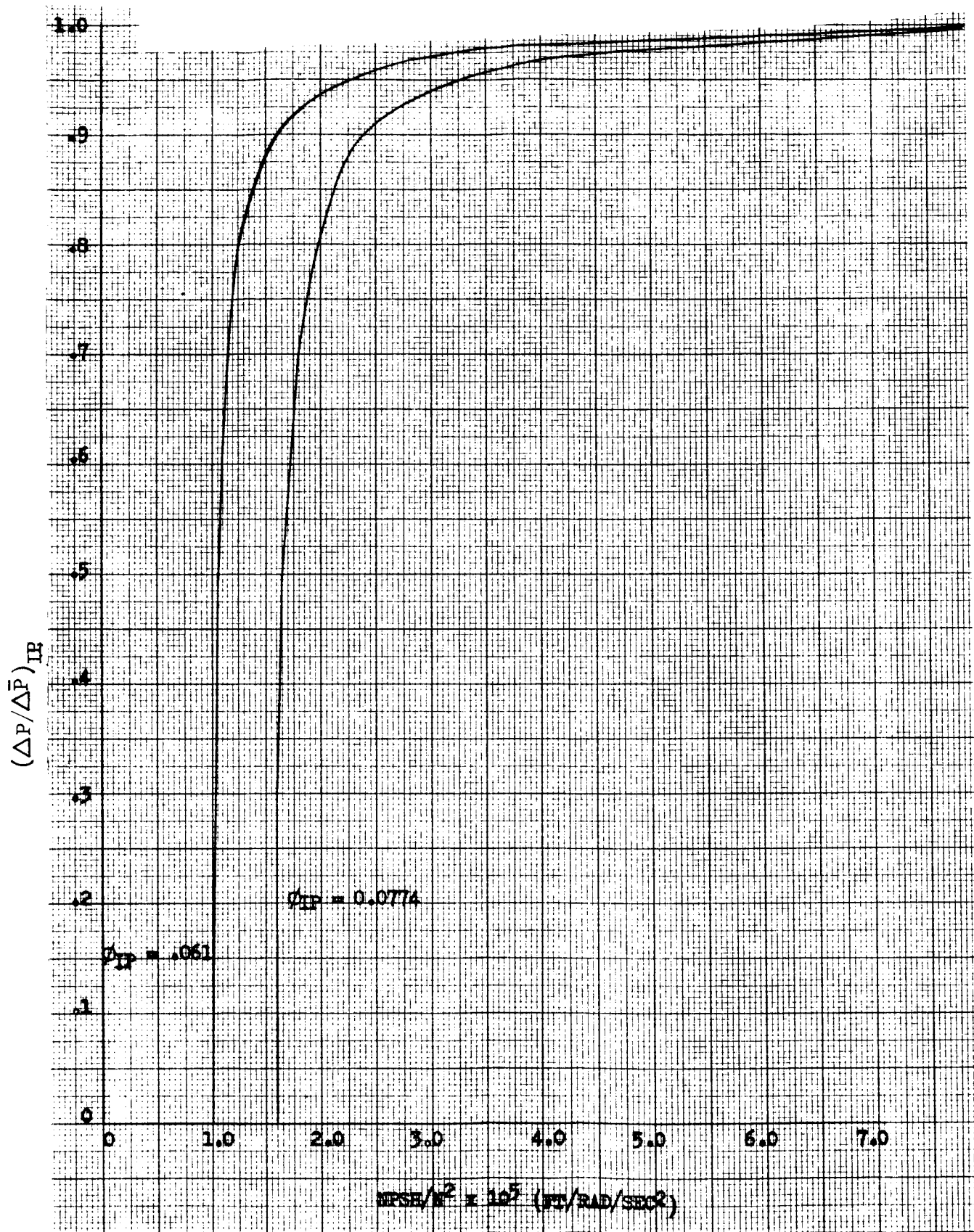


Figure 19. Preinducer Cavitation Correction

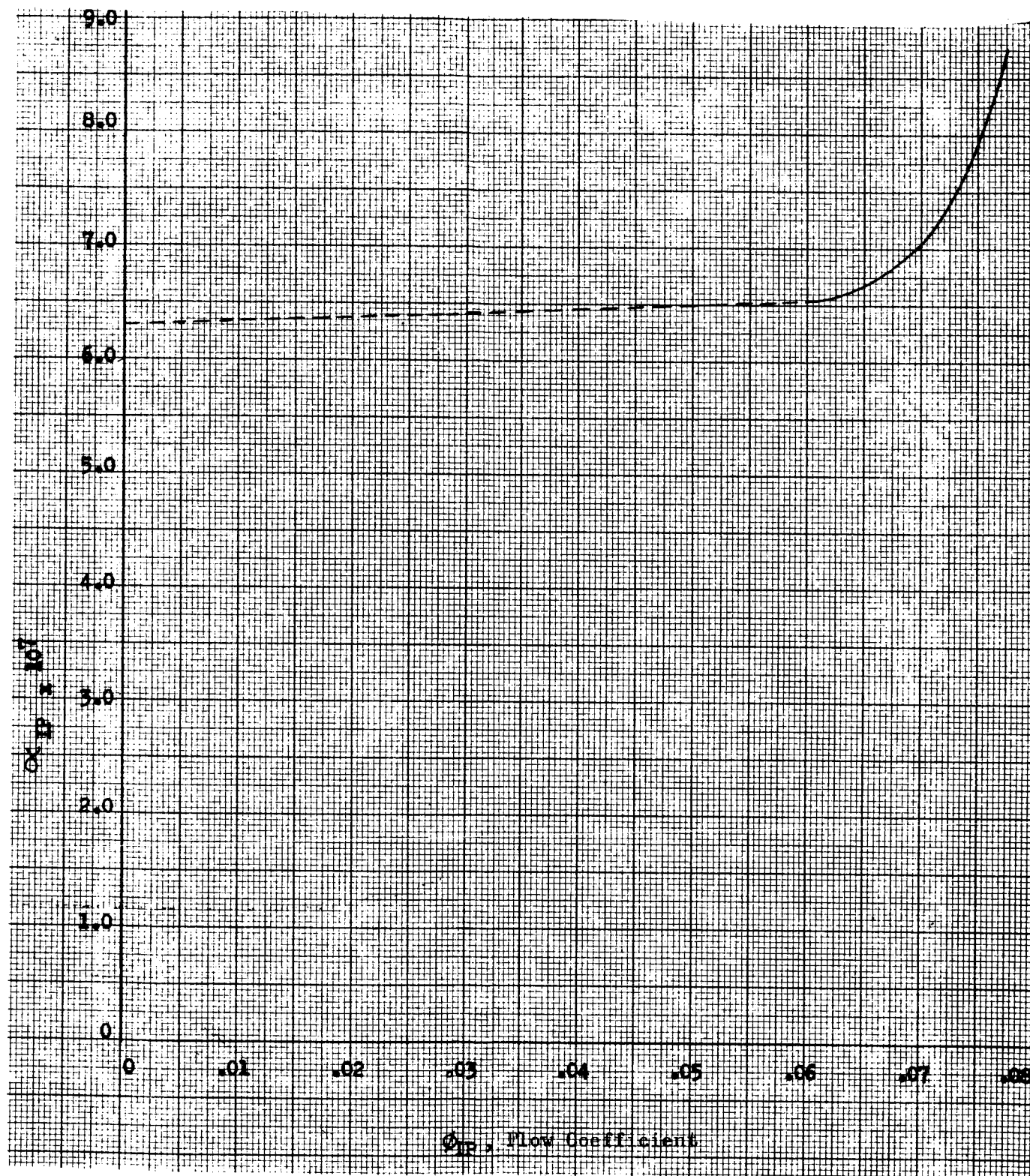


Figure 20. Preinducer (H_2O) Cavitation Correction Parameter

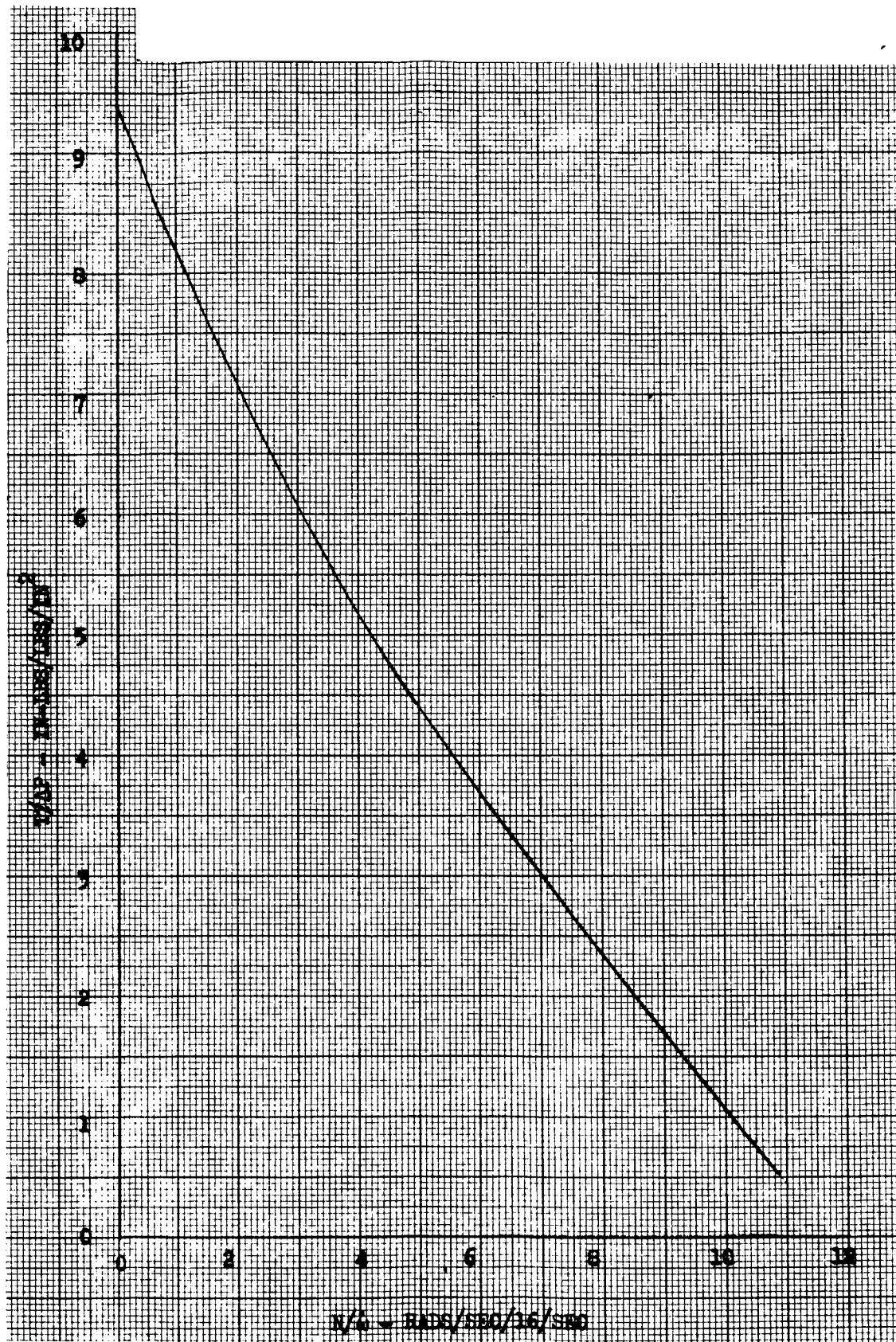


Figure 21. Hydraulic Turbine Torque Map

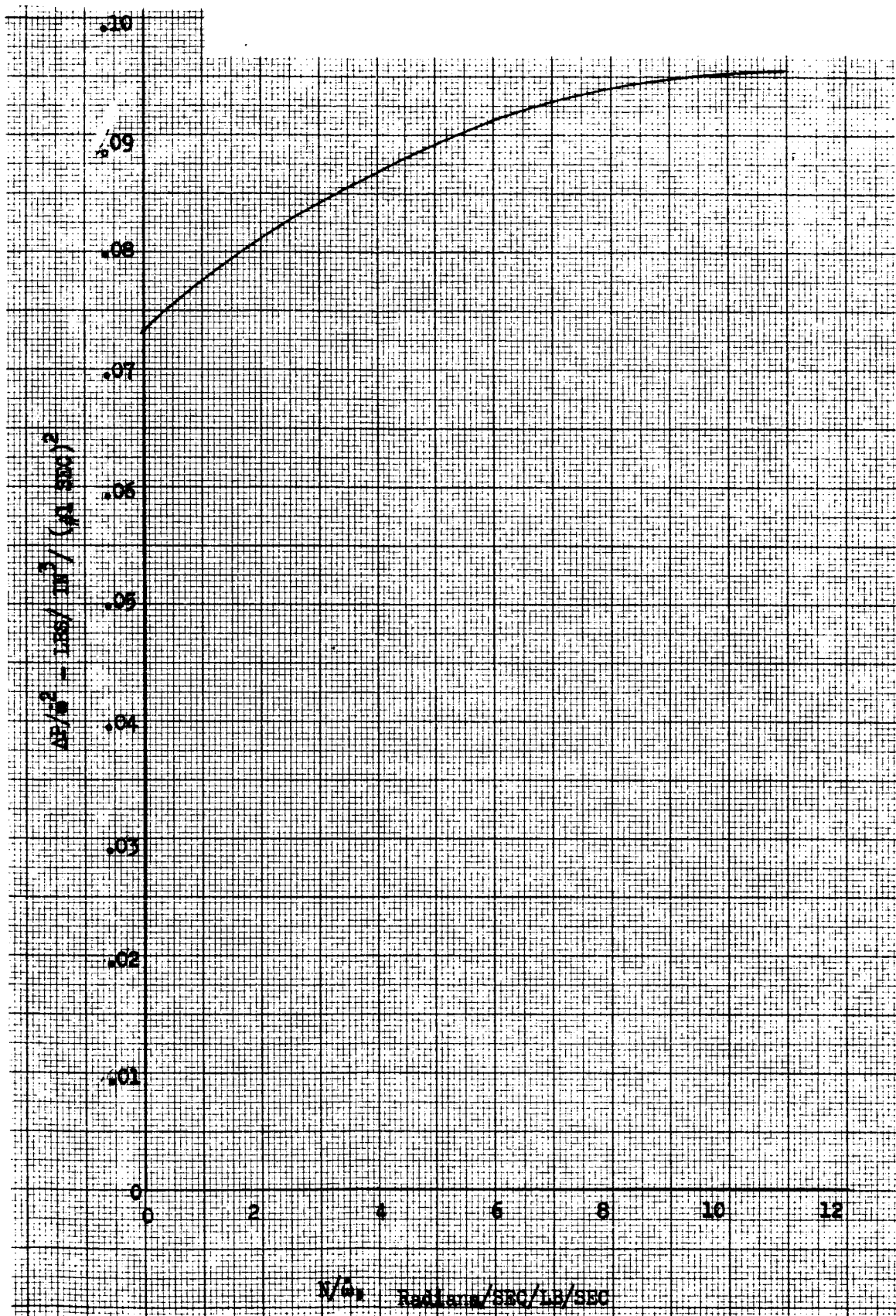


Figure 22. Hydraulic Turbine Flow Characteristic

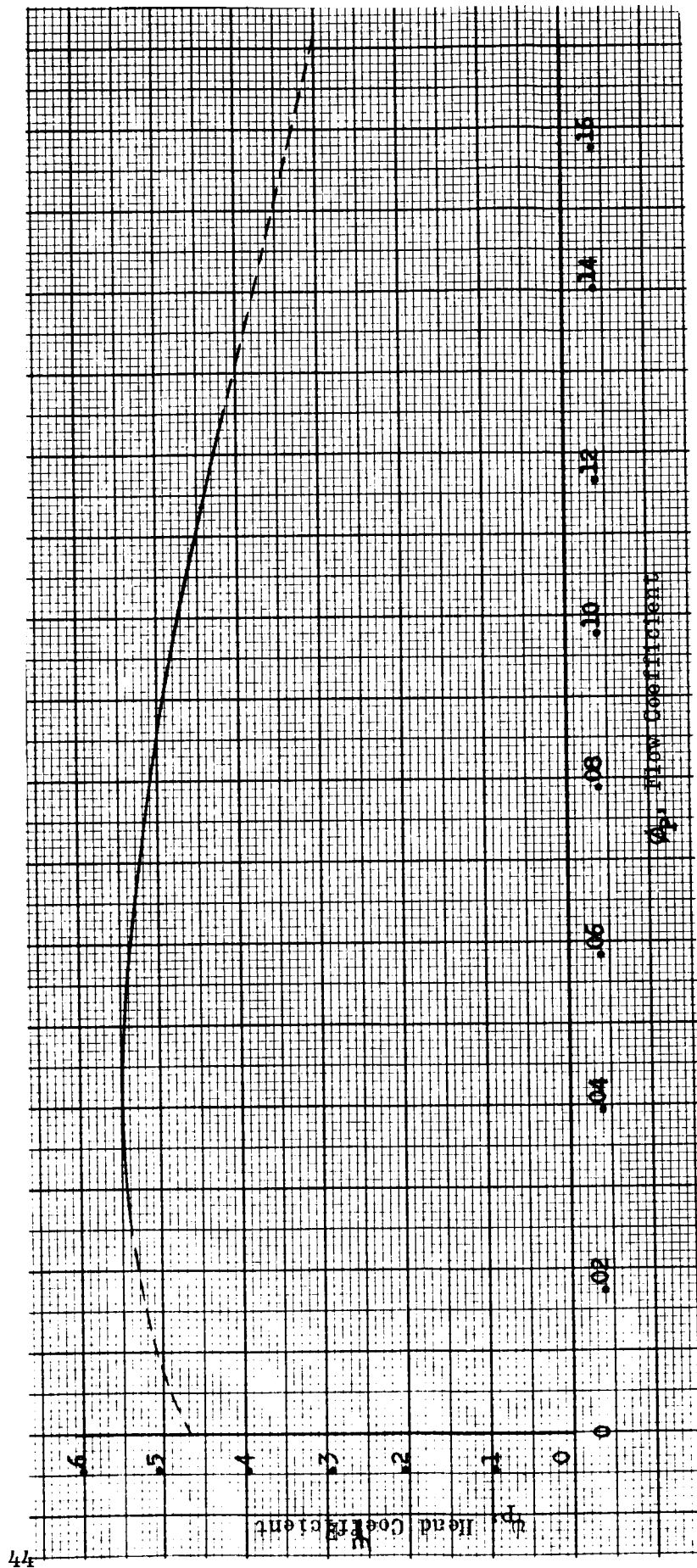


Figure 23. Main Pump Head Capacity Characteristic

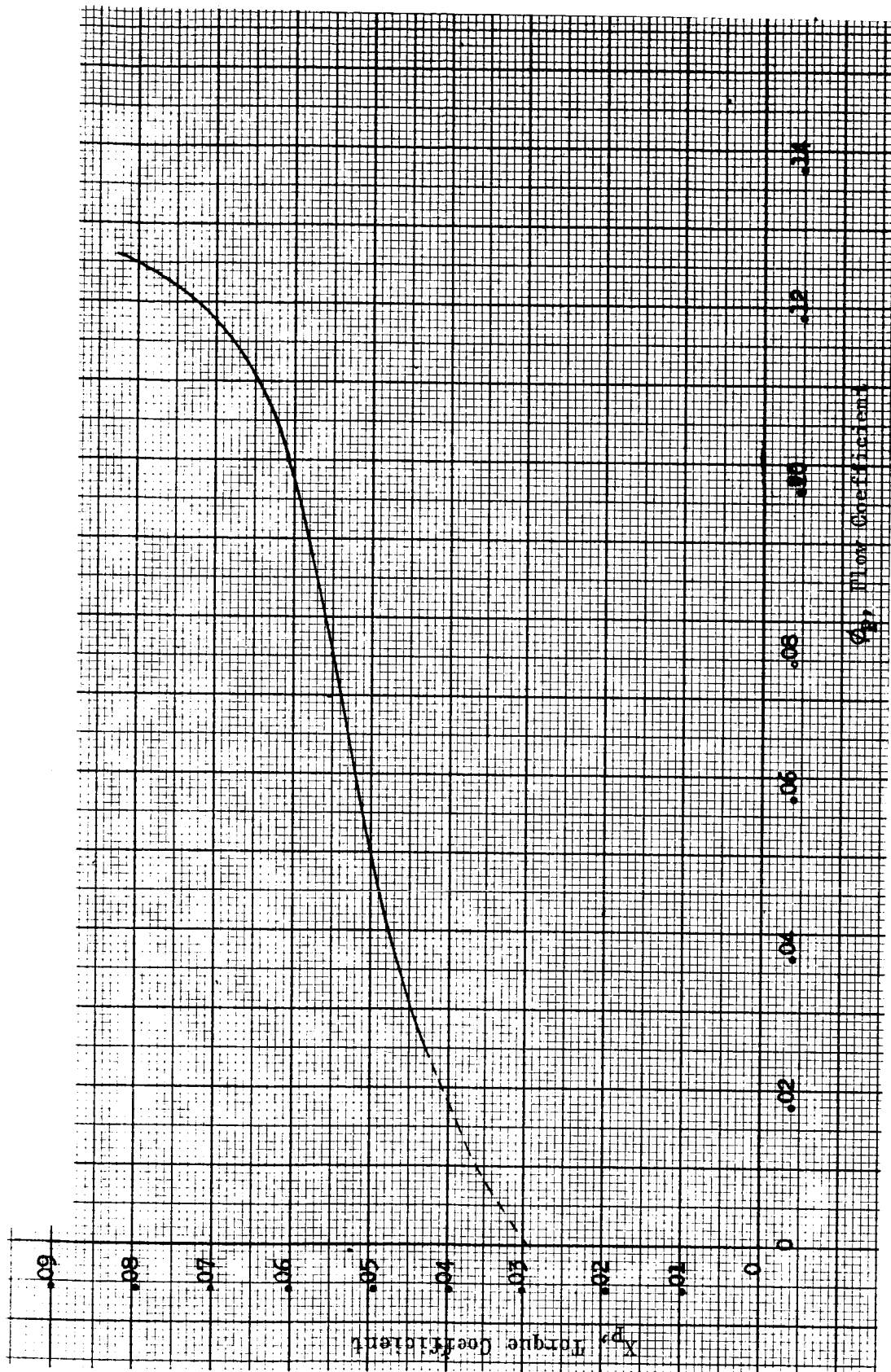


Figure 2/4. Main Pump Torque Capacity Characteristic

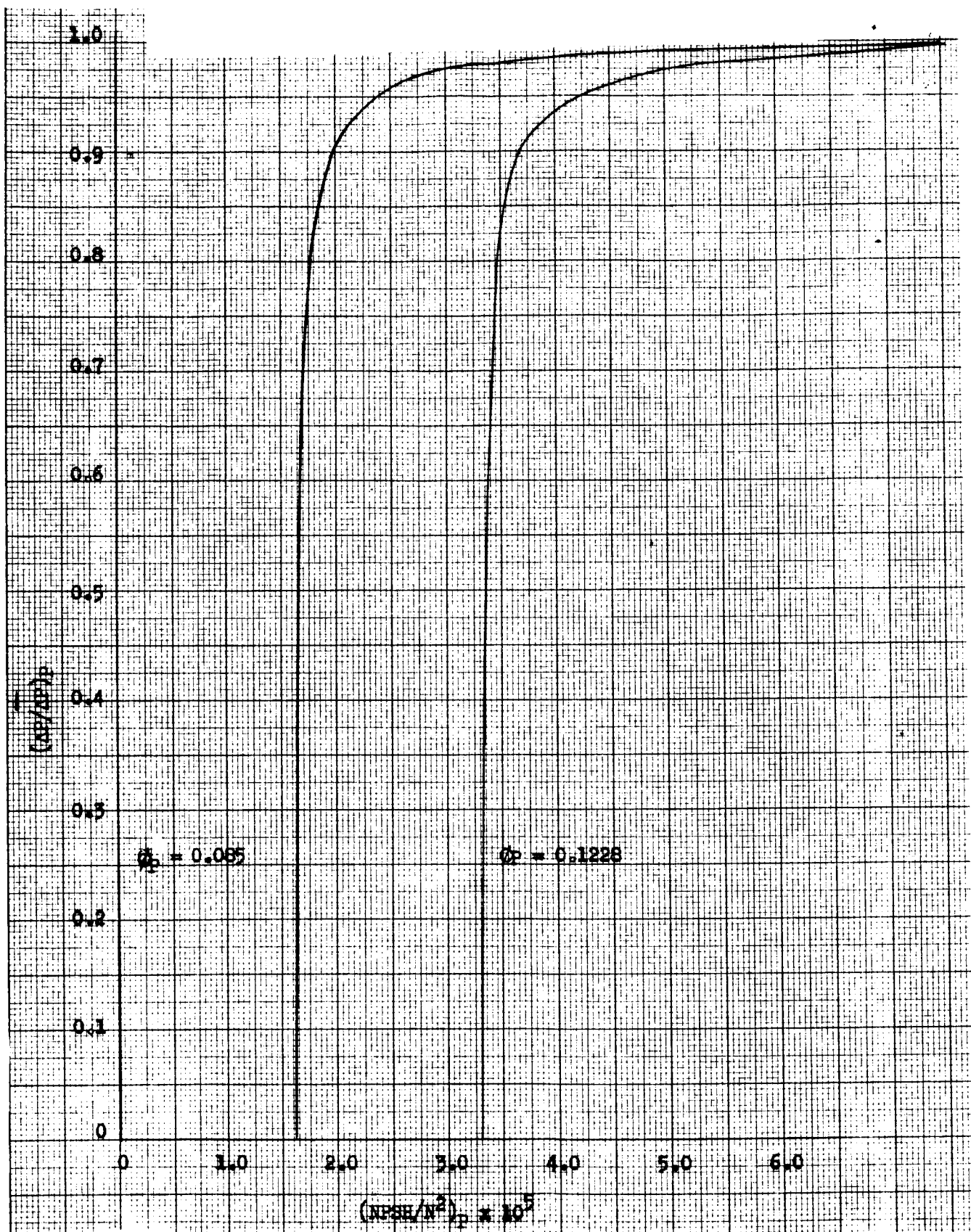


Figure 25. Main Pump, Cavitation Correction

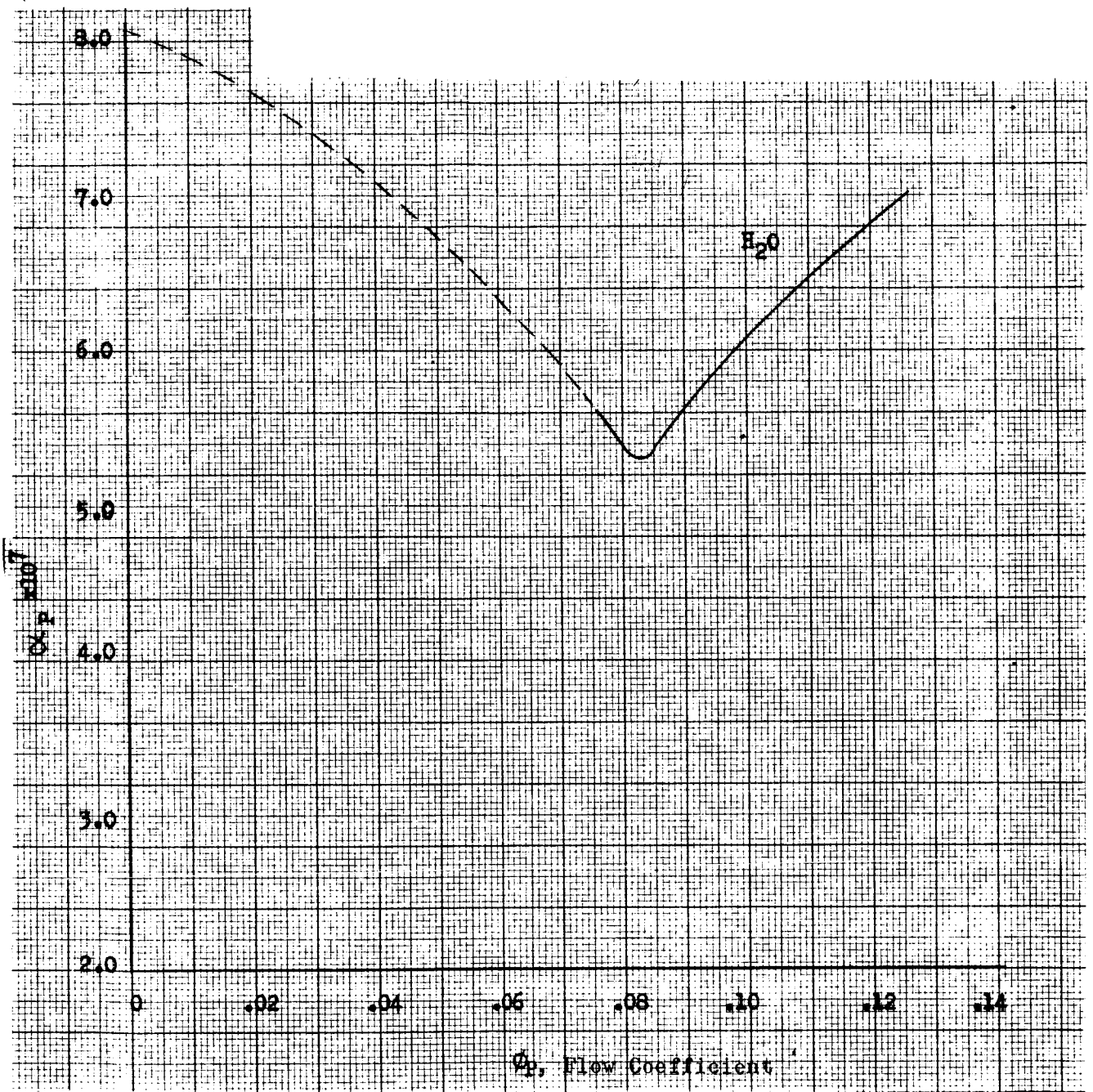


Figure 26. Main Pump Cavitation Correction Parameter

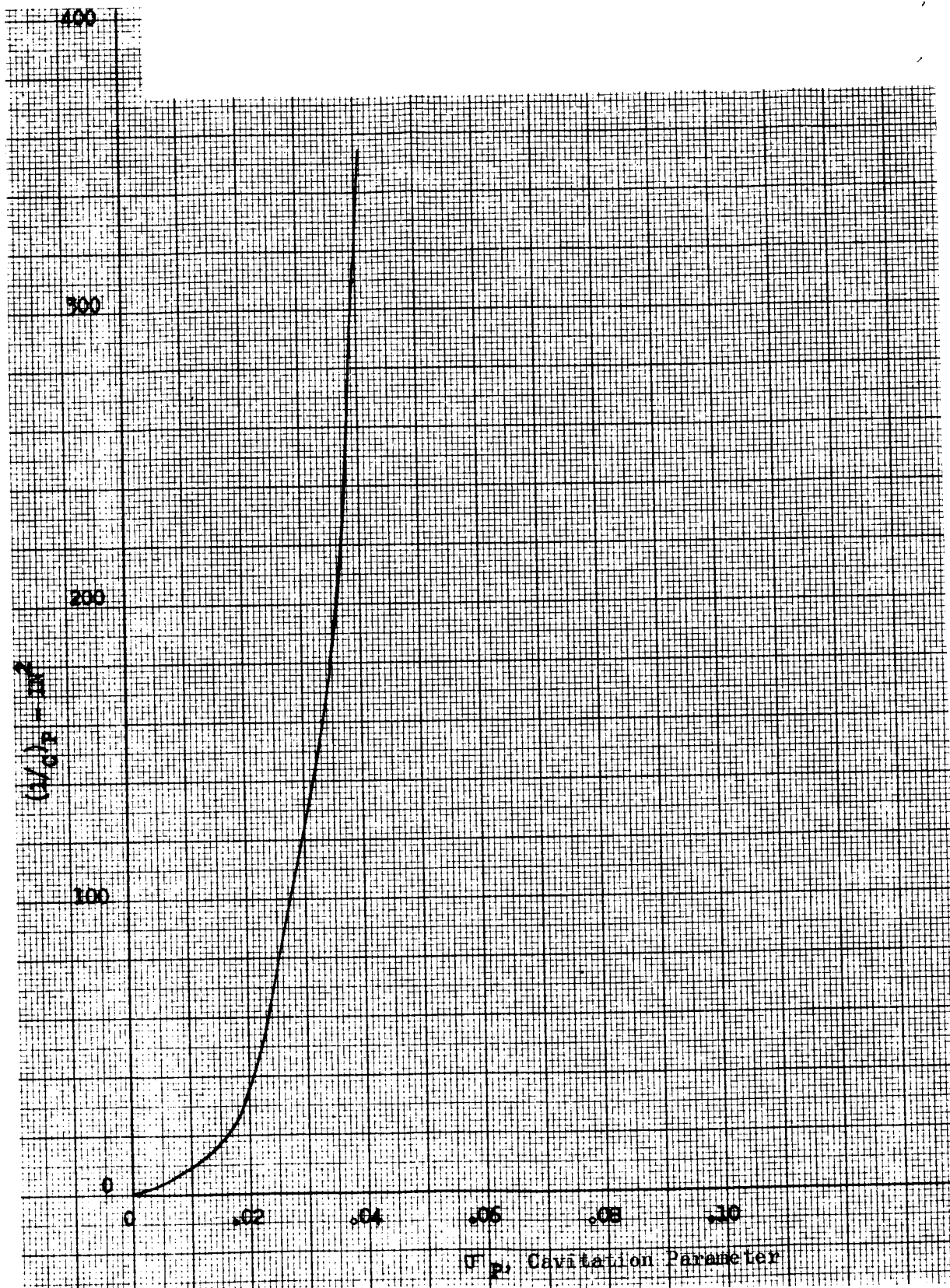


Figure 27. Main Pump Inlet Compliance

FEED LINE DESCRIPTION

Three methods of representing the feed lines were used on the line length under consideration. These are the time delay (wave equation), lumped parameter, and modal.

The digital model uses the time delay and lumped parameter representations, while the analog model uses a combination of all three.

The time delay representation is satisfactory for all frequencies; the frequency range of the modal representation is dependent on the number of modes used, while the lumped parameter (the simplest representation) is satisfactory for lines whose length is less than approximately $1/8$ wavelength of an acoustic mode at the maximum desired frequency. For water at 50 cps, $1/8$ wavelength is approximately 11 feet.

On the digital model, the lumped parameter description was used for the 2-foot section of line from the main pump discharge to the turbine feed line junction and for the turbine feed line. While the turbine feed line is approximately 20 feet long, it was believed that for the transient studies, where no external pulsing is present and the generated oscillations are low frequency, this was satisfactory. The remainder of the feed lines were represented by the time delay equations.

The analog model used the lumped parameter representation for the 2-foot section from the pump discharge to the turbine line junction, a time delay representation for the pump coupling line when the preinducer is remotely located from the main pump, and the modal description for the remainder of the lines. In general, the modal method, on the analog computer, results in a more stable solution than the time delay method and, consequently, was used when sufficient computer equipment was available.

PREINDUCER DESCRIPTION

The complete preinducer simulation includes noncavitating performance maps of head and torque coefficients versus flow coefficient, a cavitation correction factor expressing the percent of performance loss as a function of NPSH divided by speed squared, and the fluid dynamics represented by the inlet and outlet compliances and inertance.

Performance of the preinducer was represented by curves describing the non-cavitating head- and torque-capacity characteristics corrected for cavitation. The noncavitating performance curves were determined from the steady-state maps and described as a head coefficient (proportional to generated pump head divided by speed squared), and a torque coefficient (proportional to required pump torque divided by speed squared) versus a flow coefficient (proportional to flowrate divided by speed). The cavitation correction factor is a ratio of actual to noncavitating generated pump pressure versus pump NPSH divided by speed squared. The curves expressing this ratio, shown in Fig. 19, were estimated from 2-percent head loss data on the J-2 fuel pump inducer and 100-percent head loss calculations. The curves of Fig. 19 were fitted, for use in the computer models, with the equation for an equilateral hyperbola. This equation is of the form $X \cdot Y = \alpha$ where $X = (1 - \Delta P / \Delta \bar{P})$ and $Y = (NPSH / N^2 - (NPSH / N^2)_0)$, $(NPSH / N^2)_0$ being taken as the value of $NPSH / N^2$ at $\Delta P / \Delta \bar{P} = 0.0$. α was calculated from the data of Fig. 11 and is shown plotted in Fig. 20, the dashed portion of the curve being an extrapolation for use in the computer models.

Representation of the preinducer dynamics was patterned after the results of a J-2 Pogo analysis study presented in Rocketdyne Report R-6283 submitted to NASA under Contract NAS8-19, G.O. 8590. The results of this study indicated that the pump dynamics are associated with the inducer section of a pump and that a reasonable representation is two compliances separated by an inertance. This type of representation was used for the preinducer where values of the compliances and inertance were based on pump test data.

PUMP DESCRIPTION

The main pump representation includes only noncavitating performance maps (Fig. 23 and 24) and a cavitation correction factor shown in Fig. 25 and 26. Figures 25 and 26 were generated in the same manner as the pre-inducer cavitation curves based on the 2-percent head loss data of Fig. 9 and 100-percent head loss calculations. This representation also was based on the results of the previous study which indicated that the impeller section of the pump followed the noncavitation performance curves. In the case of the remote-coupled pumps, allowance is made for a compliance (Fig. 27) at the pump inlet. It also should be noted that when speed is used as an input to the main pump, the main pump torque is not required.

HYDRAULIC TURBINE DESCRIPTION

The representation of the hydraulic turbine is based on performance curves giving the developed torque divided by turbine pressure drop and turbine pressure drop divided by flowrate squared as functions of turbine speed divided by flowrate. The performance curves (Fig. 21 and 22) were supplied from the output of the steady-state mapping programs. These curves then were either curve fitted or used as point data with linear interpolation between points in the computer programs.

SYSTEM DATA

Determination of the remainder of the equation coefficients involved line lengths and diameter, fluid sonic velocity, rated operating point of the system, calculated moment of inertia of the preinducer and estimates of the compliance and inertance values from previous test programs. Table 1 presents the test system line and component data not shown as curves. The operating point data for the preinducer test system are presented in Table 2.

TABLE 1

SYSTEM DATA

Description	Value
1. Feed lines	
a. Tank exit to facility interface	
1. Length, inches	78
2. Diameter, inches	9
3. Acoustic velocity, ft/sec	3670
b. Facility interface to inducer inlet	
1. Close coupled	
a. Length, inches	264
b. Diameter, inches	10
2. Remote coupled	
a. Length, inches	84
b. Diameter, inches	10
3. Acoustic velocity, ft/sec	4090
c. Pump coupling line	
1. Length, inches	180
2. Diameter, inches	10
3. Acoustic Velocity, ft/sec	4090
d. Main pump discharge to tapoff junction	
1. Length, inches	24
2. Diameter, inches	4
e. Turbine feed line	
1. Length, inches	114
2. Diameter, inches	4
3. Length, inches	136
4. Diameter, inches	2

TABLE 1
(Concluded)

Description	Value
f. Pump discharge line	
1. Length, inches	96
2. Diameter, inches	6
3. Acoustic velocity, ft/sec	4205
g. Facility return line	
1. Length, inches	3720
2. Diameter, inches	8
3. Acoustic velocity, ft/sec	3670
2. Preinducer pump	
a. Radius, inches	4.875
b. Area, sq in.	64.25
c. Moment of inertia, in.-lb-sec ²	0.24
3. Main Pump	
a. Radius, inches	5.1
b. Area, sq in.	22.9
c. Moment of inertia, in.-lb-sec ²	1.0
4. Water density, lb/cu in.	0.0361
5. Tube bundle resistance, sec ² /in. ⁵	3.735x10 ⁻⁶
6. Inducer-turbine valve resistance, sec ² /in. ⁵	5.88x10 ⁻⁴
7. Discharge line valve resistance, sec ² /in. ⁵	2.437x10 ⁻⁴

TABLE 2

TEST SYSTEM OPERATING POINT

Parameter	Value
Tank Pressure, psia	15
Preinducer Inlet Pressure, psia	4
Preinducer Outlet Pressure, psia	79.5
Main Pump Outlet Pressure, psia	707.5
Turbine Tapoff Junction Pressure, psia	697.5
Turbine Inlet Pressure, psia	603.8
Preinducer Speed, rpm	3930
Main Pump Speed, rpm	7560
Inducer Flowrate, lb/sec	326
Hydraulic Turbine Flowrate, lb/sec	76
Main Pump Flowrate, lb/sec	402

COMPUTER PROGRAMS

To provide a solution to the system of equations, two computer programs were prepared, one for solution on a digital computer and one for solution on an analog computer. Initially, the two programs were used as a check against each other. When both programs gave comparable results, parametric studies were made. The analog program was used for analysis pertaining to the water test facility while the digital program was used to predict performance for an engine application of a hydraulic turbine driven preinducer.

DIGITAL MODEL

The digital computer model was programmed using an IBM application program called System/360 Continuous System Modeling Program (360A-CX-16X). Using this approach it was necessary to program only the statements involved in the problem along with the input data.

Listings of the problem solution portion of the program and a function called DLAY, for use with the time delay equation, are shown in the appendix for the water test facility close- and remote-coupled preinducer configurations. With a few exceptions, the coding is nonprocedural; that is, the order of solution is not dependent on the order in which the statements appear. The CSMP program translates the problem statements so that the proper order of solution is attained. The exceptions are those statements contained in the NO SORT and PROCEED sections. The table of Output Variable Sequence found at the end of the listing gives the sorted sequence.

The coding of the statements is very similar to FORTRAN and can be understood by anyone familiar with the FORTRAN language. The component performance characteristics expressed by curves use a CSMP function called AFGEN. The input for this function is a series of x and y coordinate values taken from the curves. The function determines the value of the

dependent variable by linear interpolation at the desired value of the independent variable. The remainder of the input data is supplied in statements preceded by the word PARAM.

Various methods of integration are available with the CSMP program which may be selected at the user's option. Both Simpson's and the trapezoidal method were used in running the model.

The program solves the equations as a function of time and provides printed and plotted output. A sample of these forms of output is shown in the appendix. To use the program as listed, the complete CSMP application program and manuals must be obtained from the IBM Corporation.

ANALOG MODEL

The equations for the analog model were mechanized on an Applied Dynamics AD-288 computer. This computer has bipolar amplifiers; therefore, both a positive and negative output are available from each amplifier. This is reflected in the program diagram shown in the appendix.

This program uses primarily second-order curve fits of the pump and turbine performance curves, and a modal representation for the feed lines. In the case of the remote-coupled preinducer, a time delay simulation is used for the coupling line where use is made of prepackaged time delay circuits installed at the Rocketdyne analog computing facility.

PROGRAM COMPARISON

One of the reasons for developing both an analog and a digital model of the system was to cross check the results of both programs to assist in eliminating errors. The final result of this cross checking is shown in Fig. 28 through 33 which present a comparison of the analog and digital results for the close- and remote-coupled configuration. The main pump, in all cases, was driven with a linear, 3-second ramp torque input.

It is believed that the comparison is sufficiently close to justify using the results from either program. The differences are attributed to a slightly lower speed balance used in the digital program.

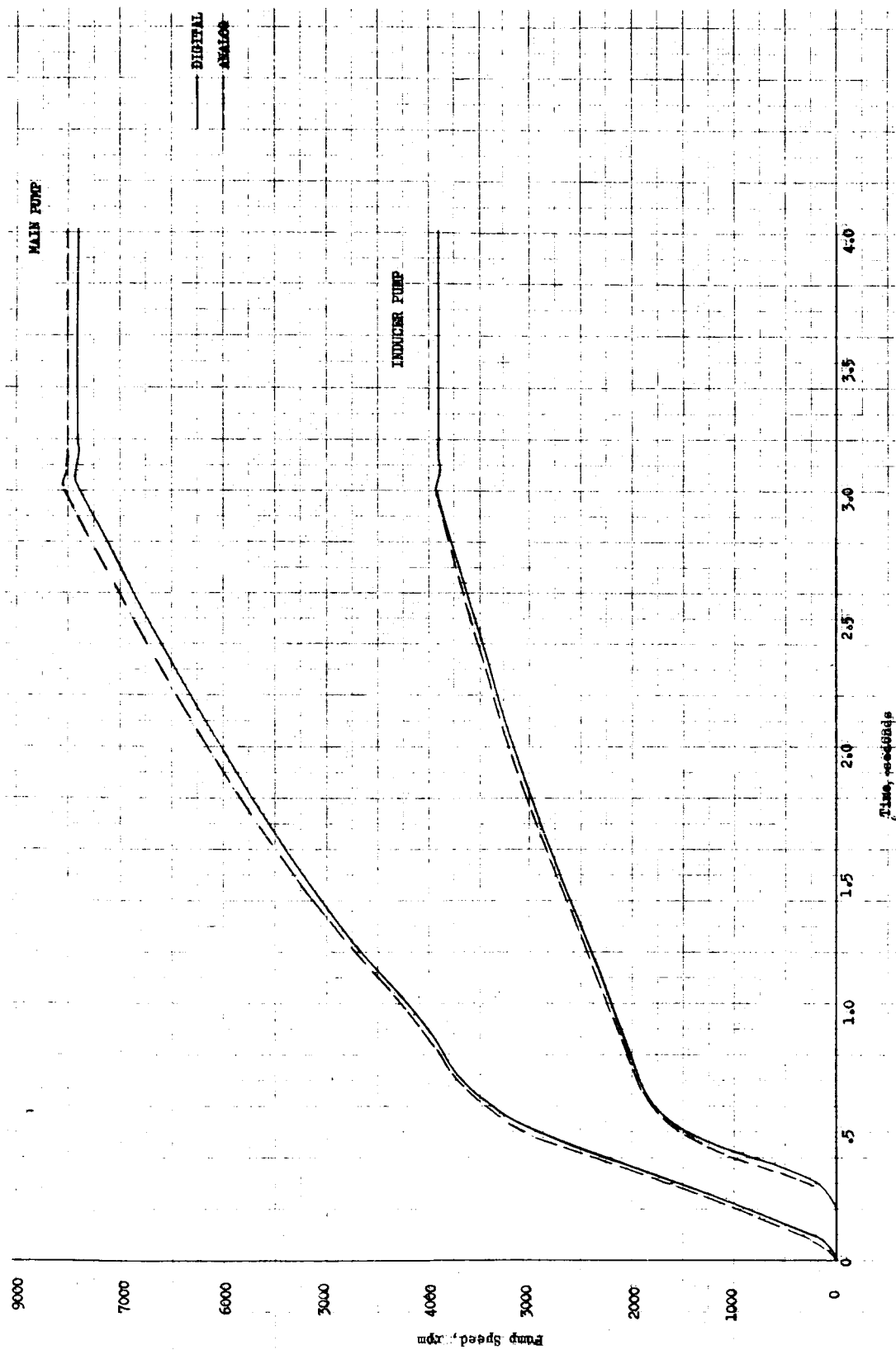


Figure 28. Inducer and Main Pump Speed, Close-Coupled Configuration

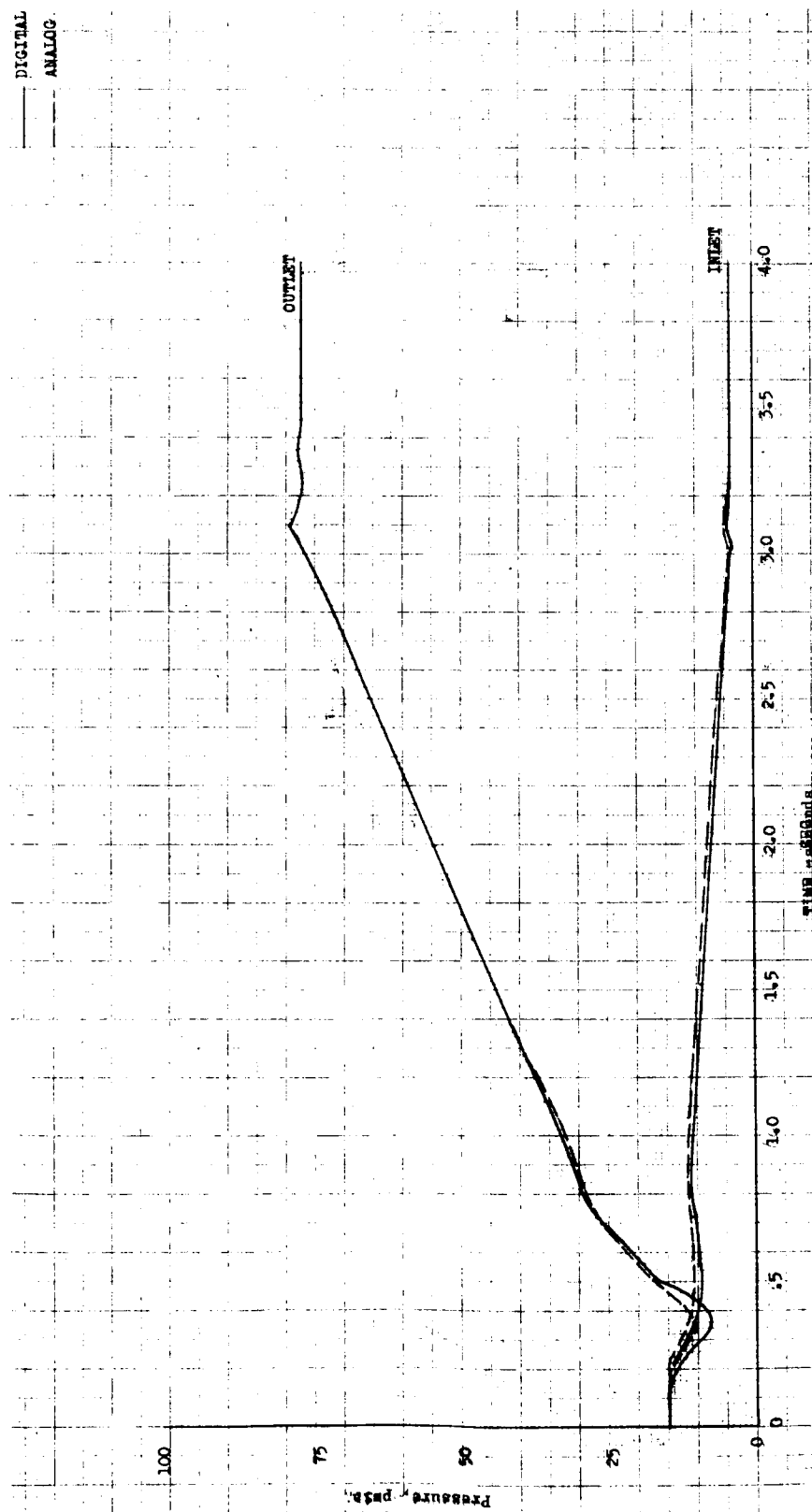


Figure 29. Inducer Pump Pressures, Close-Coupled Configuration

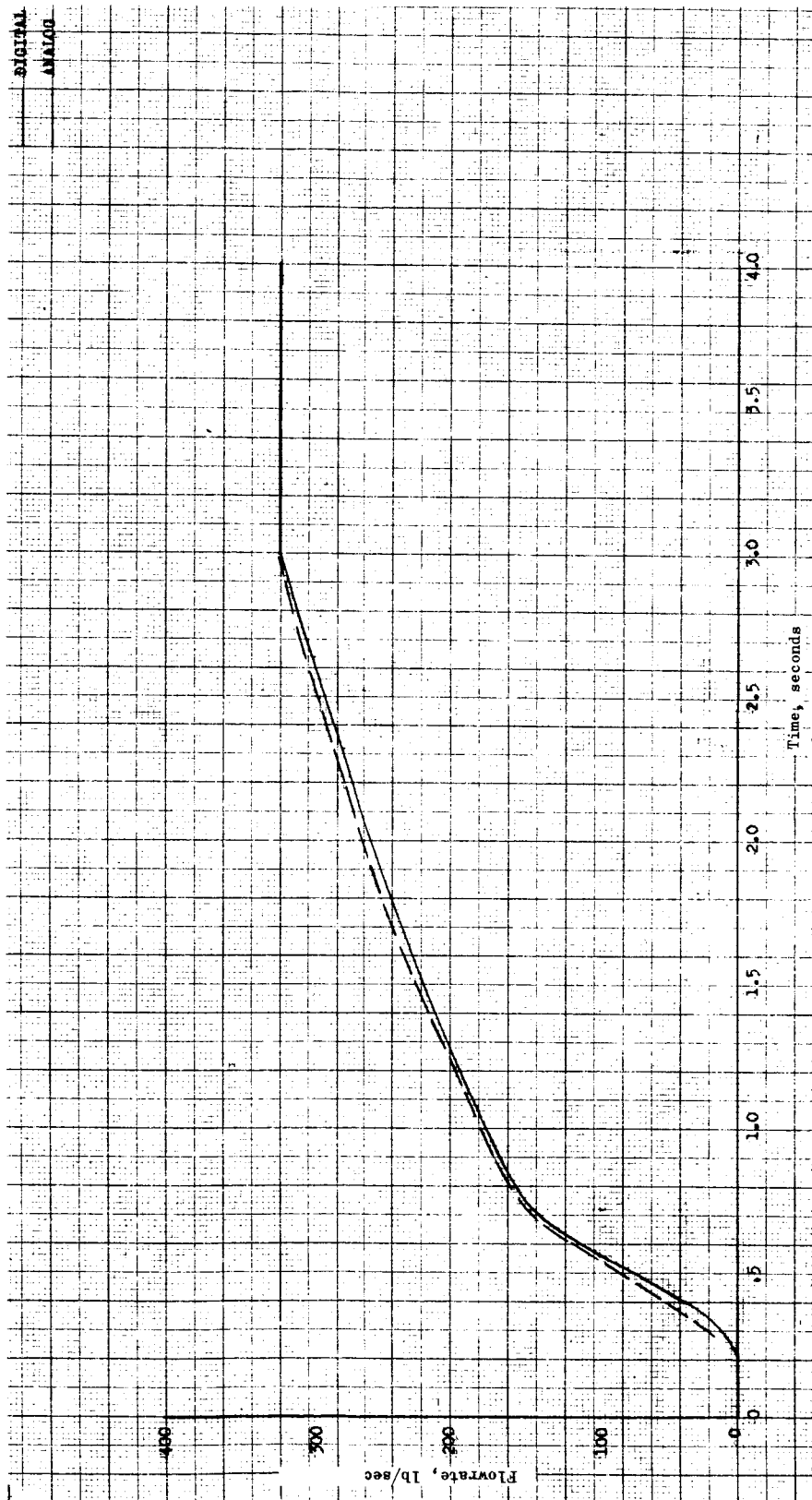


Figure 30. Inducer Pump Flowrate, Close-Coupled Configuration

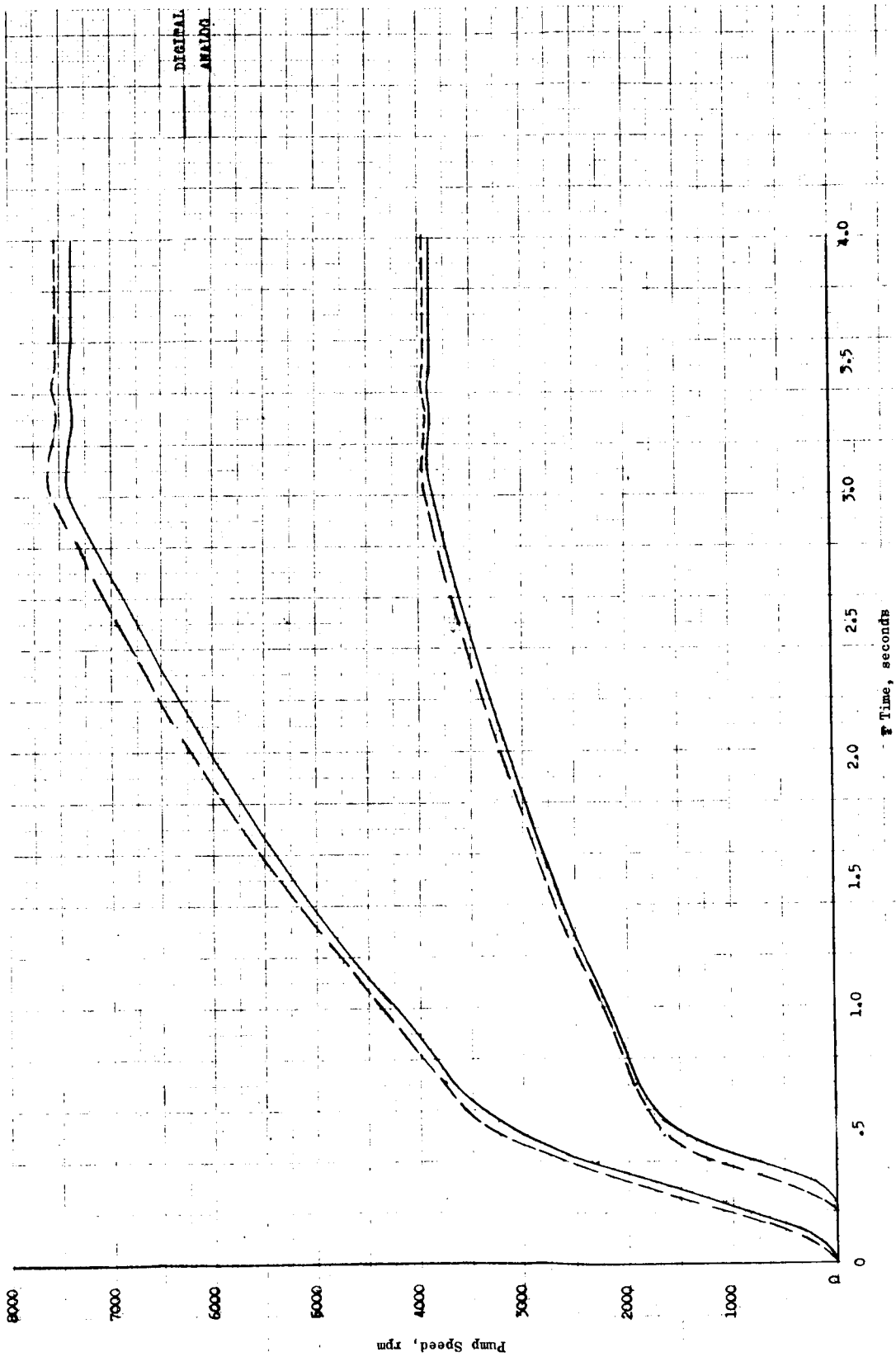


Figure 31. Inducer and Main Pump Speed, Remote-Coupled Configuration

— DIGITAL
--- ANALOG

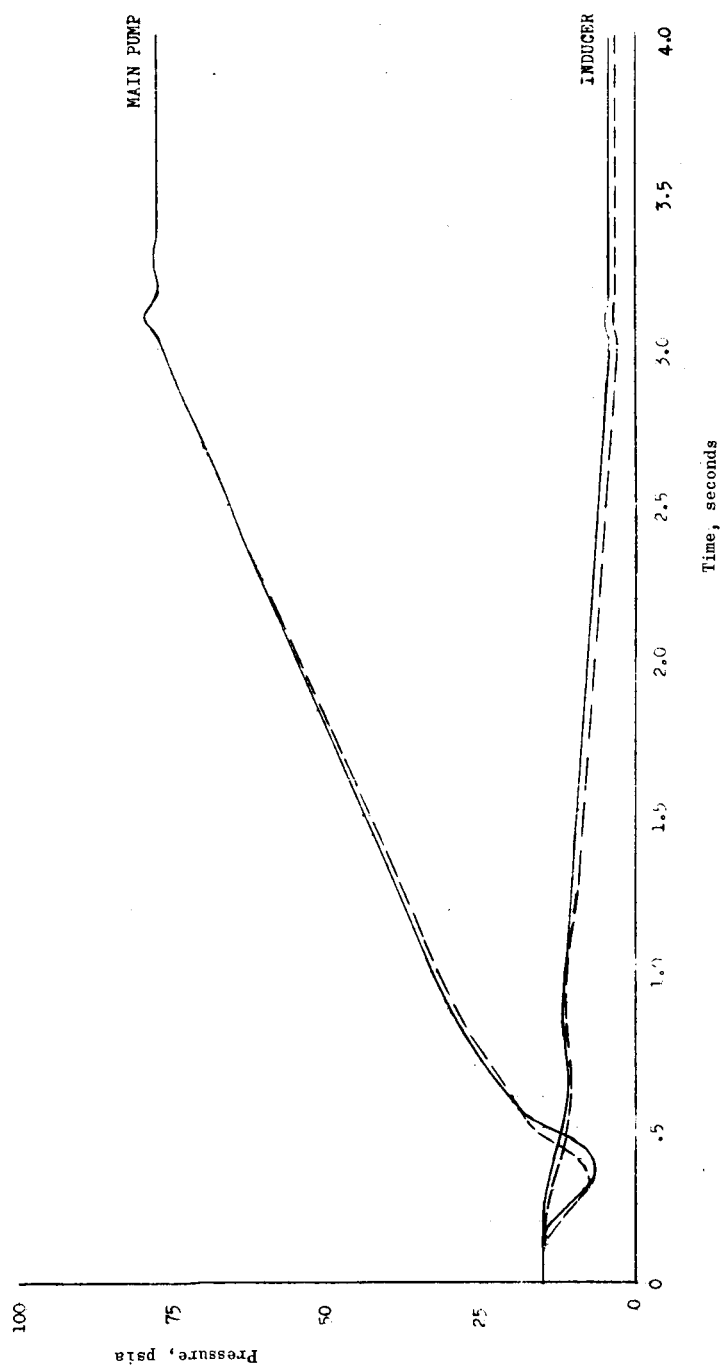


Figure 32. Pump Inlet Pressures, Remote-Coupled Configuration

— DIGITAL
-- ANALOG

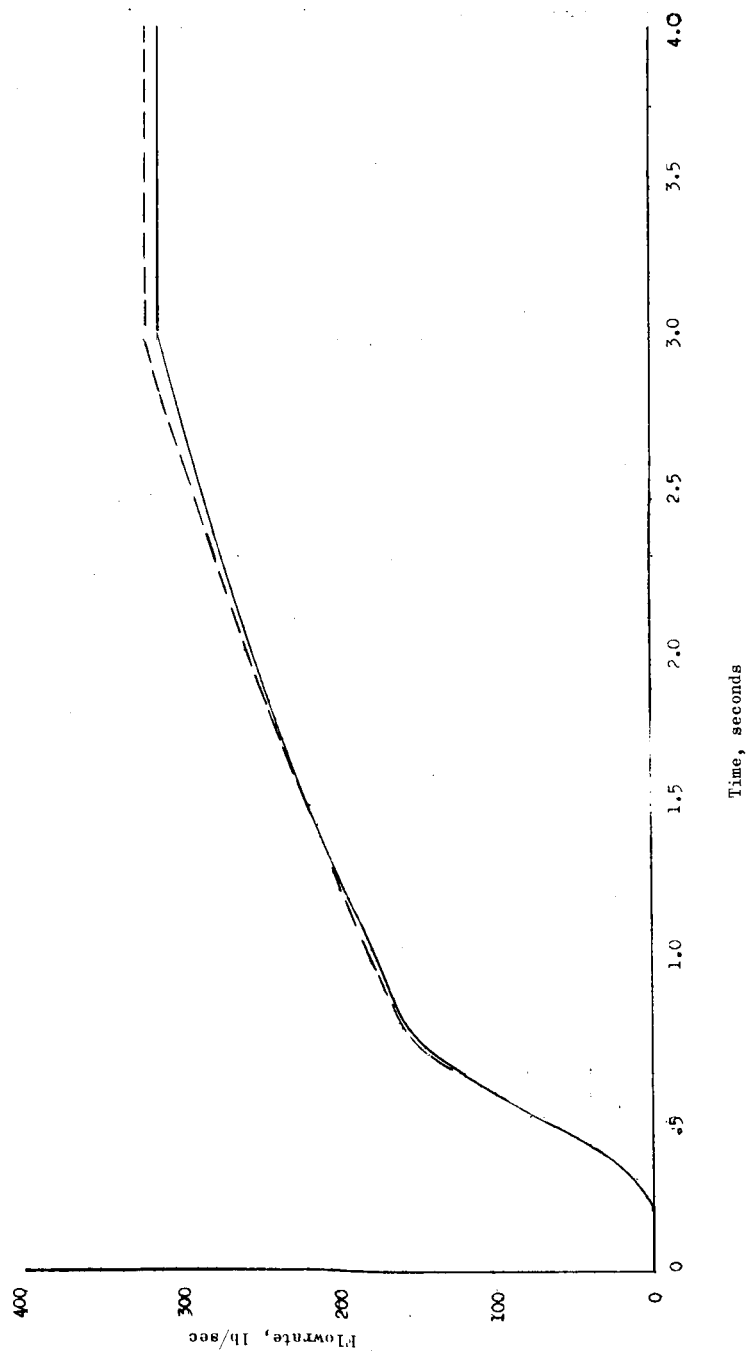


Figure 33. Inducer Pump Flowrate, Remote-Coupled Configuration

PARAMETRIC STUDIES

INTRODUCTION

A series of parametric studies was conducted, using the analog and digital computer models, to evaluate the effect of selected parameters on the transient performance of the simulated pump system and to predict the operation of hydraulic turbine driven preinducers in an LH_2 and LO_2 rocket engine feed system.

The studies can be grouped into three areas covering: (1) variations in the water test preinducer hardware and test system parameters, (2) predictions of the test program start and throttling performance, and (3) the use of preinducers in an engine feed system.

The parameter variations in group 1 were run to establish the type of hydraulic turbine which should be designed and to determine what effect selected preinducer parameter and test stand line sizes might have on the system starting performance. In this area, the following parameters were considered:

1. A two-stage vs three-stage hydraulic turbine
2. Increased and decreased preinducer moment of inertia
3. Increased diameter of the pump coupling line for the remote-located preinducer
4. Resistance of the hydraulic turbine feed line
5. Reduced turbine feed line fluid inertia
6. Low-head preinducer

The test program predictions cover 0- to 100-percent pump speed rates from 1.5 to 4.0 seconds at nominal and 120-percent pump Q/N and throttling performance from 100 to 65 percent and 65 to 100 percent at various throttling rates. The rates were taken from the proposed test plan and form a starting point for comparing the test and model performance.

The third group considers the use of preinducers in an engine feed system. The feed system used represents the Saturn S-IVB and the propellants being pumped are liquid hydrogen and liquid oxygen.

PARAMETER SURVEY

The first series of studies involved variations in the preinducer test hardware and test system configuration. To assess the effects of these variations the following reference condition was chosen:

1. High-head preinducer pump
2. Three-stage hydraulic preinducer turbine
3. J-2 LO₂ main pump
4. Run tank pressure of 15 psia
5. Tank outlet resistance to give 4 psia, 8-foot NPSH at the preinducer inlet at rated flow
6. Turbine inlet valve and discharge valve resistance set to give rated flow conditions
7. Three-second linear torque ramp input to the main pump

Data obtained from the analog computer model for the reference starts are presented in Fig. 34 and 35 for the close and remote preinducer locations, respectively.

The primary area of interest for this type of start is the initial depression in the main pump inlet pressure. The depression results from the inherent lag in the preinducer pump speed buildup due to the hydraulic turbine being driven by a feedback from the main pump. As the main pump is accelerated, flow is initiated through the discharge system. To accelerate the flow from the tank through the pumps, the preinducer inlet and outlet pressures must decrease. The drop in preinducer outlet pressure will decrease until sufficient head is generated by the speed

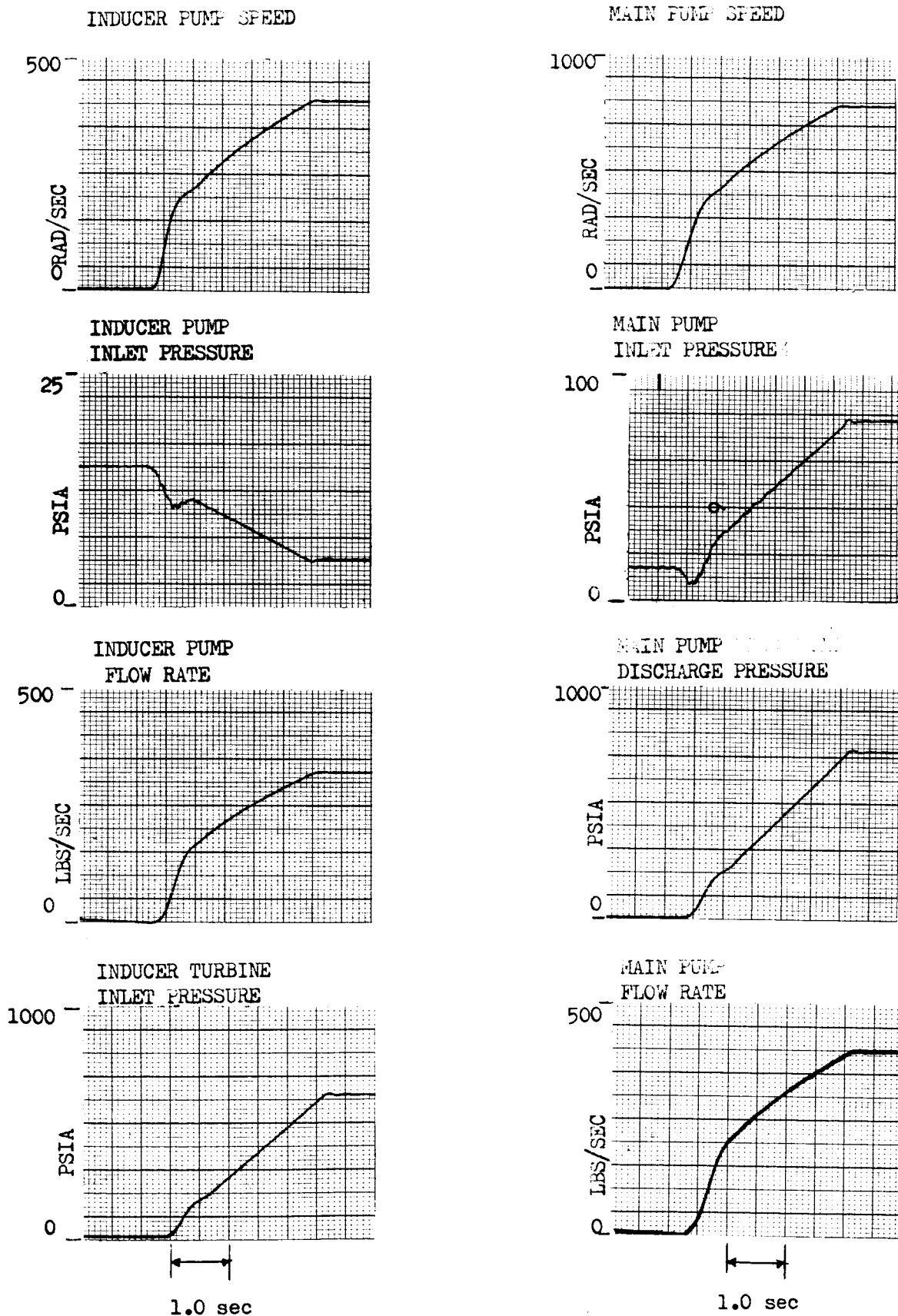


Figure 34. Close-Coupled Reference Start

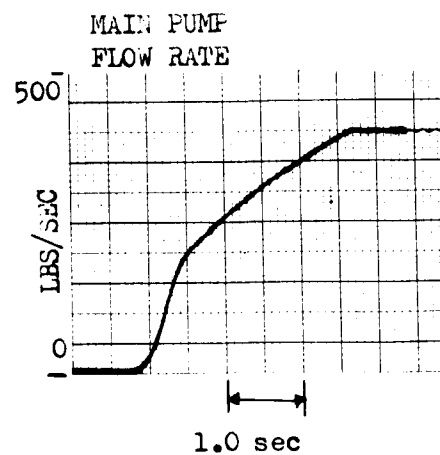
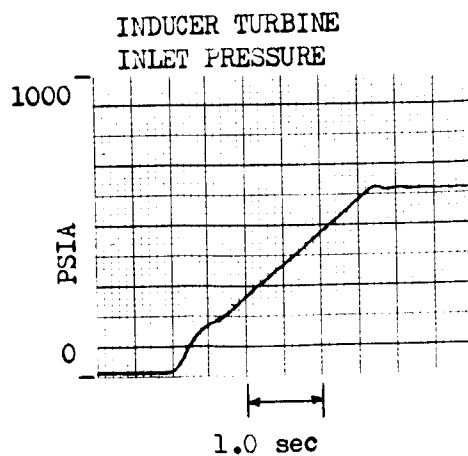
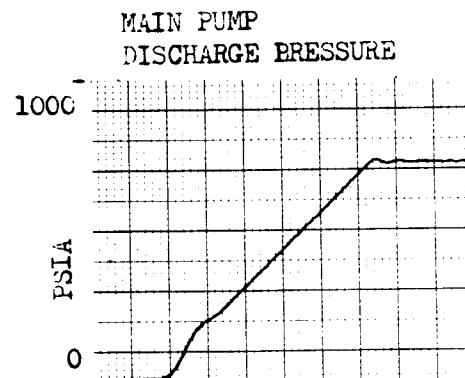
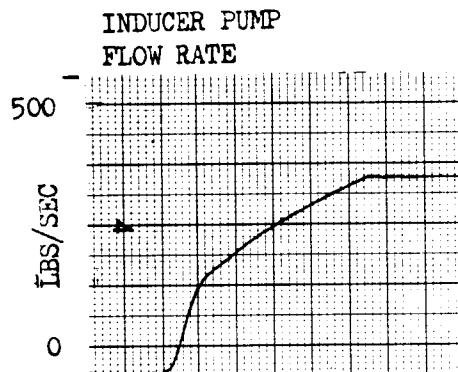
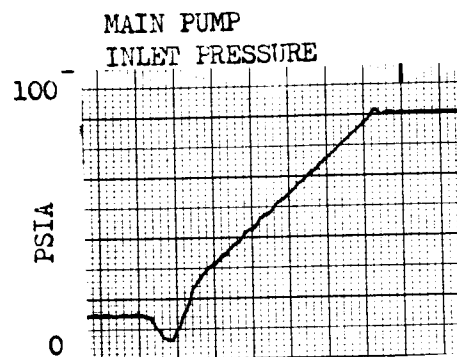
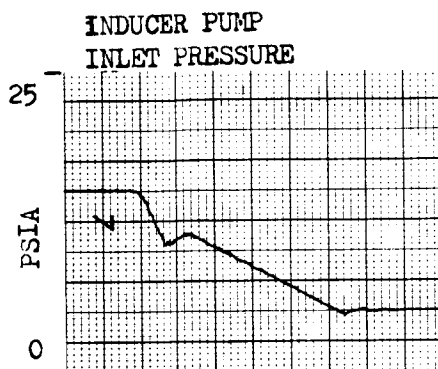
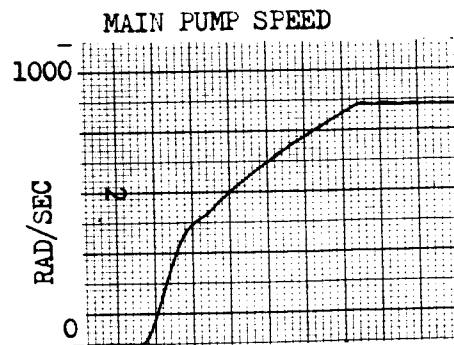
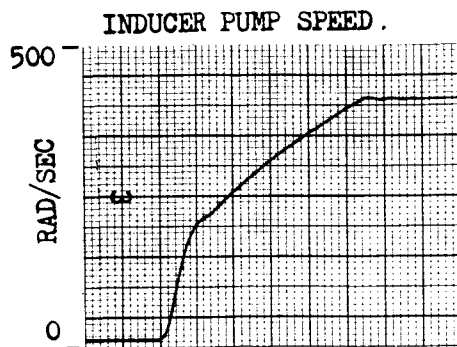


Figure 35. Remote-Coupled Reference Start

buildup of the preinducer. For the close-coupled configuration, the pre-inducer outlet and main pump inlet pressure are the same, while for the remote-coupled configuration, a section of line connects the preinducer outlet to the main pump inlet.

The effect of the depression in the preinducer discharge pressure is that as the tank pressure is lowered, the absolute pressure at the main pump inlet (due to the depression) decreases. If it reaches a low enough value, severe pump cavitation will result. Therefore, the difference between the tank pressure and minimum main pump inlet pressure has been used to compare the effect of the parametric variations. The pressure differences for the reference starts are 6 psi with a close-coupled pre-inducer and 8 psi with the remote-coupled preinducer. Comparing the curves of the inducer and main pump flowrates, it can be seen that the main pump flowrate is higher than the inducer pump flowrate, at any given time, the difference increasing to 78 lb/sec when steady-state operation is reached. This difference is the flowrate returned from the main pump discharge to drive the hydraulic turbine.

The performance curves for the hydraulic turbines, shown in Fig. 12 and 13, show the two-stage compared to the three-stage turbine has a higher torque-to-pressure drop ratio and a lower pressure drop-to-flowrate squared ratio for low values of the speed-to-flowrate ratio. The torque/ ΔP curve suggests the possibility of the two-stage turbine producing higher low-speed torque and consequently, higher preinducer speed acceleration. The system performance of the two-stage turbine driving the preinducer, shown in Fig. 36 and 37, for the close- and remote-coupled preinducer, respectively, however, indicates that no significant improvement in the starting performance was achieved. This is due to the fixed inlet valve resistance in the turbine feed line required to balance the system for rated operation. The lower two-stage turbine resistance results in an increase in turbine flowrate which produces an increase in the inlet valve pressure drop resulting in a decrease in the turbine pressure drop compared to the three-stage turbine. The decrease in turbine pressure drop results in comparable turbine torques for both the two- and three-stage turbines, and thus, the same buildup characteristics.

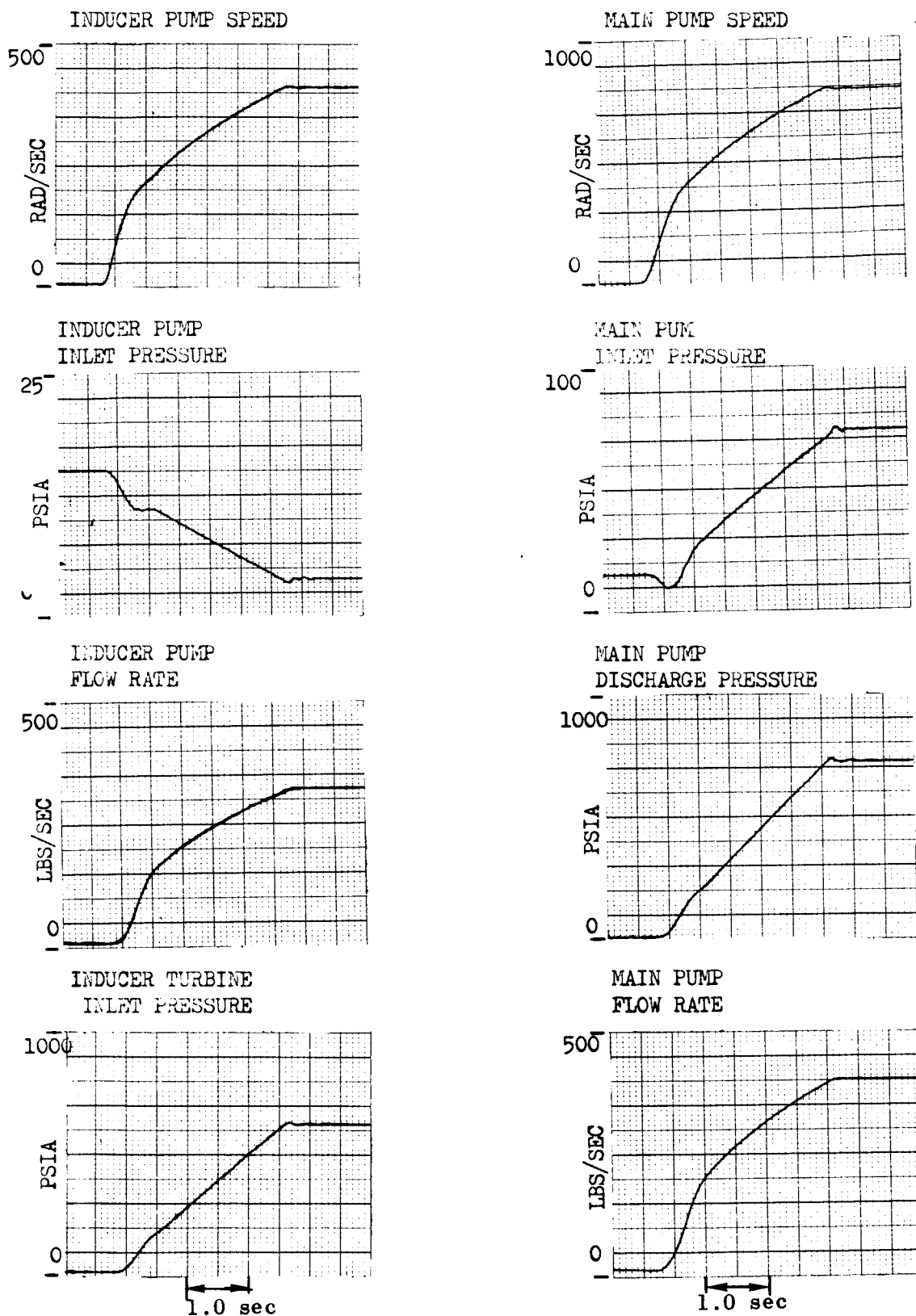


Figure 36. Close-Coupled, Two-Stage Turbine

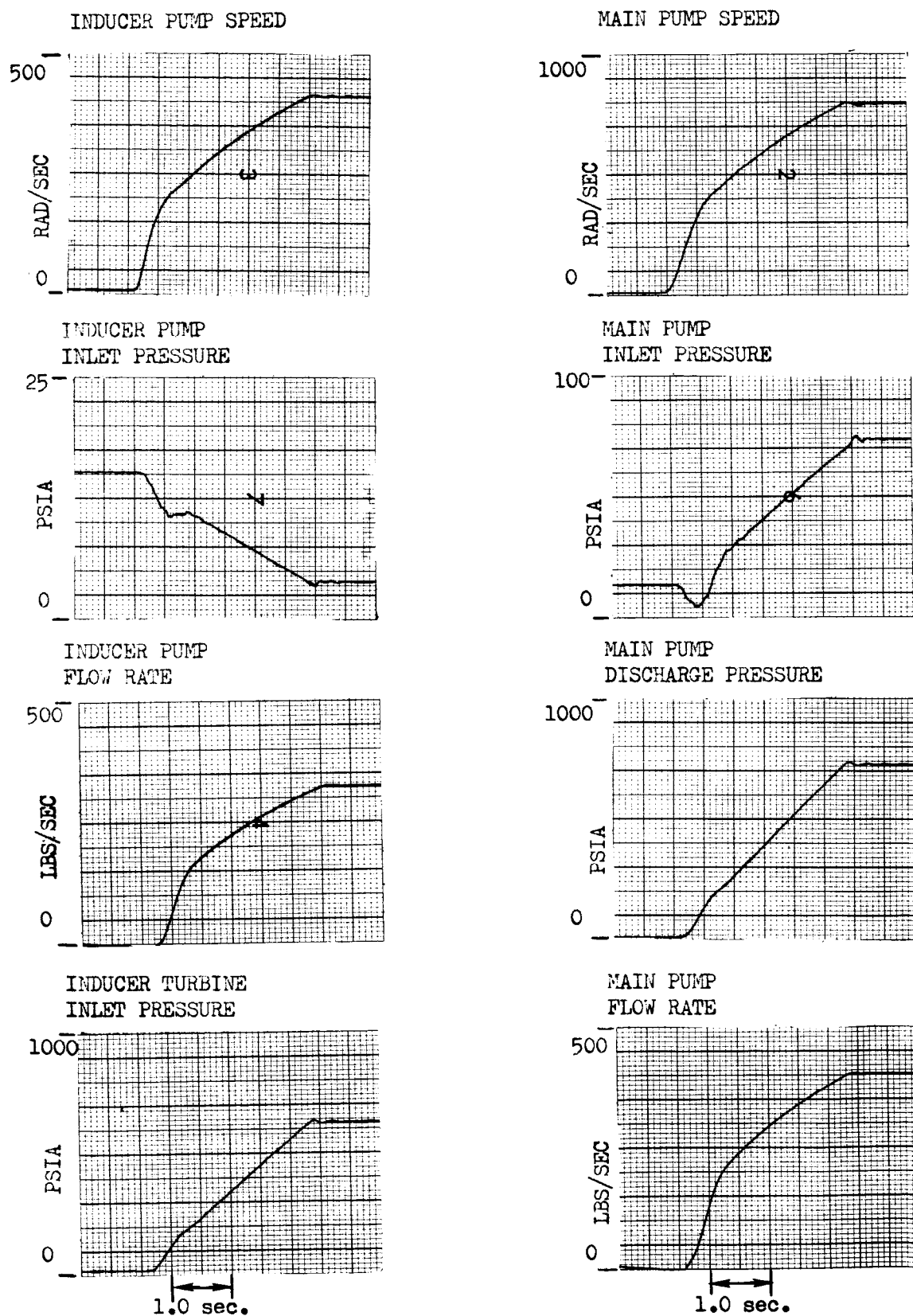


Figure 37. Remote-Coupled Two-Stage Turbine

For determining the effect of the preinducer moment of inertia, values of 0.1 and 3.0 times the design value of $0.24 \text{ in.-lb-sec}^2$ were used. The lower value of inertia does not represent any usable material. The high value of inertia could represent a preinducer made from K-monel. The results (Fig. 37 through 42) indicate a significant effect; the low moment of inertia reduced the main pump inlet pressure depression to about 2 and 5 psi below tank pressure for close- and remote-coupled pre-inducers, respectively, while the high inertia increased the depression to 12 and 14 psi, respectively. This indicates that care should be taken in the design and selection of materials for an engine preinducer to minimize the rotor moment of inertia.

The pump coupling line between the pump inlet and the preinducer outlet is used only with the remote-coupled preinducer configuration. Increasing this line area reduces the fluid inertia term which is proportional to the line length divided by the line area. The coupling line area was doubled; this resulted in a main pump inlet pressure depression of about 6.5 psi, as shown in Fig. 42. This is a significant change from the 8-psi depression of the reference case.

A variation of ± 10 percent in inducer inlet line resistance was analyzed to determine the effect of a system balancing error. These results are presented in Fig. 43 through 46; they indicate no effect upon the minimum pump inlet pressure and only a very slight effect (less than 30 rpm) on the preinducer running speed. Consequently, this does not appear to be a critical item from the standpoint of water testing.

To determine the effect of the size of the turbine feed line, the length was halved and the area was doubled, which resulted in reducing the fluid inertia by a factor of 4. The results, shown in Fig. 47 and 48, indicate little, if any, effect. Therefore, for the test system, this is not a significant factor.

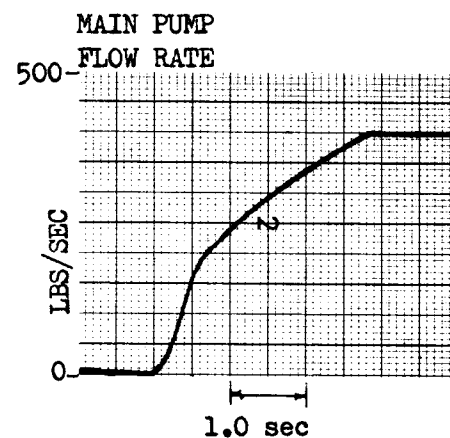
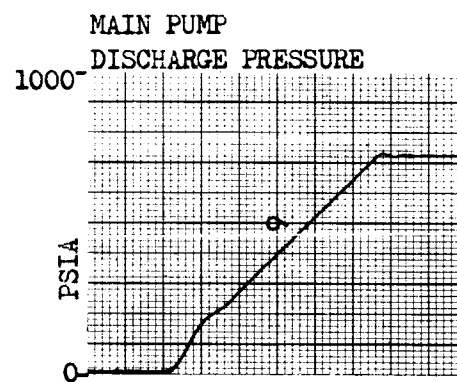
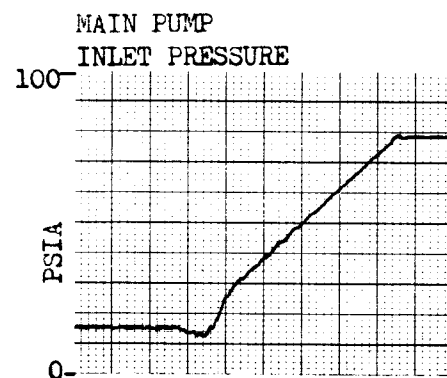
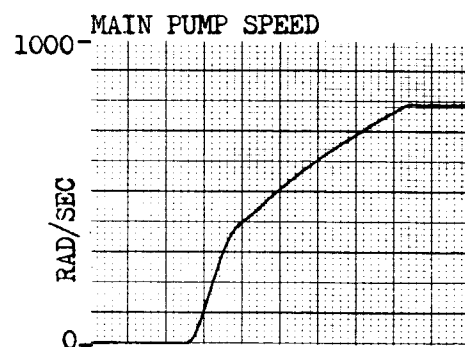
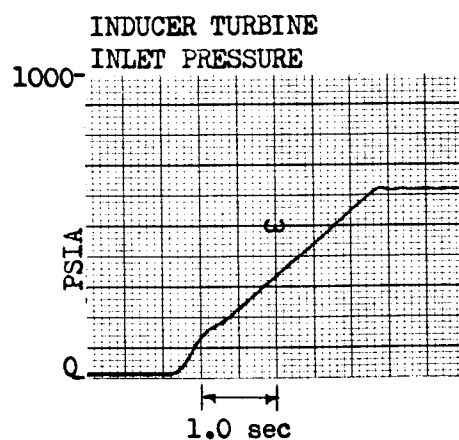
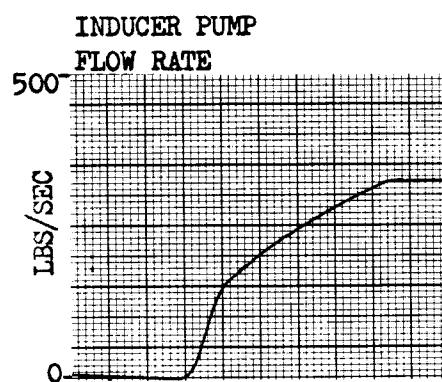
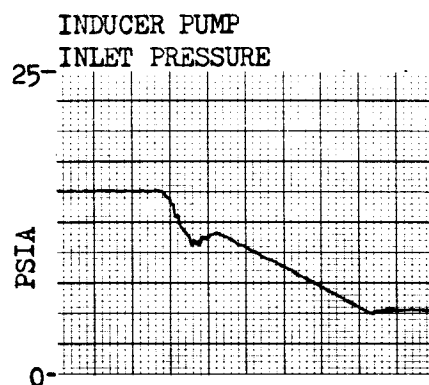
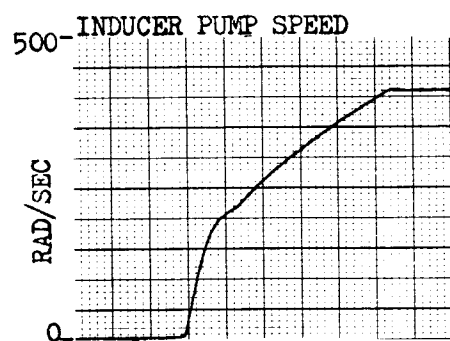


Figure 38. Close-Coupled Low Moment of Inertia

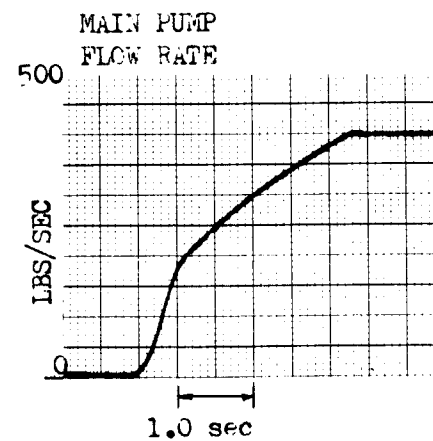
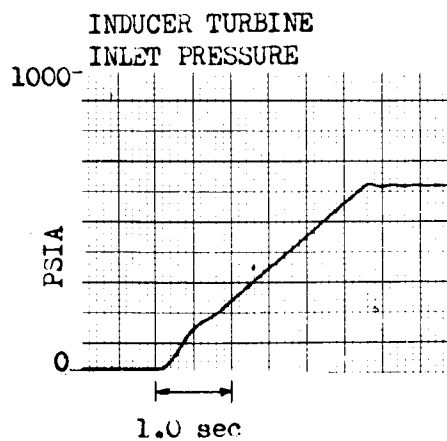
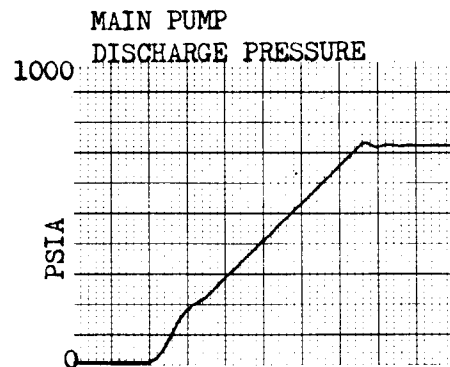
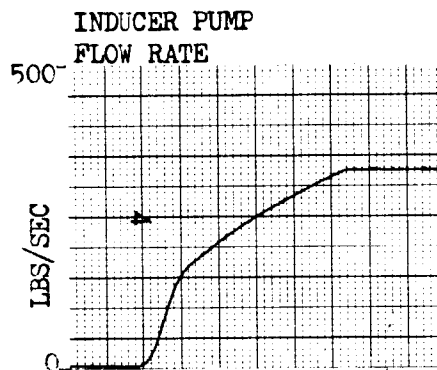
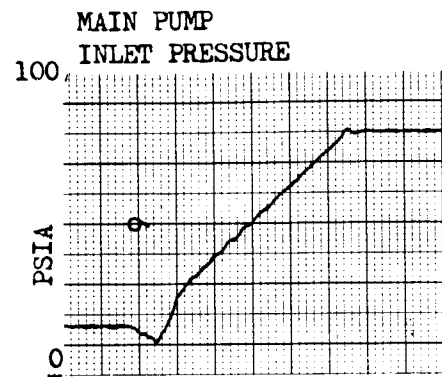
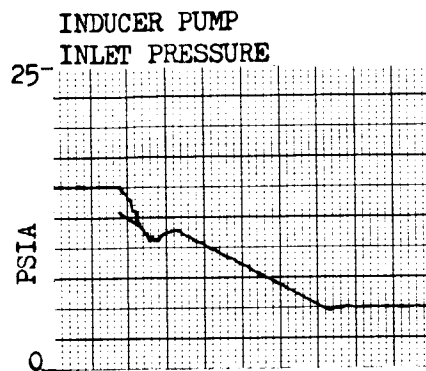
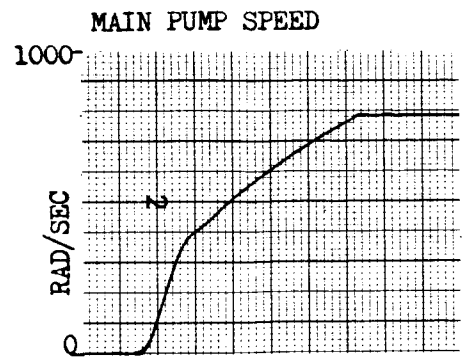
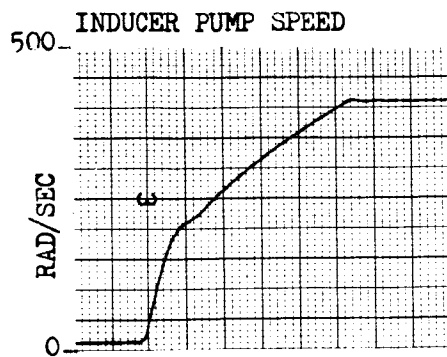


Figure 39. Remote-Coupled Low Moment of Inertia

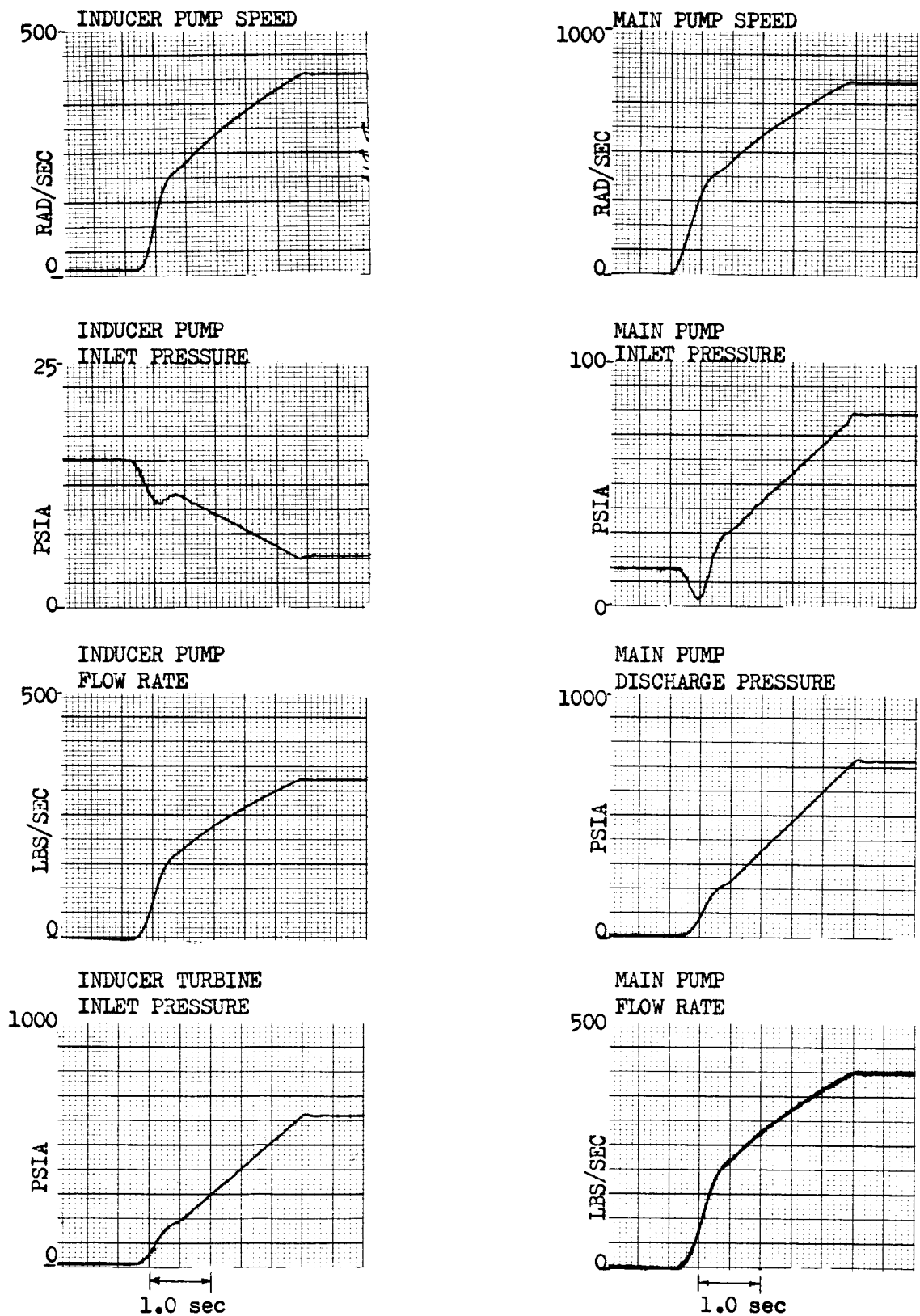


Figure 40. Close-Coupled High Moment of Inertia

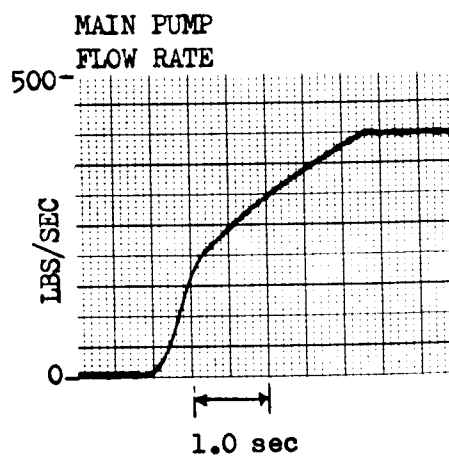
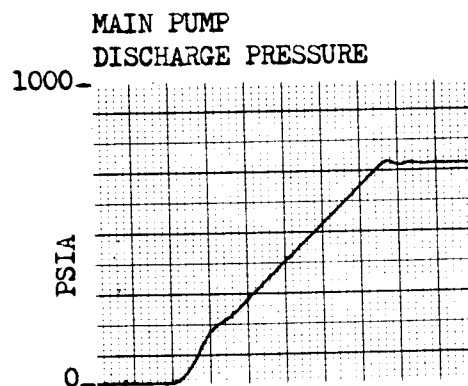
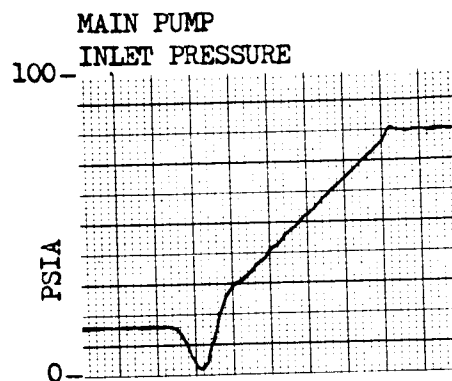
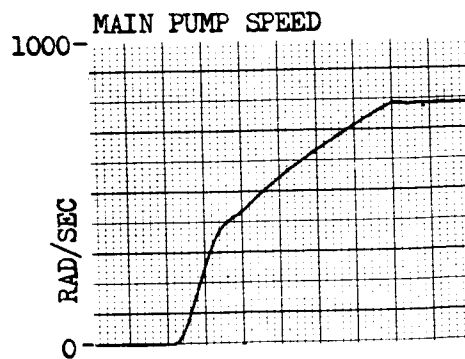
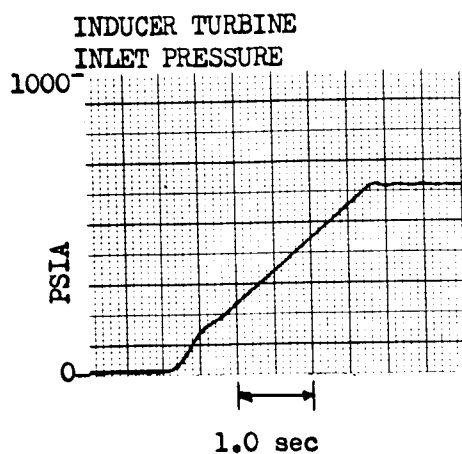
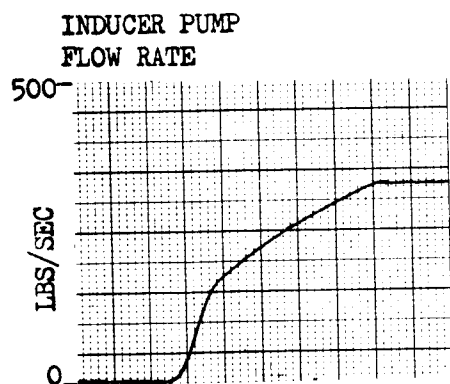
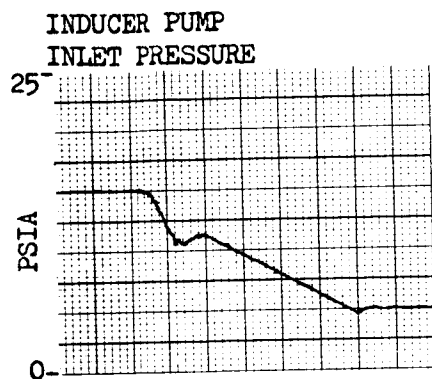
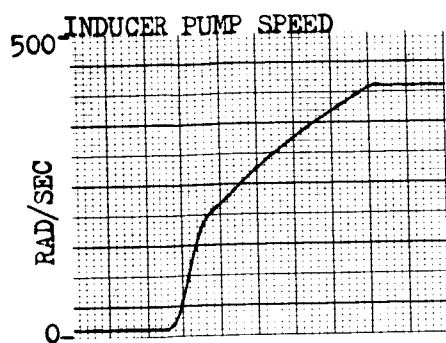


Figure 41. Remote-Coupled High Moment of Inertia

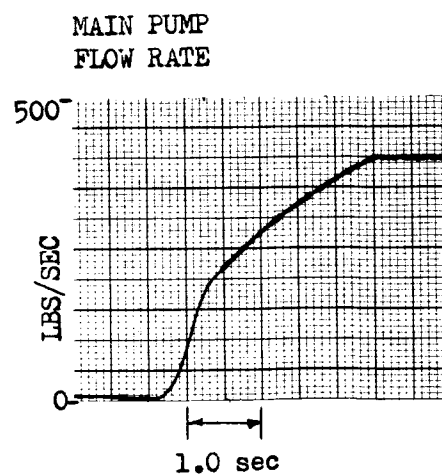
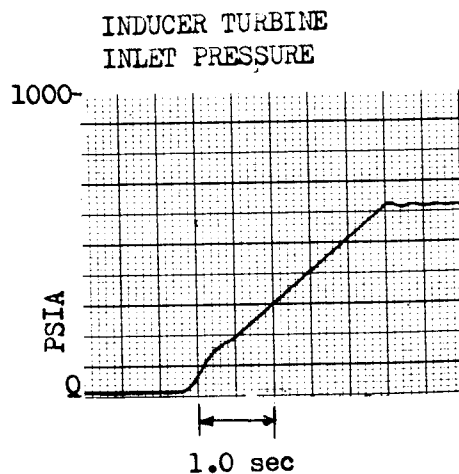
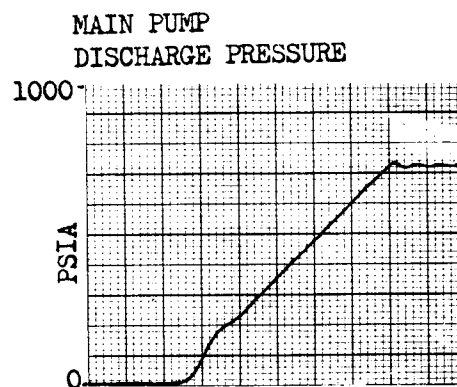
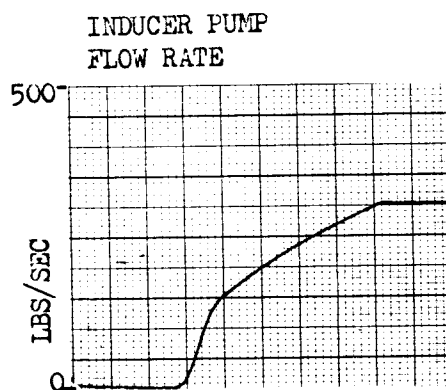
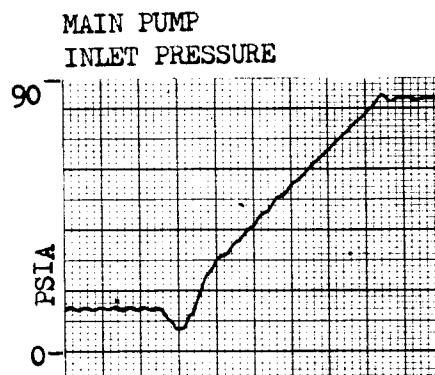
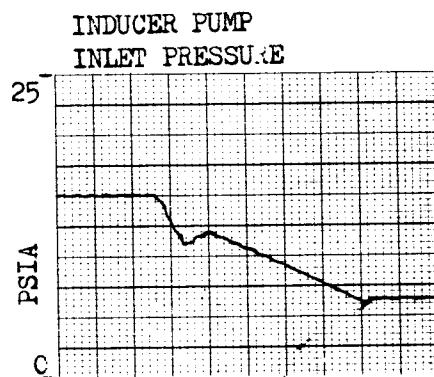
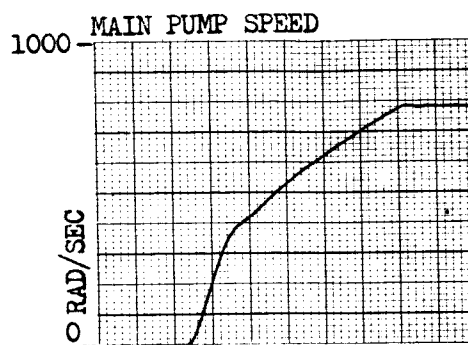
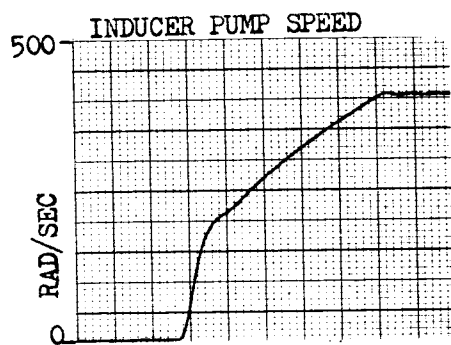


Figure 42. Remote-Coupled Low Coupling Line Fluid Inertia

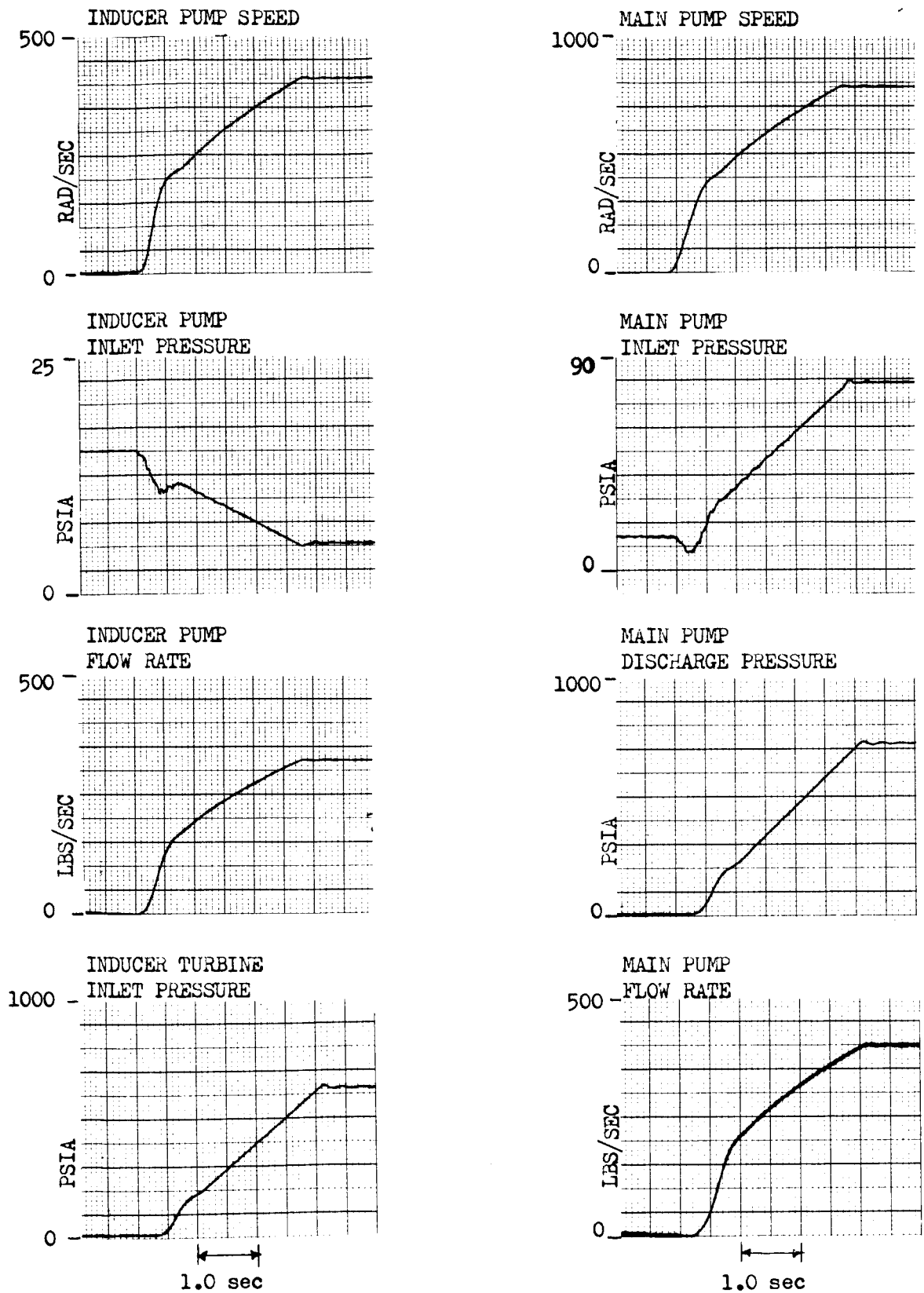


Figure 43. Close-Coupled Low Turbine Feed Line Resistance

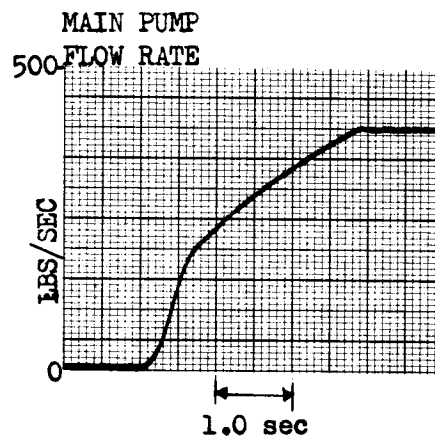
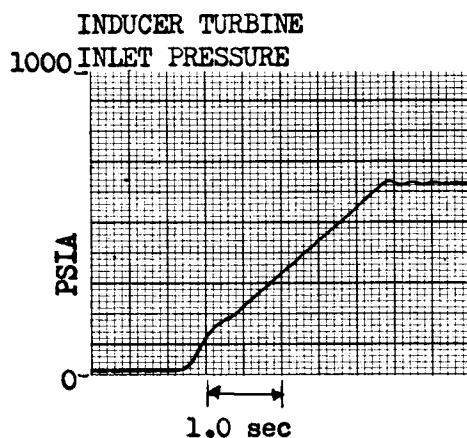
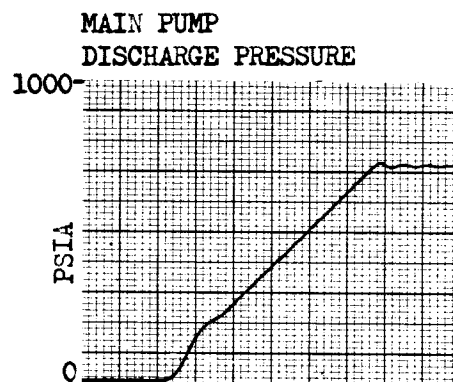
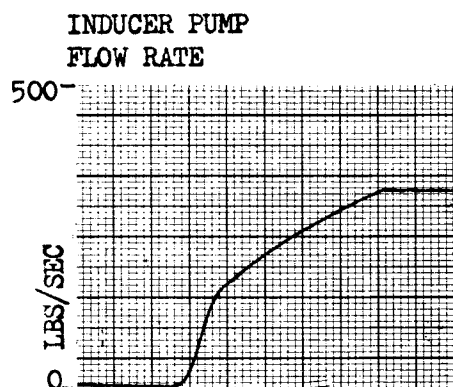
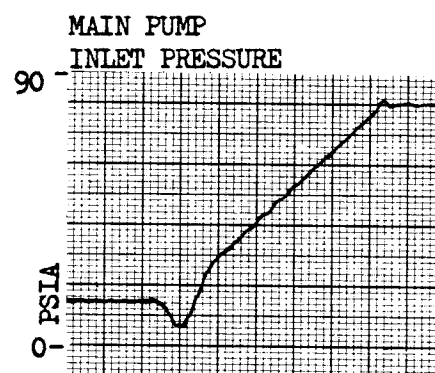
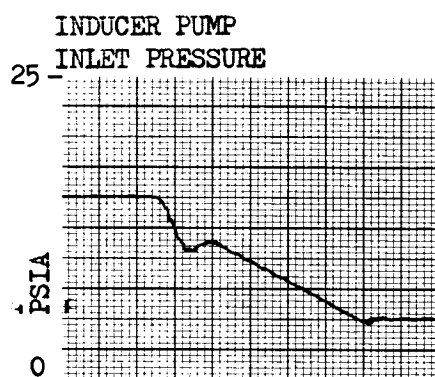
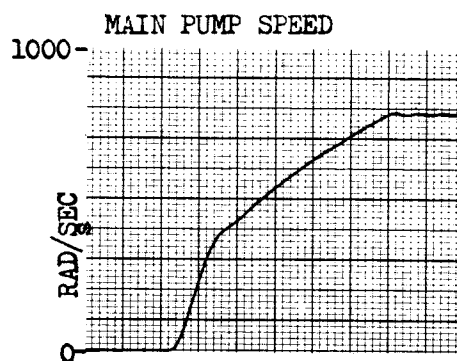
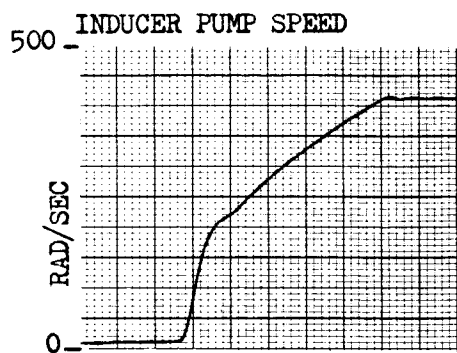


Figure 44. Remote-Coupled Low Turbine Feed Line Resistance

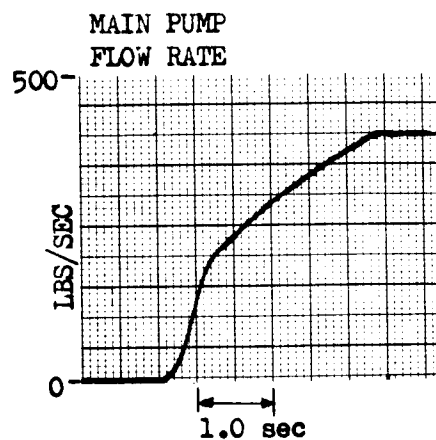
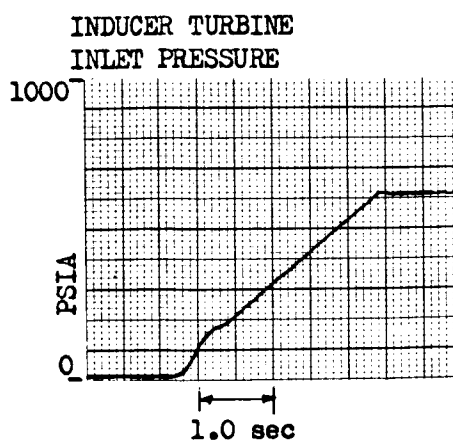
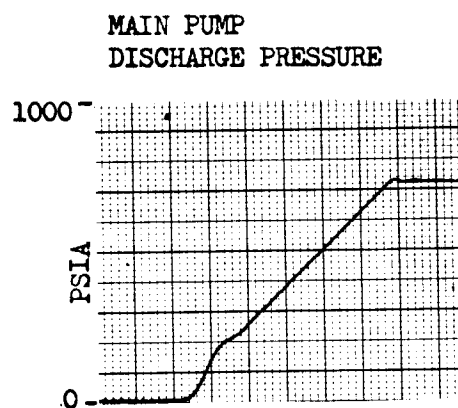
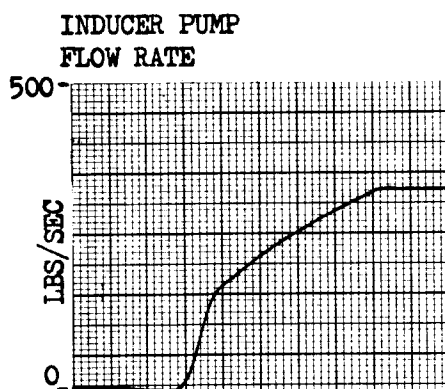
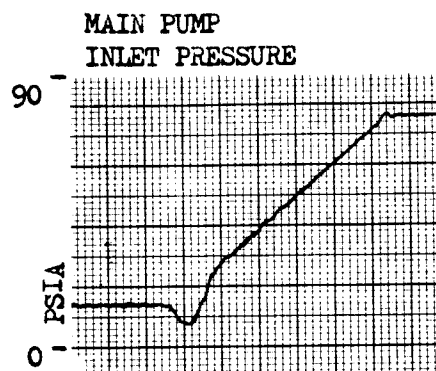
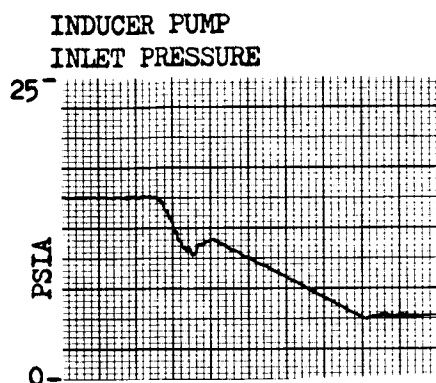
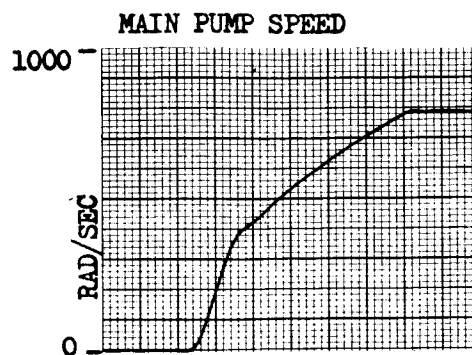
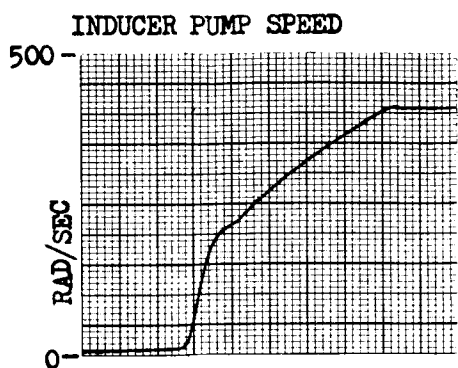


Figure 45. Close-Coupled High Turbine Feed Line Resistance

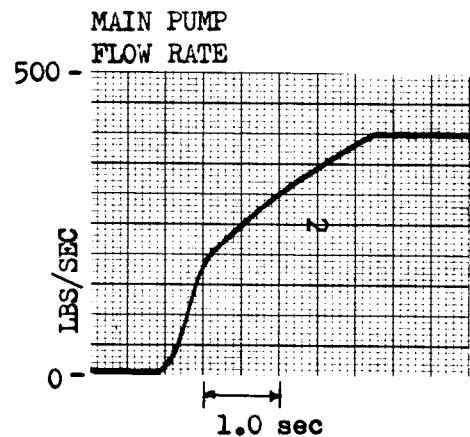
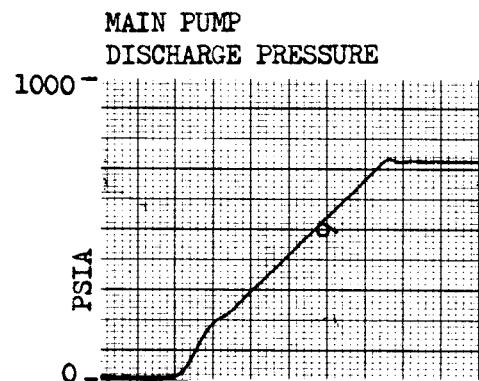
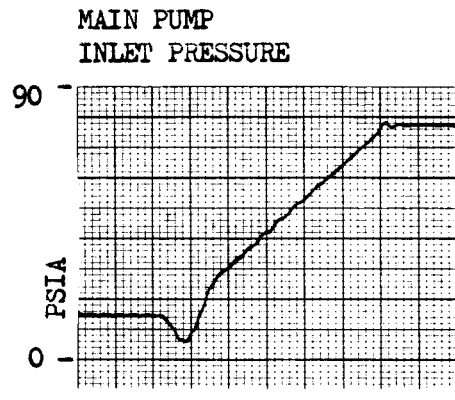
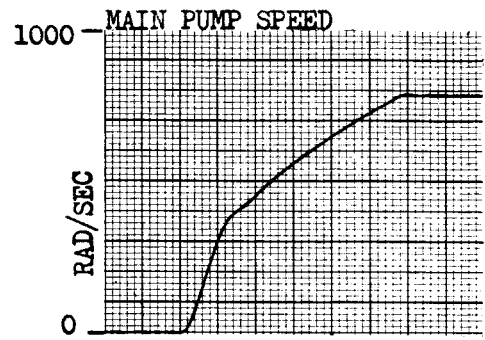
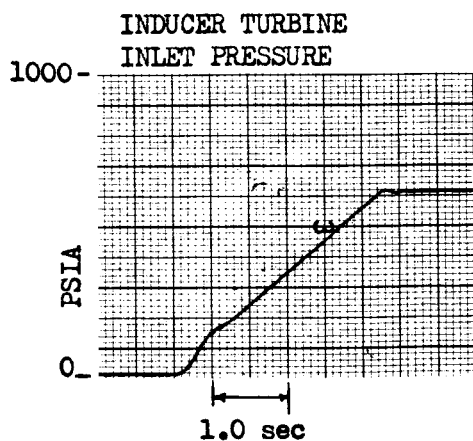
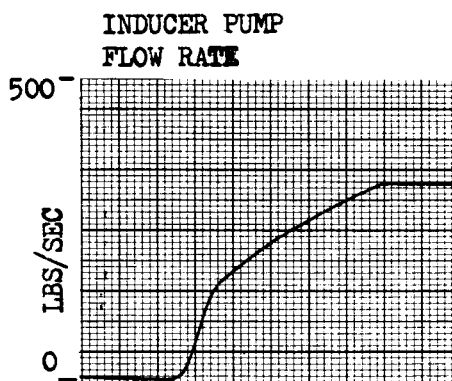
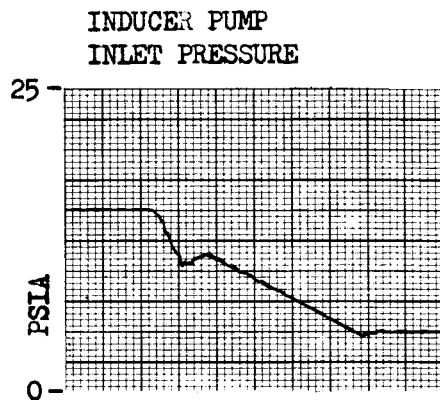
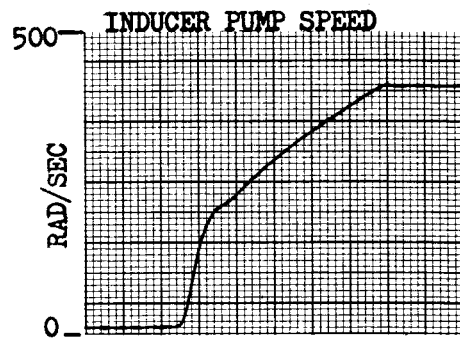


Figure 46. Remote-Coupled High Turbine Feed Line Resistance

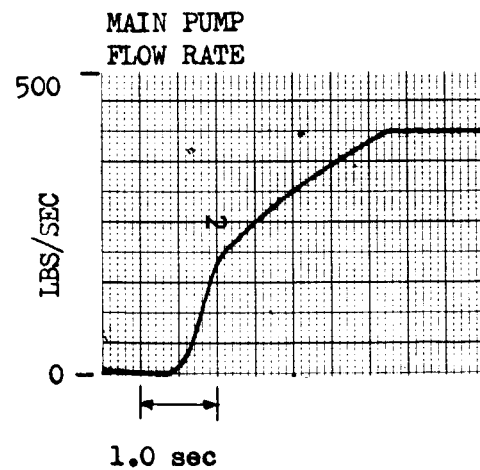
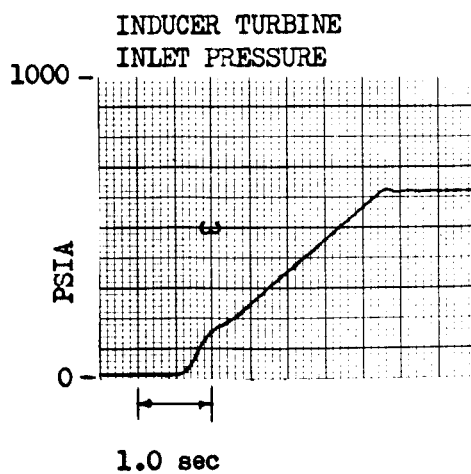
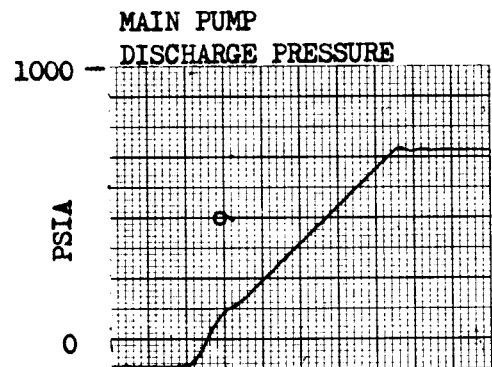
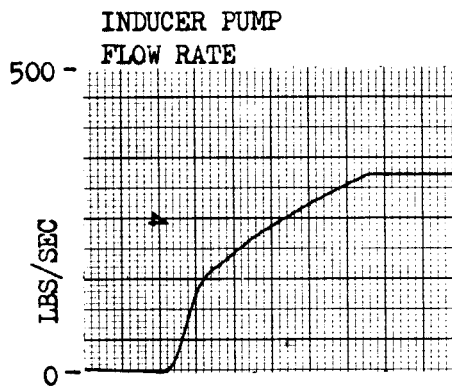
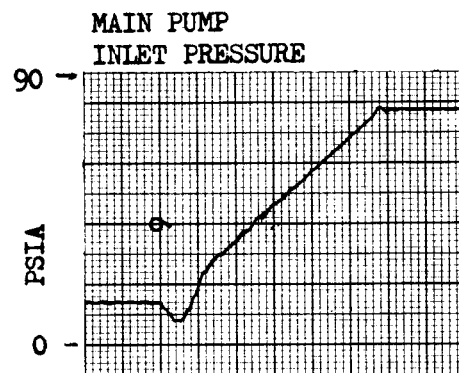
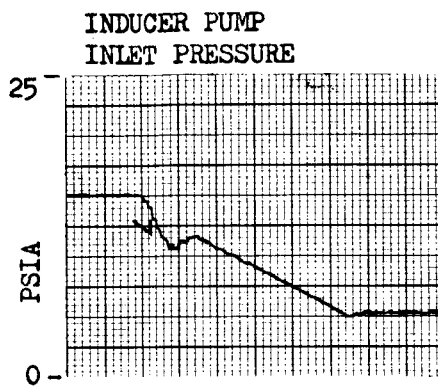
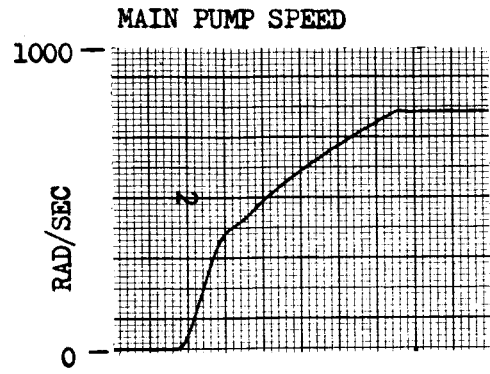
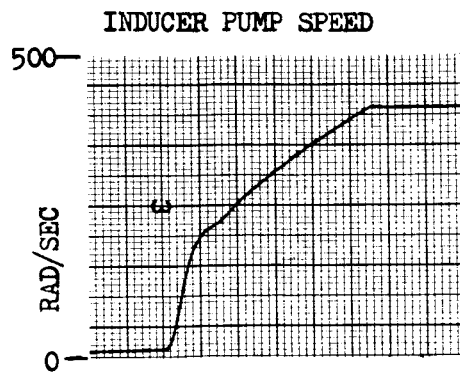


Figure 47. Close-Coupled Low Turbine Feed Line Fluid Inertia

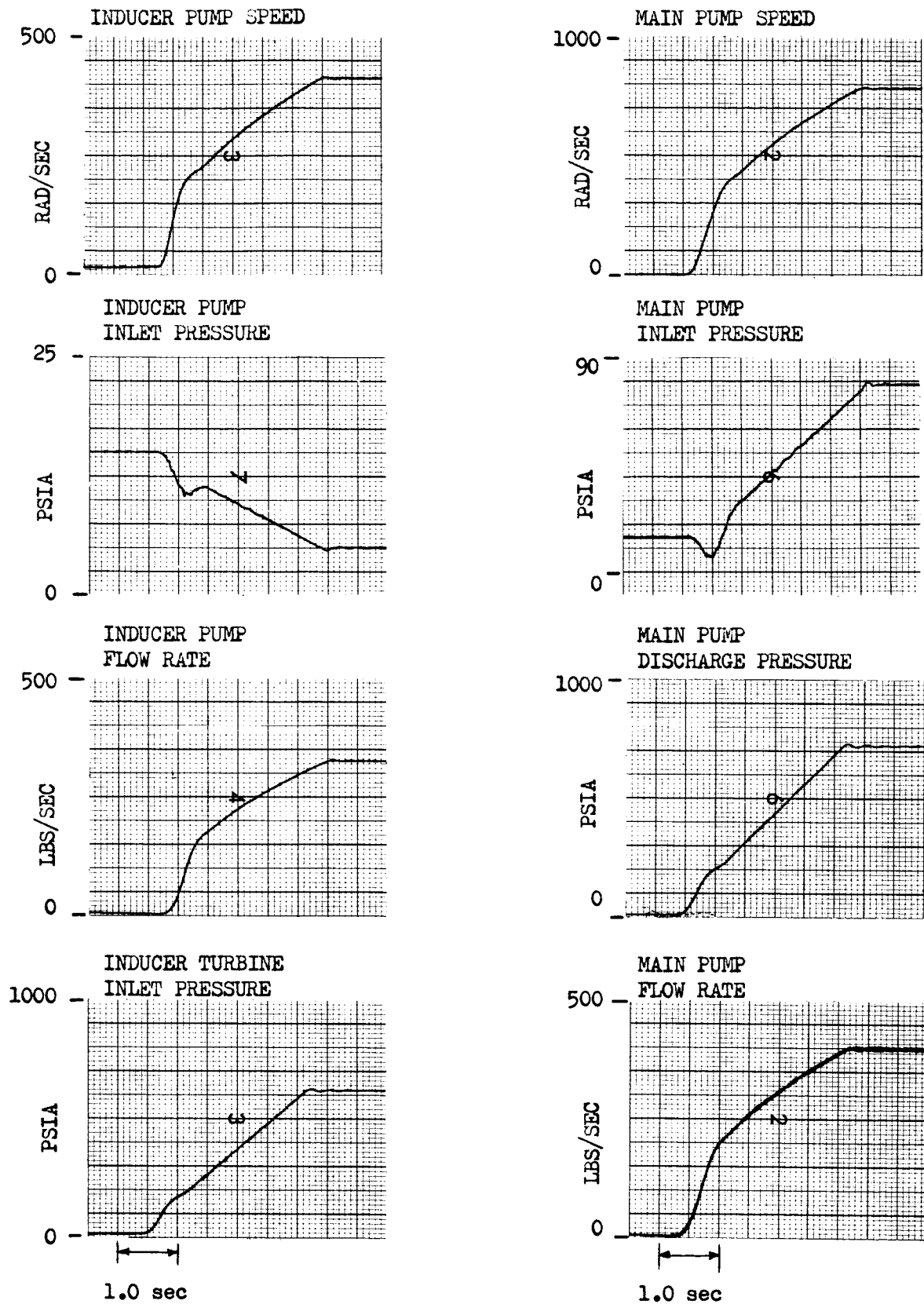


Figure 48. Remote-Coupled Low Turbine Feed Line Fluid Inertia

The final case in this portion of the study involved using the performance curves for a low-head preinducer having a pressure rise of 13 psi compared to about 75 psi for the test preinducer. Use of the low-head preinducer results in less power required to drive the preinducer and a reduction of the turbine flowrate from about 75 lb/sec to 20 lb/sec. This is a distinct advantage in that the main pump flowrate is reduced, resulting in less power required to drive the main pump. The results are presented in Fig. 49 for a close-coupled preinducer mounted in the water test facility with a 3.0-second speed ramp input to the main pump. It was found that the main pump inlet pressure depression is greater because of the reduced preinducer pump head. Slowing down the start, throttling the main flowrate during the first part of the start, or a combination of start time and throttling would improve this situation. It appears, therefore, that a practical low-head preinducer could be adapted to an engine with a possible sacrifice in start time.

TEST SYSTEM PERFORMANCE

The system performance of the proposed water test series was analyzed for both a close- and remote-coupled preinducer. For this study, the main pump drive was represented by a linear speed ramp input rather than a torque input, which results in less-severe system dynamic effects. With a torque input, the initial speed acceleration is high because of the low required pump torque at low speed and the relatively high input torque available from the drive motor. The resulting high pump acceleration produces more dynamic effects and a larger dip in the pump inlet pressure. For example, a 1.5-second speed ramp start results in less main pump inlet pressure loss than a 3.0-second torque input.

The test conditions for which predictions were made are presented in Table 3, and the results shown in Fig. 50 through 82. Smooth starts and speed changes were achieved for all ramp conditions with negligible dynamics. These results indicate that the inducer, as designed, will perform satisfactorily during transients in the range of engine start and throttling times.

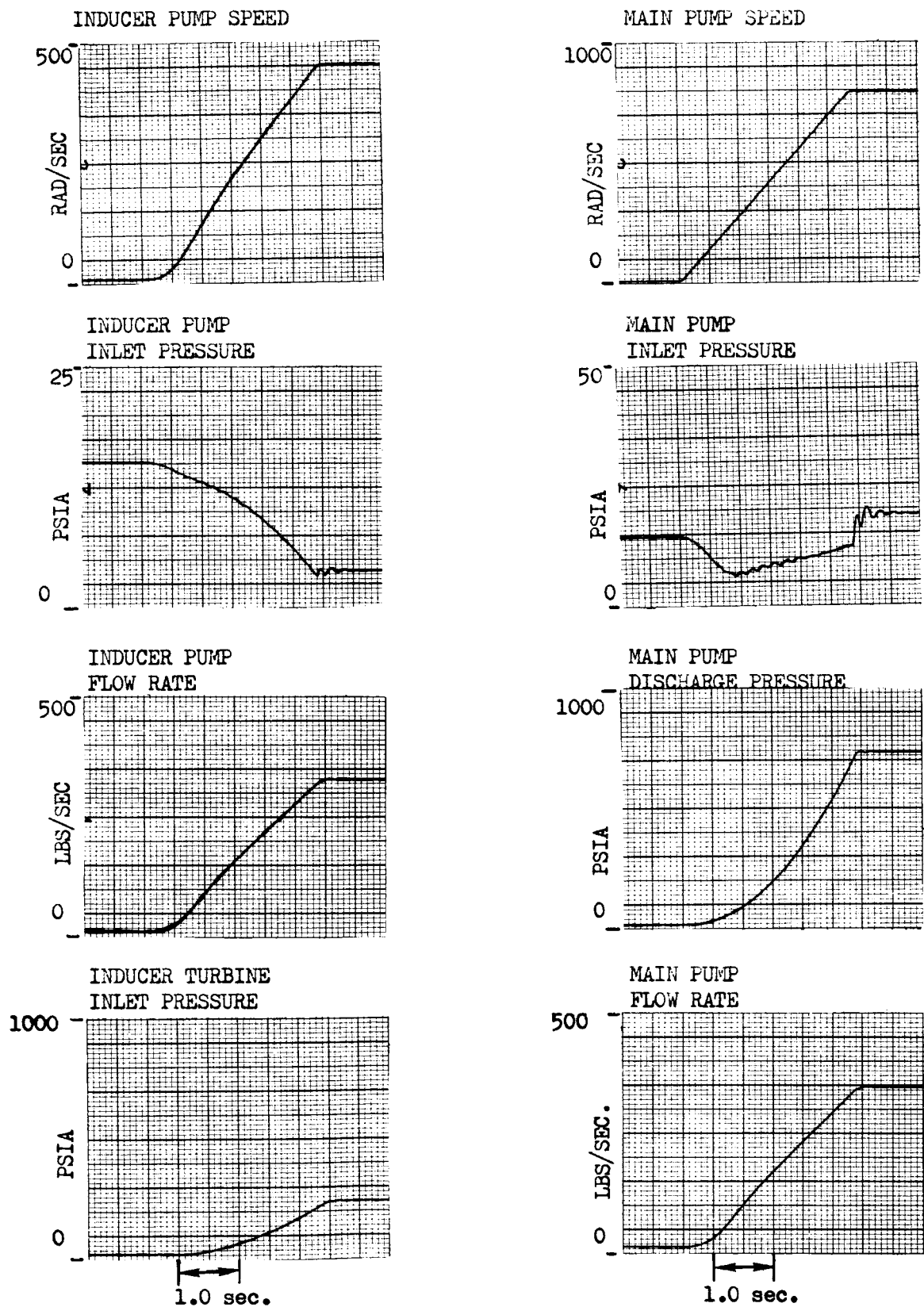


Figure 49. Close-Coupled Low-Head Inducer

TABLE 3

TRANSIENT TEST CONDITIONS*

1. Accelerate from 0- to 100-percent N and 100-percent Q/N in:	1.5	2.0	2.5	3.0	4.0
2. Accelerate from 0- to 100-percent N and 120-percent Q/N in:	2.0	3.0	4.0	--	--
3. Ramp from 100-percent N, 100-percent Q/N to 65-percent N in:	1.0	2.0	3.0	4.0	3.0
Accelerate from 65-percent N to 100-percent N in:	0.5	1.0	1.5	2.0	4.0

*Values are in seconds

N = speed

Q = flow

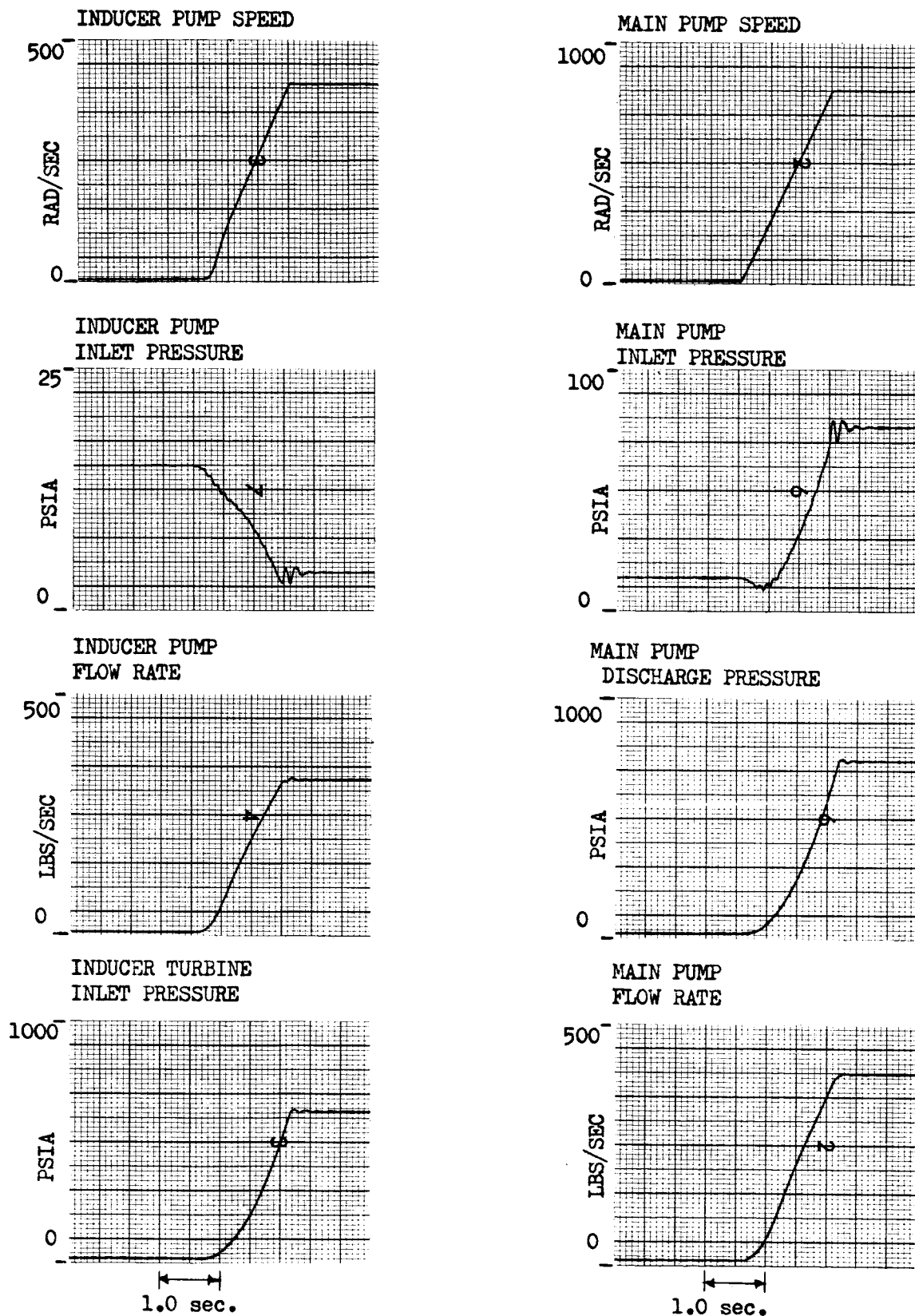


Figure 50. Close-Coupled Test Start to 100-Percent Q/N , 1.5-Second Speed Ramp

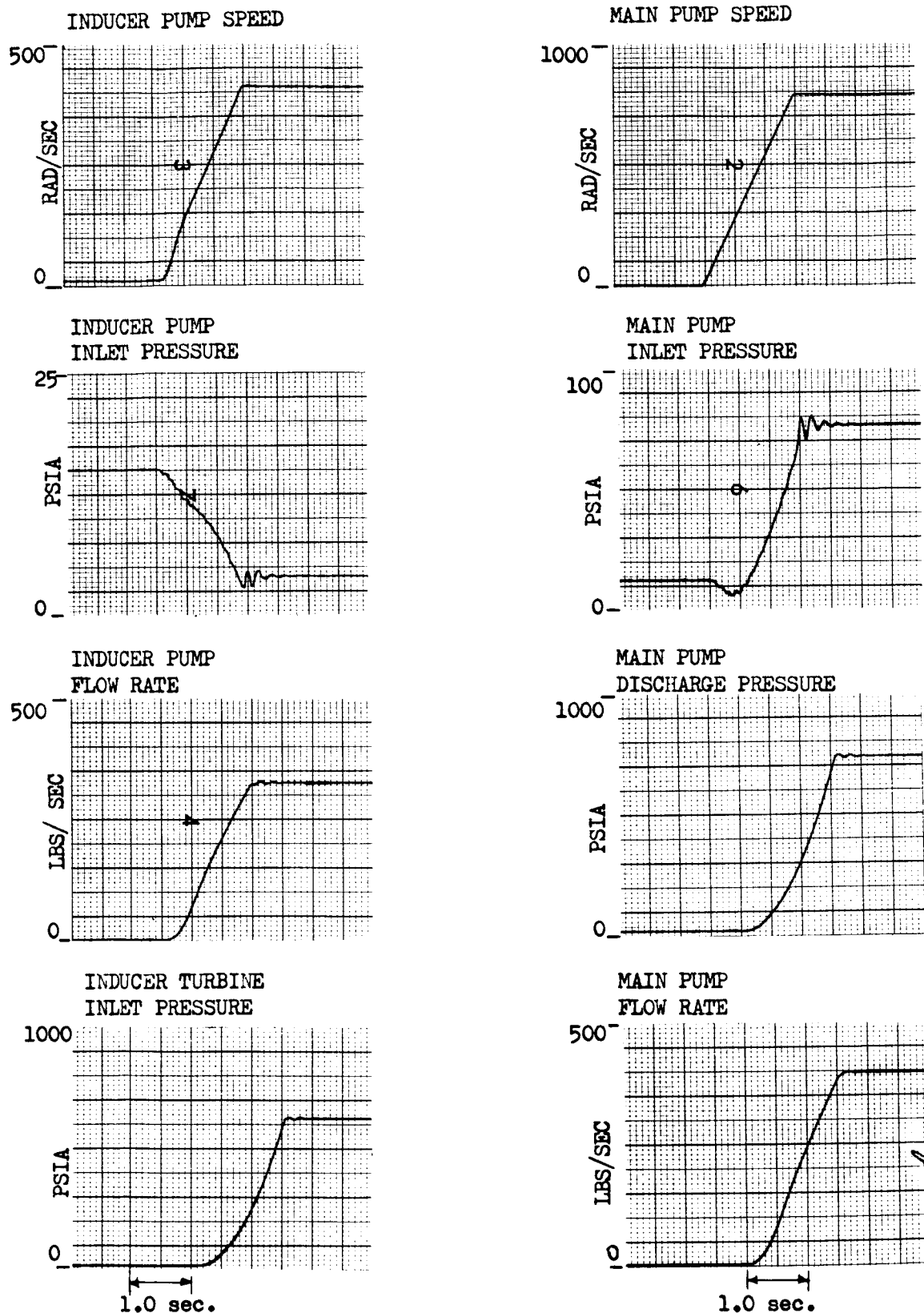


Figure 51. Remote-Coupled Test Start to 100-Percent Q/N, 1.5-Second Speed Ramp

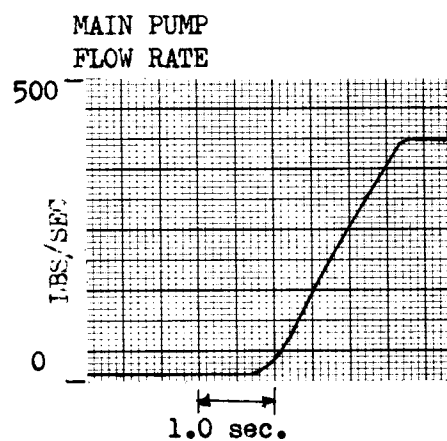
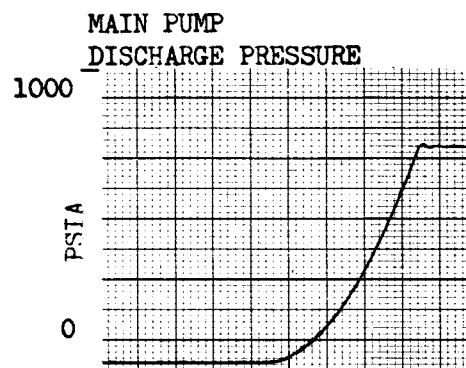
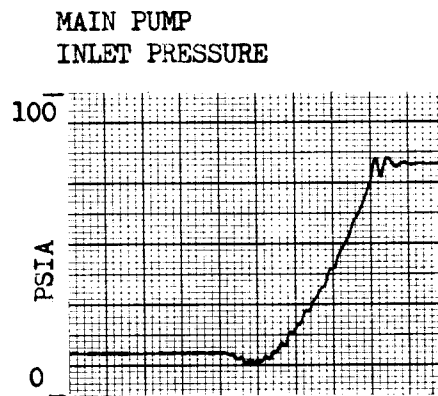
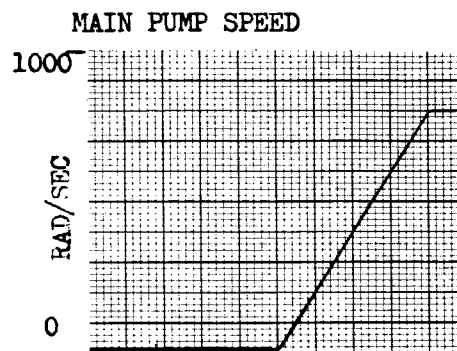
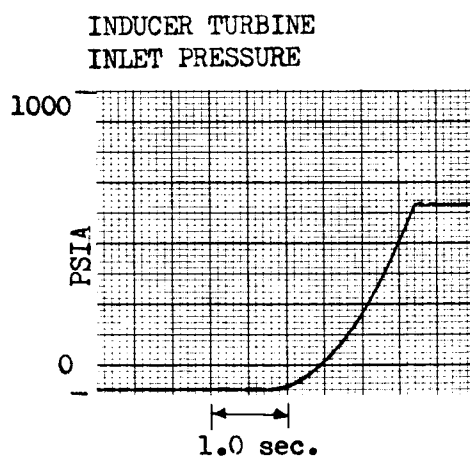
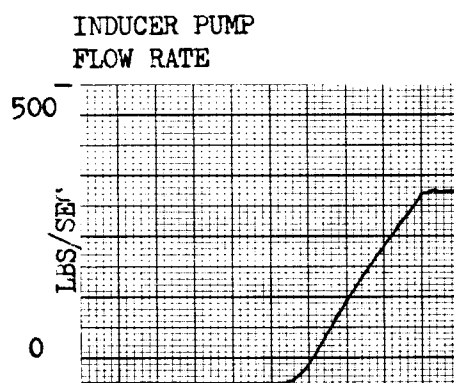
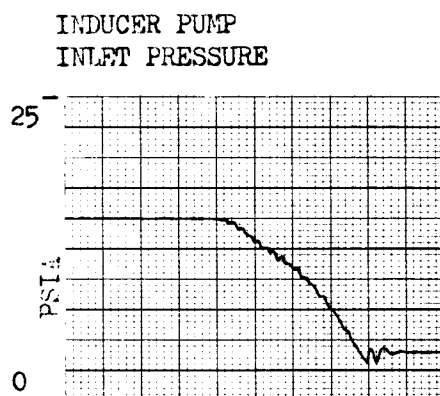
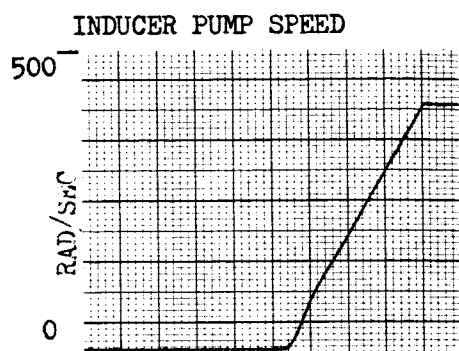


Figure 52. Close-Coupled Test Start to 100-Percent Q/N, 2.0-Second Speed Ramp

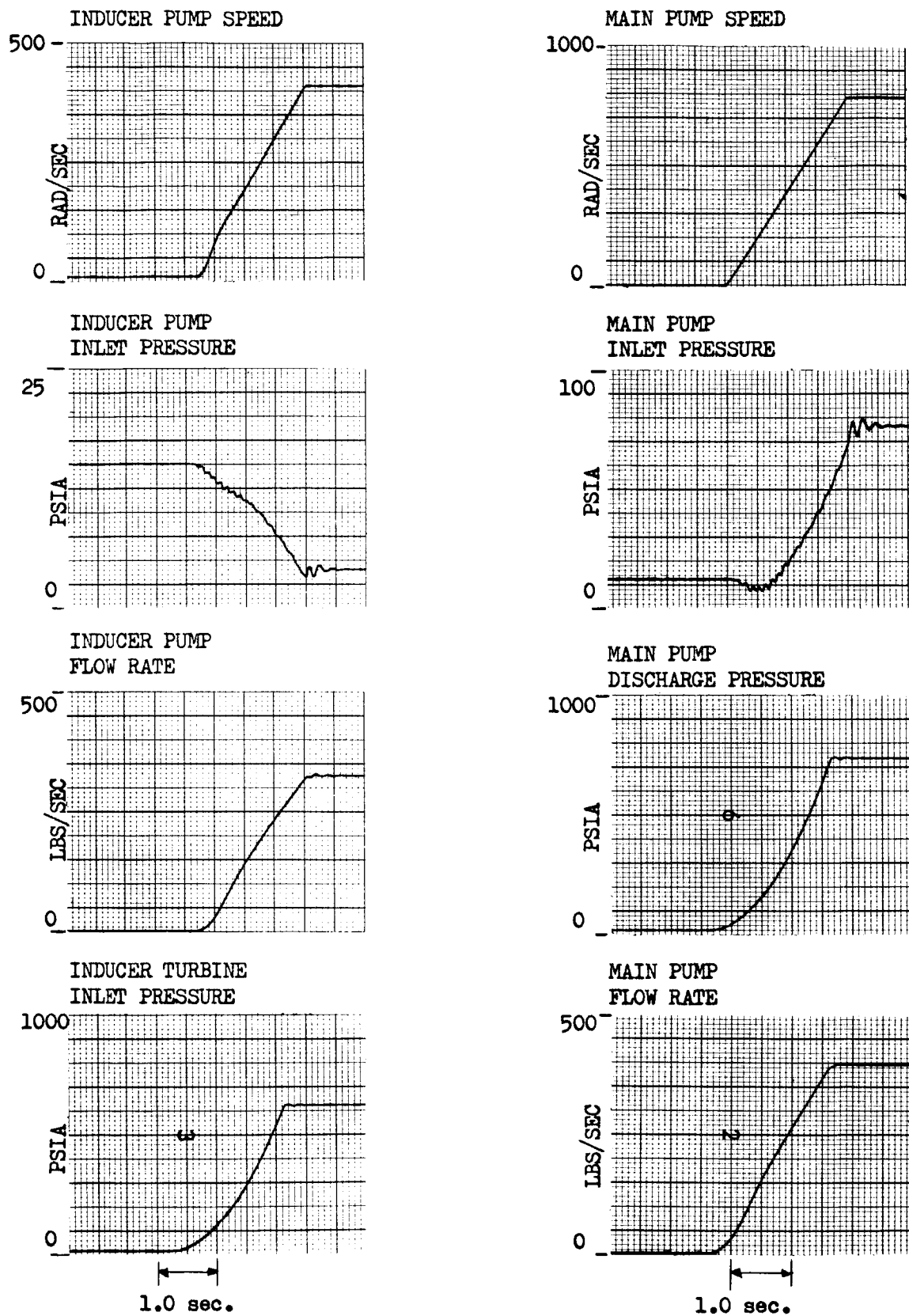


Figure 53. Remote-Coupled Test Start to 100-Percent Q/N, 2.0-Second Speed Ramp

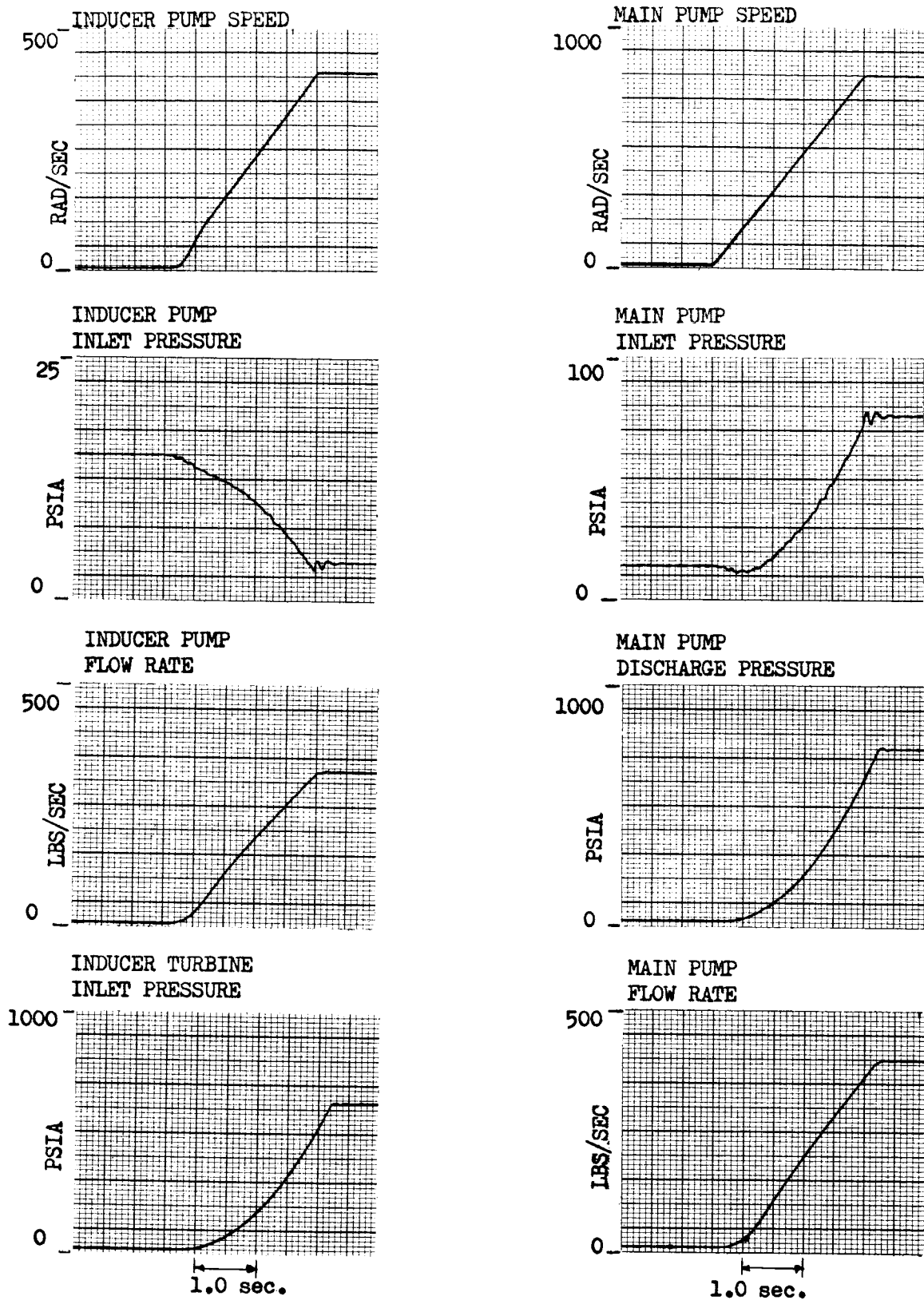


Figure 54. Close-Coupled Test Start to 100-Percent Q/N, 2.5-Second Speed Ramp

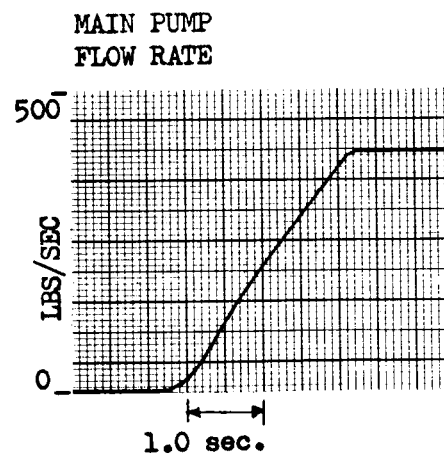
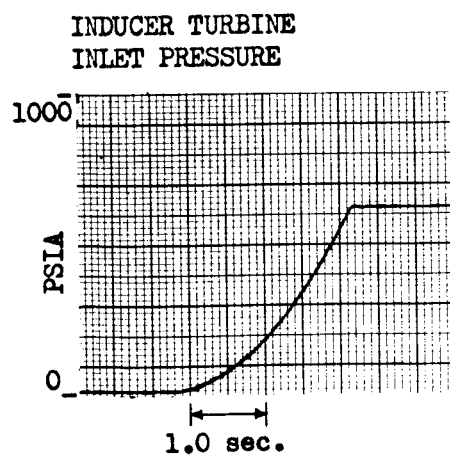
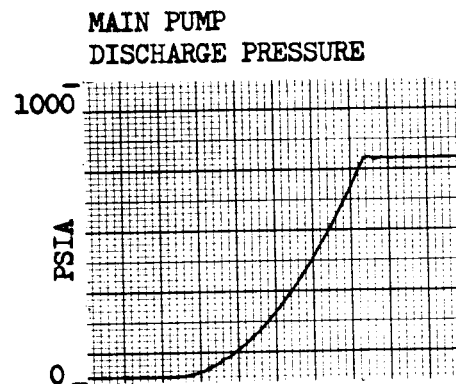
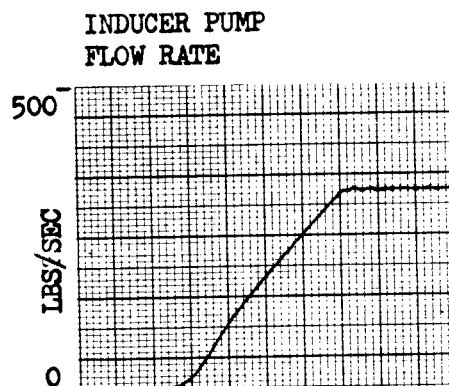
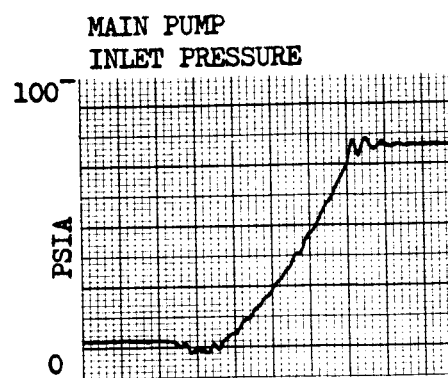
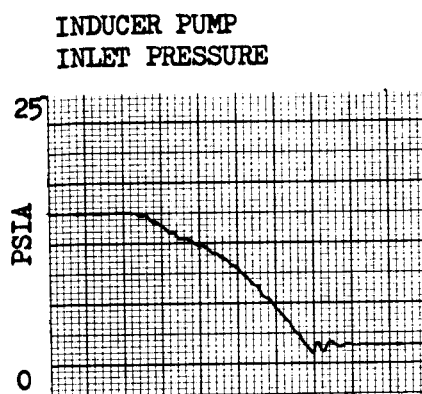
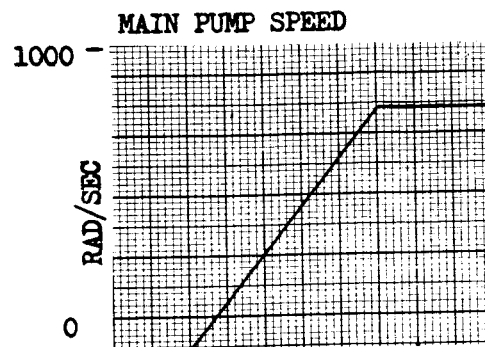
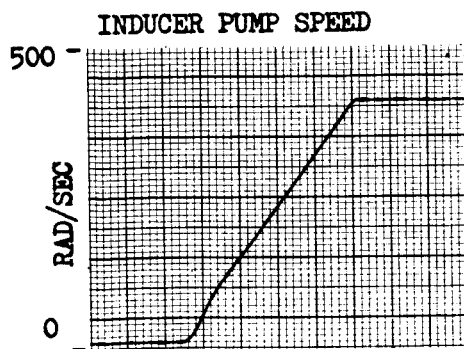


Figure 55. Remote-Coupled Test Start to 100-Percent Q/N, 2.5-Second Speed Ramp

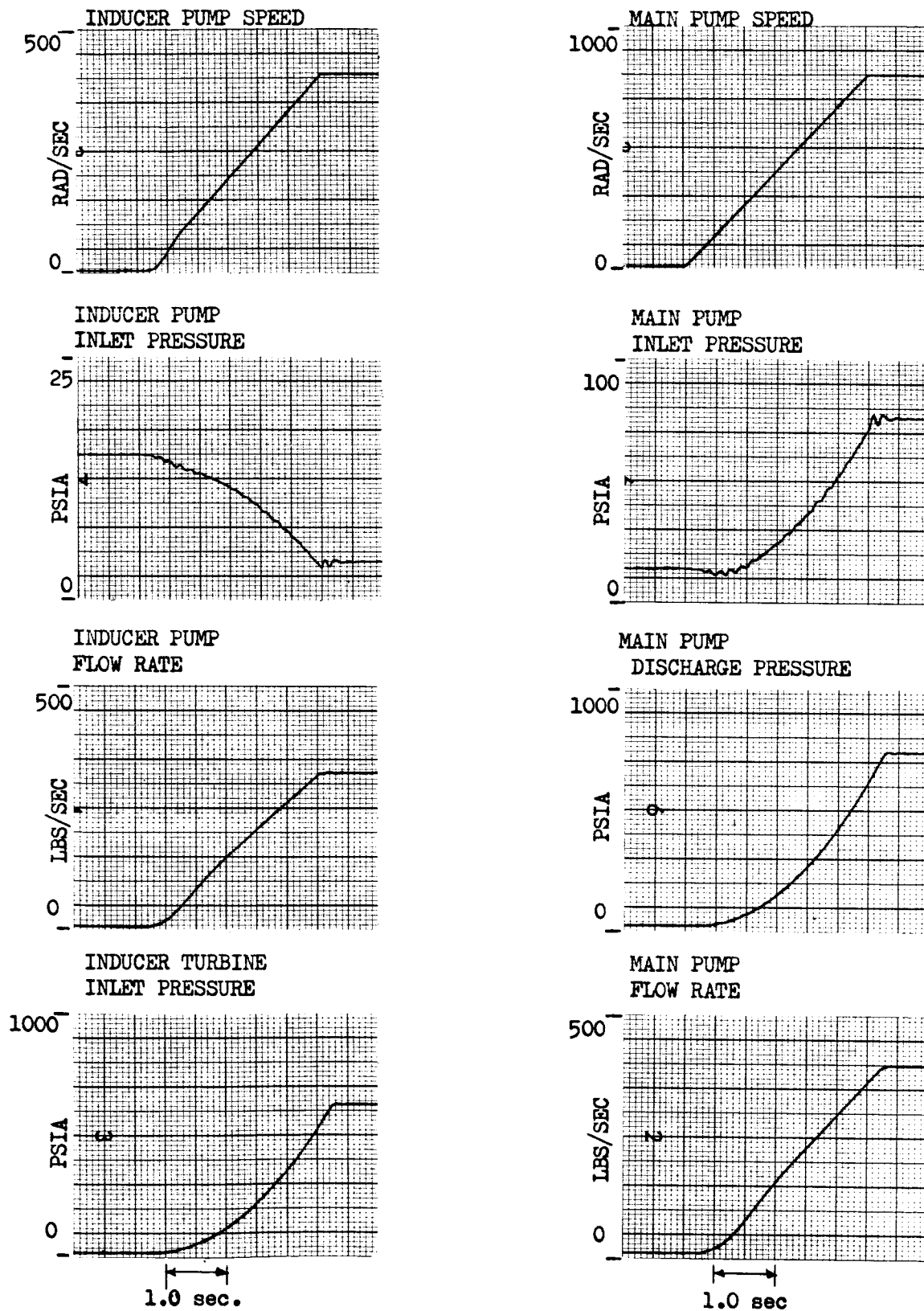


Figure 56. Close-Coupled Test Start to 100-Percent Q/N, 3.0-Second Speed Ramp

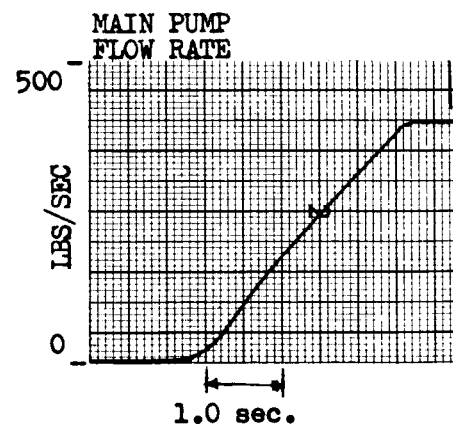
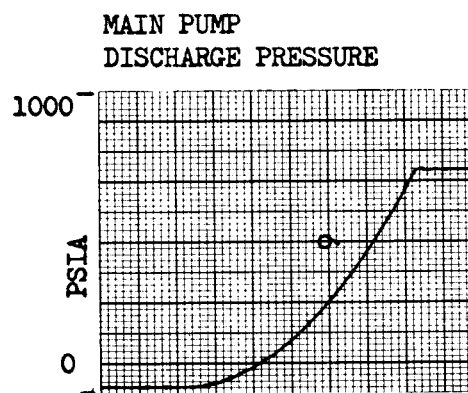
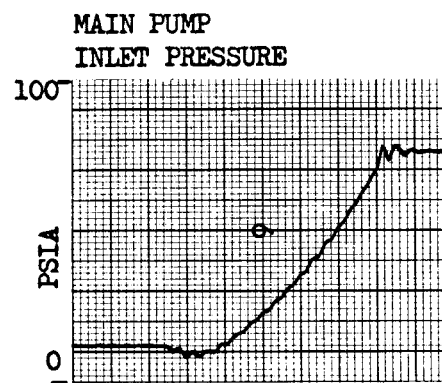
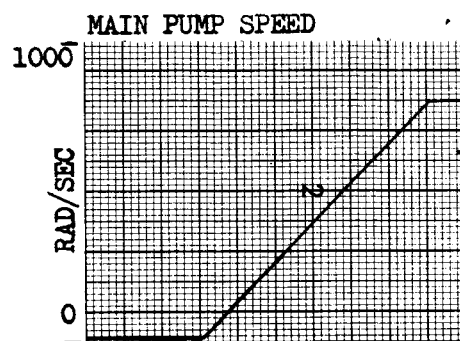
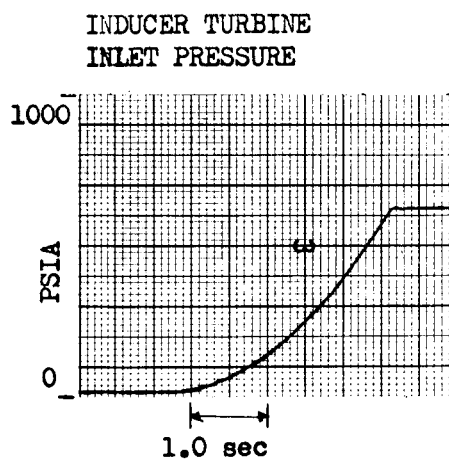
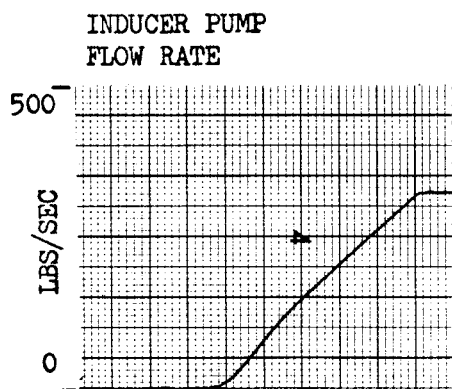
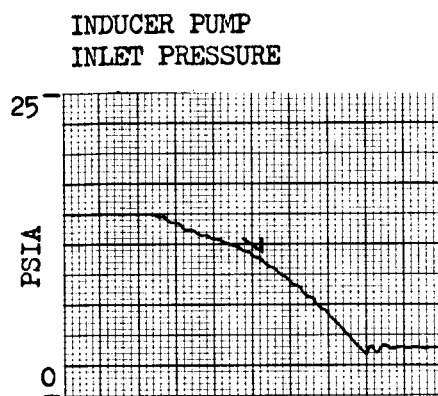
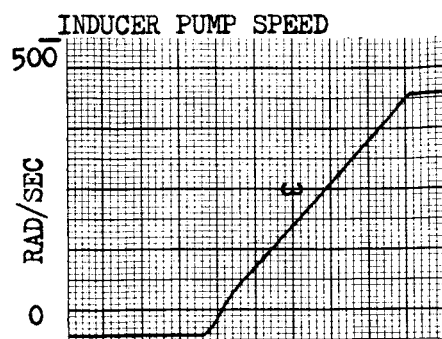


Figure 57. Remote-Coupled Test Start to 100-Percent Q/N, 3.0-Second Speed Ramp

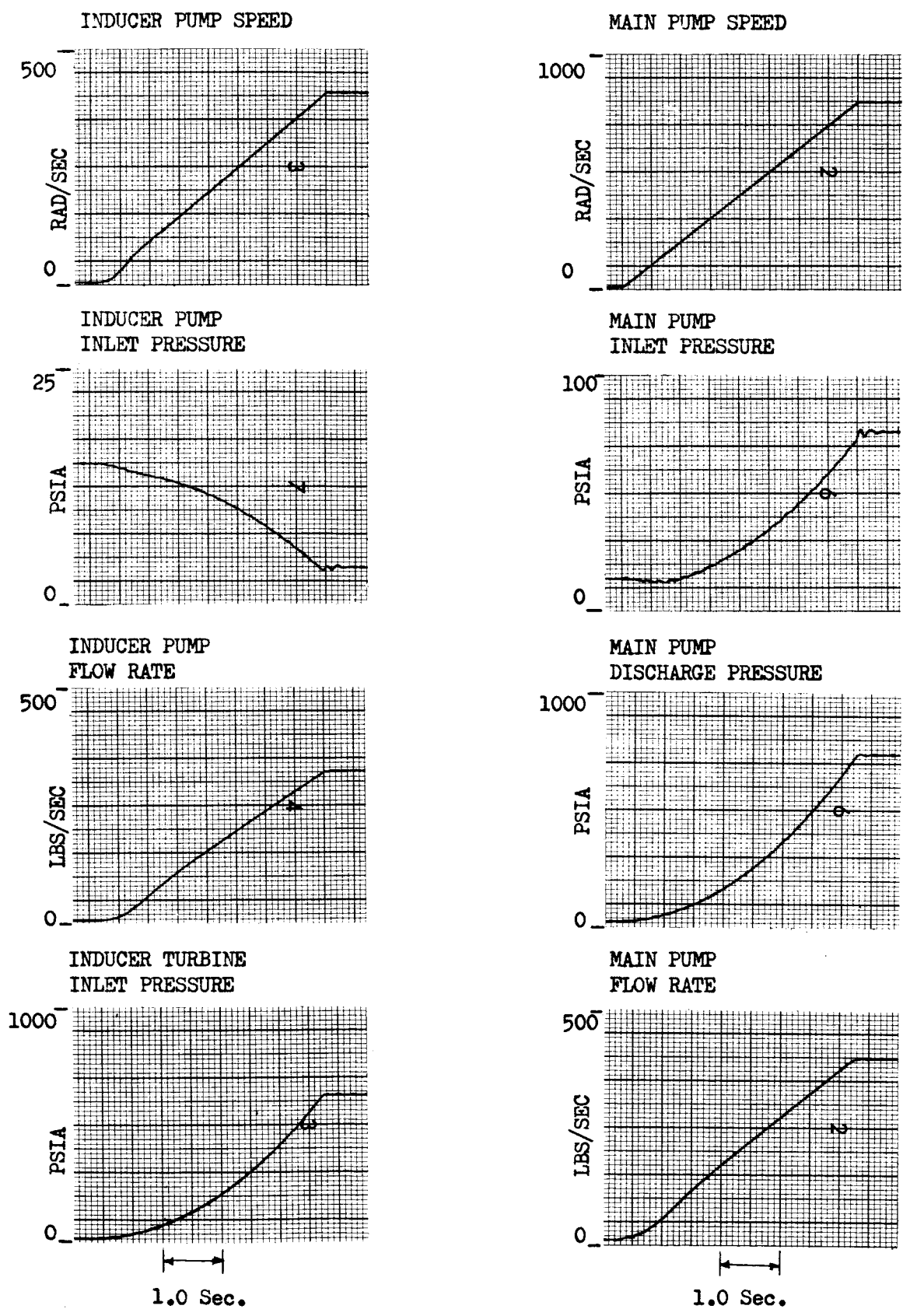


Figure 58. Close-Coupled Test Start to 100-Percent Q/N, 4.0-Second Speed Ramp

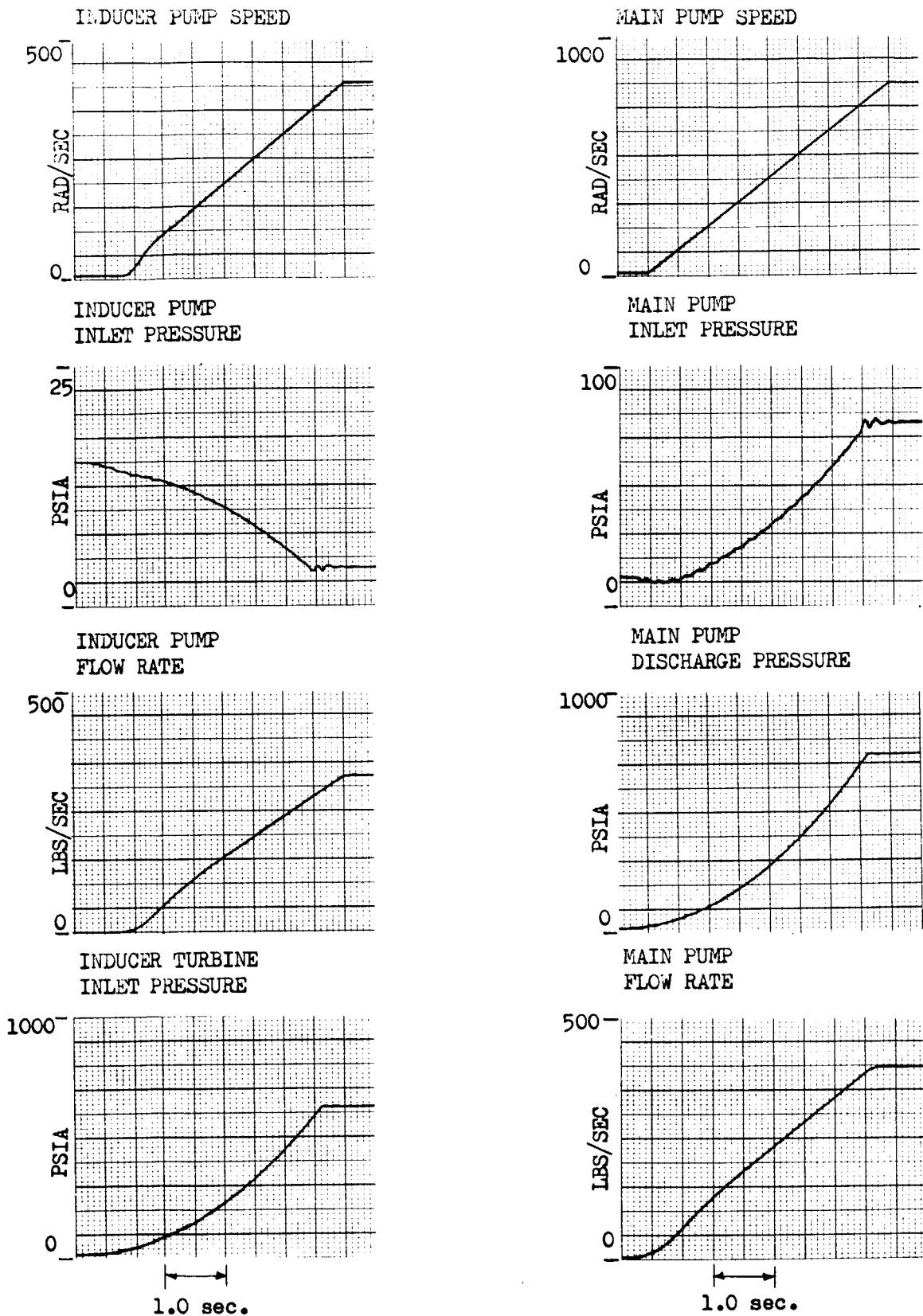


Figure 59. Remote-Coupled Test Start to 100-Percent Q/N, 4.0-Second Speed Ramp

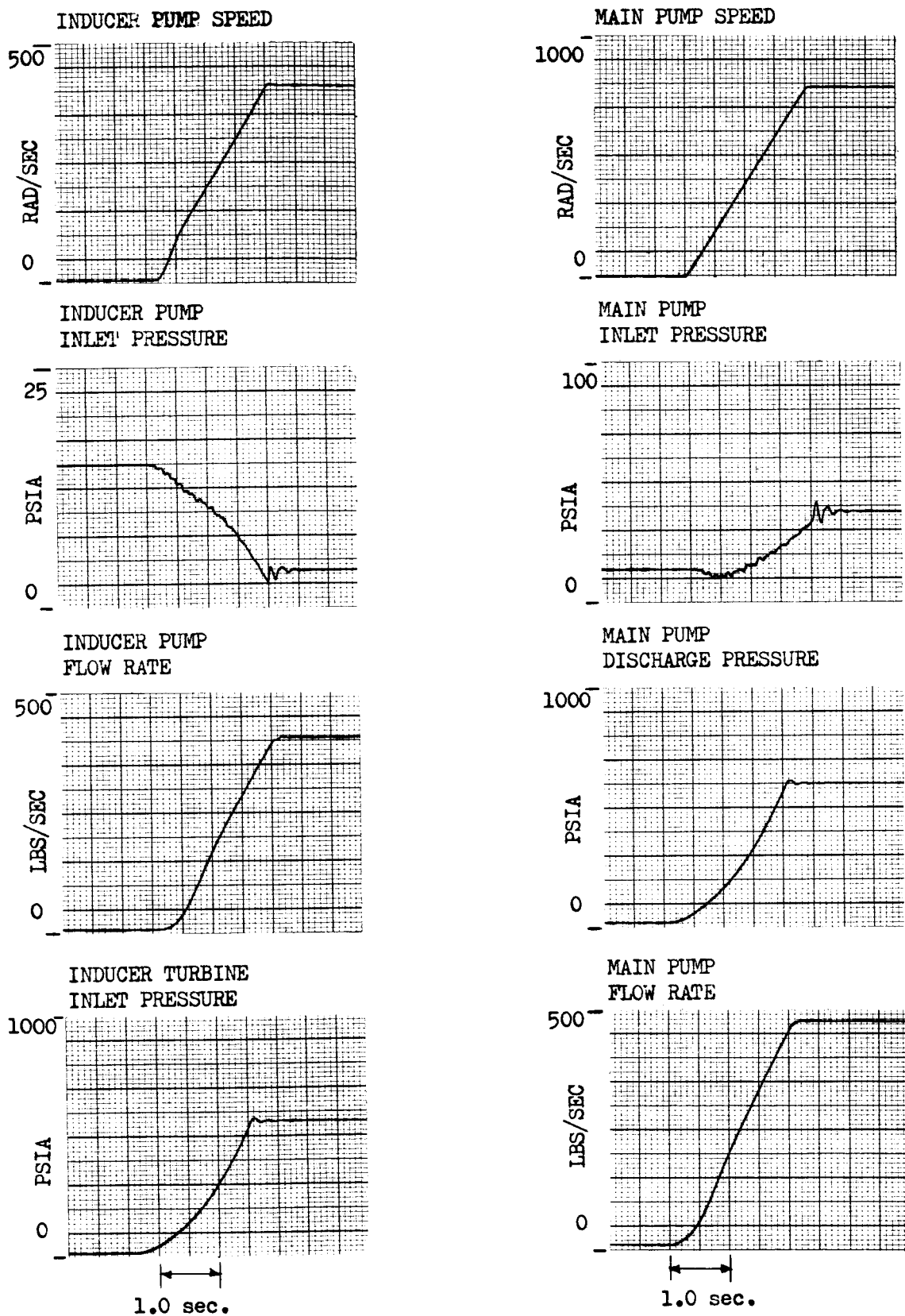


Figure 60. Close-Coupled Test Start to 120-Percent Q/N , 2.0-Second Speed Ramp

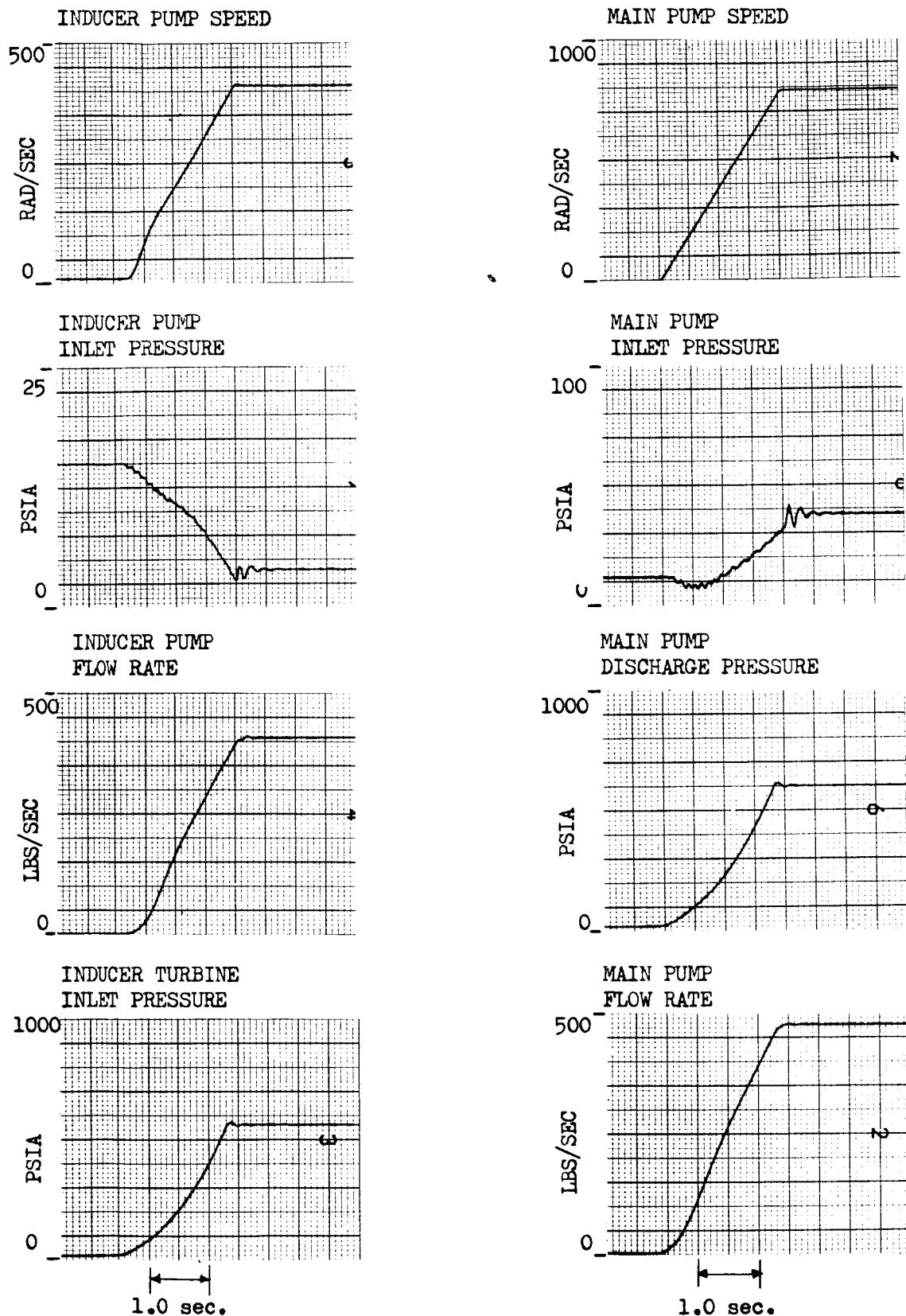


Figure 61. Remote-Coupled Test Start to 120-Percent Q/N , 2.0-Second Speed Ramp

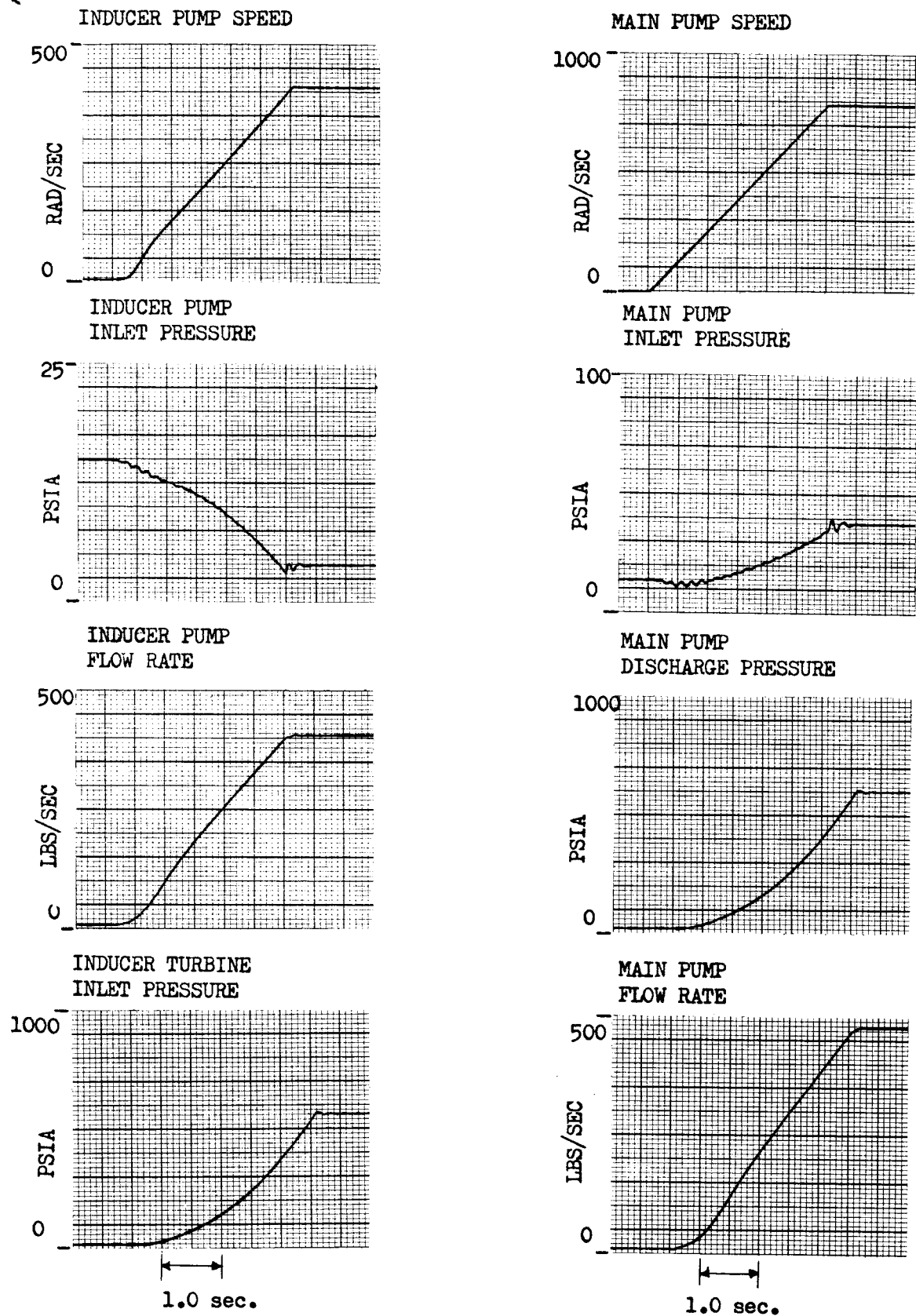


Figure 62. Close-Coupled Test Start to 120-Percent Q/N , 3.0-Second Speed Ramp

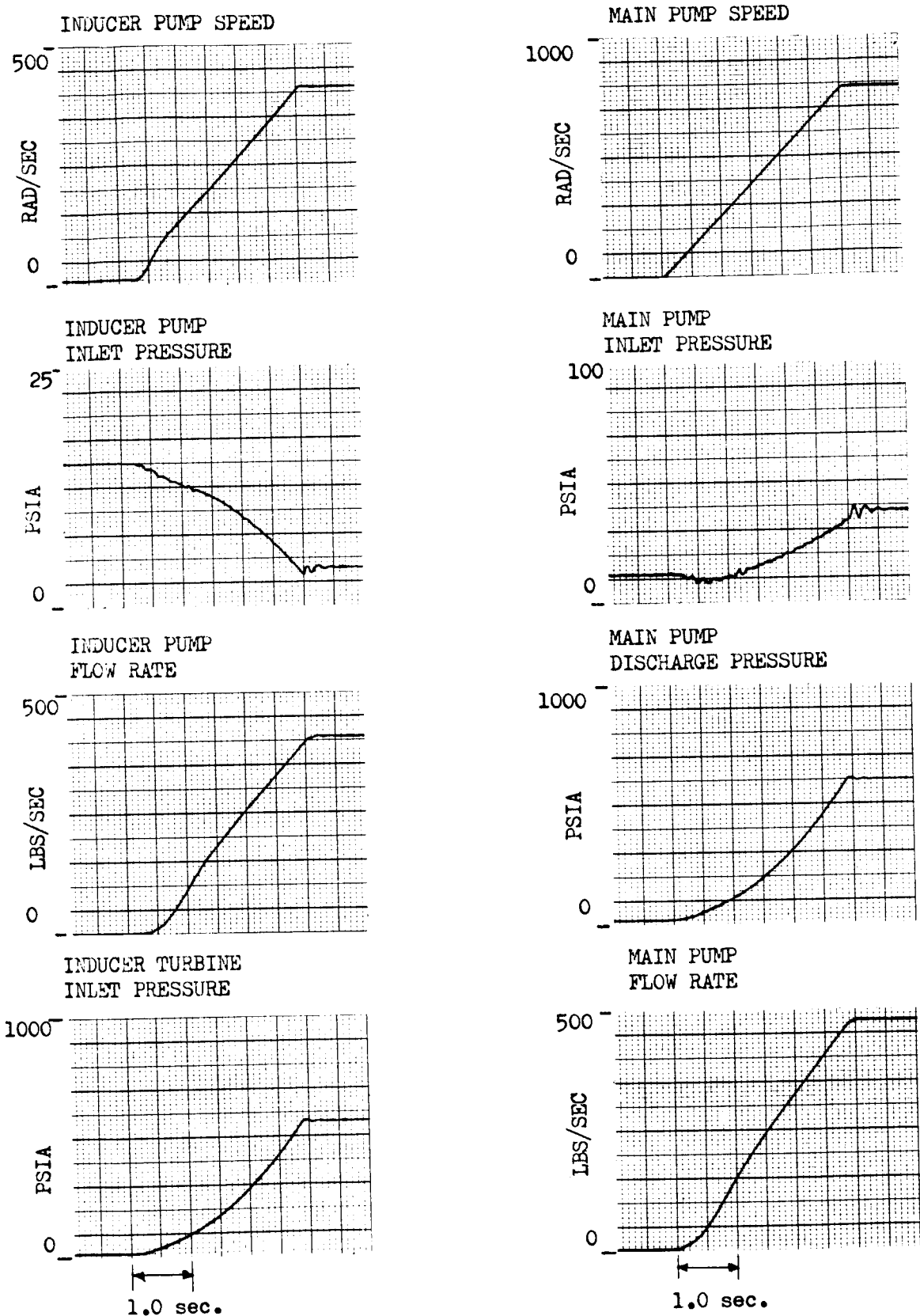


Figure 63. Remote-Coupled Test Start to 120-Percent Q/N, 3.0-Second Speed Ramp

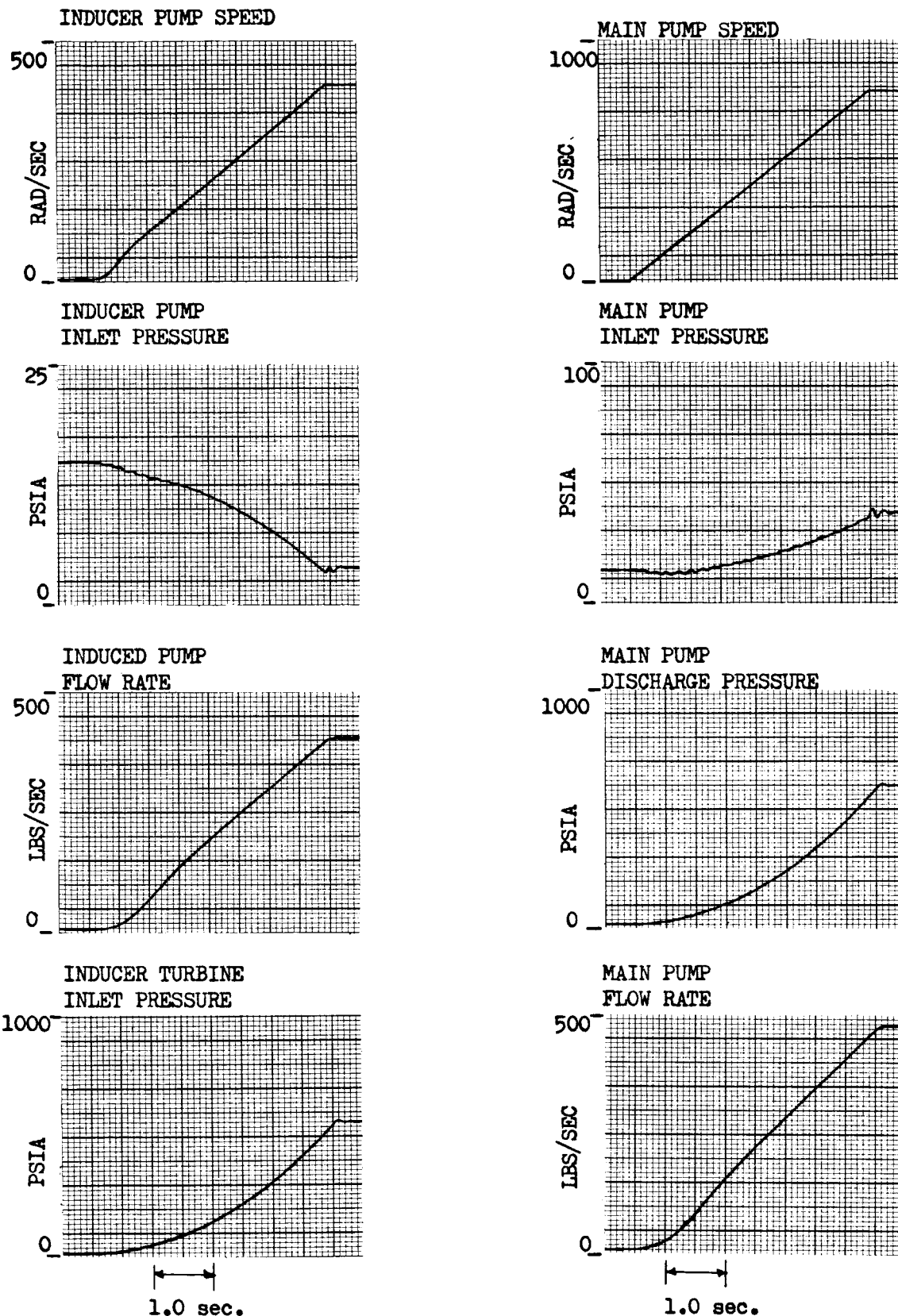


Figure 64. Close-Coupled Test Start to 120-Percent Q/N, 4.0-Second Speed Ramp

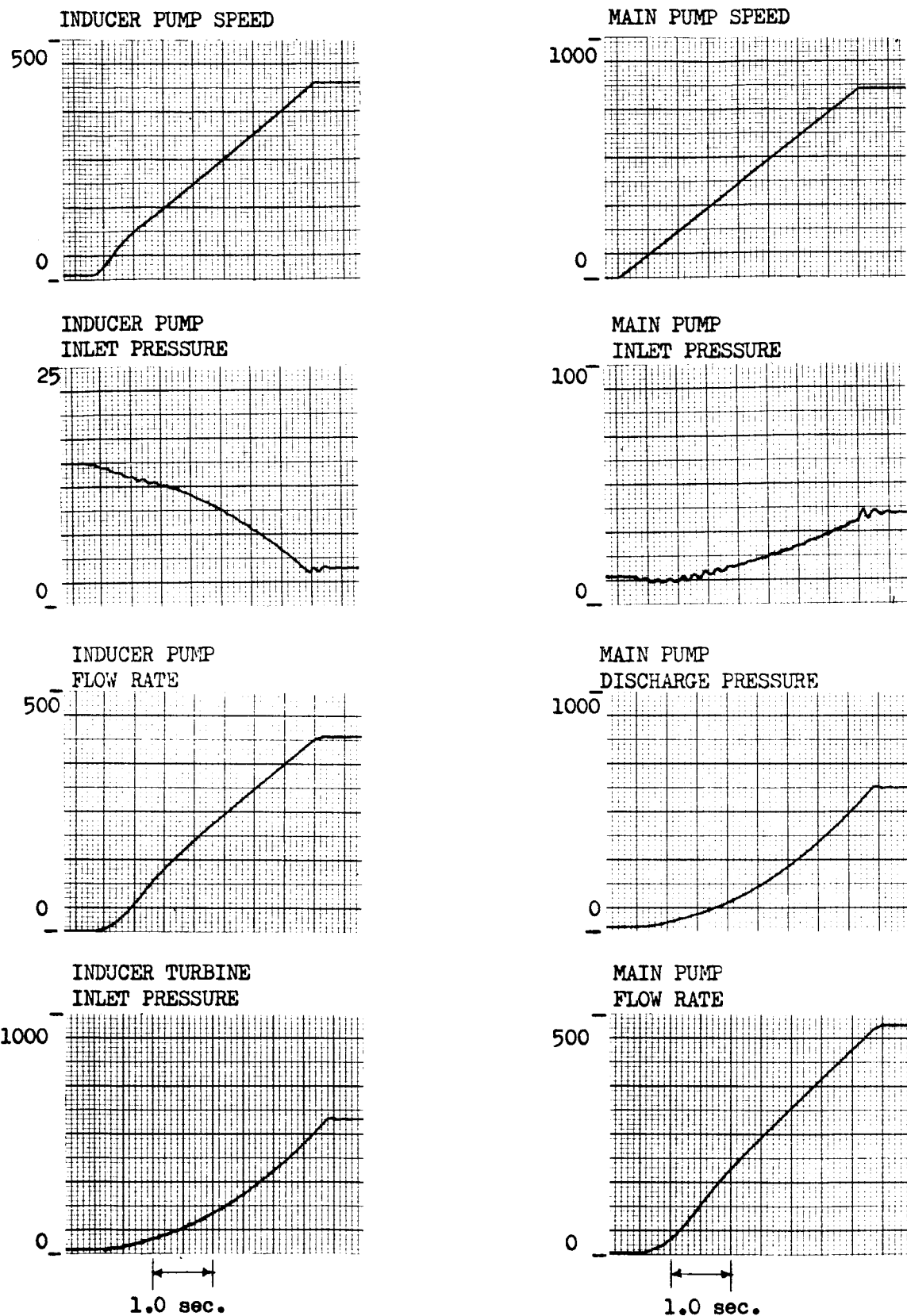


Figure 65. Remote-Coupled Test Start to 120-Percent Q/N, 4.0-Second Speed Ramp

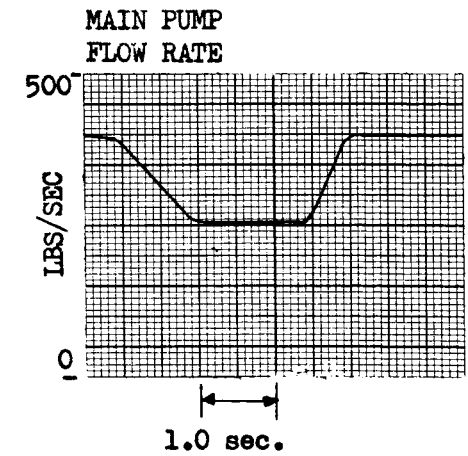
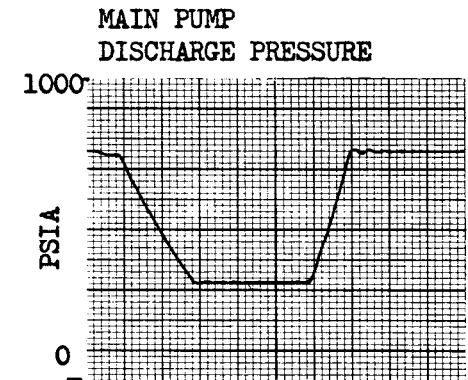
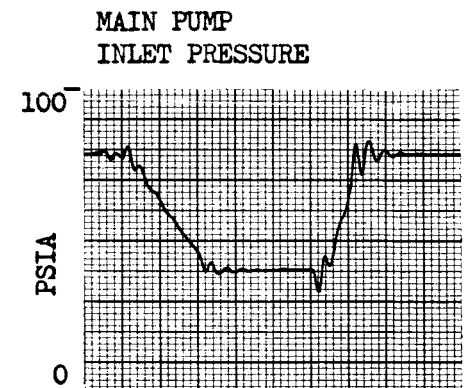
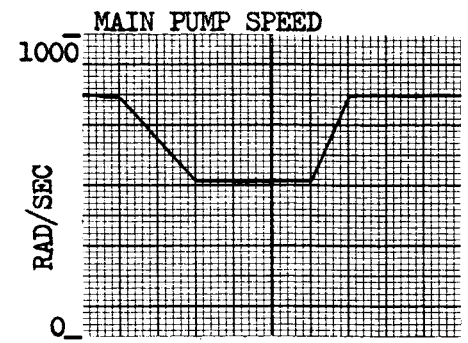
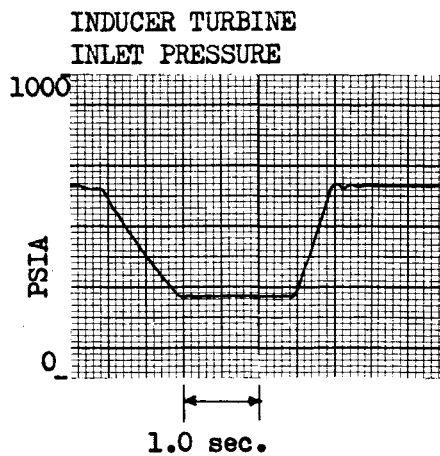
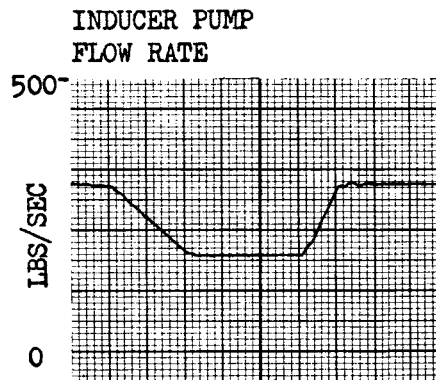
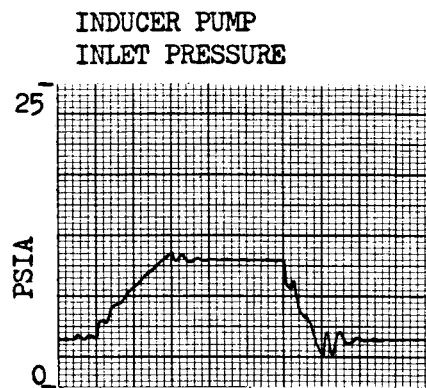
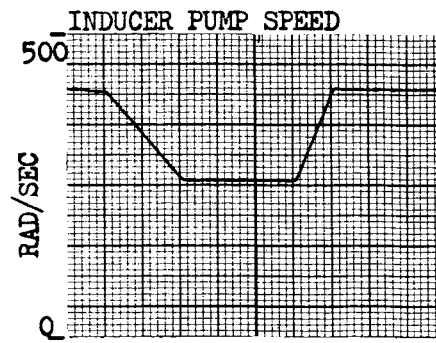


Figure 66. Remote-Coupled Test Throttling, 1.0-Second Deceleration, 0.5-Second Acceleration

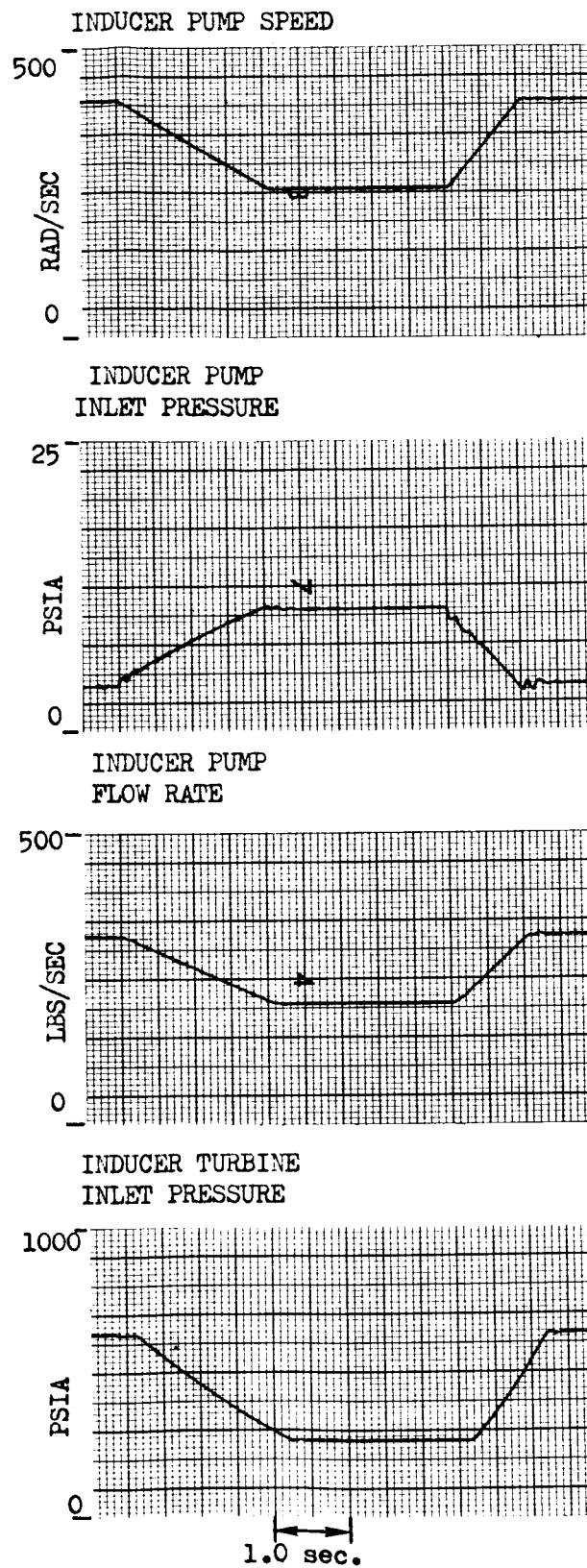


Figure 67. Close-Coupled Test Throttling, 2.0-Second Deceleration, 1.0-Second Acceleration

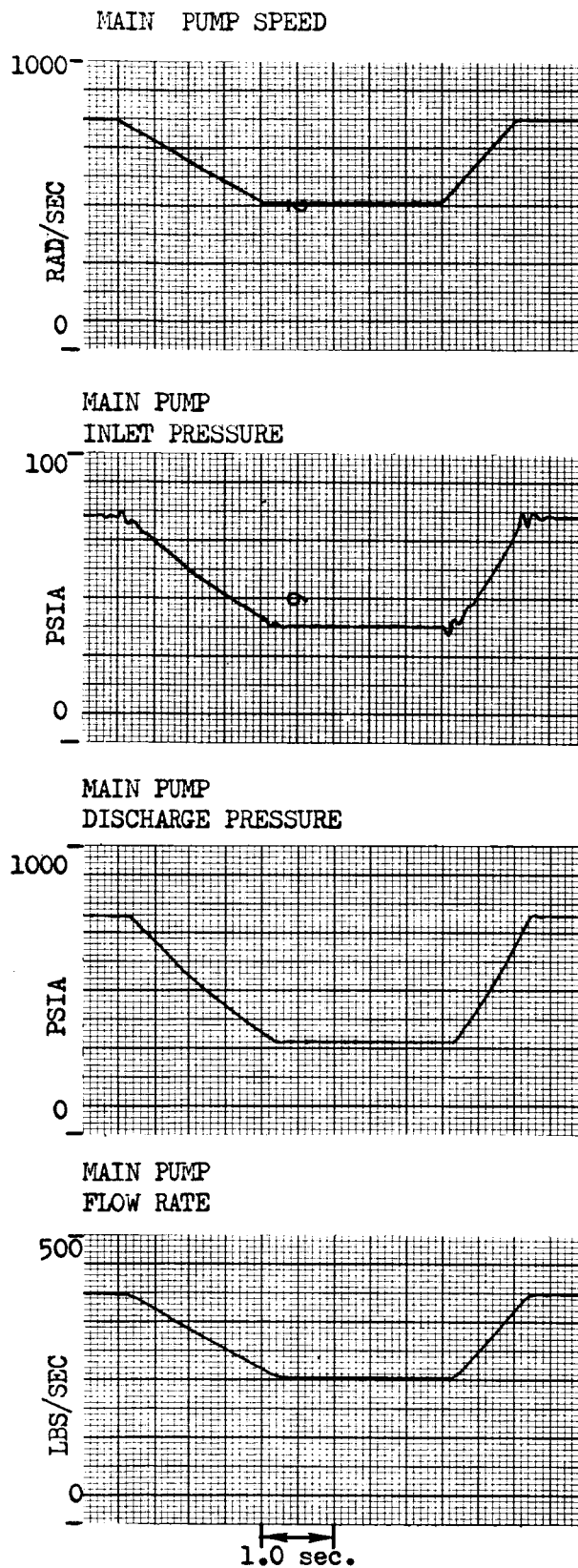


Figure 68. Close-Coupled Test Throttling, 2.0-Second Deceleration, 1.0-Second Acceleration

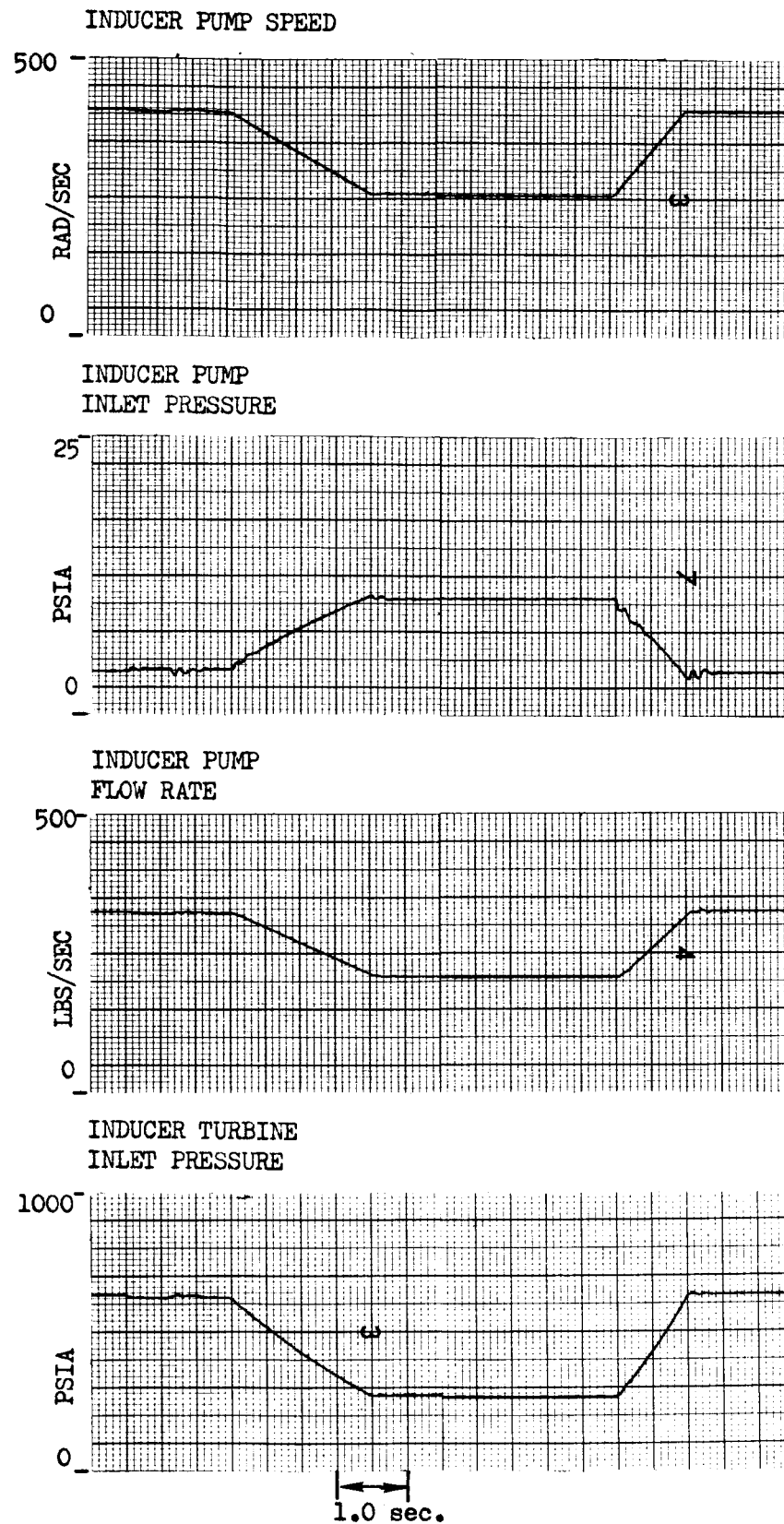


Figure 69. Remote-Coupled Test Throttling, 2.0-Second Deceleration, 1.0-Second Acceleration

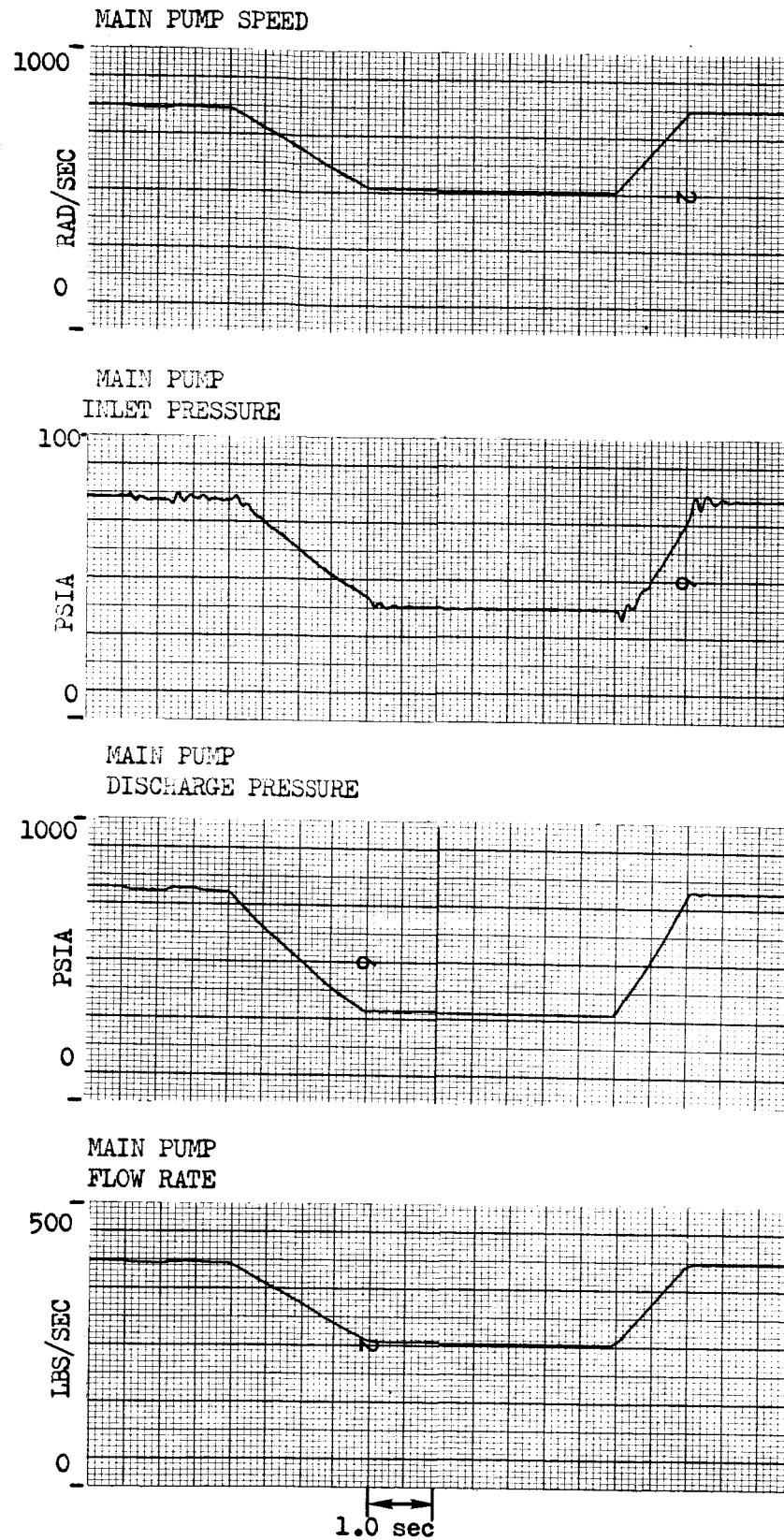


Figure 70. Close-Coupled Test Throttling, 2.0-Second Deceleration, 1.0-Second Acceleration

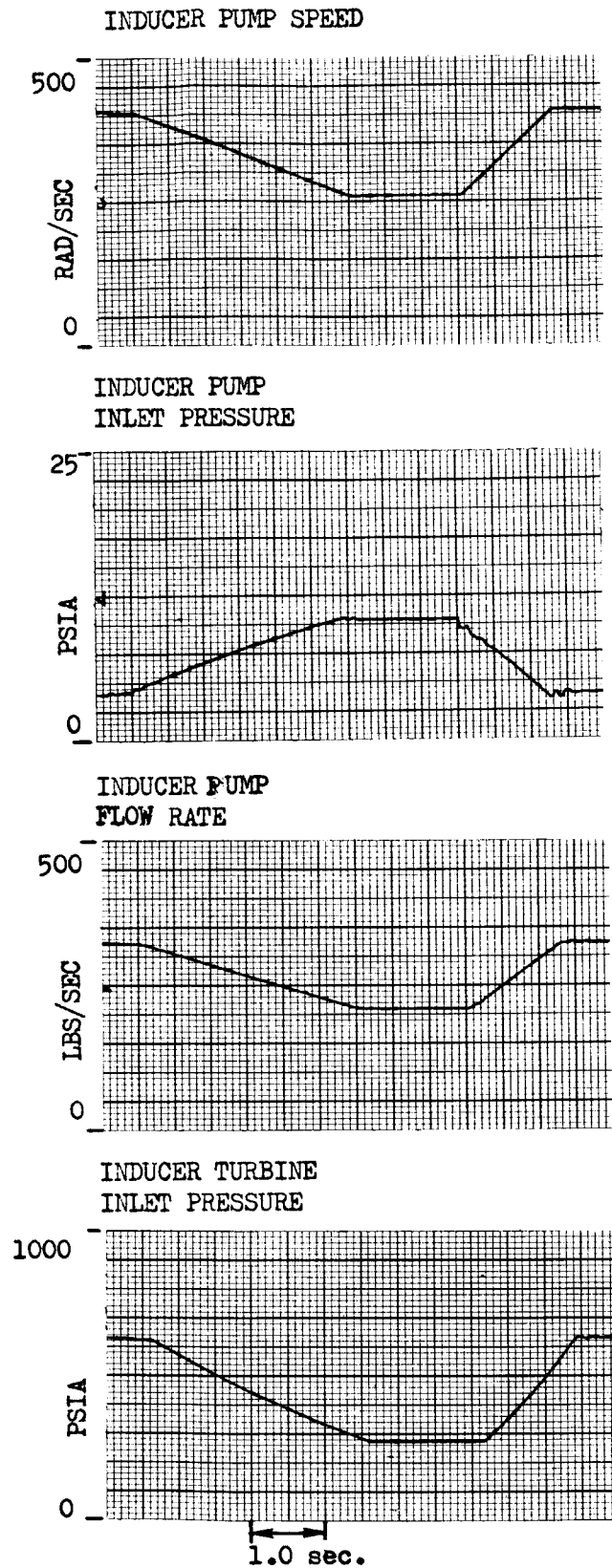


Figure 71. Close-Coupled Test Throttling, 3.0-Second Deceleration, 1.5-Second Acceleration

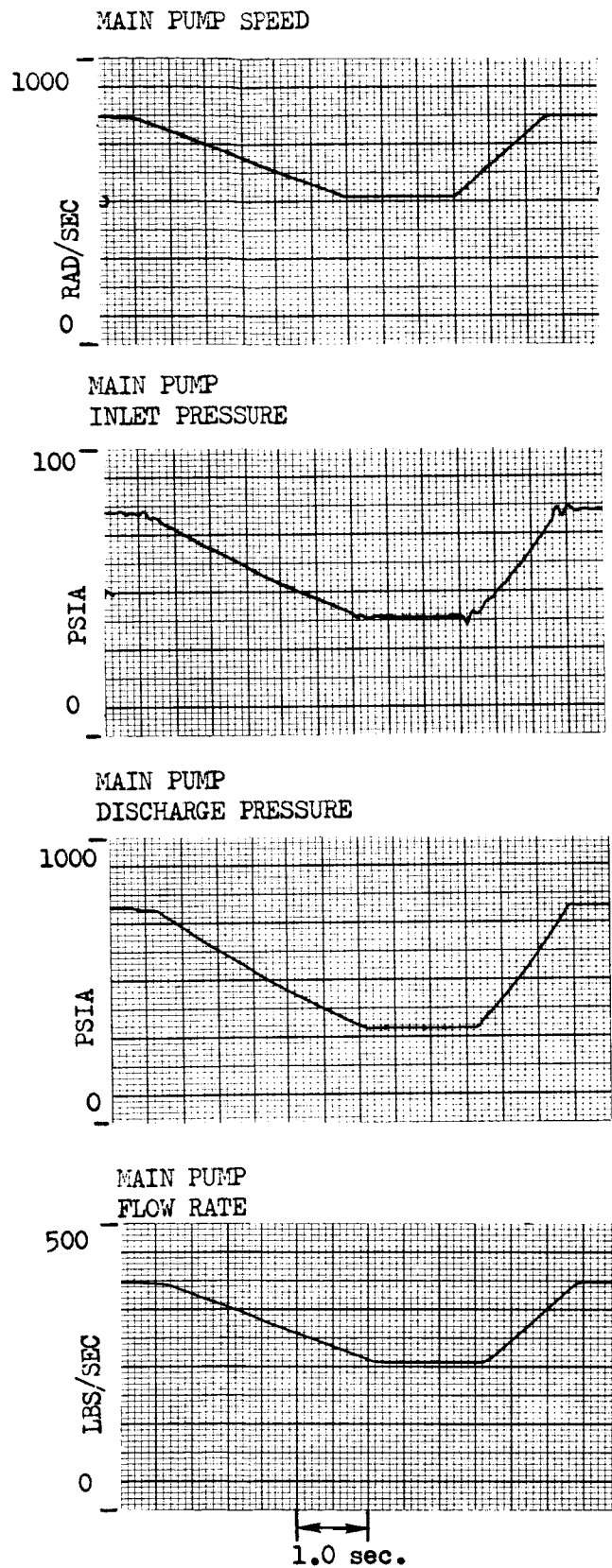


Figure 72. Close-Coupled Test Throttling, 3.0-Second Deceleration, 1.5-Second Acceleration

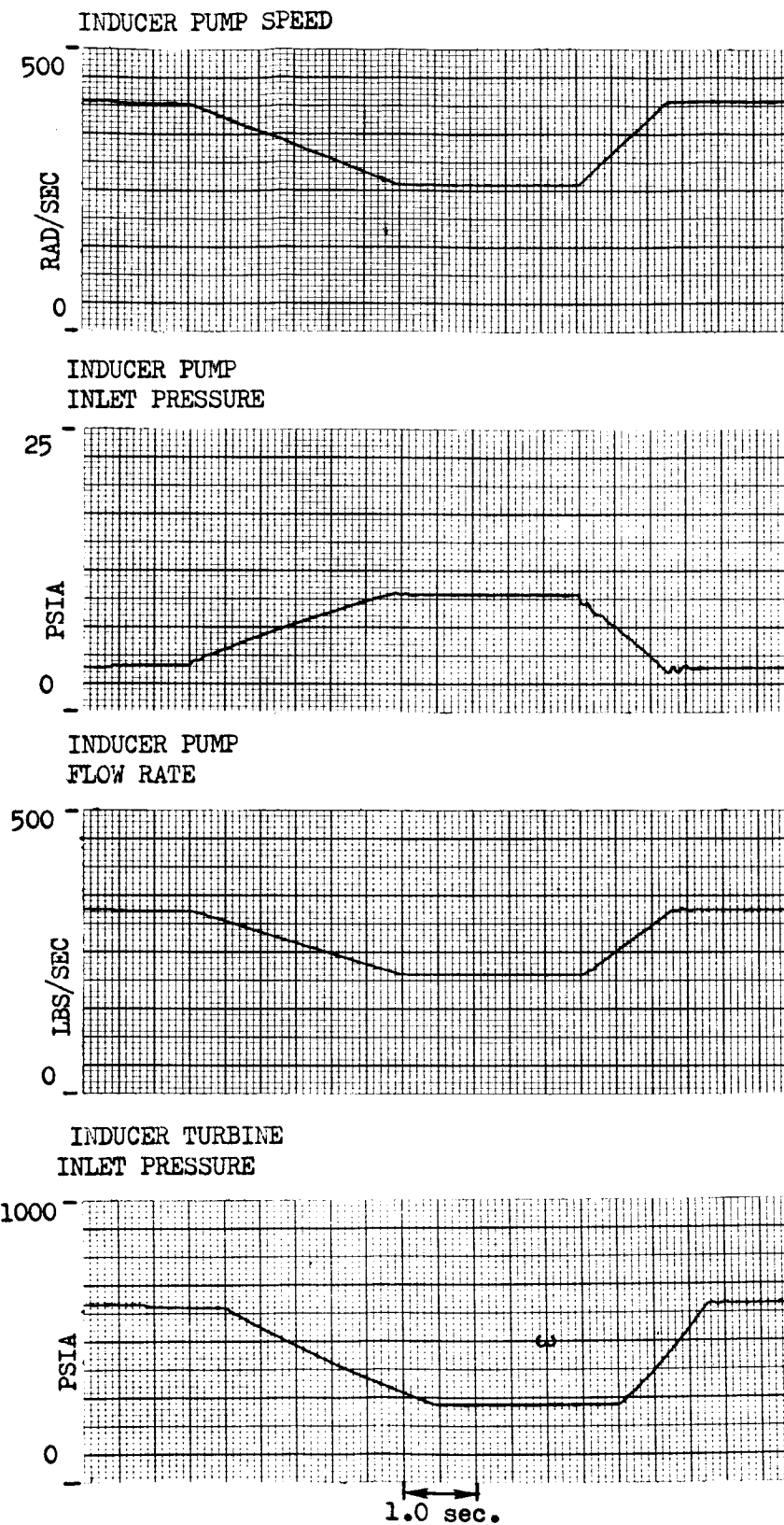


Figure 73. Remote-Coupled Test Throttling, 3.0-Second Deceleration, 1.5-Second Acceleration

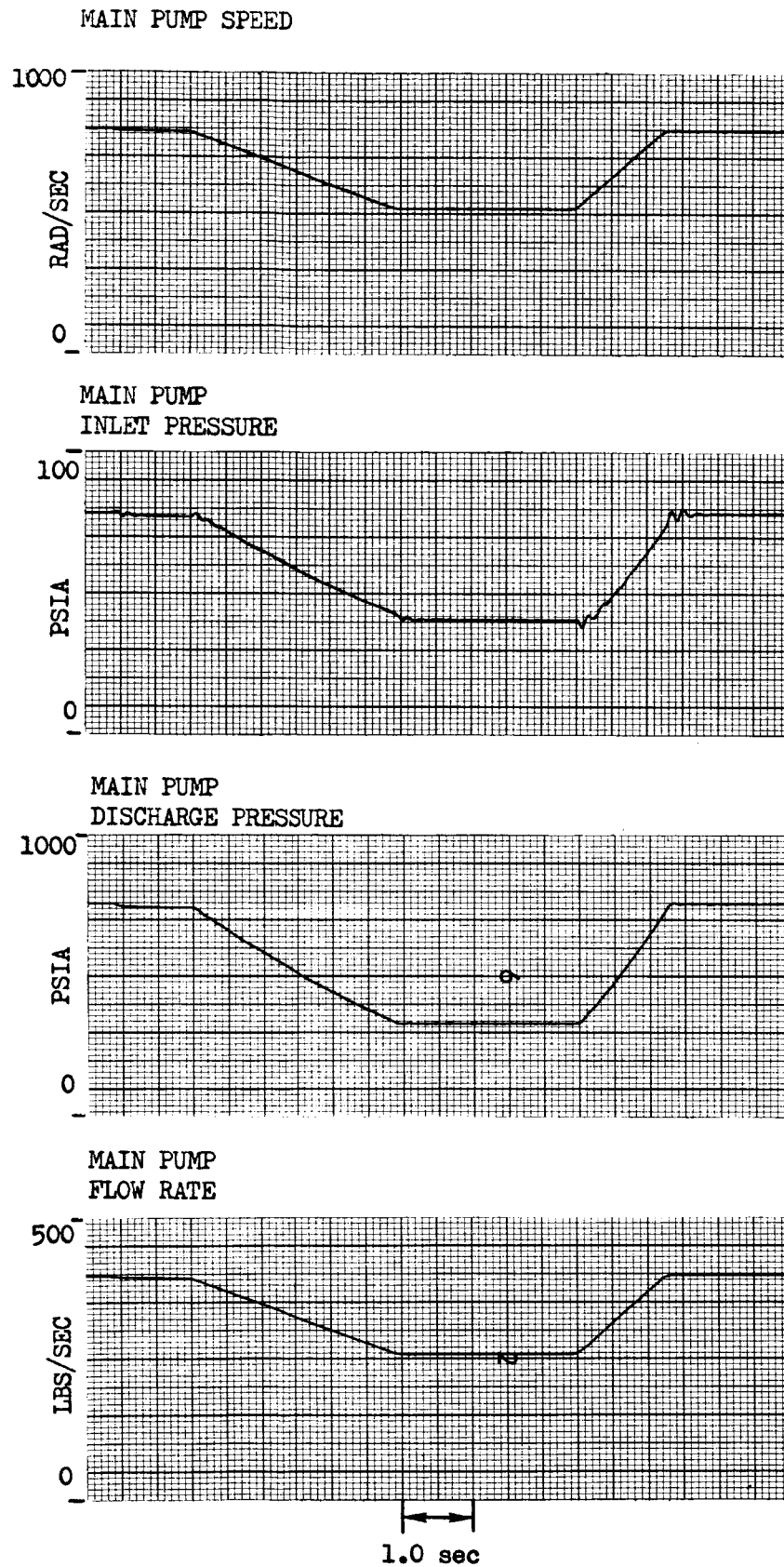


Figure 74. Remote-Coupled Test Throttling, 3.0-Second Deceleration, 1.5-Second Acceleration

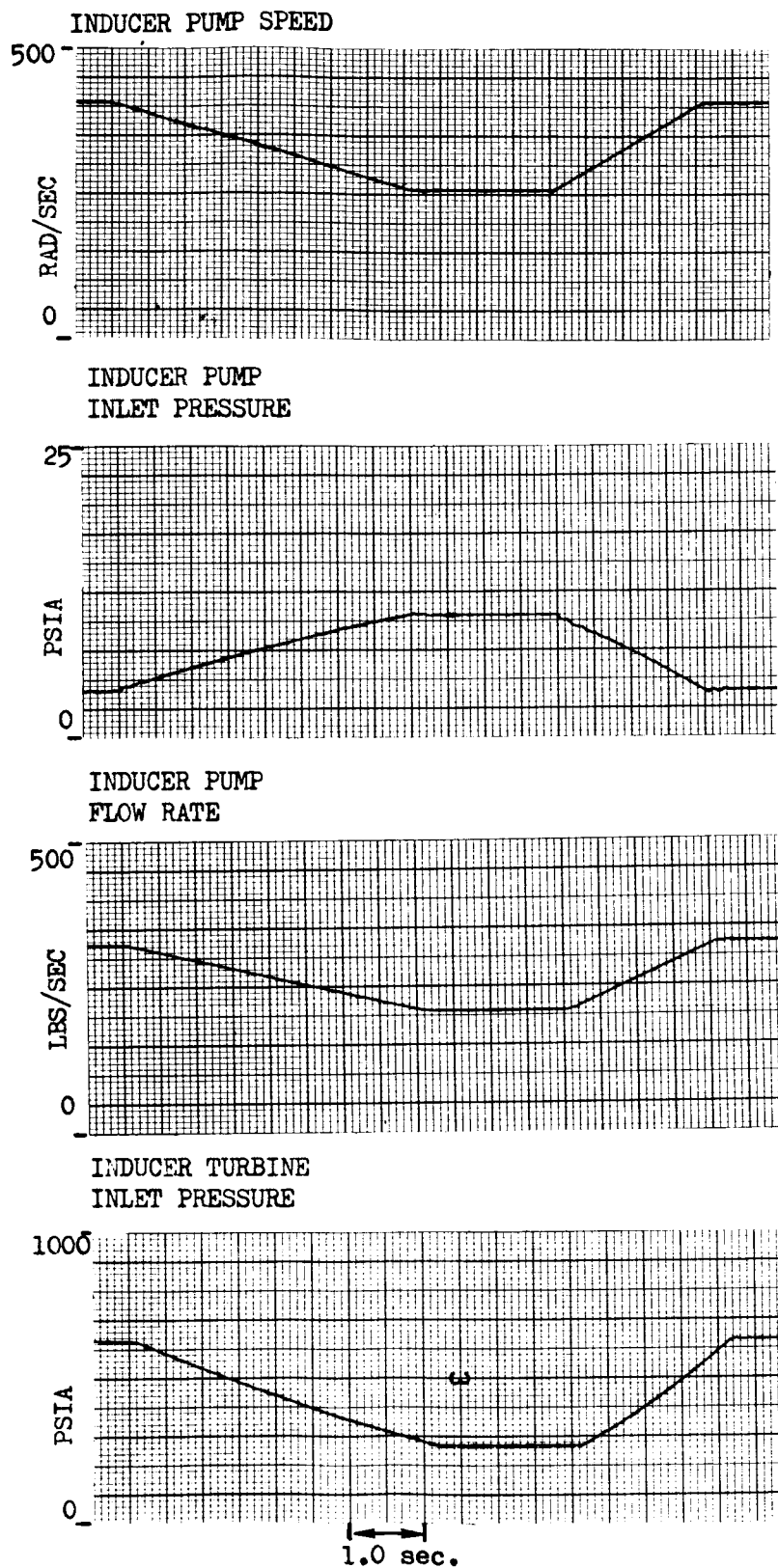


Figure 75. Close-Coupled Test Throttling, 4.0-Second Deceleration, 2.0-Second Acceleration

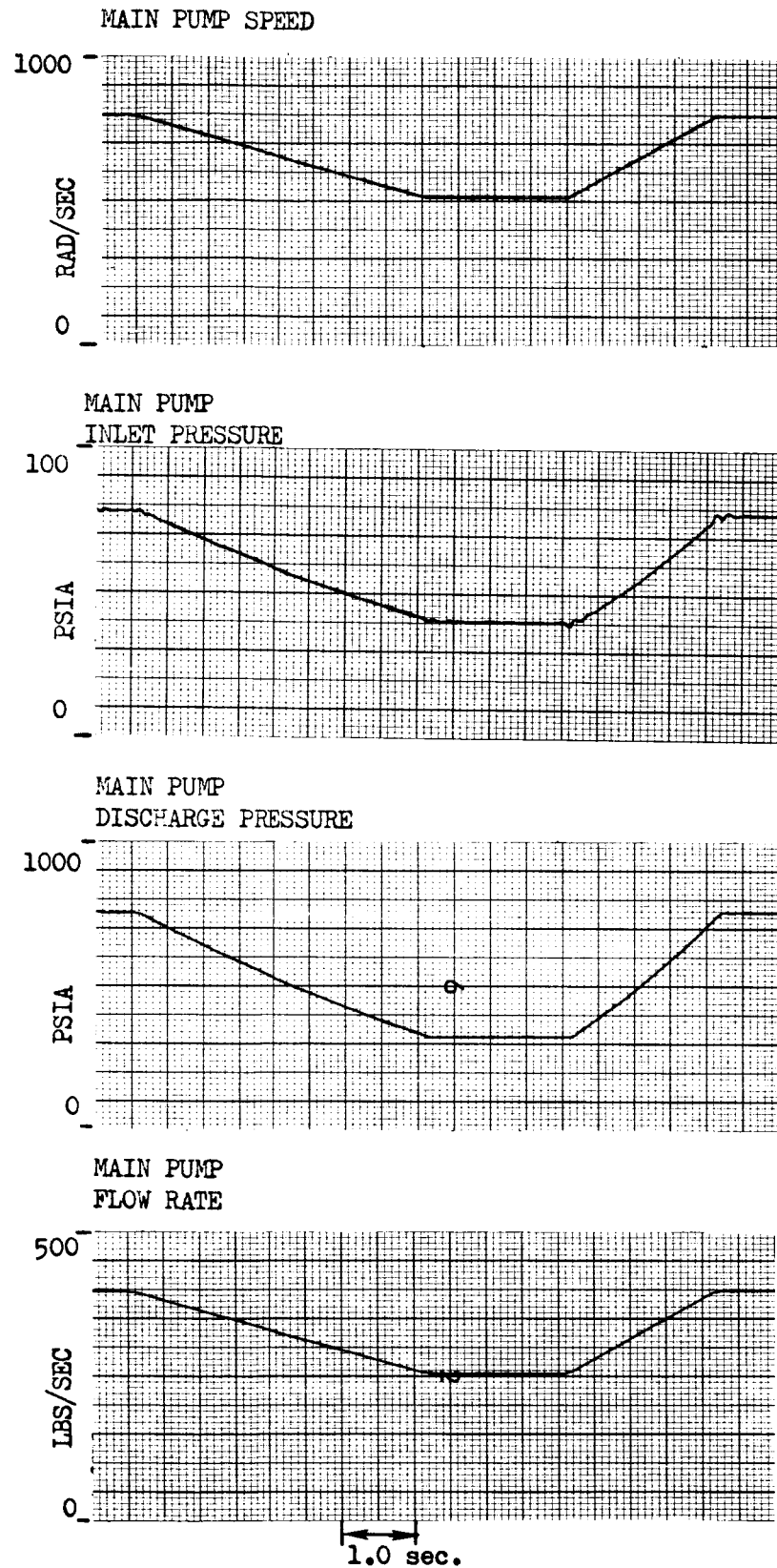


Figure 76. Close-Coupled Test Throttling, 4.0-Second Deceleration, 2.0-Second Acceleration

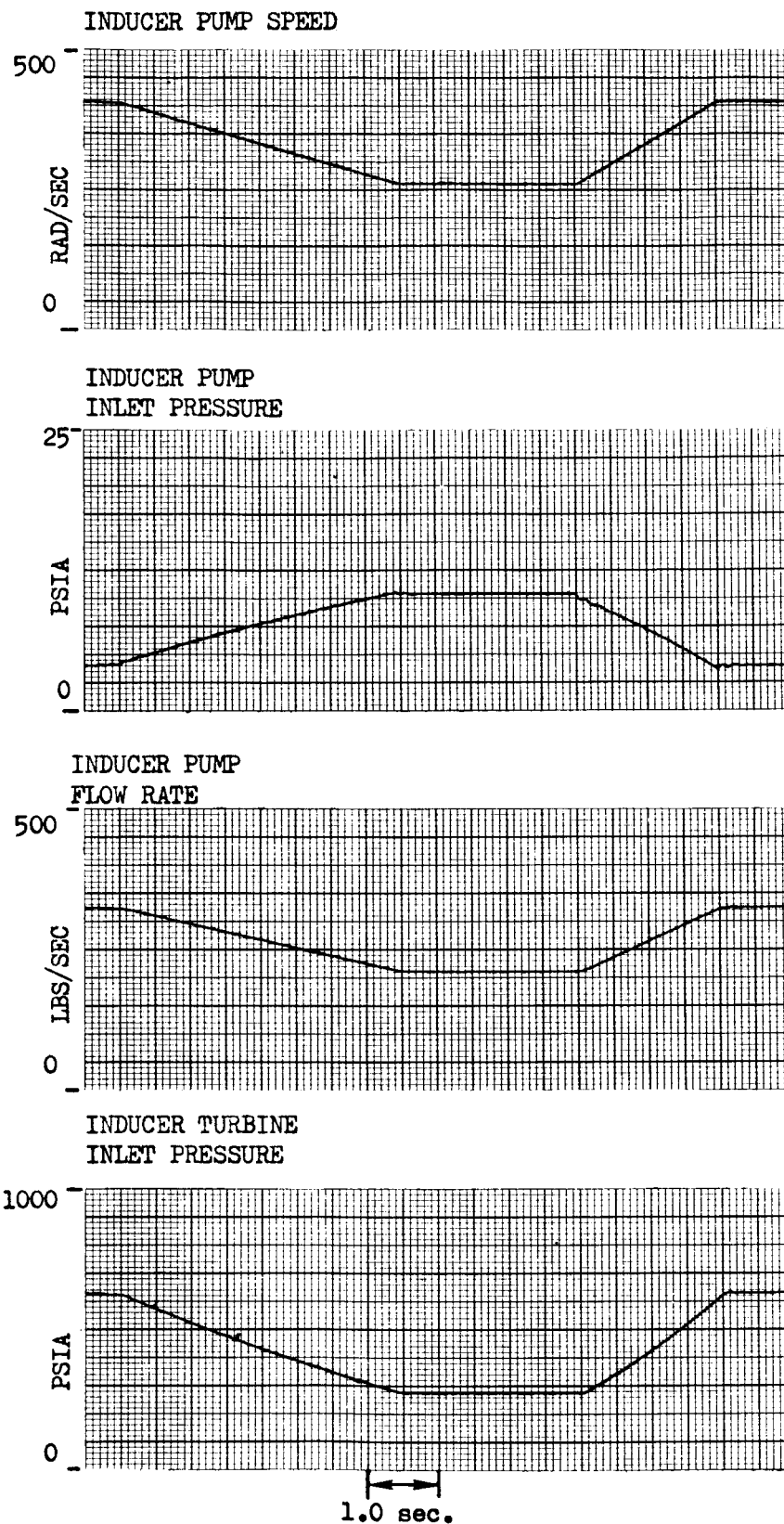


Figure 77. Remote-Coupled Test Throttling, 4.0-Second Deceleration, 2.0-Second Acceleration

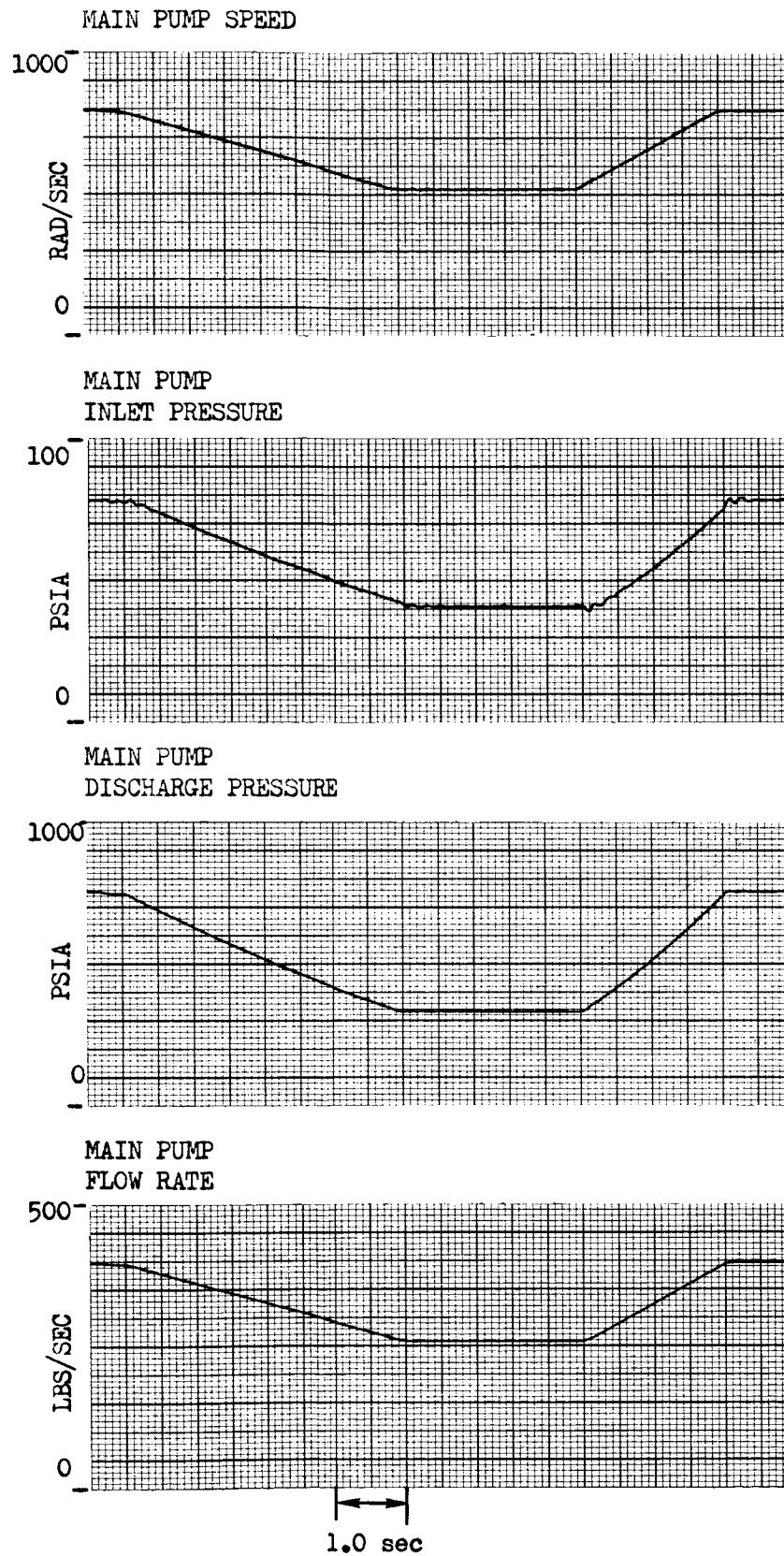


Figure 78. Remote-Coupled Test Throttling, 4.0-Second Deceleration, 2.0-Second Acceleration

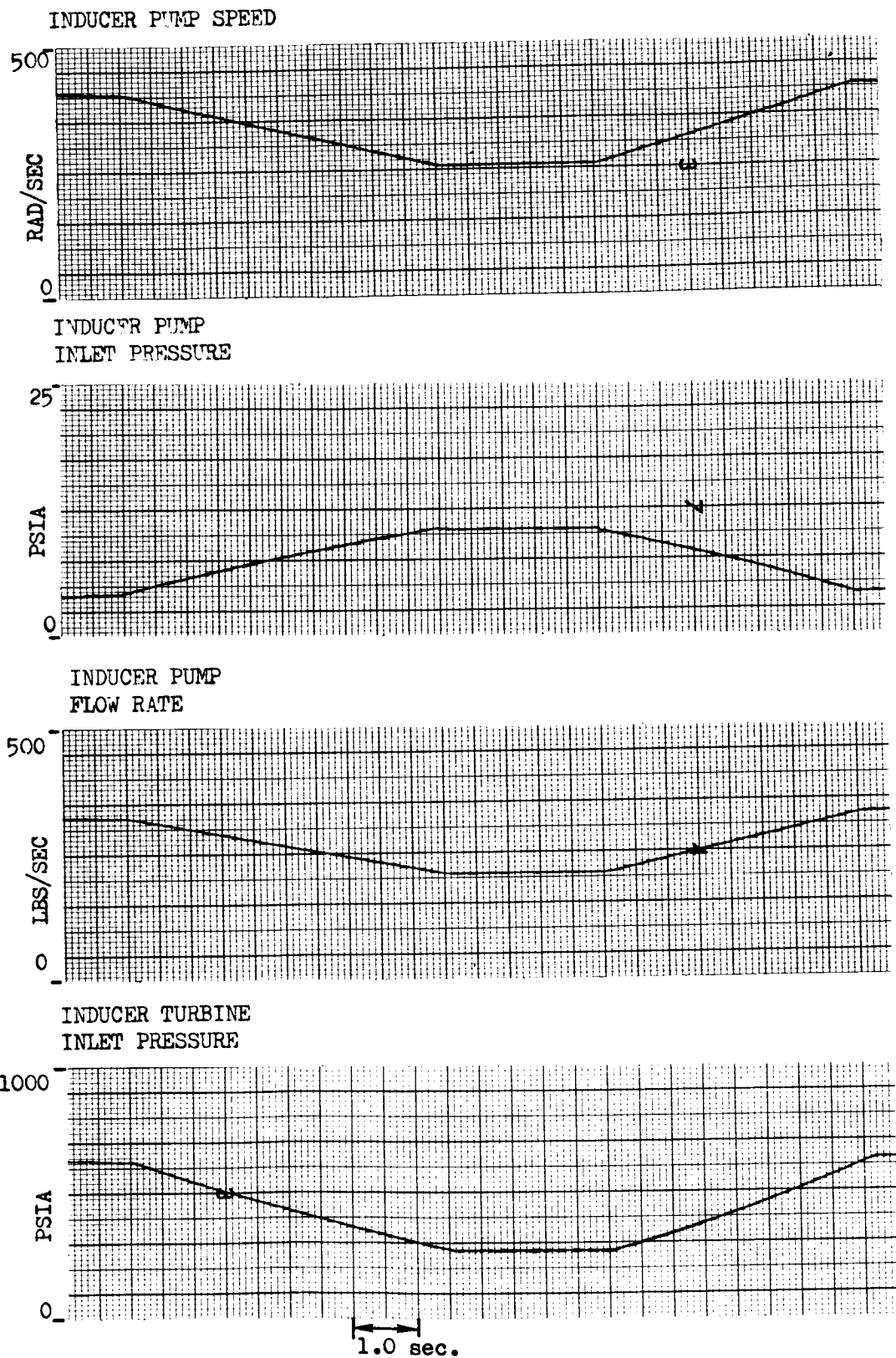


Figure 79. Close-Coupled Test Throttling, 5.0-Second Deceleration, 4.0-Second Acceleration

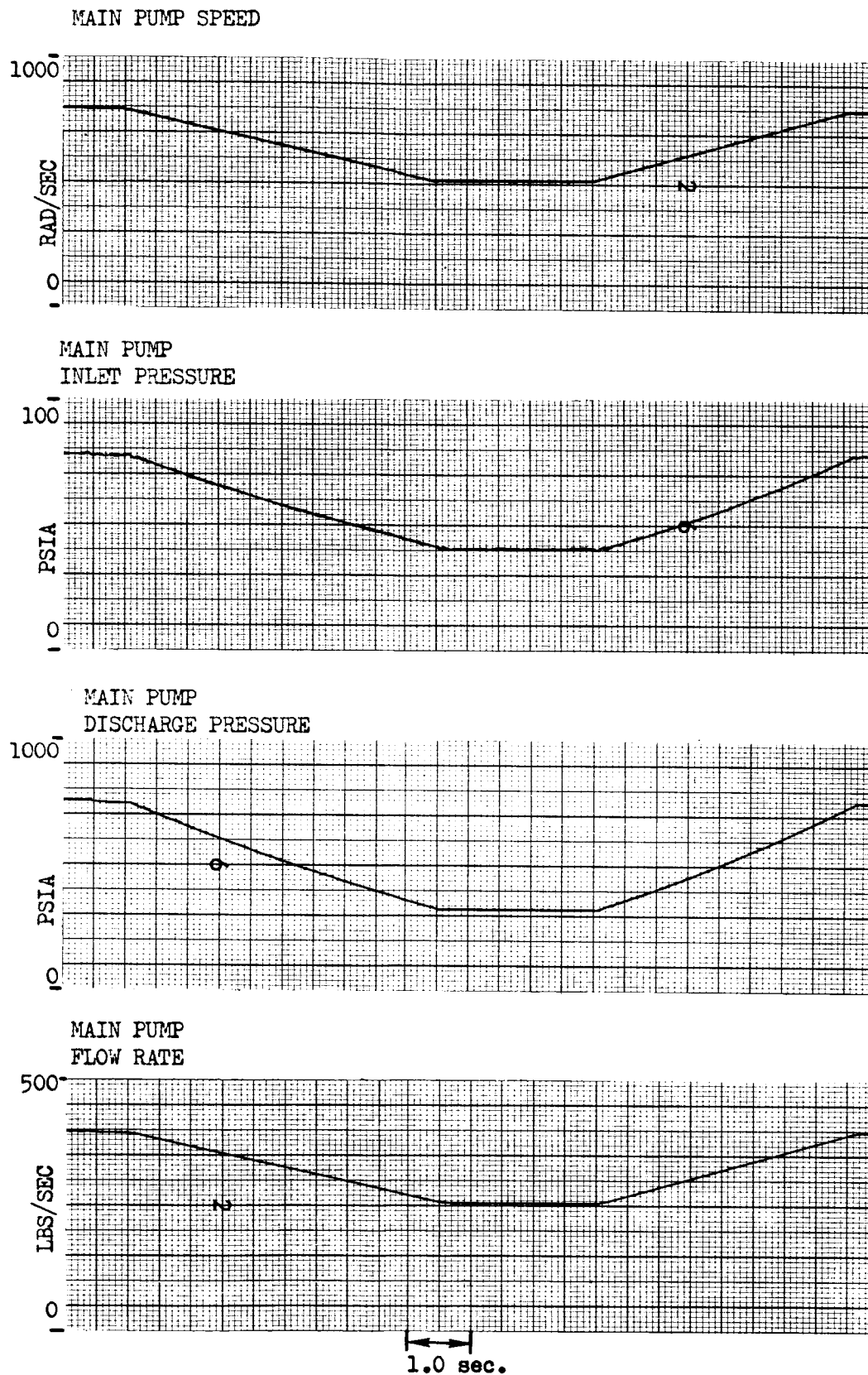


Figure 80. Close-Coupled Test Throttling, 5.0-Second Deceleration, 4.0-Second Acceleration

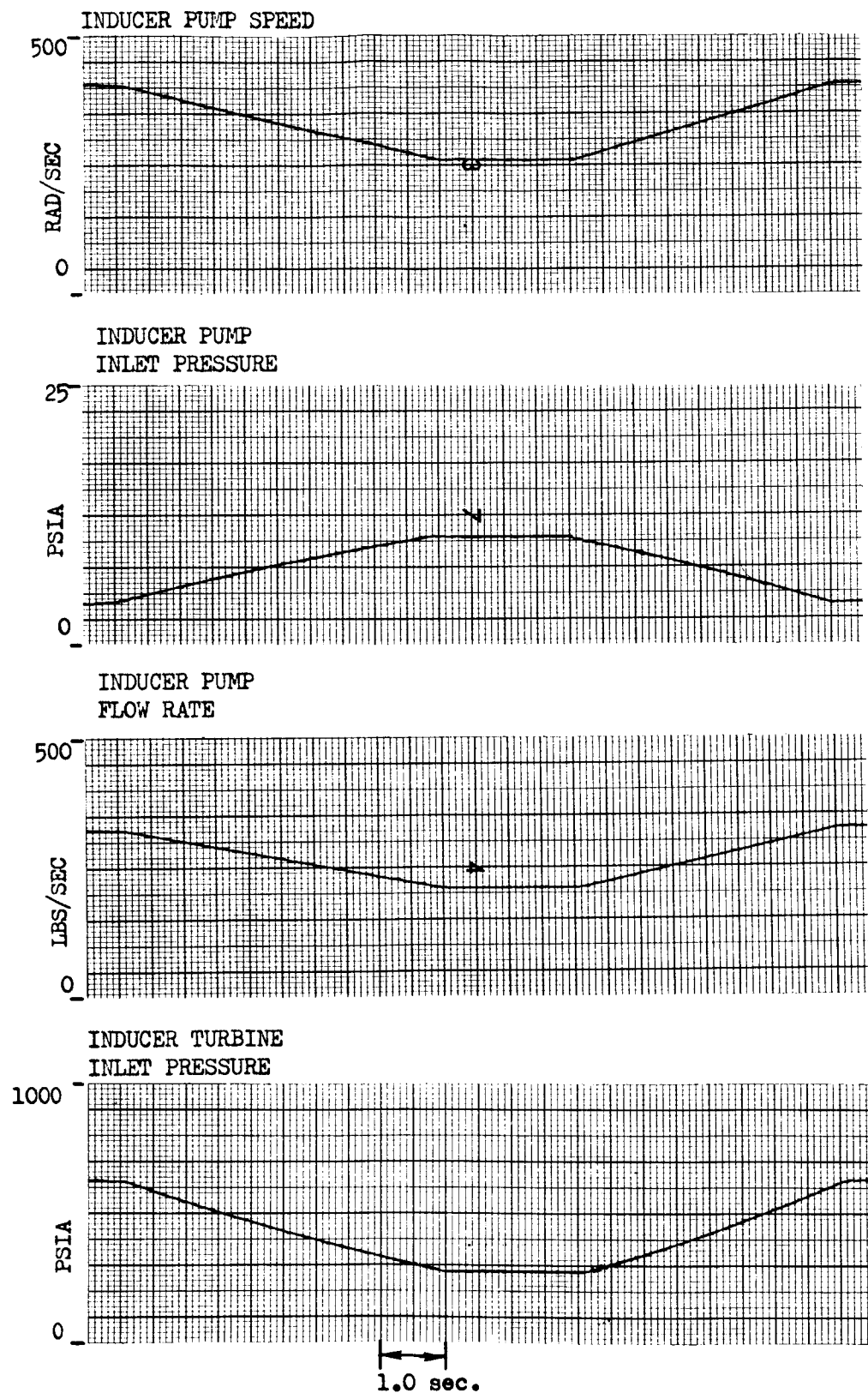


Figure 81. Remote-Coupled Test Throttling, 5.0-Second Deceleration, 4.0-Second Acceleration

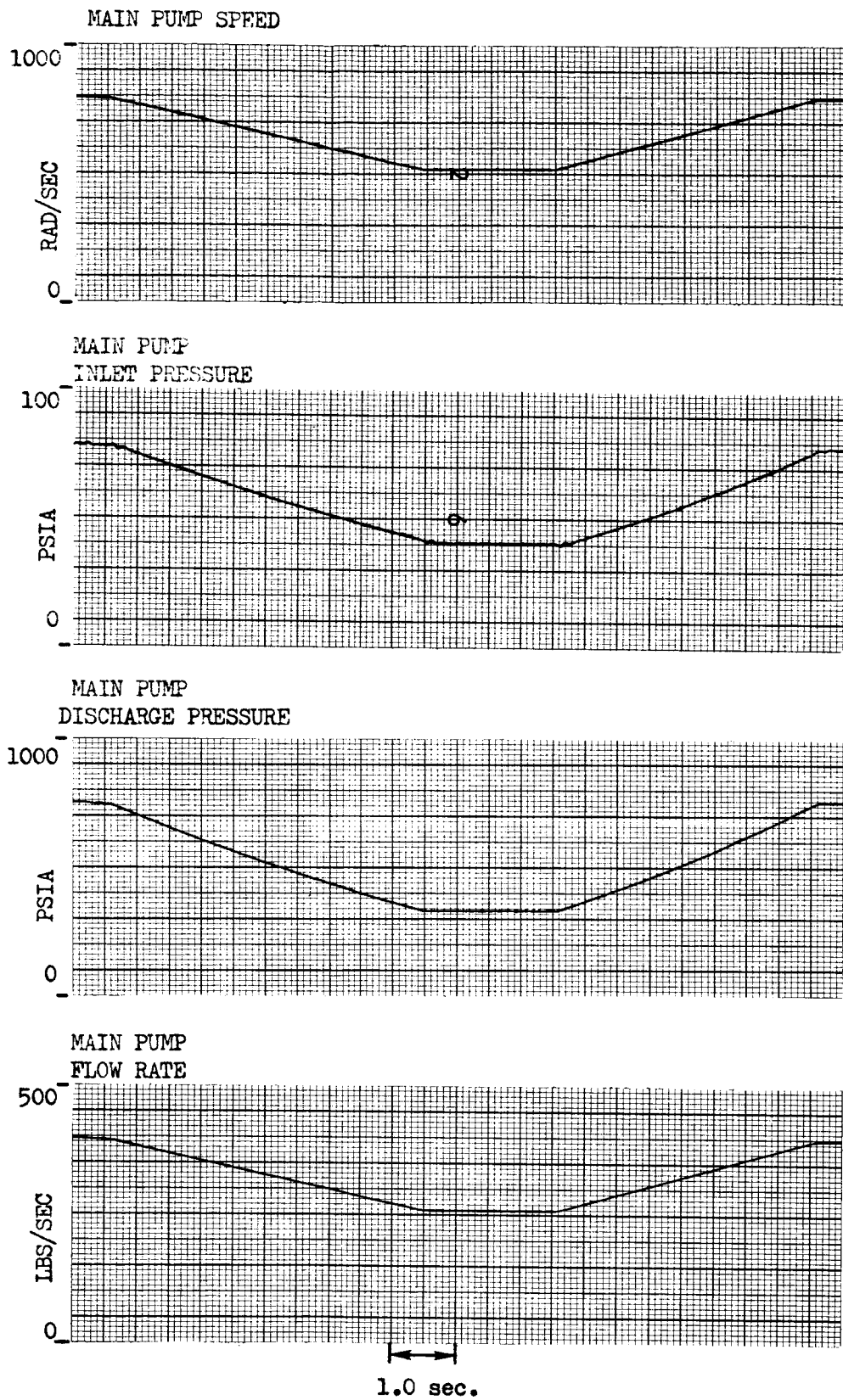


Figure 82. Remote-Coupled Test Throttling, 5.0-Second Deceleration, 4.0-Second Acceleration

ENGINE SYSTEM OPERATION

The final part of the parametric study involved consideration of the use of preinducers in an engine feed system pumping liquid oxygen and liquid hydrogen. To obtain this information, the digital computer model was used with modifications to simulate the engine configuration. The modifications included changing the preinducer inlet and main pump discharge systems to represent a J-2S engine installed in a Saturn S-IVB stage, and the use of a realistic hydrogen preinducer with the turbine drive tapped off at the main pump inducer discharge.

The oxidizer preinducer was close coupled to the main pump, and the inlet line was represented by 76 inches of 8-inch pipe, while the discharge system was represented by the resistance required to give rated flow conditions. The fuel preinducer was remote coupled with 93 inches of 10-inch pipe between the tank and preinducer inlet and 120 inches of 8-inch pipe between the preinducer discharge and main pump inlet. The hydrogen discharge system was represented by the resistance required to achieve rated flow operation. The oxidizer preinducer and main pump performance curves were the same as for the test hardware. The hydrogen preinducer and turbine performance curves are shown in Fig. 83 and 84, while the main hydrogen pump characteristics are those of the J-2 Mark 29-F shown in Fig. 85. The driving input to the main pumps was the pump speed vs time taken from a typical J-2S engine start, as shown in Fig. 86, along with the engine main valve sequencing.

The results of the LO_2 feed system simulation are presented in Fig. 87 and 88 for a preinducer NPSH of 25 and 16 feet, respectively. The 25-foot NPSH condition simulates the current J-2 starting condition without a preinducer. From the results of the two runs, there does not appear to be a problem with starting at 16 feet. Both starts exhibit pressure oscillations beginning at about 2.1 seconds because of the rapid opening of the oxidizer valve. The oscillations are more pronounced with 16 feet of NPSH, but the preinducer output is sufficient to prevent main pump cavitation. No attempt was made in this study to determine the effect

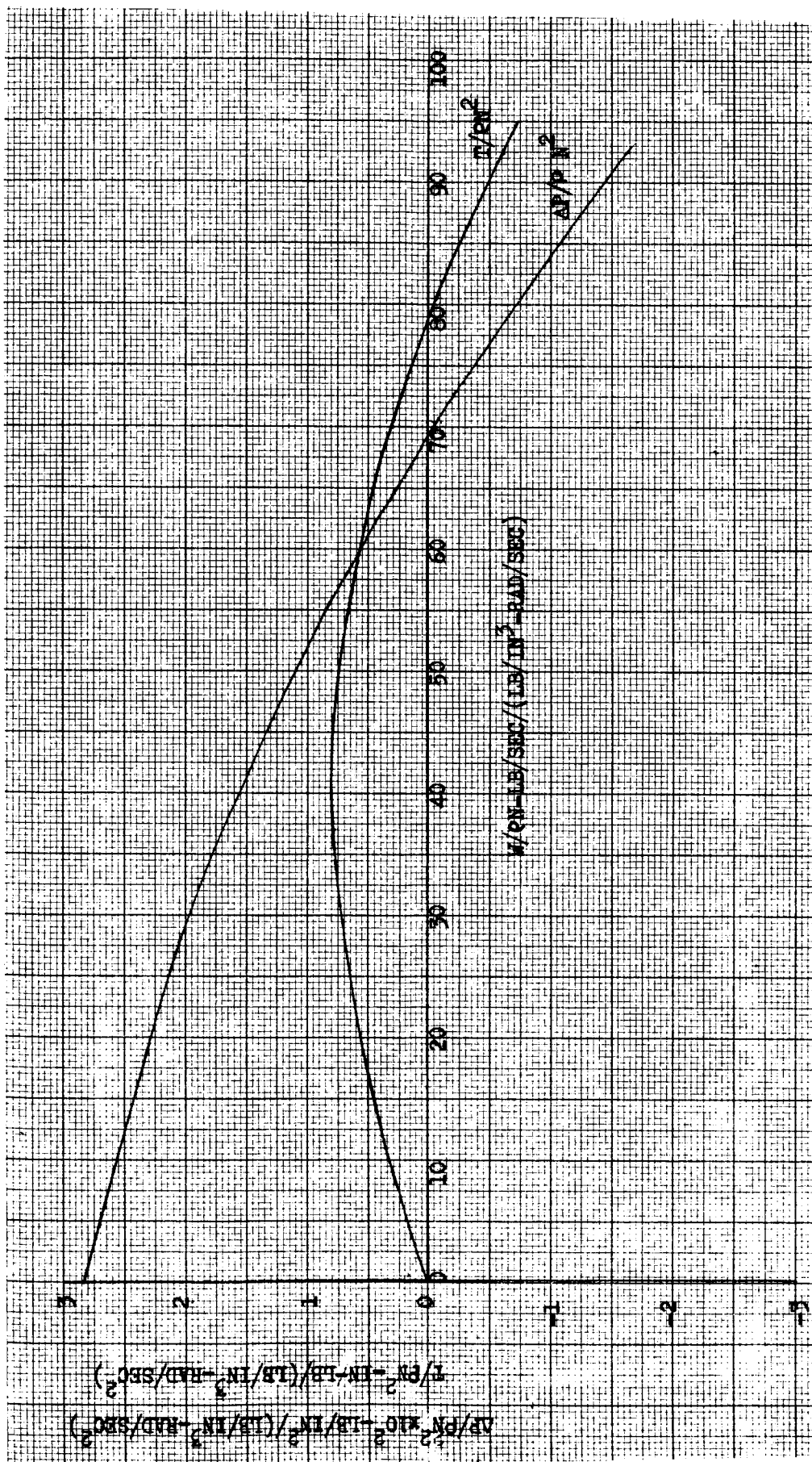


Figure 83. LH₂ Preinducer Performance

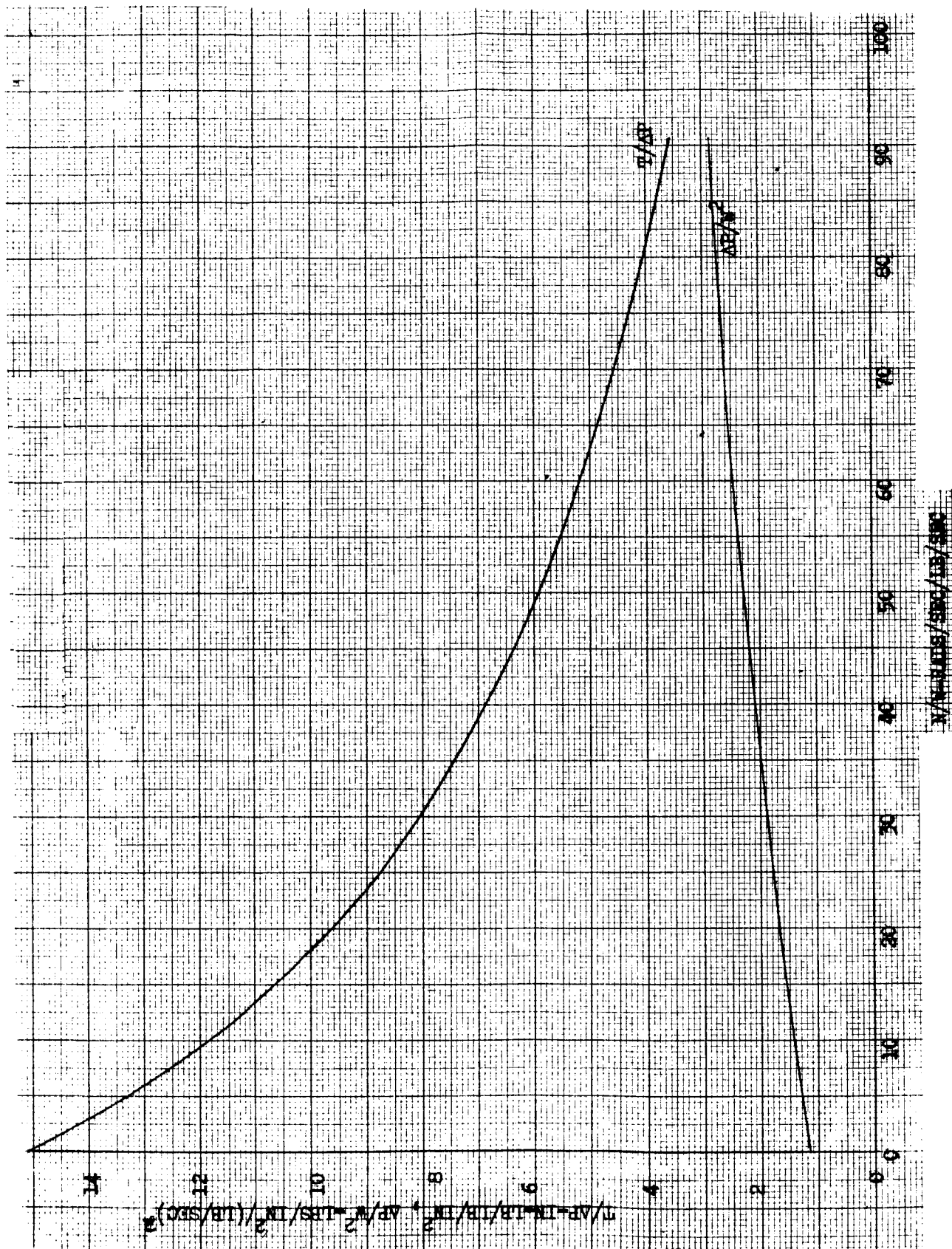


Figure 84. LH₂ Hydraulic Turbine Performance

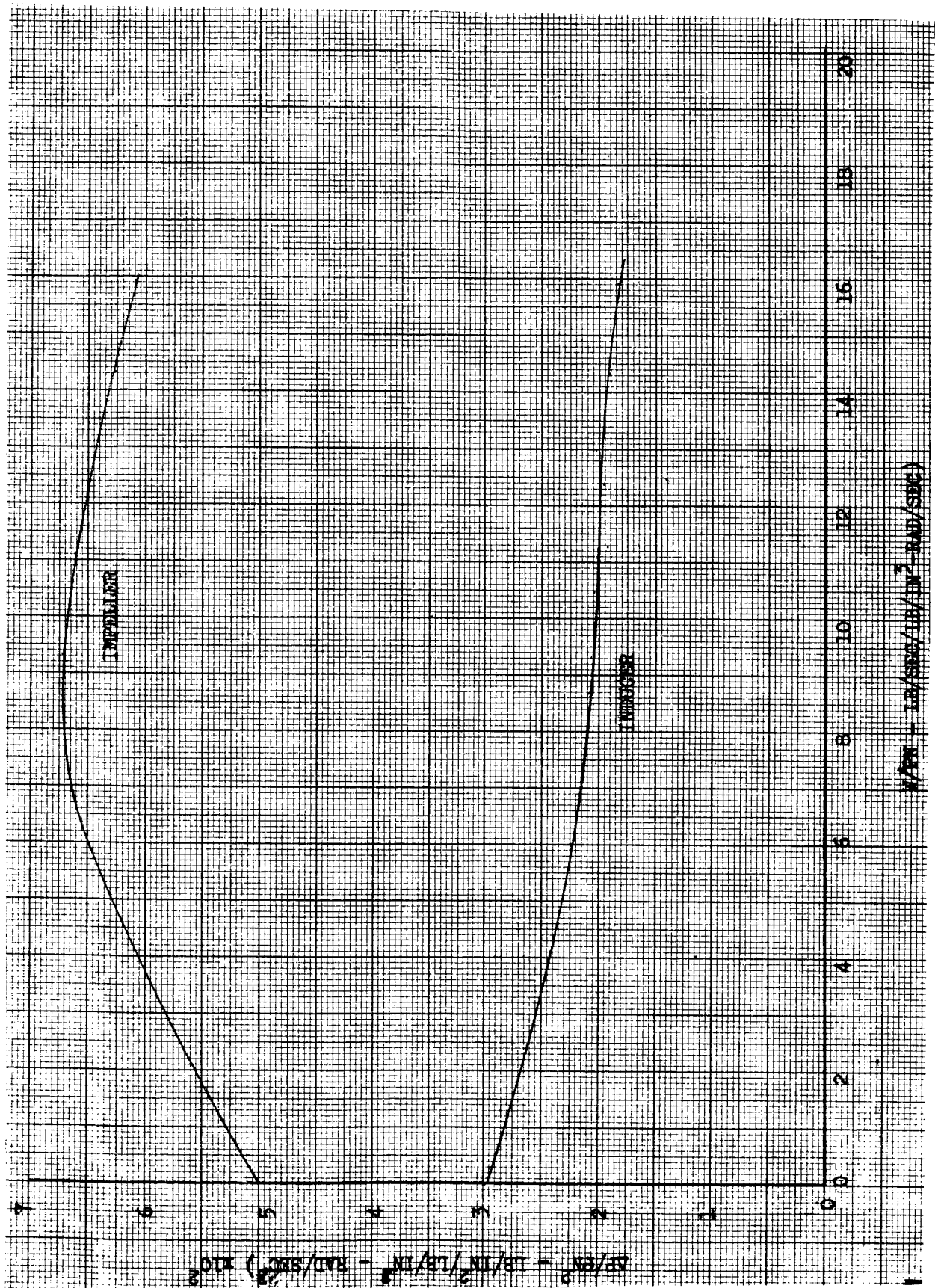


Figure 85. LH₂ Mark 29-F Pump Performance

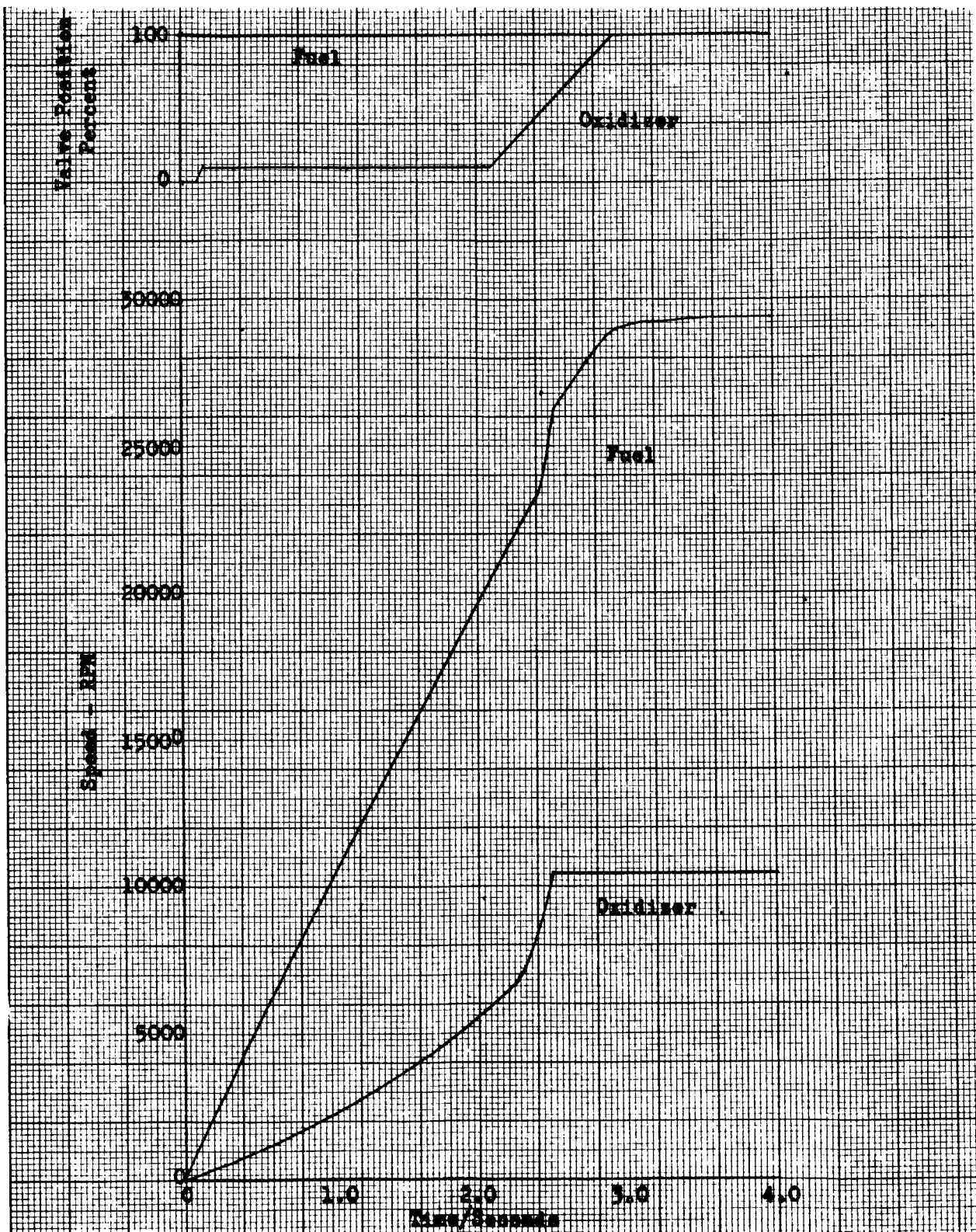


Figure 86. Typical J-2S Valve Sequencing and Pump Speed Buildup

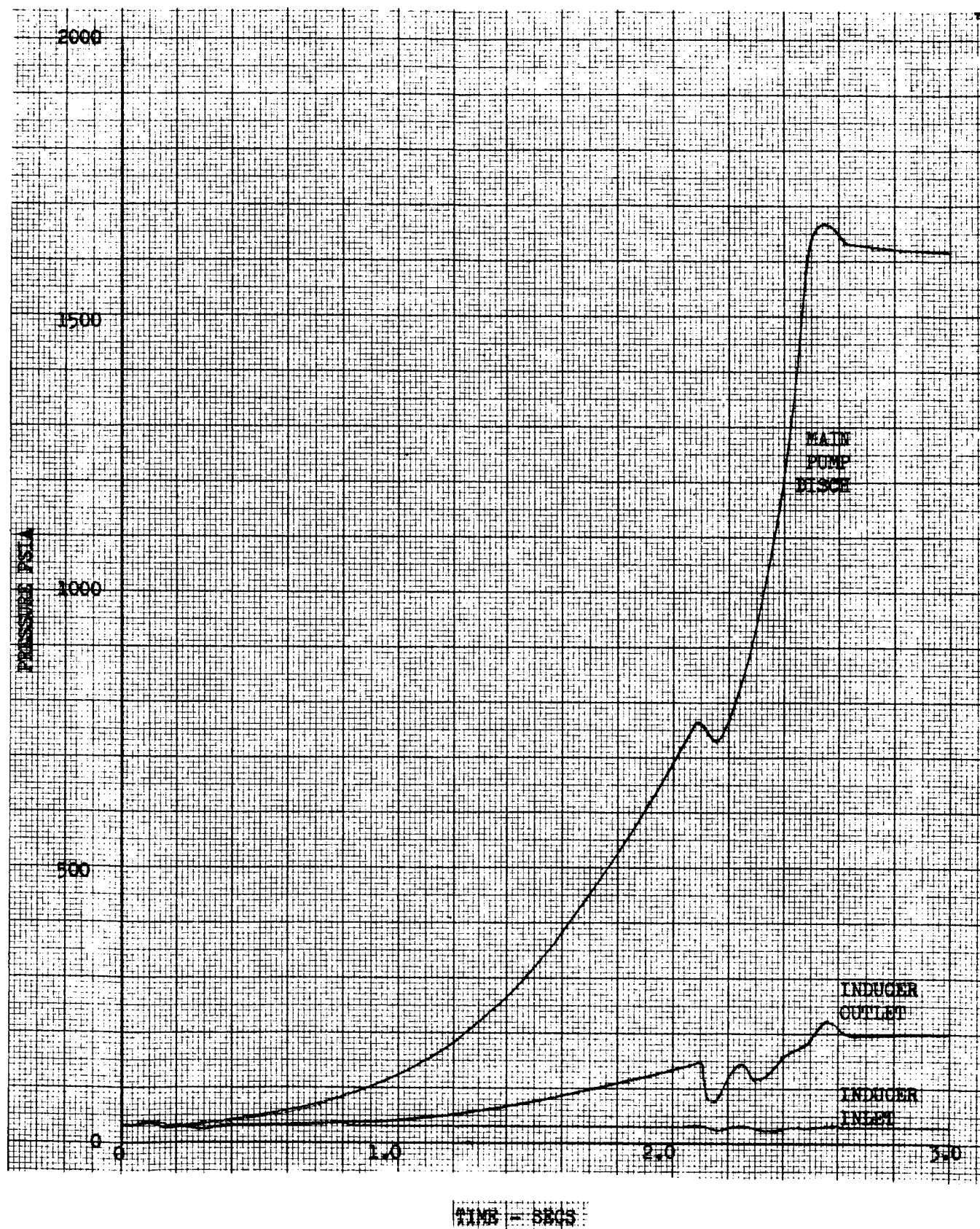


Figure 87. Simulated Oxidizer Engine Feed System, 25-Feet NPSH

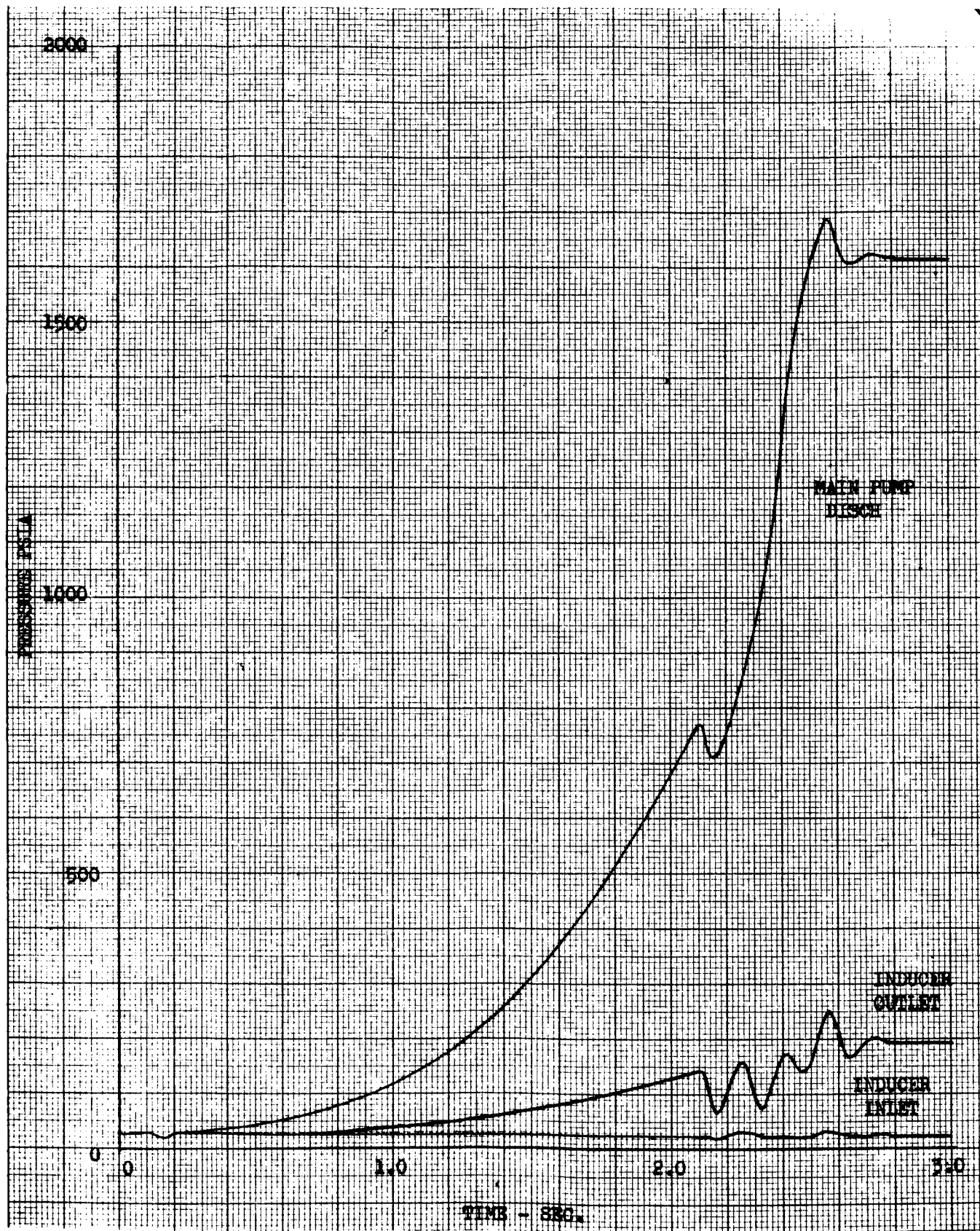


Figure 88. Simulated Oxidizer Feed System, 16-Foot NPSH

of varying the propellant valve sequencing. If the ramp opening portion of the oxidizer valve were slowed down, however, the magnitude of the oscillations would be reduced and the time to reach rated operation would be increased.

The results of the simulated fuel feed system are shown in Fig. 89. The start was run for an NPSH of 218 feet, representing current starting conditions. The start is smooth and there does not appear to be any reason why the NPSH could not be reduced. It should be noted that the depression of the fuel preinducer and pump pressures during the initial portion of the start are reduced compared to the oxidizer system because of the lower required fuel acceleration. The time to accelerate the flow is still 3.0 seconds, but the rated flowrate is only one-fifth of the oxidizer flowrate.

SUMMARY AND CONCLUSIONS

A series of parametric studies was made using the analog and digital computer models developed for predicting the dynamic performance of feed systems using a hydraulic turbine-driven preinducer in series with a high-head main pump. These studies covered the effects due to variation in preinducer design and test configuration, prediction of the planned test program performance, and predictions of start performance for an engine with preinducers used in the propellant feed systems.

From the results of these studies, the following conclusions are drawn:

1. The preinducer rotating moment of inertia has a significant effect upon the starting performance: the lower the inertia, the better the start.
2. The fluid inertia (ratio of line length to area) of the pump coupling line for a remote location of the preinducer has an effect upon the starting performance: the lower the inertia, the better the performance.

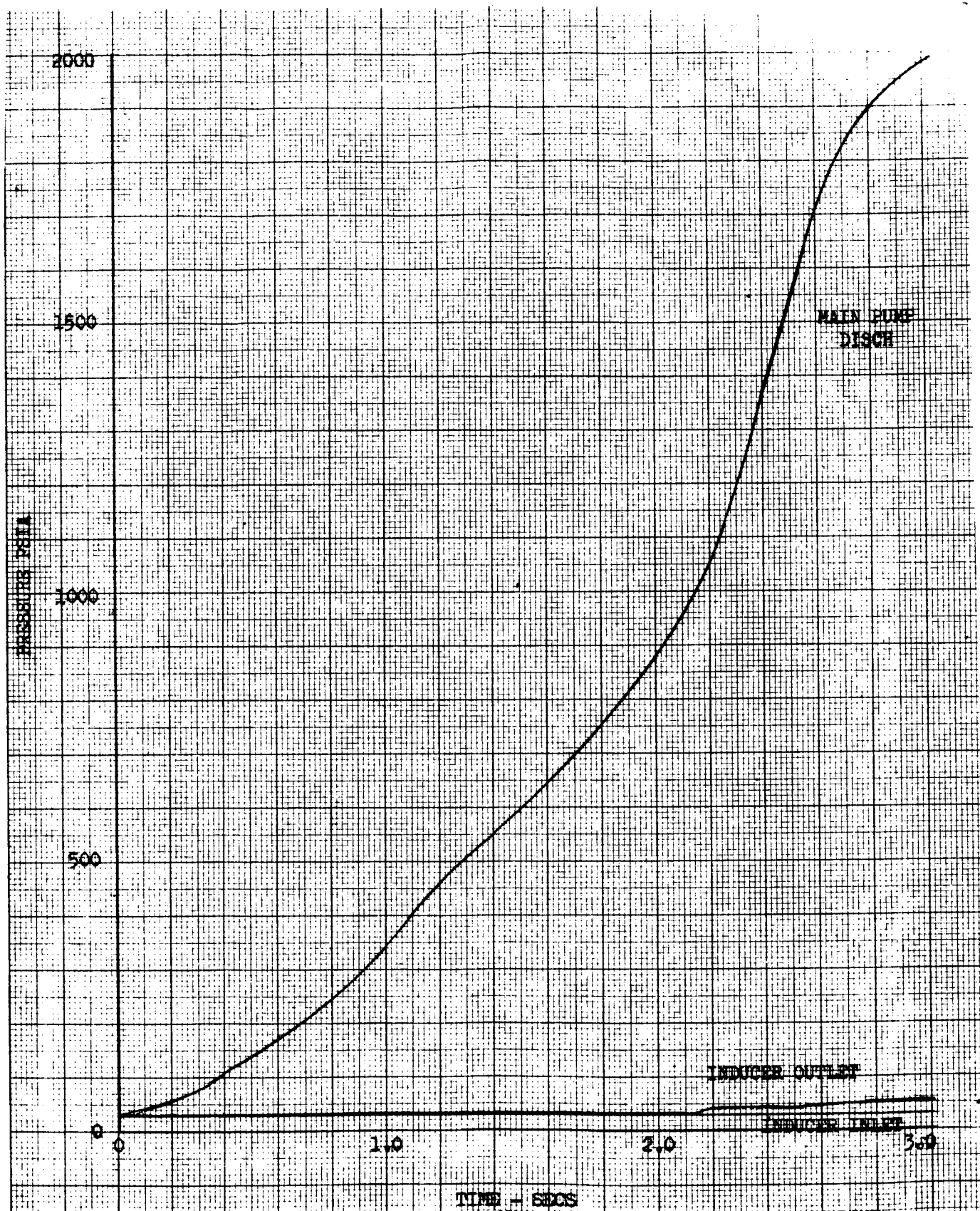


Figure 89. Simulated Fuel Feed System

3. The starting and throttling performance for the planned test series is smooth and shows little dynamic effects.
4. The use of this type of preinducer in an engine feed system is feasible, with a proper starting sequence, at low preinducer NPSH's, thereby allowing the use of lower tank pressures, and thus, reducing tank wall weights.

APPENDIX A

EQUATION NOMENCLATURE

A	=	line area, in. ²
a	=	acoustic velocity, in./sec or Eigen vectors for modal analysis
1/C	=	pump compliance, in. ⁻²
g	=	acceleration of gravity, in./sec ²
I	=	turbopump moment of inertia, in.-lb-sec ²
L	=	length, inches, or fluid inertia, sec ² /in. ²
N	=	turbopump speed, rad/sec
NPSH	=	pump net positive suction head, feet
P	=	pressure, lb/in. ²
ΔP	=	pressure difference, lb/in. ²
R	=	resistance, sec ² /in. ⁵ , or pump radius, inches
T	=	torque, in.-lb
t	=	time, seconds
Δt	=	computing interval (for digital model), seconds
\dot{W}	=	flowrate, lb/sec
\ddot{W}	=	flow acceleration, lb/sec ²
γ	=	time delay line parameter, sec/in. ²
φ	=	pump flow parameter
ψ	=	pump head parameter
χ	=	pump torque parameter
ρ	=	fluid density, lb/in. ³
σ	=	cavitation parameter
τ	=	time delay line transmission time, seconds
ω	=	undamped natural frequency
V	=	modal analysis parameter
ξ	=	modal damping constant

BASIC EQUATIONS

A. Tank and Tube Bundle

$$P_{ILI}(t) = P_T + L_T \rho - \frac{R_{TB}}{\rho} (\dot{W}_{ILI})^2 \quad (1)$$

Note: L_T is fluid height in tank

B. Inducer Inlet Line

1. Time Delay Equations

$$\tau_{IL} = L_{IL}/a_{IL}$$

$$\gamma_{IL} = a_{IL}/g A_{IL}$$

$$P_{ILI}(t) = P_{IPI}(t - \tau_{IL}) + \gamma_{IL} \left[\dot{W}_{ILI}(t) - \dot{W}_{ILO}(t - \tau_{IL}) \right] + \frac{R_{ILI}}{\rho} \left[\dot{W}_{ILI}(t) \right]^2 + \frac{R_{ILO}}{\rho} \left[\dot{W}_{ILO}(t - \tau_{IL}) \right]^2 \quad (2)$$

$$P_{IPI}(t) = P_{ILI}(t - \tau_{IL}) - \gamma_{IL} \left[\dot{W}_{ILO}(t) - \dot{W}_{ILI}(t - \tau_{IL}) \right] - \frac{R_{ILO}}{\rho} \left[\dot{W}_{ILO}(t) \right]^2 + \frac{R_{ILI}}{\rho} \left[\dot{W}_{ILI}(t - \tau_{IL}) \right]^2 \quad (3)$$

2. Modal Equations

$$\frac{L_{IL}}{gA_{IL}} \ddot{W}^* + \frac{R_{IL}}{\rho} \dot{W}^{*2} = P_{ILI}(t) - P_{IPI}(t)$$

$$\ddot{V}_i + 2\xi_i \omega_i \dot{V}_i + \omega_i^2 V_i = a_{li} P_{ILI}(t) - a_{ni} P_{IPI}(t) \quad (4)$$

($i = 2$ to number of modes)

Note: \dot{W}^* is first mode flowrate

$$\dot{W}_{ILI}(t) = \dot{W}^* + \sum_{i=2}^n a_{1i} \dot{V}_i \quad (5)$$

$$\dot{W}_{ILO}(t) = \dot{W}^* + \sum_{i=2}^n a_{1i} \dot{V}_i \quad (6)$$

C. Inducer Inlet Compliance

$$NPSH_{IP} = (P_{IPI} - P_{VAP}) / (12) (\rho) \quad (7)$$

$$\sigma_{IP} = \frac{NPSH_{IP} (12) (2g)}{(N_{IP})^2 (R_{IP})^2 (1 + (\phi_{IP})^2)} \quad (8)$$

$$P_{IPI}(t) = P_{IPI}(t - \Delta t) + \left(\frac{1}{C_1} \right)_{IP} \left[W_{ILO}(t) - W_{IP}(t) \right] \Delta t \quad (9)$$

D. Inducer Pump

1. Head

$$\phi_{IP} = \dot{W}_{IP} / \rho (N_{IP}) (R_{IP}) (A_{IP}) \quad (10)$$

$$\psi_{IP} = f(\phi_{IP})$$

For digital simulation, ψ_{IP} will be evaluated by linear interpolation between points representing the curve.

$$\overline{\Delta P}_{IP} = (\psi_{IP}) (\rho) (N_{IP})^2 \frac{(R_{IP})^2}{g} \quad (\text{noncavitating}) \quad (11)$$

Cavitation Correction

$$\frac{\Delta P}{\overline{\Delta P}_{IP}} = f \left[\left(\frac{NPSH}{N^2} \right)_{IP}, \phi_{IP} \right]$$

$$\Delta P_{IP} = \left[\frac{\Delta P}{\overline{\Delta P}} \right]_{IP} (\overline{\Delta P}_{IP}) \quad (12)$$

Note: \dot{W}^* is first mode flowrate

$$P_{IPD} = P_{IPI} + \Delta P_{IP} - \frac{L_{IP}}{\Delta t} \left[\dot{W}_{IP}(t) - \dot{W}_{IP}(t - \Delta t) \right] \quad (13)$$

2. Torque

$$\chi_{IP} = f(\varphi_{IP})$$

$$\overline{T_{IP}} = \chi_{IP} (\rho) (N_{IP})^2 (R_{IP})^3 (A_{IP})/g \quad (14)$$

$$T_{IP} = \overline{T_{IP}} \left(\frac{\Delta P}{\Delta P} \right)_{IP} \quad (15)$$

E. Inducer Turbine

1. Head-Capacity for Liquid Drive Fluid

$$\Delta P_{IT} = \frac{0.00307}{\rho} \dot{W}_{IT}^2 \quad (16)$$

2. Torque for Liquid Drive Fluid

$$(T/\Delta P)_{IT} = f(N_{IP})$$

$$T_{IT} = (T/\Delta P)_{IT} (\Delta P)_{IT} \quad (17)$$

F. Inducer Speed

$$N_{IP} = N_{IP} + 1/I_{ITP} (T_{IT} - T_{IP}) \Delta t \quad (18)$$

G. Inducer Turbine Inlet Line

1. Lumped Parameter

$$P_{ITVD}(t) - P_{ITI}(t) = \frac{L_{ITL}}{A_{ITL}} \frac{d W_{IT}}{d t} \quad (19)$$

2. Modal Equations

$$\left(L_{ITL} / g A_{ITL} \right) \dot{W}_{ITL} + \frac{R_{ITL}}{\rho} \left(\dot{W}_{ITL}^* \right)^2 = P_{ITVD} - P_{ITI} \quad (20)$$

$$\ddot{V}_i + 2\xi \omega_i'' \dot{V}_i + \omega_i''^2 V_i = a_{li}'' P_{ITVD} - a_{ni}'' P_{ITI}$$

$$\dot{W}_{ITV}(t) = \dot{W}_{ITL}^* + \sum_{i=2}^n a_{li}'' \dot{V}_i \quad (21)$$

$$\dot{W}_{IT}(t) = \dot{W}_{ITL}^* + \sum_{i=2}^n a_{ni}'' \dot{V}_i \quad (22)$$

H. Inducer Turbine Line Value

$$P_{ITVD} = P_{PD} - \frac{R_{ITV}}{\rho} \left(\dot{W}_{ITV}(t) \right)^2 \quad (23)$$

I. Inducer-Main Pump Coupling

$$\dot{W}_P = \dot{W}_{DL} + \dot{W}_{ITV} \quad (24)$$

1. If Close Coupled

$$P_{PI} = P_{IPD}$$

2. If Line Coupled (assuming line length > 10 feet)

A. Time-Delay Equations

$$\tau_{PIL} = L_{PIL} / a_{PIL}$$

$$\gamma_{PIL} = a_{PIL} / g A_{PIL}$$

$$P_{IPD}(t) = P_{PI}(t - \tau_{PIL}) + \gamma_{PIL} \left(\dot{W}_{PIL}(t) - \dot{W}_{PIL}(t - \tau_{PIL}) \right)^2 + \frac{R_{PILI}}{\rho} \left(\dot{W}_{PIL}(t) \right)^2 + \frac{R_{PIL0}}{\rho} \left(\dot{W}_{PI}(t - \tau_{PI}) \right)^2 \quad (25)$$

$$P_{PI}(t) = P_{IPD}(t - \tau_{PIL}) - \gamma_{PIL} \left(\dot{W}_{PI}(t) - \dot{W}_{PI}(t - \tau_{PIL}) \right) - \frac{R_{PIL0}}{\rho} \left(\dot{W}_{PI}(t) \right)^2 - \frac{R_{PILI}}{\rho} \left(\dot{W}_{PIL}(t - \tau_{PIL}) \right)^2 \quad (26)$$

B. Modal Equations

$$\left[\frac{L_{PIL}}{gA_{PIL}} \right] \ddot{W}^{**} + \frac{R_{IL}}{\rho} \dot{W}^{**2} = P_{IPD}(t) - P_{PI}(t) \quad (27)$$

$$\ddot{V}_i' + 2\xi \omega_i' \dot{V}_i' + \omega_i'^2 V_i' = a_{li}' IPD(t) - a_{ni}' P_{PI}(t)$$

$$\dot{W}_{PIL}(t) = \dot{W}^{**} + \sum_{i=2}^n a_{li}' \dot{V}_i' \quad (28)$$

$$\dot{W}_{PI}(t) = \dot{W}'^{**} + \sum_{i=2}^n a_{ni}' \dot{V}_i' \quad (29)$$

J. Inducer Outlet Compliance and Main Pump Inlet Compliance

1. Inducer Outlet

$$P_{IPD} = (1/C_2) IP \int_0^t (W_{IP} + W_{IT} - W_{PIL}) dt \quad (30)$$

2. Main Pump Inlet

$$\sigma_P = \frac{(NPSHP)(12)(2g)}{(N_P)^2 (RP)^2 (1 + \phi_p^2)}$$

$$(1/C)_P = f(\sigma_P)$$

$$P_{PI} = (1/C)_P \int_0^t (W_{PI} - W_P) dt \quad (31)$$

K. Main Pump

1. Head

$$\phi_P = \dot{W}_P / (\rho) (N_P) (A_P) (R_P)$$

$$\psi_P = f(\phi_P) \quad (32)$$

$$\overline{\Delta P_P} = \psi_P (\rho) (N_P)^2 (R_P^2) / g \quad (33)$$

Cavitation Correction

$$\left(\frac{\Delta P}{\overline{\Delta P}} \right)_P = f(NPSH_P, \phi_P) \quad (34)$$

$$NPSH_P = (P_{PI} - P_{VAP}) / (12) (\rho)$$

$$\Delta P_P = \left(\frac{\Delta P}{\overline{\Delta P}} \right)_P \overline{\Delta P_P} \quad (35)$$

$$P_{PD} = P_{PI} + \Delta P_P \quad (36)$$

2. Torque

$$\chi_P = f(\phi_P)$$

$$T_P = \chi_P (\rho) (N_P)^2 (R_P)^3 (A_P) / g \quad (37)$$

$$T_P = T_P \left(\frac{\Delta P}{\overline{\Delta P}} \right)_P \quad (38)$$

L. Facility Drive System Torque

1. For Program Checkout

$$N_P = f(\text{TIME}) \quad (\text{Replaces Eq. 39})$$

M. Main Pump Speed

$$N_P = N_P + 1/I_{(DS + P)} (T_{DS} - T_P) \Delta t \quad (39)$$

N. Pump Discharge Line

1. Time Delay Equations

$$\tau_{\text{PDL}} = L_{\text{PDL}}/a_{\text{PDL}}$$

$$\gamma_{\text{PDL}} = a_{\text{PDL}}/g_{\text{PDL}}^A$$

$$P_{\text{PD}}(t) = P_{\text{VI}}(t - \tau_{\text{PDL}}) + \gamma_{\text{PDL}} \dot{w}_{\text{PDL}}(t) - \dot{w}_{\text{V}}(t - \tau_{\text{PDL}}) + \frac{R_{\text{PDLI}}}{\rho} \left[\dot{w}_{\text{DL}}(t) \right]^2 + \frac{R_{\text{PDLO}}}{\rho} \left[\dot{w}_{\text{V}}(t - \tau_{\text{PDL}}) \right]^2 \quad (40)$$

$$P_{\text{VI}}(t) = P_{\text{PD}}(t - \tau_{\text{PDL}}) - \gamma_{\text{PDL}} \left[\dot{w}_{\text{V}}(t) - \dot{w}_{\text{DL}}(t - \tau_{\text{PDL}}) \right]^2 - \frac{R_{\text{PDLO}}}{\rho} \left[\dot{w}_{\text{V}}(t) \right]^2 - \frac{R_{\text{PDLI}}}{\rho} \left[\dot{w}_{\text{DL}}(t - \tau_{\text{PDL}}) \right]^2 \quad (41)$$

2. Modal Equations

$$\ddot{v}_i + 2\xi \omega_i \dot{v}_i + \omega_i^2 v_i = a_{1i} P_{\text{PD}} - a_{Vi} \Delta P_{\text{V}} - a_{ni} (P_{\text{T}} - L_{\text{T}} \rho)$$

$$\left[\frac{L_{\text{DL}}^*}{g_{\text{DL}}^A} \right] \dot{w}_{\text{DL}}^* + \frac{RV}{\rho} (\dot{w}_{\text{DL}}^*)^2 = (P_{\text{PD}} - P_{\text{T}} + L_{\text{T}} \rho) \quad (42)$$

$$\dot{w}_{\text{DL}} = \dot{w}_{\text{DL}}^* + \sum_{i=2}^n a_{1i} \ddot{v}_i \quad (43)$$

$$\dot{w}_{\text{V}} = \dot{w}_{\text{DL}}^* + \sum_{i=2}^n a_{Vi} \dot{v}_i \quad (44)$$

0. Discharge Valve

$$P_{VI} - P_{V0} = \frac{R_V}{\rho} \left[\dot{w}_{V(t)} \right]^2 + \frac{L_V}{\Delta t} \left[\dot{w}_{V(t)} - \dot{w}_{V(t - \Delta t)} \right] \quad (45)$$

or, for Analog Program

$$\Delta P_V = \frac{R_V}{\rho} \dot{w}_{V(t)}^2$$

$$R_V = f(X_V)$$

P. Return Line

1. Time Delay Equations

$$\tau_{RL} = L_{RL}/a_{RL}$$

$$\gamma_{RL} = a_{RL}/gA_{RL}$$

$$P_{V0(t)} = P_T + \gamma_{RL} \left(\dot{w}_{V(t)} - \dot{w}_{T(t - \tau_{RL})} \right) + \frac{R_{RLI}}{\rho} \left(\dot{w}_{V(t)} \right)^2 + \frac{R_{RL0}}{\rho} \left(\dot{w}_{T(t - \tau_{RL})} \right)^2 + L_T \rho \quad (46)$$

$$P_T = P_{V0(t - \tau_{RL})} - \gamma_{RL} \left(\dot{w}_{T(t)} - \dot{w}_{V(t - \tau_{RL})} \right) - \frac{R_{RL0}}{\rho} \left(\dot{w}_{T(t)} \right)^2 - \frac{R_{RLI}}{\rho} \left(\dot{w}_{V(t - \tau_{RL})} \right)^2 - L_T \rho \quad (47)$$

2. Modal Equations

$$\dot{w}_T = \dot{w}_{DL}^* + \sum_{i=2}^n a_{ni} V_i \quad (48)$$

MODEL NOMENCLATURE

Symbol	Description
A1	Time delay line junction constant
A2	Time delay line junction constant
AIP	Normalizing area for inducer pump
ALPHIP	Inducer pump cavitation curve-fit coefficient
ALPHAP	Main pump cavitation curve-fit coefficient
AP	Normalizing area for main pump
CHIMP	Main pump torque parameter
CHIP	Inducer pump torque parameter
COMPPI	Main pump inlet compliance
DENPHI	Denominator of inducer pump flow coefficient
DNPHIP	Denominator of main pump flow coefficient
DPFV	Facility valve pressure drop
DPIT	Inducer turbine pressure drop
DPPI	Main pump inlet pressure derivative
DSP	Main pump speed derivative
DSPIP	Inducer pump speed derivative
DWIT	Inducer turbine flow derivative
DWPD	Main pump flow derivative
DXCAV	Inducer pump effective NPSH/(speed) ²
DXCAPV	Main pump effective NPSH/(speed) ²
GAMDL	Time delay line characteristic, main
GAMFL	Time delay line characteristic, facility return line
GAMIL	Time delay line characteristic, tank-to-interface line
GAMIP	Time delay line characteristic, inducer inlet line
IDP	Inducer pump, cavitating pressure rise
IDPBAR	Inducer pump noncavitating pressure rise
IITP	Reciprocal of inducer rotating moment of inertia
IMP	Reciprocal of main pump rotating moment of inertia
IPICOM	Inducer pump inlet compliance
IPINER	Inducer pump fluid inertia
IPOCOM	Inducer pump outlet compliance
IPPRAT	Inducer pump cavitating to noncavitating pressure ratio

Symbol	Description
ITFLCO	Inducer turbine flow coefficient
LDL	Main pump discharge line fluid inertia
LT	Fluid height in tank
LV	Discharge valve fluid inertia
NPSHIP	Inducer pump net positive suction head
NPSHP	Main pump
PDP	Main pump cavitating pressure rise
PDPBAR	Main pump noncavitating pressure rise
PFUI	Main pump discharge valve inlet pressure
PFVD	Main pump discharge valve outlet pressure
PHIIP	Inducer pump flow coefficient
PHIP	Main pump flow coefficient
PILD	Inducer inlet line interface pressure
PILU	Tube bundle outlet pressure
PIPIN	Inducer pump inlet pressure
PIPOUT	Inducer pump outlet pressure
PITI	Inducer turbine inlet pressure
PPD	Main pump outlet pressure
PPLI	Turbine tapoff junction pressure
PPI	Main pump inlet pressure
PPRAT	Main pump cavitating to noncavitating pressure ratio
PSIIP	Inducer pump head coefficient
PSIP	Main pump head coefficient
PT	Tank pressure
PVAP	Vapor pressure
PWC	Water cooler pressure
RDL	Discharge line resistance
RITO	Fluid density
RILI	Inducer inlet line resistance
RILU	Interface line resistance
RIP	Inducer pump normalizing radius
RIT	Inducer turbine flow resistance
RITV	Inducer turbine valve resistance
RP	Main pump normalizing radius

Symbol	Description
RFMIP	Inducer pump speed
RPMP	Main pump speed
RTB	Tube bundle resistance
RV	Discharge valve resistance
SIGIP	Inducer pump cavitation parameter
SIGP	Main pump cavitation parameter
SIP	Inducer pump speed
SIPO	Inducer pump speed initial value
SP	Main pump speed
TDPIT	Inducer turbine torque to ΔP ratio
TORQF	Main pump input torque
TORQIP	Inducer pump torque
TORQIT	Inducer turbine torque
TORQP	Main pump torque
\dot{V}	Modal velocities
WCLI	Coupling line inlet flowrate
WCLD	Coupling line outlet flowrate
WFOV	Discharge valve flowrate
WILD	Inlet interface flowrate
WILU	Tube bundle outlet flowrate
WIP	Inducer pump flowrate
WIPLD	Inducer inlet line flowrate
WIT	Inducer turbine flowrate
WP	Main pump flowrate
WPD	Pump discharge flowrate
WT	Tank return flowrate
WWC	Water cooler flowrate
XDV	Discharge line valve position
XITV	Inducer turbine valve position
Y1 through Y12	Time delay line delayed values

DIGITAL MODEL PROGRAM LISTINGS

CONTINUOUS SYSTEM MODELING PROGRAM

PROBLEM INPUT STATEMENTS

```

*      CONTROL TIMES AND OUTPUT
TIMER  FINTIM=4.0,PRDEL=0.02,DELT=0.0005,OUTDEL=0.08
PRINT  P1LU,W1LU,P1LD,W1LD,NPSHIP,PHIP,PIPIN,WFV1,W1PLD,W1P,W1T,WP,...
        P1POUT,RPMIP,NPSHP,P1TI,RPMP,PPD,PFI,PFO,WT,PPLI,WPD,...
        TORQIT,TORQIP,PHIIP,SIGIP,IPICCM,IPINER,IPCCCM,IDPHAR,...
        IPPRAT,PCPBAR,PPRAT,Y1,Y2,Y3,Y4,Y5,Y6,Y7,Y8,Y9,Y10,PWC,WWC
TITLE  PRE-INDUCER-PUMP TEST SYSTEM
PRTPLT SIP(0.0,500.0),SP(0.0,1000.0),PIPCUT(0.0,100.0),PIPIN(0.0,25.0)
PRTPLT PPC(0.0,1000.0),WIP(0.0,500.0),WP(0.0,500.0),WIT(0.0,100.0)
PRTPLT PITI(C.C,500.C)
LABEL  PRE-INDUCER-PUMP TEST SYSTEM - CLOSE COUPLING
MACRO  YI=SPEED1(NUM1,DEN1,S1,Y1MAX)
PROGCD YI=SPEED1(NUM1,DEN1,S1,Y1MAX)
        IF(S1)2,2,1
1      YI=NUM1/(DEN1*S1**2)
        YI=AMIN1(Y1,Y1MAX)
        GO TO 3
2      YI=Y1MAX
3      CONTINUE
ENDPRO
ENDMAC
MACRO  Y=SPEED(NUM,DEN,S)
PROGCD Y=SPEED(NUM,DEN,S)
        IF(S)2,2,1
1      Y=NUM/(DEN*S)
        GO TO 3
2      Y=0.0
3      CONTINUE
ENDPRO
ENDMAC
*TANK AND INDUCER INLET LINES
MEMORY DLAY(200)
PARAM  PT=15.C,LT=0.0,RHJ=0.0361,RILI=0.0,RILO=0.0,RIPO=0.0,RIPI=0.0,...
        RTB=3.735E-06,GAMIL=2.04,GAMIP=1.61,TAU1=0.00158,TAU2=0.00538
INIT
        A1=GAMIP/GAMIL
        A2=1.0+A1
CYNAM
        W1LU=IMPL(C.0,0.001,W1LU1)

```

```

RIL1=(RILI+RTB)/RHO*WILL*ABS(WILU)
WILU1=(Y1+PT+LT*RH0-RIL1-15.0)/GAMIL
RILU=RILI/RHO*WILU*ABS(WILU)
PILU=PT+LT*RH0-RTB/RFO*WILL*ABS(WILU)
WILD=(Y2-PILU+15.0)/GAMIL
PILD=(Y3+A1*Y2)/A2+15.0
INDUCER PUMP
*
AFGEN FIG6=0.0,100.0,0.2,100.0
AFGEN FIG1=-2.0,14.65,0.0,0.338,0.025,0.309,0.04,0.285,0.05,0.265,...
0.06,0.237,0.065,0.218,0.07,0.195,0.075,0.168,0.085,0.106,...
0.095,0.028,0.11,-0.093,2.0,-15.29
AFGEN FIG6A=0.0,0.0225,0.2,0.0225
AFGEN FIG2=0.0,6.3E-7,0.062,6.55E-7,0.0665,6.72E-7,0.0707,7.1E-7,...
0.074,7.0E-7,0.1,16.3E-7
AFGEN FIG6B=0.0,100.0,0.2,100.0
AFGEN FIG3=0.0,0.0170,0.0115,0.01842,0.025,0.01939,0.035,0.0197,0.05,...
0.0197,0.07,0.0189,0.095,0.01685,0.115,0.0143,0.13,0.01175,...
0.15,0.00658,0.165,0.0027,0.18,-0.00318,2.0,-0.699
AFGEN TORQFD=0.0,0.0,0.5,0.12320,0.5,0.12320.0
AFGEN RVV=0.0,1000.0,100.0,0.002437,200.0,0.0002437
AFGEN ITV=0.0,1000.0,100.0,0.000588,200.0,0.000588
PARAM SIP=0.0,KIP=4.875,AIP=64.25,WIT=0.0,SIPD=0.0,...
PVAP=0.5,WIP=0.0,PIPD=15.0,IPIC=15.0,WP=0.0,...
IPIC=15.0,IPWIC=0.0
NPSHIP=AMAX1(0.3,(PIPIN-PVAP)/(12.0*RHG))
DENPHI=RHG*KIP*AIP
PHIIP=SPEED(WIP,DENPHI,SIP)

```

```

IND00060
IND00065
IND00084
IND00100
IND00115
IND00125
IND00160
IND00165
IND00170
IND00171
IND00172
IND00180
IND00190
IND00191
IND00200
IND00210
IND00211
IND00212
IND00220
IND00230
IND00240
IND00250
IND00251
IND00252
IND00260
IND00265
IND00270

```

GENERATED STRUCTURE STATEMENTS

```

PRUCEL PHIIP =SPEED( WIP , DENPHI , SIP )
IF( SIP ) 30004 , 30004 , 30003
30003 PHIIP = WIP /( DENPHI* SIP )
GC TO 30005
30004 PHIIP =0.0
30005 CONTINUE
ENDPRC

```

```

SIGNUM=NPSPHIP*9273.6
SIGDEN=(1.0+PHIIP**2)*RIP**2
SIGIP=SPEED1(SIGNUM,SIGDEN,SIP,0.1)

```

```

IND00275
IND00280
IND00285

```

GENERATED STRUCTURE STATEMENTS

```

PRUCEL SIGIP =SPEED1( SIGNUM , SIGDEN , SIP , 0.1 )

```

```

IF( SIP ) 20007 , 30007 , 30006 , SIP **2)
30006 SIGIP = SIGNUM/( SIGDEN* )
SIGIP = AMIN1( SIGIP , 0.1 )
GC TC 30008
30007 SIGIP = 0.1
30008 CONTINUE
ENDPRG

```

```

IPICOM=AFGEN(FIG6,SIGIP)
IPINER=AFGEN(FIG6A,SIGIP)
IPOCOM=AFGEN(FIG6B,SIGIP)
PSIIP=AFGEN(FIG1,PHIIP)
ICPBAR=PSIIP*RHU*(SIP*RIP)**2/386.4
ALPHIP=AFGEN(FIG2,PHIIP)
DXCAV1=SPEED1(NPSHIP,1,SIP,1.0E+5)

```

GENERATED STRUCTURE STATEMENTS

```

PRGCEC DXCAV1=SPEED1( NPSHIP, 1 , SIP , 1.0E+5)
IF( SIP ) 30010 , 30010 , 30009 , SIP **2)
30009 DXCAV1= NPSHIP/( 1 * SIP **2)
DXCAV1=AMIN1( DXCAV1, 1.0E+5)
GC TO 30011
30010 DXCAV1= 1.0E+5
30011 CONTINUE
ENDPRG

```

```

CXCAV=AMAX1(6.36E-7,DXCAV1-C.0C2545*PHIIP**2)
IPPRAT=AMAX1(0.1,1.0-ALPHIP/DXCAV)
ICP=IDPBAR*IPPRAT
WIPLD=(Y4-PIPIN+15.0)/GAMIP
IICOMW=IPICOM*(WIPLD-WIP)
PIPIN=INTGRL(IPIIC,IICOMW)
IICOMW=IPOCOM*(WIP+WIT-WP)
PIPOUT=INTGRL(IPOIC,IICOMW)
IPDW=(ICP+PIPIN-PIPOUT)/IPINER
WIP=INTGRL(IPWIC,IPDW)
CHIP=AFGEN(FIG3,PHIIP)
TORQIP=CHIP*RHU*SIP**2*RIP**3*AIIP*IPPRAT/386.4
RPMIP=SIP*9.5493
INCUCER TURBINE
*
PARAM IITP=4.16,WIIC=0.0,LITL=0.1344,XITV=100.0
AFGEN FIG5=0.C,Y.4,1.C79,8.0548,1.3488,7.7544,1.7984,7.2755,2.6976,...
6.3885,3.5568,5.5806,5.3952,4.1437,5.9947,3.7053,6.744,3.1791,...

```

```

7.7074,2.5314,8.9920,1.7047,10.79,0.58773
AFGEN ITR=0.0,0.0732,1.80,C.080345,3.5968,0.08581,5.9947,0.091212,....
7.7074,C.09375,10.79,0.09555
RITV=AFGEN(ITV,XITV)
RIT=AFGEN(ITR,ITFLCO)
DPIT=RIT*WIT*ABS(WIT)
PITI=PIPUUT+DPIT
DWIT=(PPLI-PIPUUT-(RITV/KHO+RIT)*WIT*ABS(WIT))/LITL
WIT=INTGRL(WIT0,DWIT)
TDPIT=AFGEN(FIG5,ITFLCO)
TORQIT=TDPIT*DPIT
DSPIP=(TORQIT-TORQIP)*IITP
SIP=INTGRL(SIP0,DSPIP)
SIP=AMAX1(C.0,SIP)

```

```

TURB0022
TURB0025
TURB0026
TURB0035
TURB0039
TURB0040
TURB0045
TURB0050
TURB0055
TURB0060
TURB0065
TURB0070
TURB0075
TURB0080

```

****CUTPUT NAME NOT UNIQUE ** WARNING ONLY****

****INPUT NAME SAME AS OUTPUT NAME**WARNING ONLY****

```

PROCD ITFLCO=FLCO(SIP,WIT)
IF(WIT)10,20,10
10 ITFLCO=SIP/WIT
GO TO 25
20 ITFLCO=C.0
25 CONTINUE
ENDPRO
* MAIN PUMP
PARAM AP=22.5,KP=5.1,SP=0.0,IMP=1.0
AFGEN FIG9=-4.0,C.2,C.0,0.029,0.024,0.0425,0.0375,0.047,0.0505,....
0.0502,C.0085,C.057,C.105,0.0607,0.113,0.0655,0.1203,0.0728,....
0.16,0.125
AFGEN FIG7=-4.0,48.86,0.0,C.465,0.012,0.52,0.03,0.545,0.043,0.545,....
0.062,C.536,0.0,C89,0.498,C.107,0.46,0.16,0.332,0.3803,-0.2
AFGEN FIG8=0.0,0.06E-07,0.03,7.4E-07,0.05,6.74E-07,0.07,5.96E-07,....
0.081,5.32E-07,0.082,5.3E-07,0.0843,5.32E-07,0.10,5.1E-07,....
0.11,6.5E-07,0.12,6.82E-07,0.14,7.44E-07
PARAM LCL=C.00488,RDL=2.235E-6
NPSHP=AMAX1(0.3,(PIPUUT-PVAP)/(12.0*RHC))
UNPHIP=KHO*KP*AP
PHIP=SPEED(WP,DNPHIP,SP)

```

```

TURB0085
TURB0090
TURB0095
TURB0100
TURB0105
TURB0110
TURB0115
PUMP0010
PUMP0020
PUMP0025
PUMP0026
PUMP0027
PUMP0030
PUMP0031
PUMP0035
PUMP0036
PUMP0037
PUMP0045
PUMP0055
PUMP0060
PUMP0065

```

GENERATED STRUCTURE STATEMENTS

```

PROCCED      PHIP =SPEED(
  IF( SP      ) 30012 ,      WP      ,      DNPHIP ,      SP      )
30012      PHIP =      WP      / (      DNPHIP*      SP      )
GC TO 30014
30013      PHIP =0.0
30014      CONTINUE
ENCLPRG

```

PUMP0070
PUMP0075
PUMP0080
PUMP0085

```

PSIP=AFGEN(FIG7,PHIP)
PDPBAR=PSIP*RHO*(SP*RP)**2/386.4
ALPHAP=AFGEN(FIG8,PHIP)
CXCAVP=SPEED1(NPSHP,1,SP,1.0E+5)

```

GENERATED STRUCTURE STATEMENTS

```

PROCCED      DXCAVP=SPEED1(      NPSHP ,      1      ,      SP      ,      1.0E+5)
  IF( SP      ) 30016 ,      30015      ,      SP      **2)
30015      CXCAVP=      NPSHP / (      1      *      SP      **2)
CXCAVP=AMIN1(      CXCAVP ,      1.0E+5)
GC TO 30017
30016      CXCAVP=      1.0E+5
30017      CONTINUE
ENCLPRG

```

```

DCAVP=AMAX1(5.3E-07,DXCAVP-0.00122*PHIP**2)

```

```

PPRAT=AMAX1(0.1,1.0-ALPHAP/DCAVP)
PDP=PDPBAR*PPRAT
PPD=PI*PUUT+PDP
DWPL=(PPD-PPL1-RUL/RHO*WP*ABS(WP))/LDL
WP=INTGRL(C.0,DWPD)
RPM=SP*5.5453
TORQF=AFGEN(TORQFD,TIME)
CFIMP=AFGEN(FIG5,PHIP)
TORQP=CFIMP*RHO*SP**2*RP**3*AP*PPRAT/386.4
DSP=IMP*(TORQF-TORQP)
SP=INTGRL(C.0,DSP)
PUMP DISCHARGE AND FACILITY LINE
* PARAM GAMDL=4.51,RDLI=0.0,KDLO=0.0,TAU3=0.0019,TAU4=0.035,...
  GAMFL=2.085,RFLI=0.0,RFL0=0.0,XDV=100.0,LV=0.00416,TAU5=0.0455
  WPD=WP-WIT
  PPLI=Y5+GAMDL*WPD+15.0
  RV=AFGEN(RDV,XDV)

```

PUMP0090
PUMP0095
PUMP0100
PUMP0105
PUMP0107
PUMP0108
PUMP0110
PUMP0120
PUMP0130
PUMP0140
PUMP0150
PUMP0160
REFL0010
REFL0020
REFL0025
REFL0090
REFL0110
REFL0125

RETL 0165
 RETL 0185
 RETL 0210
 RETL 0230
 RETL 0240
 RETL 0250
 RETL 0260
 TDV00010
 TDV00015
 TDV00020
 TDV00030
 TDV00040
 TDV00050
 TDV00060
 TDV00070
 TDV00080
 TDV00085
 TDV00089
 TDV00090
 TDV00095
 TDV00096
 TDV00100
 TDV00110
 TDV00120
 TDV00130
 TDV00140
 TDV00150
 TDV00160
 TDV00170
 TDV00290
 TDV00350
 MISC0020
 MISC0030
 MISC0040

PFV1=Y6-GAMDL*WFFV1+15.0
 PFVU=Y7+GAMFL*WFFV1+15.0
 WT=(Y10-LT*RHU)/GAMFL
 ICFVW=(PFV1-PFVU-RV/RHO*WFFV1*ABS(WFFV1))/LV
 WFFV1=INTGKL(C.G,ICFVW)
 WWC=(Y8-Y5)/(2*GAMFL)
 PWC=Y8-GAMFL*WWC+PT
 NG:SUPT
 IF(KEEP)IG,IG,50
 50 TUPPD=PFV1-GAMDL*WFFV1+KDLO/RHO*WFFV1*ABS(WFFV1)-PT
 Y5=CLAY(4,TAU3,TDPPD)
 TDPVI=PPLI+GAMDL*WPD-KDLI/RHO*WPD*ABS(WPD)-PT
 Y6=CLAY(4,TAU3,TDPI)
 TDFVU=PWC-GAMFL*WWC-PT
 Y7=CLAY(78,TAU4,TDPVU)
 TDTW=PWC+GAMFL*WWC-PT
 Y10=CLAY(91,TAU5,TDTW)
 TDWC=PFVU+GAMFL*WFFV1-PT
 Y8=CLAY(79,TAU4,TDWC)
 TDTWC=-GAMFL*WT
 Y9=CLAY(51,TAU5,TDTW)
 TDWIL=-PILD+GAMIL*WILD-RILO/RHC*WILD*ABS(WILD)+15.0
 Y1=CLAY(4,TAU1,TDWIL)
 TCDWL=PILU+GAMIL*WILU-RILI/RHO*WILU*ABS(WILU)-15.0
 Y2=CLAY(4,TAU1,TDWDL)
 TCDPL=PIPIN-GAMIP*WIPLD+RIPO/RHC*WIPLD*ABS(WIPLD)-15.0
 Y3=CLAY(12,TAU2,TDPI)
 TDWPI=PILD+GAMIP*WILD-RIPC/RHC*WILD*ABS(WILD)-15.0
 Y4=CLAY(12,TAU2,TDWPI)

100 CONTINUE

SCRT

METHGD TRAPZ

ENC

STOP

OUTPUT VARIABLE SEQUENCE

A1	A2	WIPLD	SIP	DENPHI	PHIIP	SIGDEN	NPSHIP	SIGNUM	SIGIP
IPICOM	IICOMW	PIPIN	IPOCOM	IUCOMW	PIPOLT	IPINER	DXCAV1	DXCAV	ALPHIP
IPPRAT	PSIIP	ICPBAR	ICP	IPDW	WIP	ITFLCC	RIT	RITV	WPI
PPLI	CMIT	WIT	CHIP	TORQIP	DPIT	TDPIIT	TORQIT	DSPIP	SIP
LNPHIP	PHIP	NPSHP	EXCAVP	UCAVP	ALPHAP	PPRAT	PSIP	POPPAR	PPF
FWC	FWPC	WP	CHIMP	TORQP	TORQF	DSP	SP	RV	PFVU
PFV1	ICFVW	WFFV1	ZZCCCL	RIL1	WILU1	WILU	RILU	PILU	PILU

WILD	RPMIP	PITI	RPMP	WT	WMC	PWC	ZZ0013	TDPPD	Y5
TDPVI	Y6	TDPVO	Y7	TDTW	Y10	TDWC	Y8	TDTWC	Y9
TDWIL	Y1	TDWCL	Y2	TDPDL	Y3	TDWIPI	Y4		

PARAMETERS NOT INPUT OR OUTPUTS NOT AVAILABLE TO SORT SECTION***SET TO ZERO***

Y1	Y2	Y3	Y4	Y5	Y6	Y7	Y10
Y8	Y9						

OUTPUTS	INPUTS	PAKAMS	INTEGS +	MEM	BLKS	FORTAN	DATA	CDS
104(500)	161(1400)	73(400)	8+	10=	18(300)	130(600)		49

CONTINUOUS SYSTEM MODELING PROGRAM

PROBLEM INPUT STATEMENTS

```

*      CONTROL TIMES AND OUTPUT
TIMER  FINTIM=4.C,PRODEL=0.02,DELT=0.0005,OUTDEL=0.08
PRINT  P1LU,W1LU,P1LD,W1LD,NPSHIP,PHIP,PIPIN,WFVI,W1PLD,W1P,W1T,W1P,...
        P1POLT,FPMIP,NPSHP,P1TI,KPMP,PPD,PFVI,PFVC,W1T,P1LI,WPD,...
        TORQIT,TORQIP,PHIIP,SIGIP,IPICCM,IPINER,IPCCM,ICPBAR,...
        IPPRAT,PPBAR,PPRAT,PWC,WWC,PPI,WCLL,WCLC
TITLE  PRE-INDUCER-PUMP TEST SYSTEM-REMCIE COUPLING
PR1PLT SIP(C.C,500.C),SF(0.0,1000.0),PIPCUT(0.0,100.0),PIPIN(0.0,25.0)
PR1PLT PPD(0.0,1000.0),W1P(0.0,500.0),WP(0.0,500.0),W1T(0.0,100.0)
PR1PLT P1TI(C.C,500.C),PPI(0.0,100.0)
LABEL  PRE-INDUCER-PUMP TEST SYSTEM-REMCIE COUPLING
MACRO  Y1=SPEED1(NUM1,DEN1,S1,Y1MAX)
PROCED Y1=SPEED1(NUM1,DEN1,S1,Y1MAX)
      IF(S1)2,2,1
      1 Y1=NUM1/(DEN1*S1**2)
        Y1=AMIN1(Y1,Y1MAX)
        GO TO 3
      2 Y1=Y1MAX
      3 CONTINUE
ENDPRO
ENDMAC
MACRO  Y=SPEED(NUM,DEN,S)
PROCED Y=SPEED(NUM,DEN,S)
      IF(S)2,2,1
      1 Y=NUM/(DEN*S)
        GO TO 3
      2 Y=0.C
      3 CONTINUE
ENDPRO
ENDMAC
*TANK AND INDUCER INLET LINES
MEMORY DLAY(200)
PARAM  PT=15.0,LT=0.0,RHC=0.0361,RILI=0.0,RILC=0.0,RIPO=0.0,RIPI=0.0,...
      RTB=3.735E-06,GAMIL=2.04,GAMILP=1.61,TAU1=0.00158,TAU2=0.001714
INIT
      A1=GAMILP/GAMIL
      A2=1.0+A1
DYNAM
      W1LU=IMPL(C.0,C.C01,W1LU1)

```

CT-00010
CT-00020
CT-00050
CT-00060
CT-00061
CT-00062
CT-00100
CT-00110
CT-00111
CT-00112
CT-00115
SPED1010
SPED1015
SPED1020
SPED1025
SPED1030
SPED1035
SPED1040
SPED1045
SPED1050
SPED1055
SPED0010
SPED0020
SPED0030
SPED0040
SPED0050
SPED0060
SPED0070
SPED0080
SPED0090
IND00010
IND00015
IND00021
IND00022
INDC0030
IND00035
IND00040
IND00045
IND00055


```

RIL1=(KILI+RTB)/RHO*WILU*ABS(WILU)
WILU1=(Y1+PI+LT*RHO-RIL1-15.0)/GAMIL
RILU=RILI/RHO*WILU*ABS(WILU)
PILU=PI+LT*RHO-RTB/RHC*WILU*ABS(WILU)
WILU=(Y2-PILD+15.0)/GAMIL
PILD=(Y3+A1*Y2)/A2+15.0
* INDUCER PUMP
AFGEN FIG6=C.C.100.C.C.2.100.0
AFGEN FIG1=-2.0,14.65,C.C.0.338,0.025,0.309,0.04,0.285,0.05,0.265,...
AFGEN 0.06,0.237,0.065,0.218,0.07,0.195,0.075,0.168,0.085,C.106,...
0.095,C.C.28,C.11,-0.093,2.0,-15.29
AFGEN FIG6A=C.C.C.C.0.225,0.2,0.0225
AFGEN FIG2=C.C.0.6,3E-7,0.062,6.55E-7,0.0665,6.72E-7,0.0777,7.1E-7,...
C.074,7.6E-7,0.1,16.3E-7
AFGEN FIG68=C.C.0.64,C.C.2.64,0
AFGEN FIG3=0.C.C.0.0170,0.0115,0.01842,0.025,0.01939,0.035,0.0197,0.05,...
C.0197,0.07,C.C.189,0.095,C.C.01685,0.115,0.0143,0.13,0.01175,...
C.15,0.00698,C.C.165,0.0027,0.18,-0.00318,2.0,-0.699
AFGEN TORQFD=C.C.C.C.3.0,12320.0,5.0,12320.0
AFGEN RDV=C.C.1000.C.C.100.0,0.0002437,200.0,0.0002437
AFGEN ITV=C.C.1000.C.C.100.0,0.000538,200.0,0.000588
PARAM SIP=C.C.0,RIP=4.875,AIP=64.25,WIT=0.0,SIPC=0.0,...
PVAP=C.5,WIP=0.0,PIPD=15.0,PIIC=15.0,WP=0.0,...
IPOIC=15.0,IPWIC=C.C
NPSHIP=AMAX1(C.3,{PIPIN-PVAP)/(12.0*RHC))
DENPHI=RHC*RIP*AIP
PHIIP=SPEED(WIP,DENPHI,SIP)

```

```

IND00060
IND00065
IND00084
IND00100
IND00115
IND00125
IND00160
IND00165
IND00170
IND00171
IND00172
IND00180
IND00190
IND00191
IND00200
IND00210
IND00211
IND00212
IND00220
IND00230
IND00240
IND00250
IND00251
IND00252
IND00260
IND00265
IND00270

```

```

GENERATED STRUCTURE STATEMENTS
PROCED PHIIP =SPEED( WIP , DENPHI, SIP )
IF( SIP ) 3CCC4 , 30004 , 30003
3CC03 PHIIP = WIP /( DENPHI* SIP )
GO TO 3CC05
3CCC4 PHIIP =C.C
3CC05 CONTINUE
ENDPROC

```

```

IND00275
IND00280
IND00285

```

```

SIGNUM=NPSHIP*9273.6
SIGDEN=(1.0+PHIIP**2)*RIP**2
SIGIP=SPEED1(SIGNUM,SIGDEN,SIP,0.1)

GENERATED STRUCTURE STATEMENTS
PROCED SIGIP =SPEED1( SIGNUM, SIGDEN, SIP , 0.1 )

```

```

IF( SIP ) 3CCC7 , 30007 , 30006 , SIP **2)
30CC6 SIGIP = SIGNUM/( SIGDEN* SIP **2)
SIGIP =AMINI( SIGIP , 0.1 )
GO TO 3CCC8
3CCC7 SIGIP = C.1
30CC6 CONTINUE
ENDPRO

```

INDC0290
 INDC0295
 INDC0300
 INDC0305
 INDC0310
 INDC0315
 INDC0320

GENERATED STRUCTURE STATEMENTS

```

PROCED DXCAV1=SPEED1( NPSHIP, 1 , SIP , 1.CE+5)
IF( SIP ) 3CC1C , 30010 , 30009 , SIP **2)
3CCCS DXCAV1= NPSHIP/( 1 * SIP **2)
DXCAV1=AMINI( DXCAV1, 1.0E+5)
GO TO 3CC11
3CC1C DXCAV1= 1.CE+5
3CC11 CONTINUE
ENDPRO

```

```

DXCAV=AMAX1( 6.367E-7,DXCAV1-0.002545*PHIIP**2)
IPPRAT=AMAX1( C.1,1.0-ALPHIP/DXCAV)
IDP=IDPBAR*IPPRAT
WIPLD=(Y4-PIPIN+15.0)/GAMIP
IICOMW=IPICOM*(WIPLD-WIP)
PIPIN=INTGRL(IPIIC,IICOMW)
IUCOMW=IPOCCM*(WIP+WIT-WCLI)
PIPOUT=INTGRL(IPCIC,ICCOMW)
IPDW=(IDP+PIPIN-PIPOUT)/IPINER
WIP=INTGRL(IPWIC,IPDW)
CHIP=AFGEN(FIG3,PHIIP)
TORQIP=CHIP*RHCH*SIP**2*RIIP**3*AIPI*IPPRAT/386.4
RPMIP=SIP*.5493
* INDUCER TURBINE
PARAM IITP=4.16,WITO=C.0,LITL=0.1344,XITV=100.0
AFGEN FIG5=C.C.9.4,1.C79,8.0548,1.3488,7.7544,1.7984,7.2755,2.6976,...
6.3885,3.5968,5.5806,5.3952,4.1437,5.9947,3.7053,6.744,3.1791,...
TURB0020
TURB0015
TURB0010
INDC0425
INDC0420
INDC0415
INDC0410
INDC0405
INDC0400
INDC0395
INDC0390
INDC0385
INDC0360
INDC0335
INDC0330
INDC0325

```

```

7.7074,2.5314,8.9920,1.7047,10.79,10.79,0.58773
AFGEN ITR=C.C,0.0732,1.8C,0.080345,3.5968,0.08581,5.9947,0.091212,...
7.7074,0.09375,10.79,0.09555
RITV=AFGEN(ITV,XITV)
RIT=AFGEN(ITR,ITFLCG)
DPIT=RIT*WIT*ABS(WIT)
PITI=PIPCUT+DPIT
DWIT=(PPLI-PIPCUT-(RITV/RHC+RIT)*WIT*ABS(WIT))/LITL
WIT=INTGRL(WITC,DWIT)
TDPIIT=AFGEN(FIG5,ITFLCC)
TORQIT=TDPIIT*DPIT
DSPIP=(TCRQIT-TCRQIP)*IITP
SIP=INTGRL(SIPC,DSPIP)
SIP=AMAX1(C.C,SIP)

```

TURB0022
TURB0025
TURB0026
TURB0035
TURB0039
TURB0040
TURB0045
TURB0050
TURB0055
TURB0060
TURB0065
TURB0070
TURB0075
TURB0080

****OUTPUT NAME NOT UNIQUE ** WARNING ONLY****

****INPUT NAME SAME AS OUTPUT NAME**WARNING ONLY****

```

PROCED ITFLCO=FLCG(SIP,WIT)
IF(WIT)10,20,10
10 ITFLCO=SIP/WIT
GO TO 25
20 ITFLCO=C.C
25 CONTINUE
ENDPRO
PARAM GAMCL=1.61,TAU6=C.003665,ICPPI=15.C
AFGEN FIG1C=0.0,1.0,C.01,8.5,0.016,20.0,0.02,40.0,0.025,72.0,0.03,...
120.C,0.035,200.C,0.04,340.0,0.045,460.0,0.2,460.0
WCLT=(Y12+PIPCUT-PT)/GAMCL
WCLU=(Y11-PTI+PT)/GAMCL
SIGNL=NPSHP*9273.6
SIGDE=(1.C+PHIP**2)*RP**2
SIGP=SPEED1(SIGNL,SIGDE,SP,0.1)

```

TURB0085
TURB0090
TURB0095
TURB0100
TURB0105
TURB0110
TURB0115
PCL00010
PCL00020
PCL00021
PCL00030
PCL00040
PCL00050
PCL00060
PCL00070

GENERATED STRUCTURE STATEMENTS

```

PROCED      SIGP =SPEED1(      SIGNL ,      SIGDE ,      SP ,      0.1 )
IF( SP ) 30013 , 30013 , 30012
30012      SIGP = SIGNL / ( SIGNL * SP **2)
SIGP =AMIN1( SIGP , 0.1 )

```

3C01S DXCAVP= 1.0E+5
 3C02C CONTINUE
 ENDPRO

```

DCAVP=AMAX1(5.3E-07,DXCAVP-0.00122*PHIP**2.0)
PPRAT=AMAX1(0.1,1.0-ALPHA/DXCAVP)
PDP=DPBAR*PPRAT
PPD=PPI+PDP
DMPD=(PPD-PPI-RDL/RHO*WP*ABS(WP))/LDL
WP=INTGRL(0.0,DMPD)
RMP=SP*9.5493
TORQF=AFGEN(TORQFD,TIME)
CHIMP=AFGEN(FIG9,PHIP)
TORQP=CHIMP*RHO*SP**2*RP**3*AP*PPRAT/386.4
DSP=IMP*(TORQF-TORQP)
SP=INTGRL(C.0,DSP)
* PUMP DISCHARGE AND FACILITY LINE
PARAM GAMDL=4.51,RDLI=C.0,RDLC=0.0,TAU3=0.0019,TAU4=0.039,...
GAMFL=2.085,RFLI=0.0,RFL0=0.0,XDV=100.0,LV=0.00416,TAU5=0.0455
WPD=WP-WIT
PLI=Y5+GAMDL*WPD+15.0
RV=AFGEN(RDV,XDV)
PFVI=Y6-GAMDL*WFVI+15.0
PFVO=Y7+GAMFL*WFVI+15.0
WT=(Y10-LT*RHO)/GAMFL
ICFVW=(PFVI-PFVO-RV/RHC*WFVI*ABS(WFVI))/LV
WFVI=INTGRL(0.0,ICFVW)
WVC=(Y8-Y5)/(2*GAMFL)
PWC=Y8-GAMFL*WVC+PT
NOSORT
IF(KEEP)100,100,50
50 TOPPD=PFVI-GAMDL*WFVI+RDLC/RHO*WFVI*ABS(WFVI)-PT
Y5=DLAY(4,TAU3,TDPPD)
TOPVI=PPI+GAMDL*WPD-RDLI/RHO*WPD*ABS(WPD)-PT
Y6=DLAY(4,TAU3,TDPMI)
TOPVO=PWC-GAMFL*WVC-PT
Y7=DLAY(78,TAU4,TDPVC)
TDTW=PWC+GAMFL*WVC-PT
Y10=DLAY(91,TAU5,TDTW)
TDWC=PFVO+GAMFL*WFVI-PT
Y8=DLAY(78,TAU4,TDWC)
TDWC=-GAMFL*WT
Y9=DLAY(91,TAU5,TDWC)
PUMP0090
PUMP0095
PUMP0100
PUMP0105
PUMP0107
PUMP0108
PUMP0110
PUMP0120
PUMP0130
PUMP0140
PUMP0150
PUMP0160
RETL0010
RETL0020
RETL0025
RETL0090
RETL0110
RETL0125
RETL0165
RETL0185
RETL0210
RETL0230
RETL0240
RETL0250
RETL0260
TDV00010
TDV00015
TDV00020
TDV00030
TDV00040
TDV00050
TDV00060
TDV00070
TDV00080
TDV00085
TDV00089
TDV00090
TDV00095
TDV00096

```

```

GO TO 3CC14          SIGP = C.1
3CC13
3CC14 CONTINUE
ENDPRO

      COMPPI=AFGEN(FIG10,SIGP)
      DPPI=COMPPI*(WCLG-WP)
      PPI=INTGRL(ICPPI,DPPI)
      * MAIN PUMP
      PARAM AP=22.9,RP=5.1,SP=0.0,IMP=1.0
      AFCEN FIG9=-4.0,C.2,C.C,0.029,0.024,0.0425,0.0375,0.047,0.0505,...
      0.0502,C.0885,C.057,0.105,0.0607,0.113,0.0655,0.1203,0.0728,...
      0.16,C.135
      AFCEN FIG7=-4.0,49.96,C.0,0.465,0.012,0.52,0.03,0.545,0.043,0.545,...
      0.062,0.536,C.089,0.498,0.107,0.46,0.16,0.332,0.3803,-0.2
      AFCEN FIG8=0.C,8.06E-07,0.03,7.4E-07,0.05,6.74E-07,0.07,5.96E-07,...
      0.081,5.32E-07,0.082,5.3E-07,0.0843,5.32E-07,0.1C,6.1E-07,...
      0.11,6.5E-07,C.12,6.82E-07,0.14,7.44E-07
      PARAM LDL=C.0048P,RDL=2.235E-6
      NP SHP=AMAX1(C.3,(PPI-PVAP)/(12.0*RHCI))
      DNPHIP=RH0*2P*AP
      PHIP=SPEED(WP,DNPHIP,SP)

GENERATED STRUCTURE STATEMENTS
PROCED PHIP =SPEED( WP , DNPHIP, SP )
IF( SP ) 30016 , 30016 , 30015
3CC15 PHIP = WP /( DNPHIP* SP )
GO TO 3CC17
3CC16 PHIP =C.C
3CC17 CONTINUE
ENDPRO

      PSIP=AFGEN(FIG7,PHIP)
      PDPHAR=PSIP*RHCI*(SP*RP)**2/386.4
      ALPHAP=AFGEN(FIG8,PHIP)
      DXCAVP=SPEED1(NP SHP,1,SP,1.0E+5)

PUMP0070
PUMP0075
PUMP0080
PUMP0085

GENERATED STRUCTURE STATEMENTS
PROCED DXCAVP=SPEED1( NP SHP , 1 , SP , 1.0E+5)
IF( SP ) 30019 , 30019 , 30018
3CC18 DXCAVP= NP SHP /( 1 * SP **2)
CXCAVP=AMINI( DXCAVP , 1.0E+5)
GO TO 3C02C

```

TDVCO100
TDVCO110
TDVCO120
TDVCO130
TDVCO140
TDVCO150
TDVCO160
TDVCO170
TDVCO180
TDVCO190
TDVCO200
TDVCO210
TDVCO290
TDVCO350
MISC0020
MISC0030
MISC0040

TDWIL=-PILD+GAMIL*WILD-RILC/RHO*WILD*ABS(WILD)+15.0
Y1=OLAY(4,TAU1,TDWIL)
TDWDL=PILU+GAMIL*WILU-RILI/RHO*WILU*ABS(WILU)-15.0
Y2=OLAY(4,TAU1,TDWDL)
TOPDL=PIPIN-GAMIP*WIPLD+RIPC/RHC*WIPLC*ABS(WIPLD)-15.0
Y3=OLAY(4,TAU2,TDPD)
TDWPI=PILD+GAMIL*WILD-RIPC/RHO*WILD*ABS(WILD)-15.0
Y4=OLAY(4,TAU2,TDWPI)
TDCL0=-PPI+GAMCL*WCLC+PT
Y12=OLAY(8,TAU6,TDCLC)
TDCLI=PIPOUT+GAMCL*WCLI-PT
Y11=OLAY(8,TAU6,TDCLI)

100 CONTINUE

STOP

METHOD TRAPZ

END

STOP

OUTPUT	VARIABLE	SEQUENCE	DENPHI	PHIIP	SIGDEN	NPSHIP	SIGNUM	SIGIP
A1	A2	WIPLD	SIP	IPCCM	IPCCM	PIPCT	IPINER	CXCAV1
IPICOM	IPICOM	PIPIN	WCLI	IPDW	WIP	ITFLCC	RIT	RITV
ALPPIP	IPPRAT	PSIIP	IDPBAR	CHIF	TCRCIP	DPIT	TCPIIT	TORQIT
WPC	PPLI	DWIT	WIT	CHIF	TCRCIP	DPIT	TCPIIT	TORQIT
SIP	WCLC	DNPHIP	PHIP	SIGDE	NPSHP	SIGNU	SIGP	COMPPI
PPI	DXCAVP	ALPHAP	PPRAT	PSIP	PDPBAR	PDP	PPD	DWPC
CHIMP	TORQP	TORQF	OSP	SP	RV	PFVC	PFVI	ICFVW
ZZCCO1	RILI	WILU1	WILU	RILL	PILU	PILD	WILD	RPMIP
DCAVP	RPMP	WT	WWC	PWC	ZZOO14	TDPPD	Y5	TDPII
TCPVO	Y7	TDIW	Y10	TDWC	Y8	TDIWC	Y9	TDWIL
TCWDL	Y2	TOPDL	Y3	TDWPI	Y4	TDCLC	Y12	TECLI

PARAMETERS NOT INPUT OR OUTPUTS NOT AVAILABLE TO SCRT SECTION***SET TO ZERO***

PARAMETERS	NOT INPUT	OR OUTPUTS	NOT AVAILABLE	TO SCRT	SECTION***SET TO ZERO***
Y1	Y2	Y3	Y4	Y11	Y5
Y7	Y1C	Y8	Y9	Y12	Y6

OUTPUTS	INPLTS	PARAMS	INTEGS	+ MEM	BLKS	FORTRAN	DATA	CDS
116(500)	177(1400)	75(400)	9+	12=	21(300)	147(600)	52	

LEVEL 2 FEB 67

DS/360 FORTRAN H

DATE 67.34

COMPILER OPTIONS - NAME= MAIN,OPT=00,LINECNT=40,SCURCF,ERCDIC,NOLIST,NODECK,LOAD,MAP,NREDIT,ID

```

ISN 0002      FUNCTION DLAY(L,N,TD,XIN)
ISN 0003      DIMENSION KX(1),X(1)
ISN 0004      COMMON DDUM1(64),C(8000),NALARM,DDUM2(12),KPT1,DDUM3(405),KEEP
ISN 0005      COMMON DDUM4(1316),SYMB(1)
ISN 0006      EQUIVALENCE(C(1),TIME),C(12),DELT),(X(1),KX(1),SYMB(1))
ISN 0007      K=L+6+(KPT1-1)
ISN 0008      IF(TIME-0.000C)100C,100C,1000,1010
ISN 0009      X(K-6)=TD/FLOAT(N)
ISN 0010      X(K-5)=X(K-6)
ISN 0011      KX(K-4)=C
ISN 0012      KX(K-3)=K
ISN 0013      KX(K-2)=N+N+2
ISN 0014      KX(K-1)=K+KX(K-2)-2
ISN 0015      X(K)=0.
ISN 0016      X(K+1)=XIN
ISN 0017      CLAY=0.0
ISN 0018      GO TO 1210

ISN 0019      C.... TEST IF TIME FOR OUTPUT
ISN 0020      101C TIME=TIME-TD+DELT
ISN 0021      IF(TIME+.5*DELT)1020,1030,1030
ISN 0022      102C CLAY=0.0
ISN 0023      GO TO 1140
ISN 0024      103C IF(TIME-TD)1120,104C,1040
ISN 0025      104C KEND=KX(K-1)-4
ISN 0026      INDEX=KX(K-3)
ISN 0027      IF(KX(K-4)-KX(K-2))1080,1080,1050
ISN 0028      105C IF(INDEX-KEND)106C,1080,1080
ISN 0029      106C I2=INDEX+2
ISN 0030      KEND1=KX(K-1)
ISN 0031      DG 1070 I=I2,KEND1,2
ISN 0032      IF(TIME-X(I))1130,1110,1070
ISN 0033      107C CONTINUE
ISN 0034      108C GO 1090 I=K,INDEX,2
ISN 0035      IF(TIME-X(I))1130,111C,1090
ISN 0036      109C CONTINUE
ISN 0037      110C CLAY=XIN-TD*(XIN-X(I+1))/(TIME-X(I))
ISN 0038      GO TO 1140
ISN 0039      111C CLAY=X(I+1)
ISN 0040      GO TO 1140

```

DELA0010
DELA 20DELA 70
DELA 80
DELA0090
DELA 100
DELA 110
DELA 120
DELA 130
DELA 140
DELA 150
DELA 160
DELA 170
DELA0180
DELA 190
DELA 200
DELA0210
DELA 220
DELA0230
DELA 240
DELA0250
DELA0260
DELA 270
DELA 280
DELA0290
DELA 300
DELA0305
DELA0310
DELA 320
DELA 330
DELA 340
DELA 350
DELA 360
DELA0370
DELA 380
DELA0390
DELA 400

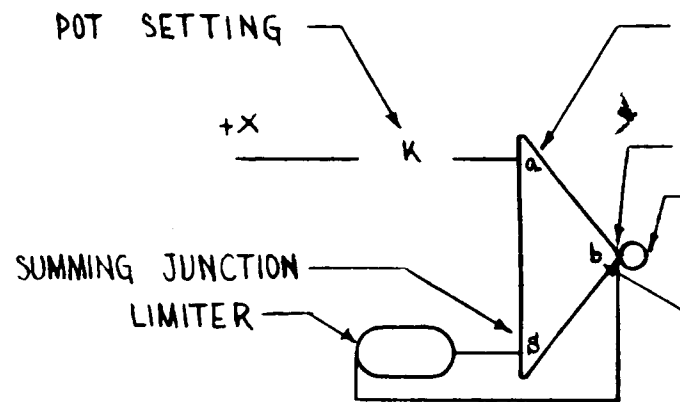
ISN 0040	1120	CLAY=X(K+1)	DELA 0410
ISN 0041		GU TO 1140	DELA 420
ISN 0042	1130	CLAY=X(I-1)+(X(I+1)-X(I-1))*(TIMEX-X(I-2))/(X(I)-X(I-2))	DELA 0430
		C... TEST IF TIME TO STORE INPUT	DELA 440
ISN 0043	1140	IF(KEEP)1210,121C,1150	DELA 450
ISN 0044	1150	IF(X(K-5)-TIME-0.5*DELT)1160,1160,1210	DELA 460
ISN 0045	1160	KX(K-4)=KX(K-4)+2	DELA 470
ISN 0046		X(K-5)=X(K-5)+X(K-6)	DELA 480
ISN 0047		IF(X(K-5)-TIME)1170,1170,1180	DELA 490
ISN 0048	1170	X(K-5)=TIME+X(K-6)	DELA 500
ISN 0049	1180	I=MOD(KX(K-4),KX(K-2))	DELA 510
ISN 0050		IF(I)1100,119C,1200	DELA 520
ISN 0051	1190	X(K)=X(INDEX)	DELA 530
ISN 0052		X(K+1)=X(INDEX+1)	DELA 540
ISN 0053		I=2	DELA 550
ISN 0054		KX(K-4)=KX(K-4)+2	DELA 560
ISN 0055	1200	INDEX=I+K	DELA 570
ISN 0056		KX(K-3)=INDEX	DELA 580
ISN 0057		X(INDEX)=TIME	DELA 590
ISN 0058		X(INDEX+1)=XIN	DELA 600
ISN 0059	1210	RETURN	DELA 610
ISN 0060		END	DELA 620

SAMPLE PRINTED OUTPUT

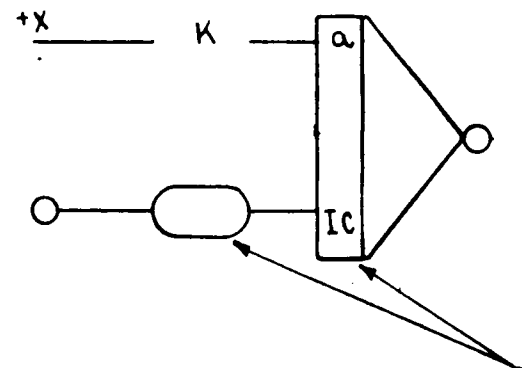
PRE-INDUCER-PUMP TEST SYSTEM-REMOTE COUPLING

TIME	PRE-INDUCER-PUMP TEST SYSTEM-REMOTE COUPLING	TRAPZ		INTEGRATION	
		TRAPZ	INTEGRATION	TRAPZ	INTEGRATION
TIME = 6.6667E-01	PILU = 1.3212E 01	PILU = 1.3145E 02	PILU = 1.1766E 01	WILD = 1.3146E 02	
	NPISHP= 2.3147E 01	PHIP = 9.4499E-02	PIPIN = 1.0527E 01	WFV1 = 1.2495E 02	
	WIPLO = 1.3148E 02	WIP = 1.3161E 02	WIT = 3.1759E 01	WP = 1.5688E 02	
	PIPOUT= 4.2738E 00	RPMIP = 1.2869E 03	NPSHP = 2.3013E 00	PITI = 9.0048E 01	
	KPMP = 3.7600E 03	PPD = 1.7755E 02	PFI = 1.7180E 02	PFO = 6.4386E 01	
	WT = 1.2572E 02	PPLI = 1.7440E 02	WPD = 1.2512E 02	TORQIT= 2.6854E 02	
	TORQIP= 1.3943E 02	PHIIP = 8.6366E-02	SIGIP = 1.0000E-01	IPICOM= 1.0000E 02	
	IPINER= 2.2500E-02	IPOCOM= 6.4000E 01	IDPBAR= 3.8451E 00	IPPRAT= 9.9907E-01	
	PUPBAR= 1.8325E 02	PPRAT = 9.6075E-01	PWC = 4.0050E 01	WMC = 1.2599E 02	
	PPI = 1.4969E 00	WCLI = 1.6298E 02	WCLO = 1.6292E 02		
	PILU = 1.2871E 01	PILU = 1.4344E 02	PILD = 1.1435E 01	WILD = 1.4345E 02	
	NPISHP= 2.2408E 01	PHIP = 9.7909E-02	PIPIN = 1.0207E 01	WFV1 = 1.3235E 02	
	WIPLO = 1.4346E 02	WIP = 1.4352E 02	WIT = 3.2612E 01	WP = 1.6512E 02	
TIME = 6.9533E-01	PIPOUT= 5.4670E 00	RPMIP = 1.4206E 03	NPSHP = 6.2652E 00	PITI = 9.5910E 01	
	KPMP = 3.8197E 03	PPD = 1.8607E 02	PFI = 1.8126E 02	PFO = 6.1048E 01	
	WT = 1.3257E 02	PPLI = 1.8354E 02	WPD = 1.3251E 02	TORQIT= 2.9322E 02	
	TORQIP= 1.7070E 02	PHIIP = 3.5322E-02	SIGIP = 1.0000E-01	IPICOM= 1.0000E 02	
	IPINER= 2.2500E-02	IPOCOM= 6.4000E 01	IDPBAR= 5.0852E 00	IPPRAT= 9.9885E-01	
	PUPBAR= 1.3631E 02	PPRAT = 9.8469E-01	PWC = 4.0432E 01	WMC = 1.3331E 02	
	PPI = 3.2141E 00	WCLI = 1.7492E 02	WCLO = 1.7466E 02		
	PILU = 1.2555E 01	PILU = 1.5373E 02	PILD = 1.1963E 01	WILD = 1.5369E 02	
	NPISHP= 2.5348E 01	PHIP = 1.3123E-01	PIPIN = 1.1481E 01	WFV1 = 1.3938E 02	
	WIPLO = 1.5351E 02	WIP = 1.5141E 02	WIT = 3.3197E 01	WP = 1.7277E 02	
	PIPOUT= 1.8168E 01	RPMIP = 1.5469E 03	NPSHP = 2.0886E 01	PITI = 1.1189E 02	
	KPMP = 3.8657E 03	PPD = 1.9667E 02	PFI = 1.9245E 02	PFO = 5.9701E 01	
	WT = 1.4028E 02	PPLI = 1.9392E 02	WPD = 1.3957E 02	TORQIT= 3.1367E 02	
	TORQIP= 2.0491E 02	PHIIP = 8.2066E-02	SIGIP = 1.0000E-01	IPICOM= 1.0000E 02	
	IPINER= 2.2500E-02	IPOCOM= 6.4000E 01	IDPBAR= 7.0189E 00	IPPRAT= 9.9889E-01	
	PUPBAR= 1.8803E 02	PPRAT = 9.9518E-01	PWC = 4.0282E 01	WMC = 1.3978E 02	
	PPI = 9.5479E 00	WCLI = 1.7754E 02	WCLO = 1.7488E 02		
TIME = 7.4667E-01	PILU = 1.2651E 01	PILU = 1.4939E 02	PILD = 1.3206E 01	WILD = 1.4941E 02	
	NPISHP= 3.0343E 01	PHIP = 1.5447E-01	PIPIN = 1.3645E 01	WFV1 = 1.4666E 02	
	WIPLO = 1.4950E 02	WIP = 1.5062E 02	WIT = 3.3392E 01	WP = 1.8041E 02	
	PIPOUT= 2.6913E 01	RPMIP = 1.6509E 03	NPSHP = 5.6718E 01	PITI = 1.2174E 02	
	KPMP = 3.9113E 03	PPD = 2.1443E 02	PFI = 2.0846E 02	PFO = 6.0922E 01	
	WT = 1.4754E 02	PPLI = 2.1098E 02	WPD = 1.4702E 02	TORQIT= 3.2558E 02	
	TORQIP= 2.3951E 02	PHIIP = 7.7051E-02	SIGIP = 1.0000E-01	IPICOM= 1.0000E 02	
	IPINER= 2.2500E-02	IPOCOM= 6.4000E 01	IDPBAR= 1.0304E 01	IPPRAT= 9.9914E-01	
	PILU = 1.2555E 01	PILU = 1.5373E 02	PILD = 1.1963E 01	WILD = 1.5369E 02	
	NPISHP= 2.5348E 01	PHIP = 1.3123E-01	PIPIN = 1.1481E 01	WFV1 = 1.3938E 02	
	WIPLO = 1.5351E 02	WIP = 1.5141E 02	WIT = 3.3197E 01	WP = 1.7277E 02	
	PIPOUT= 1.8168E 01	RPMIP = 1.5469E 03	NPSHP = 2.0886E 01	PITI = 1.1189E 02	
	KPMP = 3.8657E 03	PPD = 1.9667E 02	PFI = 1.9245E 02	PFO = 5.9701E 01	
	WT = 1.4028E 02	PPLI = 1.9392E 02	WPD = 1.3957E 02	TORQIT= 3.1367E 02	
	TORQIP= 2.0491E 02	PHIIP = 8.2066E-02	SIGIP = 1.0000E-01	IPICOM= 1.0000E 02	
	IPINER= 2.2500E-02	IPOCOM= 6.4000E 01	IDPBAR= 7.0189E 00	IPPRAT= 9.9889E-01	
	PUPBAR= 1.8803E 02	PPRAT = 9.9518E-01	PWC = 4.0282E 01	WMC = 1.3978E 02	
	PPI = 9.5479E 00	WCLI = 1.7754E 02	WCLO = 1.7488E 02		

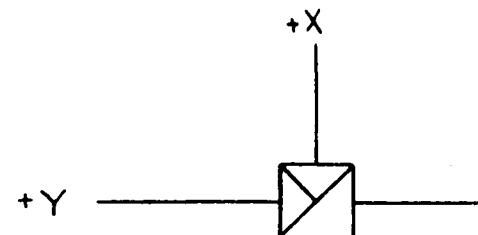
SUMMER



INTEGRATOR



MULTIPLIER



RS — REFERENCE

τ — TIME DELAY

— TRUNK IN

INPUT RESISTOR $\begin{cases} 1 = 1 \text{ MEGOHM} \\ .1 = 0.1 \text{ MEGOHM} \end{cases}$

-KX
+KX

FEED BACK
RESISTOR

0.1 MEGOHM IF NOT NOTED
10 DENOTES 1 MEGOHM
100 DENOTES 10 MEGOHMS

$+\int KX dt$

1 μ F FEEDBACK
IF NOT NOTED

INITIAL CONDITION DOT

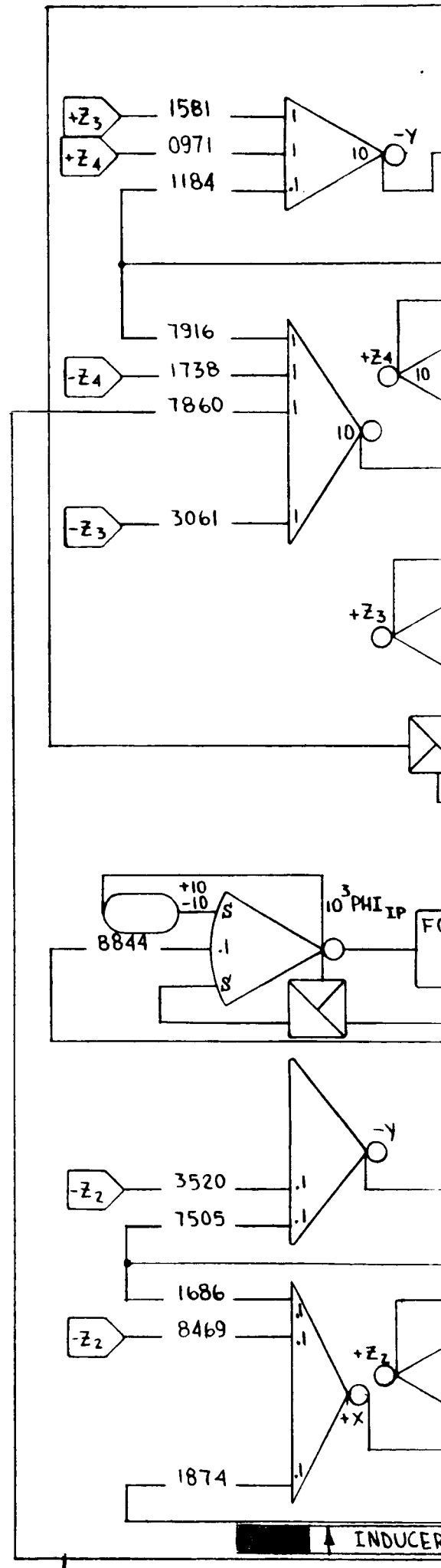
+XY/100

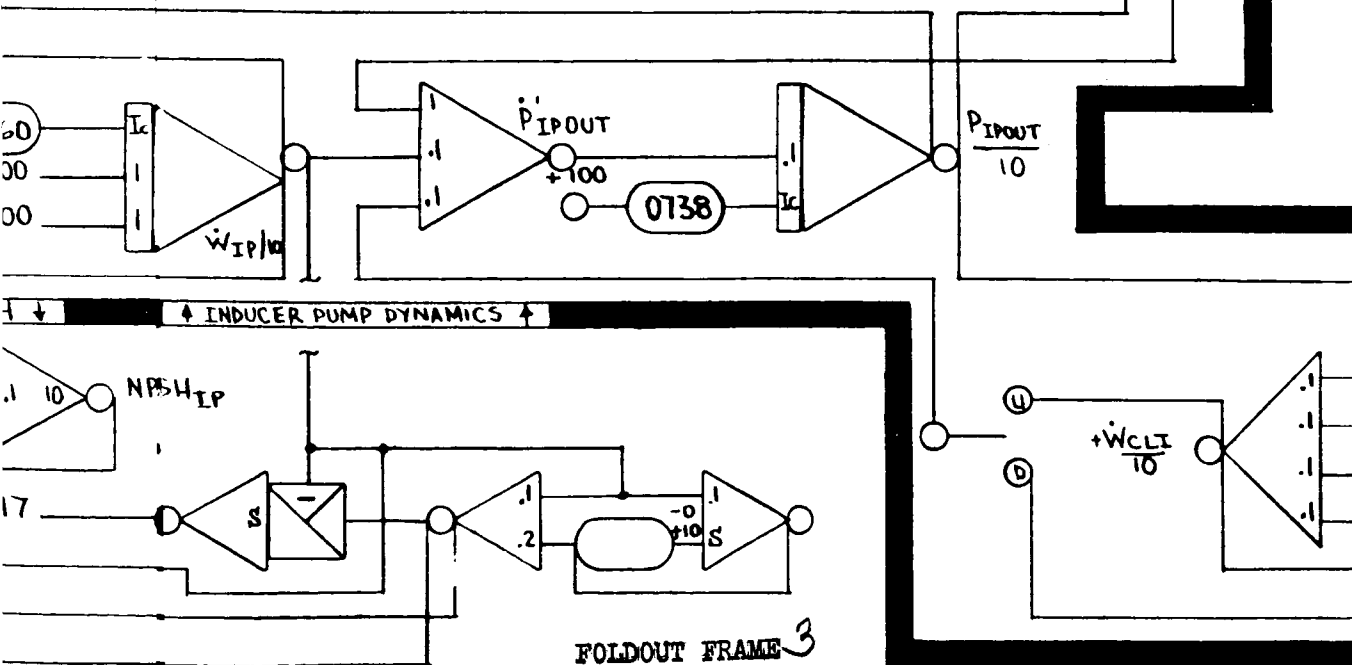
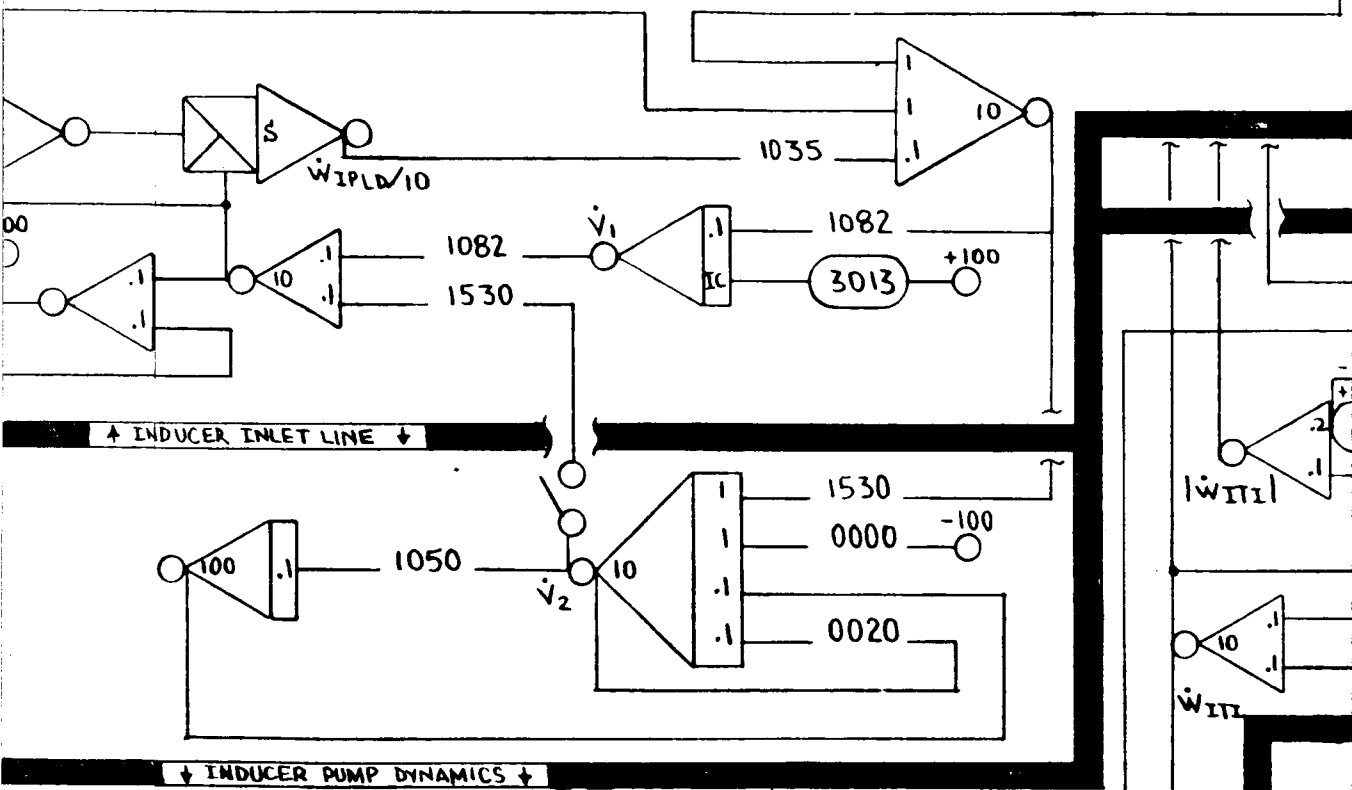
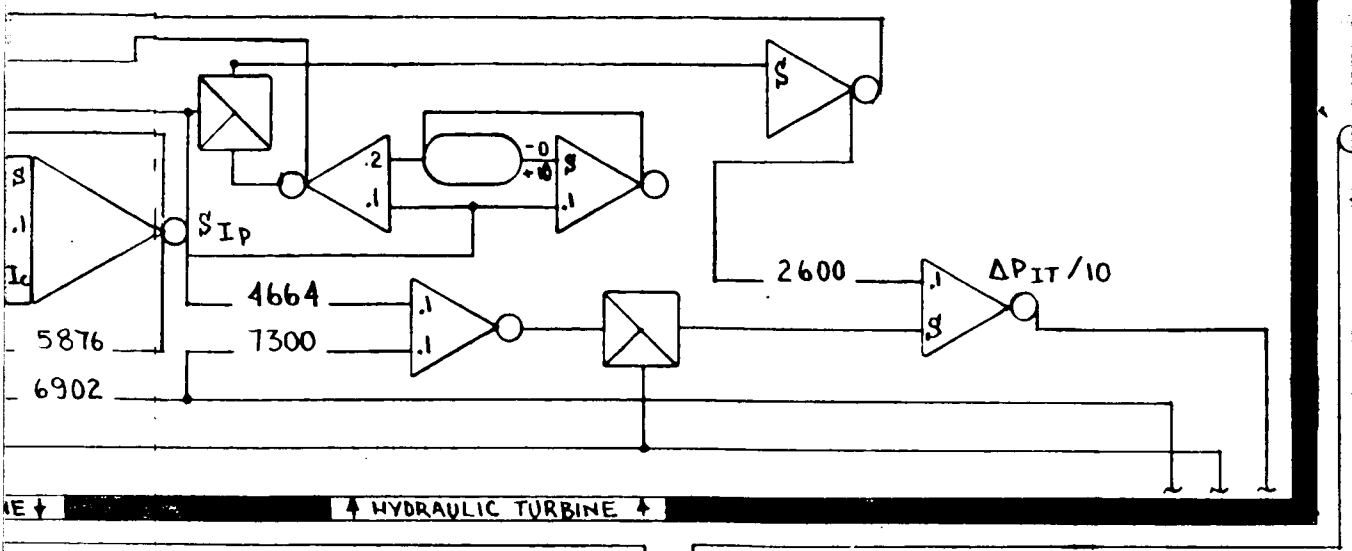
SWITCH

Y

INTERCONNECT

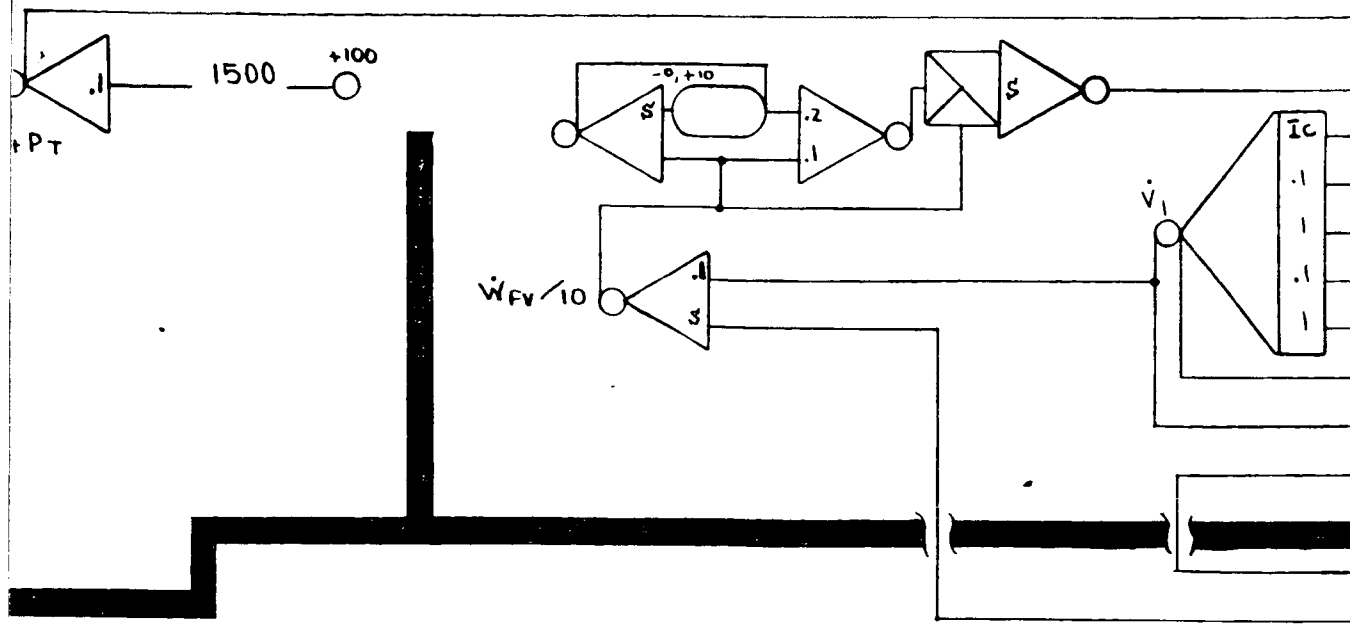
FOLDOUT FRAME



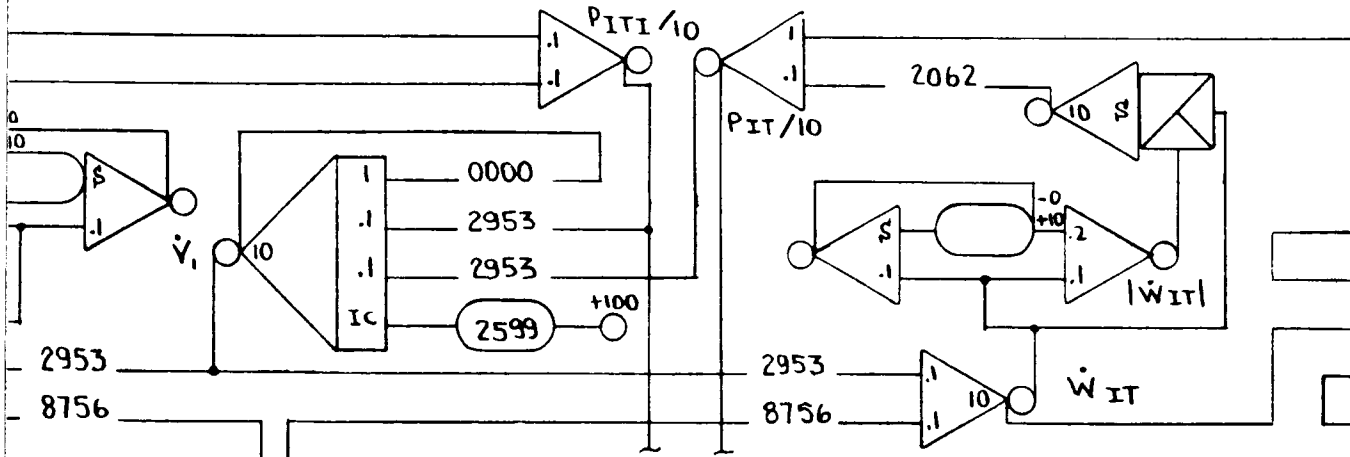


TANK

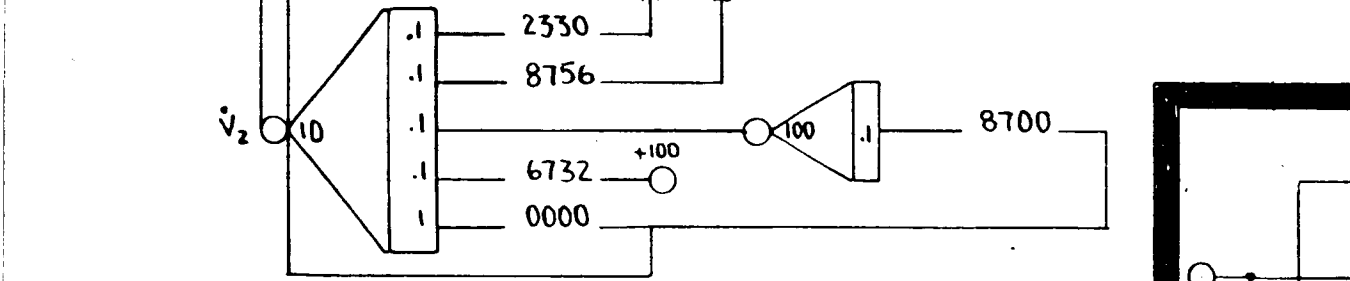
↓ RETURN LINE 1ST MODE ↓



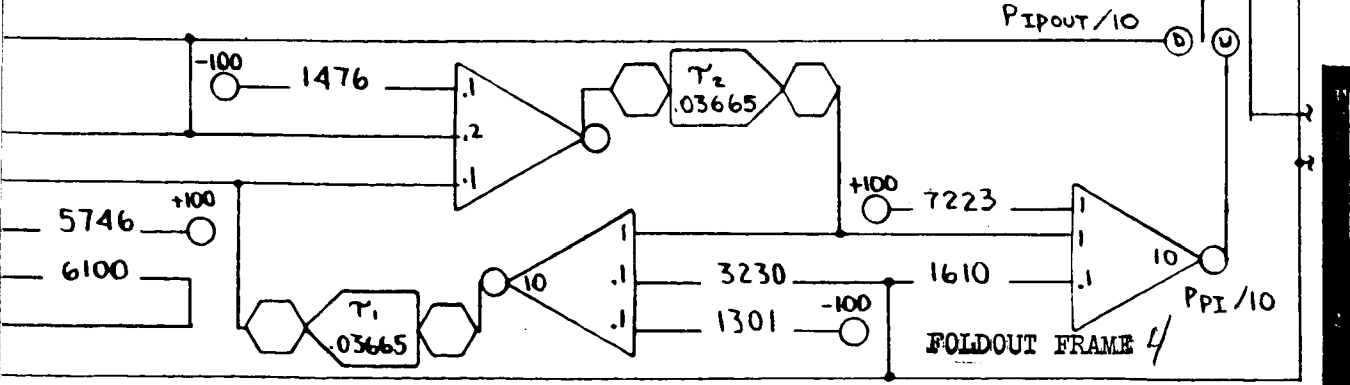
↓ HYDRAULIC TURBINE FEED LINE ↓



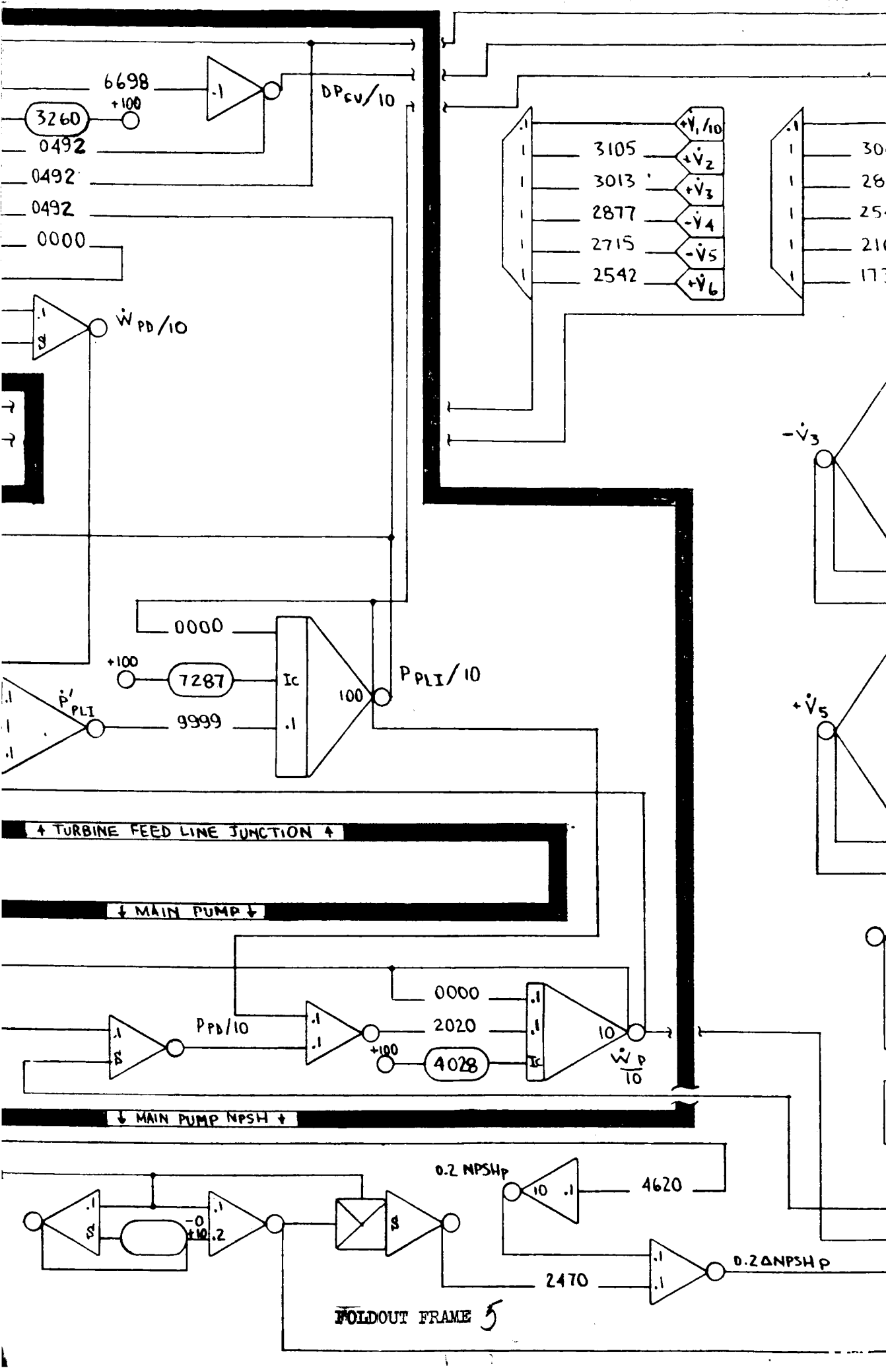
↓ HYDRAULIC TURBINE FEED LINE ↓



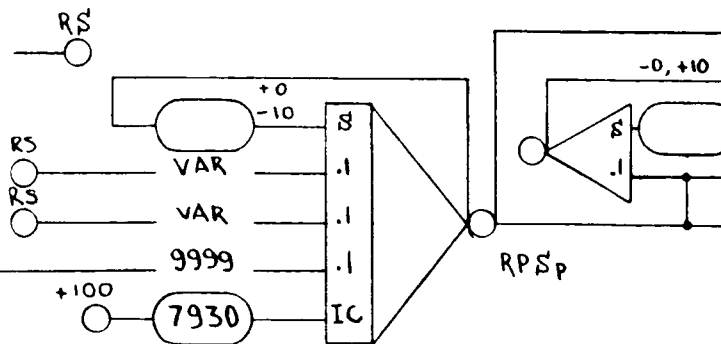
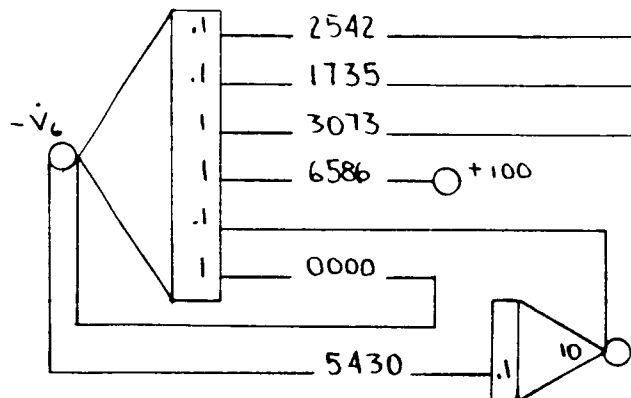
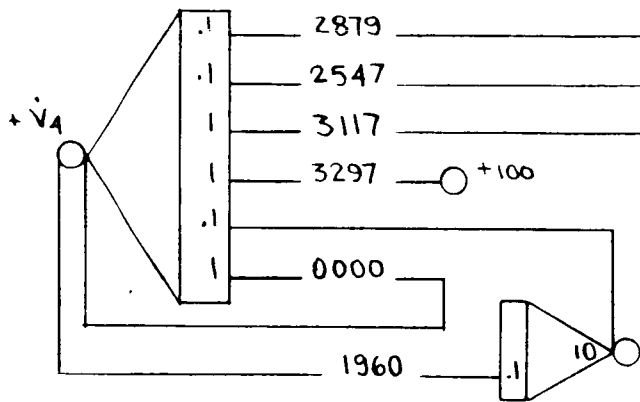
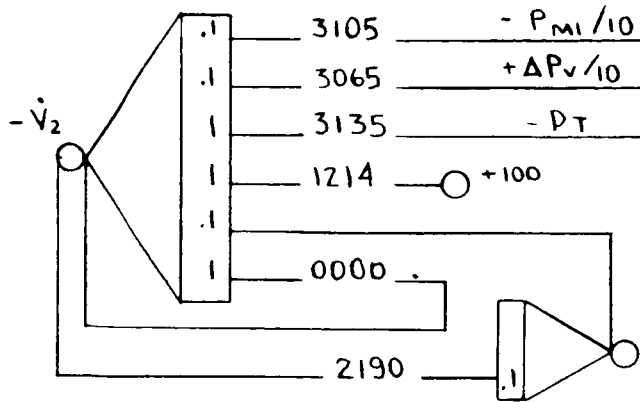
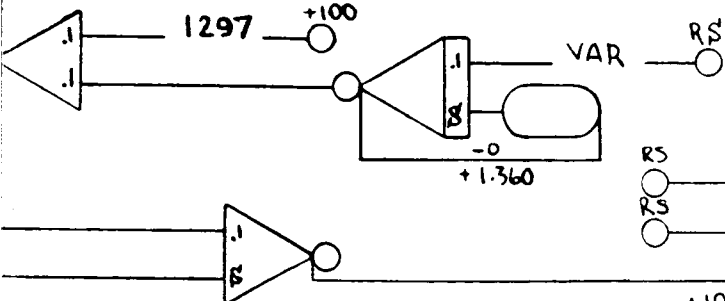
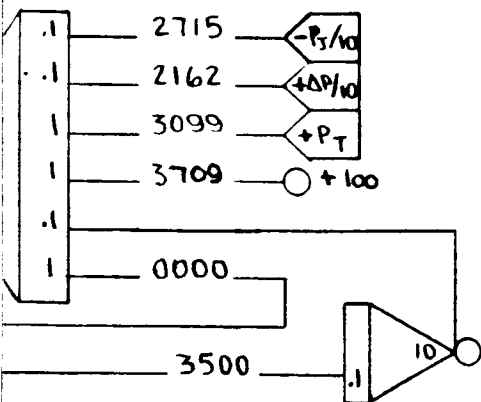
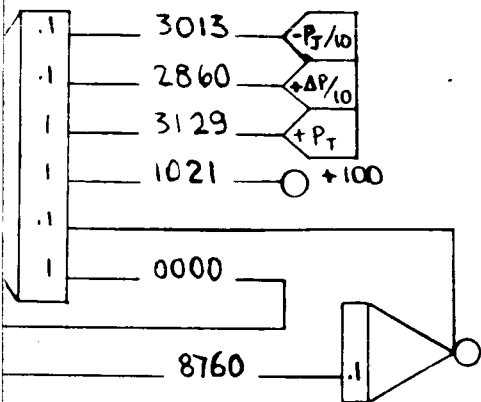
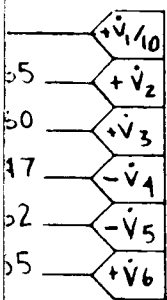
↓ PUMP COUPLING LINE ↓



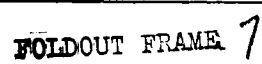
↓ PUMP COUPLING LINE ↓

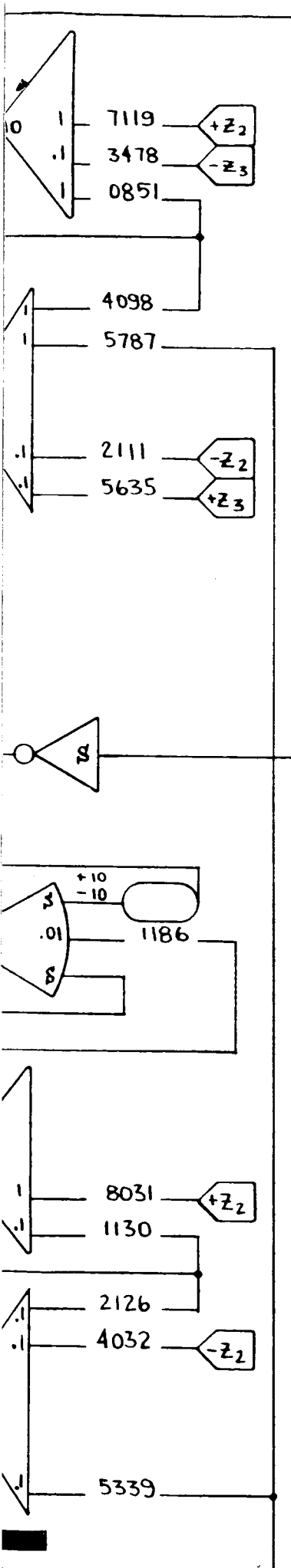


↓ RETURN LINE HIGHER FREQUENCY MODES ↑



↑ MAIN PUMP DRIVE ↓





Preinducer Analog Model Diagram

SAMPLE PLOTTED OUTPUT

PRE-INDUCER-PUMP TEST SYSTEM-REMOTE COUPLING

MINIMUM
0.0

PIPIN VERSUS TIME

I

TIME PIPIN

0.0	1.5000E 01	-----+
8.0000E-02	1.4995E 01	-----+
1.6000E-01	1.4883E 01	-----+
2.4000E-01	1.4489E 01	-----+
3.2000E-01	1.3826E 01	-----+
4.0000E-01	1.3170E 01	-----+
4.8000E-01	1.2628E 01	-----+
5.6000E-01	1.1993E 01	-----+
6.4000E-01	1.0928E 01	-----+
7.2000E-01	1.1481E 01	-----+
8.0000E-01	1.0506E 01	-----+
8.8000E-01	1.1466E 01	-----+
9.6000E-01	1.1417E 01	-----+
1.0400E 00	1.1192E 01	-----+
1.1200E 00	1.0583E 01	-----+
1.2000E 00	1.0082E 01	-----+
1.2800E 00	1.0042E 01	-----+
1.3600E 00	9.7575E 00	-----+
1.4400E 00	9.4584E 00	-----+
1.5200E 00	9.1624E 00	-----+
1.6000E 00	8.8486E 00	-----+
1.6800E 00	8.5690E 00	-----+
1.7600E 00	8.3016E 00	-----+
1.8400E 00	8.0104E 00	-----+
1.9200E 00	7.7281E 00	-----+
2.0000E 00	7.4331E 00	-----+
2.0800E 00	7.1430E 00	-----+
2.1600E 00	6.8485E 00	-----+
2.2400E 00	6.5564E 00	-----+
2.3200E 00	6.2600E 00	-----+
2.4000E 00	5.9676E 00	-----+
2.4800E 00	5.6732E 00	-----+
2.5600E 00	5.3830E 00	-----+
2.6400E 00	5.0912E 00	-----+
2.7200E 00	4.8001E 00	-----+

PREINDUCER ANALOG MODEL DIAGRAM

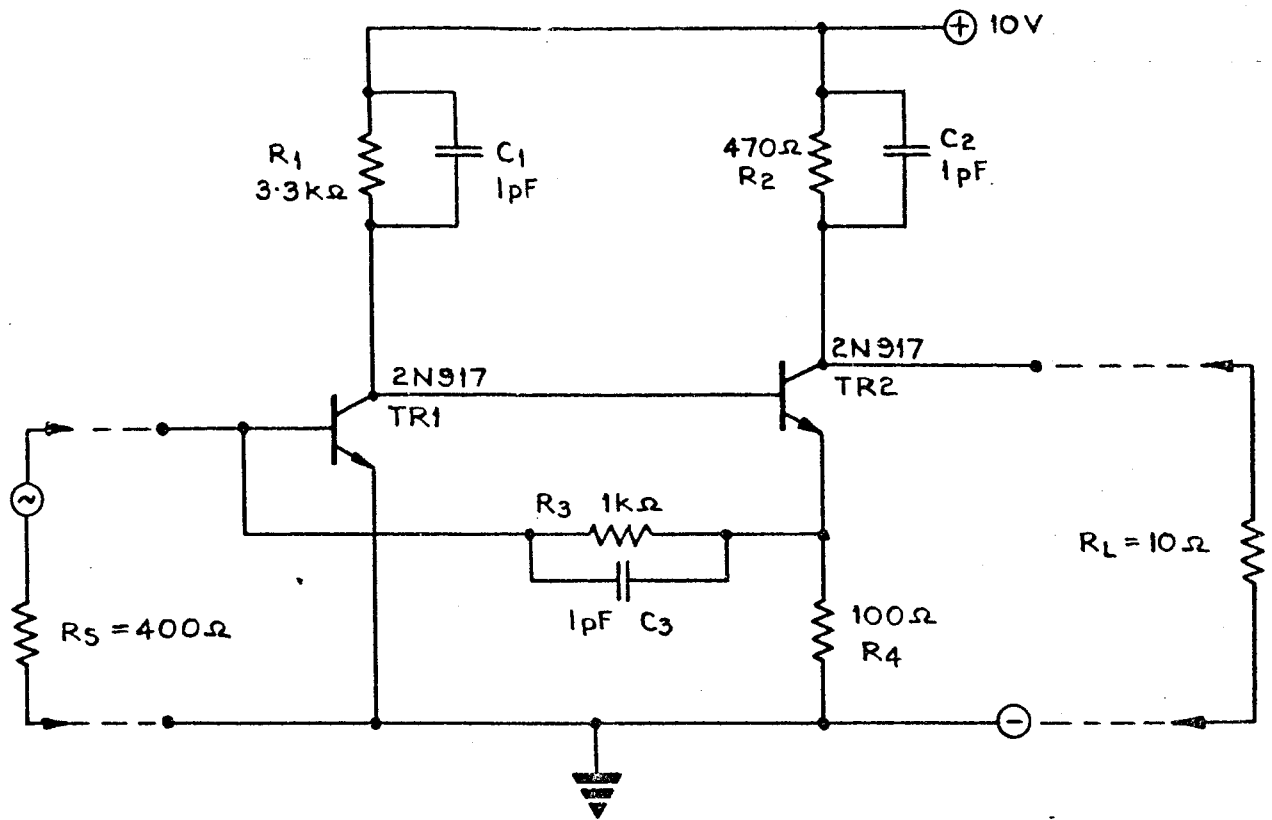


FIG.4a TYPICAL CIRCUIT TO BE ANALYSED

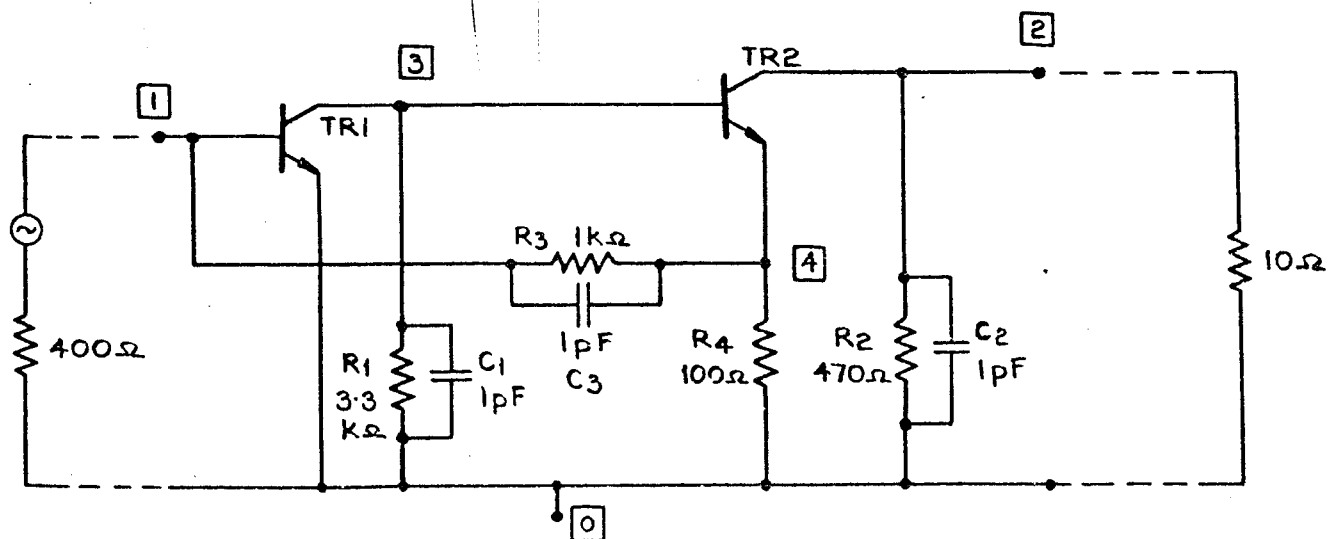
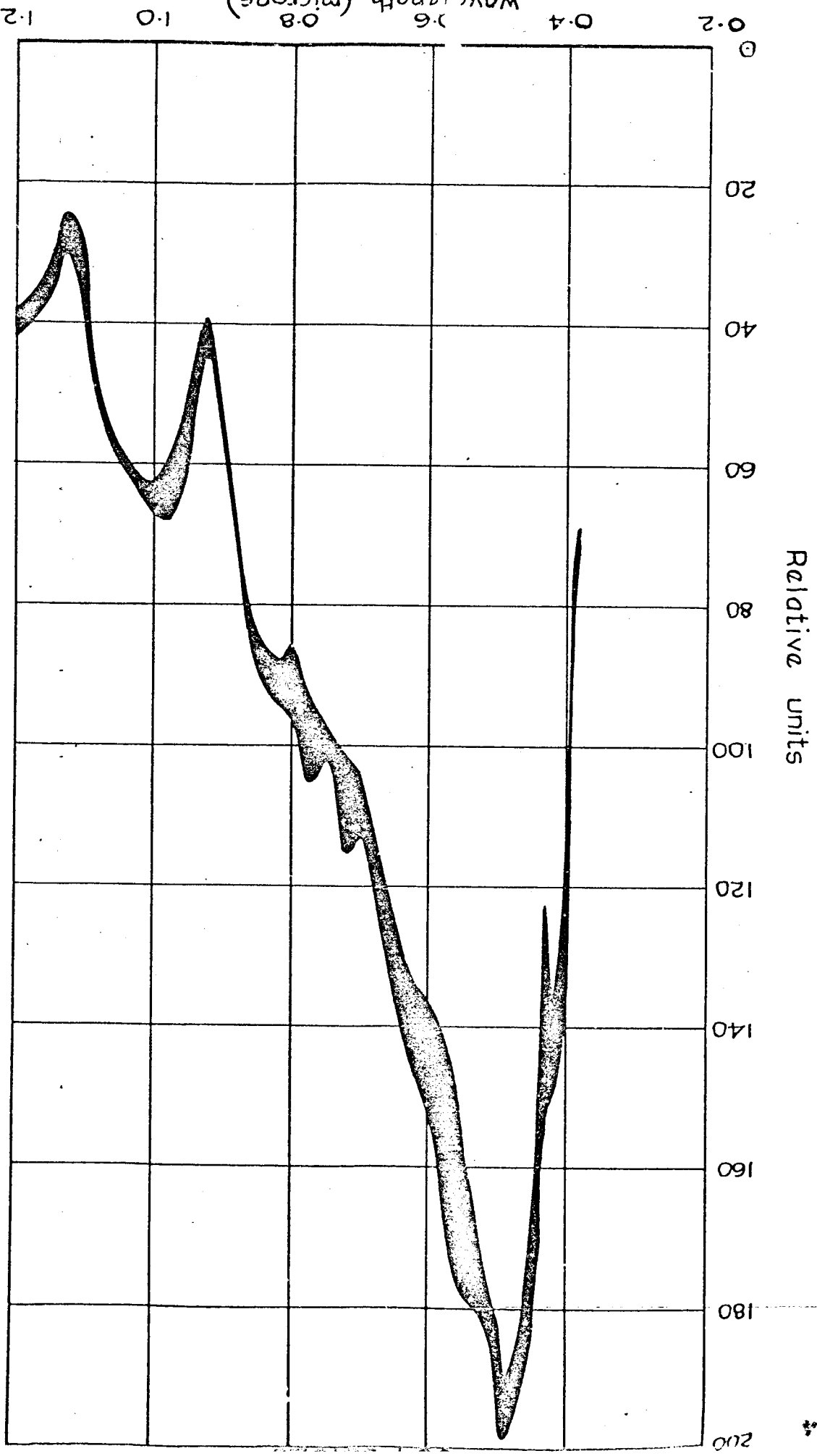


FIG.4b CIRCUIT RE-DRAWN FOR COMPUTER ANALYSIS

Fig.14 Variation of relative energy spectral distribution noon,2,3&4 July 1966



DISTRIBUTION LIST

	<u>Copies</u>
National Aeronautics and Space Administration	
Lewis Research Center	
21000 Brookpart Road	
Cleveland, Ohio 44135	
Attention: Contracting Officer, MS 500-313	1
Large Engine Technology Branch, MS 500-305	15
Technical Report Control Office, MS 5-5	1
Technology Utilization Office, MS 3-16	1
AFSC Liaison Office, MS 4-1	1
Library, MS 60-3	2
National Aeronautics and Space Administration	
Washington, D.C. 20546	
Attention: Code RPX	2
RPL	1
Scientific and Technical Information Facility	
P. O. Box 33	
College Park, Maryland 20740	
Attention: NASA Representative	
Code CRT	1
National Aeronautics and Space Administration	
Ames Research Center	
Moffett Field, California 94035	
Attention: Library	1
Dr. Leonard Roberts	1
National Aeronautics and Space Administration	
Flight Research Center	
P. O. Box 273	
Edwards, California 93523	
Attention: Library	1
National Aeronautics and Space Administration	
Goddard Space Flight Center	
Greenbelt, Maryland 20771	
Attention: Library	1

Copies

National Aeronautics and Space Administration
John F. Kennedy Space Center
Cocoa Beach, Florida 32931

Attention: Library

1

National Aeronautics and Space Administration
Langley Research Center
Langley Station
Hampton, Virginia 23365

Attention: Library

1

National Aeronautics and Space Administration
Manned Spacecraft Center
Houston, Texas 77001

Attention: Library

1

J. G. Thibodaux

1

National Aeronautics and Space Administration
George C. Marshall Space Flight Center
Huntsville, Alabama 35812

Attention: Library

1

Keith Chandler, R-P & VE-PA

1

Loren Gross, R-P & VE-PAC

1

Jet Propulsion Laboratory
4800 Oak Grove Drive
Pasadena, California 91103

Attention: Library

1

Henry Burlage

1

UNCLASSIFIED

Security Classification

DOCUMENT CONTROL DATA - R & D

(Security classification of title, body of abstract and indexing annotation must be entered when the overall report is classified)

1. ORIGINATING ACTIVITY (Corporate author) Rocketdyne, a Division of North American Rockwell Corporation, 6633 Canoga Avenue, Canoga Park, California 91304		2a. REPORT SECURITY CLASSIFICATION UNCLASSIFIED	
3. REPORT TITLE INDUCER DYNAMICS, PARTIAL FLOW HYDRAULIC TURBINE DRIVE		2b. GROUP	
4. DESCRIPTIVE NOTES (Type of report and inclusive dates) Interim Report			
5. AUTHOR(S) (First name, middle initial, last name) King, J. A.			
6. REPORT DATE February 1968		7a. TOTAL NO. OF PAGES 172 & xii	7b. NO. OF REFS
8a. CONTRACT OR GRANT NO. NAS3-10280		9a. ORIGINATOR'S REPORT NUMBER(S) R-7427	
b. PROJECT NO.		9b. OTHER REPORT NO(S) (Any other numbers that may be assigned this report) NASA CR-72379	
c.			
d.			
10. DISTRIBUTION STATEMENT			
11. SUPPLEMENTARY NOTES		12. SPONSORING MILITARY ACTIVITY Technical Management NASA Lewis Research Center Cleveland, Ohio	
13. ABSTRACT Two computer programs, an analog and a digital, have been developed that will predict the transient performance of a low-speed inducer driven by a hydraulic turbine. An inducer-turbine unit has been designed and fabrication is in progress. Steady-state maps of the pertinent components of this unit have been constructed from existing test data and by synthetic mapping procedures. These maps have been used in the computer programs to predict the performance of this unit in the system in which it will eventually be tested. Parametric studies have been made to determine the effect of selected changes in this system. The computer program has also been used to investigate several inducer-turbine combinations in simulated rocket engine installations.			

14	KEY WORDS	LINK A		LINK B		LINK C	
		ROLE	WT	ROLE	WT	ROLE	WT
	Turbomachinery Inducer dynamics Hydraulic turbine drive Preinducer Inducer						